UNIVERSITY OF CALIFORNIA, MERCED

Coupled water-food system analysis of agriculture in California's San Joaquin Valley: vulnerabilities, adaptations and policy trade-offs

A dissertation submitted in partial satisfaction of the
requirements for the degree
Doctor of Philosophy

in

Environmental Systems

by

José Manuel Rodríguez Flores

Committee in charge:

Dr. Josué Medellín Azuara, Chair
Dr. Colleen Naughton
Dr. Erin L. Hestir
Dr. Alvar Escriva Bou
Dr. Jonathan D. Herman

2023

The dissertation of José Manuel Rodríguez Flores is approved, and it is acceptable in quality and form for publication on microfilm and electronically:

(Dr. Colleen Naughton)

(Dr. Erin L. Hestir)

(Dr. Alvar Escriva Bou)

(Dr. Jonathan D. Herman)

(Dr. Josué Medellín Azuara, Chair)

University of California, Merced

2023

TABLE OF CONTENTS

LIST OF FIGURES

LIST OF TABLES

ACKNOWLEDGEMENTS

I am profoundly grateful to Josué Medellin Azuara, for his invaluable support and guidance throughout my Ph.D. journey. I was fortunate to join him for a summer research internship in 2018 while doing my Master's degree in México. Following that experience, he extended me the opportunity to pursue my Ph.D. with him, an opportunity that changed my life for the better. Josué has been more than a mentor and advisor; he has become a friend. I have learned so much from him, including water and agriculture in California, modeling, and writing. Most importantly, he has taught me the importance of collaboration and kindness. Working with Josué has been an amazing experience, he always showed his support and listened to me which I will be always grateful for.

I want to thank my parents José Manuel and Norma Lilia who have gone above and beyond to provide me with every opportunity to pursue my goals. They have supported me unconditionally offering encouragement, guidance and love no matter the challenges. I want to thank my sister Lili who has always motivated me to keep dreaming. Thanks to my grandmother Lore for her support and generosity, and for her kind sponsorship that covered the expenses necessary to pay my TOEFL, Visa, GRE, and a first month of rent (when moving to the US), which allowed me to pursue my educational aspirations.

The past four years have been filled with numerous challenges, from long hours of research to moments of uncertainty during the COVID pandemic, that started during my second semester of the program. I cannot imagine going through all these without the support and love of my partner Elena Bischak. Who I met during the first week of our PhD and since then we haven't stop enjoying our lives together. Elena's presence has been essential in maintaining a balanced life and providing incredible support. Her support was key for my PhD journey, helping me prepare for qualifying exams, offering editing assistance for my English, cheering me up when I felt stuck and exhausted from research, and consistently motivating me. Also thanks to our dogs, Sage and Tule, keeping my mood up everyday and being the best home office mates.

I am immensely grateful to my friends at UC Merced who have become like family to me - Naivy, Anshika, Humberto, Pablo, Toshi, Edwin, and others who have been a significant part of my life in recent years. I am specially grateful to Angel Fernandez, a dear friend since 2018, with whom I have also shared numerous ideas and collaborations. Spencer Cole, with whom I spent

countless hours in zoom and coffee shops working on coding, data collection, and data analysis. I want to thank my amazing lab mates Jorge and Liying for listening and helping to each other. My path during the PhD was influenced by amazing mentors along the way, including Alvar Escriva Bou, Josh Viers, Tom Harmon and Jay Lund, all people who I admire and from whom I have learned invaluable lessons about understanding and communicating about water in California.

I want to thank my committee for they thoughtful feedback over the course of my PhD, Colleen Naughton, Erin Hestir, Jon Herman and Alvar Escriva Bou. And to numerous collaborators with whom I have had the privilege to work and learn. I look forward to continuing our collaboration on cool research projects. Special thanks to Nick Santos, Patrick Reed, Rohini Gupta, Harrison Zeff, Keyvan Malek, and Tina Karimi for their valuable contributions.

This milestone would have not been possible without the help of many people who have helped and believed in me in my academic journey prior to joining the Ph.D. program. I am profoundly grateful to all of them. In particular, I want to thank Ramon Valdivia Alcalá, who has been both a mentor and a friend since my early years in college. His support was key in providing me with various academic opportunities, including my internship at UC Merced in 2018. I am forever grateful for his guidance and encouragement.

Throughout the past four years, I have been fortunate to receive significant support from the UC Mexus-CONACyT scholarship, which covered my tuition expenses and provided a portion of my monthly allowance. I am immensely grateful to UC Alianza and the Mexican government (and the people who contributed through their tax payments) for their support in awarding me this scholarship. Additionally, my work was funded by the NSF INFEWS program grant number 1639268, by the California Department of Food and Agriculture grant agreement 21-0557-000-SO and by the Agriculture and Food Research Initiative Competitive Grant number 2021-69012-35916 from the USDA National Institute of Food and Agriculture. Their financial support has played a key role in the successful pursuit of my academic and research goals.

CURRICULUM VITAE

EDUCATION

2019-2023	University of California Merced, USA **Doctor of Philosophy in Environmental Systems** *Coupled water-food system analysis of agriculture in California's San Joaquin Valley: vulnerabilities, adaptations and policy trade-offs*
2016-2018	Colegio de Postgraduados, México **Master of Science in Economics** Field of study: Agricultural Economics *Economic valuation of water for irrigation under scarcity scenarios in the irrigation district DR011, Alto Río Lerma, Guanajuato, Mexico.*
2011-2015	Universidad Autónoma Chapingo,México **Bachelor of Science in Economics** Field of study: Agricultural Economics

PUBLICATIONS

Rodríguez-Flores, J.M., Fernandez-Bou, A.S.,Ortiz-Partida, J.P. and Medellín-Azuara, J. (2023). Drivers of domestic wells vulnerability during droughts in California's Central Valley, *In-Preparation*

Rodríguez-Flores, J.M., Gupta, R.S., Zeff, H.B., Reed, P.M. and Medellín-Azuara, J. (2023). Identifying robust adaptive irrigation operating policies to balance deeply uncertain economic food production and groundwater sustainability trade-offs. *In-Review*

Ortiz Partida, J.P., Fernandez-Bou, A.S., Maskey, M., **Rodriguez-Flores, J.M.**, Medellin-Azuara, J., Sandoval-Solis, S., Ermolieva, T., Wada, Y.and Kahil, T. (2023). Hydro-economic modeling of water resources management challenges: current applications and future directions. *Water Economics and Policy*. DOI:10.1142/S2382624X23400039

Fernandez-Bou, A.S., **Rodríguez-Flores, J.M.**, Guzman, A., Ortiz-Partida, J.P., Classen-Rodriguez, L.M., Sánchez-Pérez, P.A., Valero-Fandiño, J., Pells, C., Flores-Landeros, H., Sandoval-Solís, S., Characklis, G.W., Harmon, T.C., McCullough, M., and Medellín-Azuara,J. (2023). Water, environment, and socioeconomic justice in California: A multi-benefit cropland repurposing framework. *Science of The Total Environment*. DOI: 10.1016/j.scitotenv.2022.159963

Rodríguez-Flores,J.M., Valero Fandiño, J.A., Cole, S.A., Malek, K., Karimi,T., Zeff,H.B., Reed, P.M., Escriva-Bou, A., and Medellín-Azuara, J. (2022). Global Sensitivity Analysis of a Coupled Hydro-Economic Model and Groundwater Restriction Assessment. *Water Resources Management*,pp. 6115–6130. 2022. DOI: 10.1007/s11269-022-03344-5

Fernandez-Bou,A.S., Ortiz-Partida,J.P., Classen-Rodriguez, L.M., Pells, C., Dobbin, K.B., Espinoza, V., **Rodríguez-Flores, J.M.**, Thao,C., Hammond W., Courtney R., Fencl,A., Flores-Landeros, H., Maskey, M.L.,Cole, S.A., Azamian, S.,Gamiño, E.,Guzman,A., Alvarado, A.G., Campos-Martínez, M.S., Weintraub, C., Sandoval, E., Dahlquist-Willard, R.M., Bernacchi, L.A., Naughton,C., DeLugan, R.M., and Medellín-Azuara,J., (2021). 3 Challenges, 3 Errors, and 3 Solutions to Integrate Frontline Communities in Climate Change Policy and Research: Lessons From California. *Frontiers in Climate*, 3, 717554. DOI: 10.3389/fclim.2021.717554

Rodríguez-Flores, J.M., Medellín-Azuara, J., Valdivia-Alcalá, R., Arana-Coronado, O.A., and García-Sánchez, R.C. (2019). Insights from a Calibrated Optimization Model for Irrigated Agriculture under Drought in an Irrigation District on the Central Mexican High Plains. *Water* p. 858. 2019. DOI: 10.3390/w11040858

REPORTS

Medellín-Azuara, J., Escriva-Bou, A., **Rodríguez-Flores, J.M.**, Cole, S.A., Abatzoglou, J., Viers, J.H., Santos, N., and Sumner, Daniel A. (2022). Economic Impacts of the 2020–22 Drought on California Agriculture. *A report for the California Department of Food and Agriculture, University of California, Merced*

Medellín-Azuara, J., Escriva-Bou, A., Abatzoglou, J., Viers, J.H., Cole, S.A., **Rodríguez-Flores, J.M.**, and Sumner, Daniel A. (2022). Economic Impacts of the 2021 Drought on California Agriculture. Preliminary Report. *A report for the California Department of Food and Agriculture, University of California, Merced*

Whipple, A., Grenier, L., Safran, S., Zeleke, D., Wells, E., Deverel, S., Olds, M., Cole, S., **Rodríguez-Flores, J.M.**, Guzman, A., and Medellín-Azuara, J. (2022). Resilient Staten Island: Landscape Scenario Analysis Pilot Application. *Prepared for the U.S. Fish and Wildlife Service, San Francisco Estuary Institute, Richmond, CA*

Fernandez-Bou, A.S., Ortiz-Partida, J.P., Pells, C., Classen-Rodriguez, L.M., Espinoza, V., **Rodríguez-Flores, J.M.**, and Medellin-Azuara, J. (2021). Regional Report for the San Joaquin Valley Region on Impacts of Climate Change. *California's Fourth Climate Assesment, California Natural Resources Agency SUM-CCCA4-2021-003, Sacramento*

SELECTED CONFERENCE PRESENTATIONS

Rodríguez-Flores, J.M., Gupta, R.S., Zeff, H.B., Reed, P.M., Medellín-Azuara, J. (2022). Implementing adaptive operating policies to achieve agricultural, economic, and groundwater sustainability goals for the San Joaquin Valley using Evolutionary Multi-Objective Direct Policy Search. *Oral Presentation, AGU Fall Meeting*

Medellin-Azuara, J., **Rodriguez-Flores, J.M.**, Cole, S., Escriva-Bou, A., A., John, Viers, J.H., and Santos, N. (2022). On Assessing Drought Economic Impacts on Agriculture and Communities: Lessons Learned from California Droughts. *Poster - Presenting Author, AGU Fall Meeting*

Rodríguez-Flores, J.M., Valero Fandiño, J.A., Cole, S.A., Malek, K., Karimi,T., Zeff,H.B., Reed, P.M., Escriva-Bou, A., and Medellín-Azuara, J. (2020). Global Sensitivity Analysis for a coupled Hydro-economic model under a groundwater management policy in Kern County, California. *Poster, AGU Fall Meeting*

PROFESSIONAL TRAINING

Climate Adaptation Science Academy - Experiential Learning Expedition (CASA ELE)
Secure Water Future (SWF), UC Merced - 2022

Introduction to Groundwater, Watersheds, and Groundwater Sustainability Plans
University of California, Division of Agriculture and Natural Resources - 2020

SERVICE

UC Merced Environmental Systems Program Seminar Lead (Fall 2021 - Spring 2022)

Journal Reviewer - Journal of Water Resources Planning and Management

ABSTRACT OF THE DISSERTATION

Coupled water-food system analysis of agriculture in California's San Joaquin Valley: vulnerabilities, adaptations and policy trade-offs

by

José Manuel Rodríguez Flores

Doctor of Philosophy in Environmental Systems

University of California Merced, 2023
Josué Medellín Azuara, Graduate Advisor

The San Joaquin Valley has experienced a significant rise in water demand for irrigation, met to a large extent by groundwater resources. Groundwater serves as a dependable water source not only for irrigation but also for sustaining local communities and ecosystems. However, inadequate management of groundwater over the past few decades has led to detrimental outcomes such as aquifer depletion, subsidence, deteriorating water quality, and the failure of domestic wells. In response, the implementation of the Sustainable Groundwater Management Act (SGMA) since 2014 has fostered the development of Groundwater Sustainability Plans (GSPs) aimed at achieving groundwater sustainability goals by 2040. Consequently, it is crucial to develop approaches that allow us to identify vulnerabilities within the food-water system and evaluate potential strategies for addressing groundwater sustainability challenges. This dissertation is driven by five objectives: 1) model the food-water system, including the feed-back between agriculture and groundwater 2) incorporate uncertainty into water management policy assessment and exploration, 3) seek dynamic and adaptive policies that offer flexibility in wet and dry years, 4) assess the trade-offs between groundwater sustainability and economic revenues derived from food production, and 5) identify factors contributing to domestic well failures to inform domestic well protection efforts. These objectives are addressed through three comprehensive studies, corresponding to manuscripts published or currently under review. Chapter 2 employs Global Sensitivity Analysis to examine influential factors in a candidate groundwater pumping restriction, discovering parameters that affect its performance. Chapter 3 advances the incorporation of uncertainty within a multi-objective

optimization framework, enabling the search for dynamic policies adapting to system changes and achieve economic and groundwater sustainability objectives. Finally, in Chapter 4, a spatial analysis is developed to identify specific components within the food-water system that can be targeted through effective land and water management strategies, thus reducing the risk of domestic well failures. This dissertation provides significant insights into the implementation of sustainable groundwater management practices in the San Joaquin Valley, with a particular emphasis on four groundwater basins. However, the findings and results derived from this research have broader applicability across the San Joaquin Valley region, offering valuable implications for groundwater management practices beyond the study area.

Chapter 1

Introduction

1.1 Background

Global groundwater resources are facing unprecedented pressures due to the escalating water demand for food production. Agriculture heavily relies on groundwater as source for irrigation (Dalin et al., 2017; Qin et al., 2019), particularly in semi-arid regions such as California (W.-Y. Wu et al., 2020). Moreover, the combined effects of anthropogenic climate change and unsustainable water management practices have exacerbated global water scarcity, intensifying the strain on groundwater sources (Lall et al., 2020; Scanlon et al., 2021; Taylor et al., 2013). Consequently, this has led to the depletion of groundwater reserves in several of the most important agricultural regions worldwide (de Graaf et al., 2017; Famiglietti, 2014; Huggins et al., 2022). The depletion of groundwater reserves poses a significant threat to safe and reliable water access for various sectors, including agriculture, domestic use (Jasechko and Perrone, 2021), and ecosystems (Bierkens and Wada, 2019). Thus, addressing these challenges is of crucial importance to ensure sustainable water management and safeguard the long-term availability of groundwater.

Groundwater depletion has prompted the need to pursue sustainable use, leading to the development and implementation of policies and economic instruments (Elshall et al., 2020). However, it is important to recognize that the embedded food-water system, with its co-evolving dynamics and interdependencies, possesses distinct characteristics that must be considered when developing policies that can effectively achieve sustainability objectives. Coupled food-water systems,

as other socio-ecological or human-natural systems, exhibit co-evolving dynamics and feedback mechanisms (Konar et al., 2019; J. Liu et al., 2007; Polhill et al., 2016). Moreover, the evolution of these systems is subject to uncertainties arising from exogenous factors (Di Baldassarre et al., 2016; Pérez-Blanco, 2022; Yung et al., 2019), and the implementation of management policies may give rise to trade-offs (Lu et al., 2021; Null et al., 2021; Schreckenberg et al., 2018; Torhan et al., 2022).

To comprehensively investigate the complexities inherent in the food-water system, it is imperative to consider multiple dimensions. Modeling frameworks have been developed to capture the dynamic interplay of the coupled food-water system, such as Hydro-economic models (HEMs). These models have been successfully applied to study the evolving dynamics of food production and its feed-backs, encompassing aspects such as reservoir releases, environmental flows, and groundwater dynamics (Ortiz Partida et al., 2023). Extensive literature exists on the application of HEMs in climate change adaptation and the search for water management policies (Pérez-Blanco et al., 2021; Ward, 2021). However, there remain research gaps in exploring key uncertainties that can be included in the development of modeling as a decision-making support tool, for example through the application of sensitivity analysis (Lo Piano et al., 2022).

Furthermore, it is crucial to address the limitations of static assumptions prevalent in many HEMs, which do not account for the adaptive nature of policies in response to system changes. Modeling frameworks used in water systems have made remarkable advancements in integrating uncertainties and addressing trade-offs within multi-objective optimization frameworks. Implementations can be observed in various domains, such as reservoir operation (Gupta et al., 2020; W. Wu et al., 2022), water pollution control (Leng et al., 2021; Quinn et al., 2017; Rong et al., 2019), ecosystem preservation (Dalcin et al., 2023; Lu et al., 2021), social equity (Deng et al., 2022; Nyahora et al., 2020; Yuan et al., 2022) and groundwater management (Banihabib et al., 2019; Habibi Davijani et al., 2016; Mehrabi et al., 2021). These frameworks can also consider the potential for dynamic adaptiveness in decision-making processes (Giuliani et al., 2016; Reed et al., 2013). Moreover, the evaluation of policies can be augmented by assessing their capacity to achieve stakeholders' objectives under potential states of the system via robustness analysis (Herman et al., 2015; McPhail et al., 2018).

In addition to the utilization of optimization and simulation modeling frameworks (Harou

et al., 2009), water systems have also been extensively studied using statistical models (Müller and Levy, 2019). These methods have demonstrated their efficacy in numerous applications to develop a comprehensive understanding of the food-water system while capturing spatial processes (Di Baldassarre et al., 2019). Notably, they have proven instrumental in capturing complex associations, such as those between land use changes and streamflows (M. C. Levy et al., 2018), groundwater pumping and subsidence, groundwater pumping and water quality (M. C. Levy et al., 2020; Z. F. Levy et al., 2021), and complex socio-hydrological associations that drive shifts in water use and conservation (Breyer et al., 2018; Deines et al., 2019; Worland et al., 2018). Importantly, these modeling frameworks offer flexibility in incorporating inference methods to address data complexities, including spatial and temporal autocorrelation, and assumptions that we have of the system. These methods hold the potential to identify critical relationships among system components, particularly during drought events when feedback loops and associations between components of the system intensify. For instance, during dry periods, agriculture heavily relies on groundwater pumping, leading to exacerbated externalities affecting other sectors, such as domestic well failures (Jasechko and Perrone, 2020).

1.2 Agriculture and groundwater in the San Joaquin Valley

The agricultural sector in the California's San Joaquin Valley occupies the first place in value in the US and is a vital economic sector in the region, leading with Kern, Fresno and Tulare Counties (CDFA, 2022). Its production value is $24 billion in annual gross revenues, mainly from orchards and vines with almost $20 billion, and employs 340 thousand people (17% of the employment in the Valley) (Escriva-Bou et al., 2023). This region hosts approximately 1.8 million (in 2018) hectares of irrigated agriculture, which is 73% of the irrigated land in the Central Valley. The water use in the region accounts to 19.8 km^3 sourced from both surface water (60%) and groundwater (40%). Notably, during dry years, groundwater supplies the majority of water, as observed in 2021 when it accounted for 70% of the total supply (Medellin-Azuara et al., 2022).

One of the main reasons this region has achieved the scale and specialization tree and vine crops is the use of reliable groundwater pumping. The expansion of perennial tree crops, as shown in Figure 1.1, especially of nut trees, has become economically significant but poses higher

financial risk and inflexible water demands due to higher establishment costs compared to other crops (Mall and Herman, 2019). However, groundwater pumping has been used to mitigate surface water shortages, that in addition to uncoordinated management has resulted in significant declines in groundwater levels (P.-W. Liu et al., 2022; Qin et al., 2019).

Transitioning to a sustainable groundwater use in the San Joaquin Valley has challenges that need comprehensive understanding of the food-water system. This dissertation highlights three key trends that pose challenges to the development of sustainable groundwater policies in the region. First, the current proportion of perennial crops, has heightened vulnerability to surface water shortages and resulted in a surge of well drilling and groundwater pumping. Second, despite intermittent wet periods following droughts, intensive pumping practices have not allowed groundwater recovery. Finally, communities that rely heavily on groundwater are disproportionately affected by basin-wide declines in groundwater levels and the pumping activities of neighboring agricultural operations.

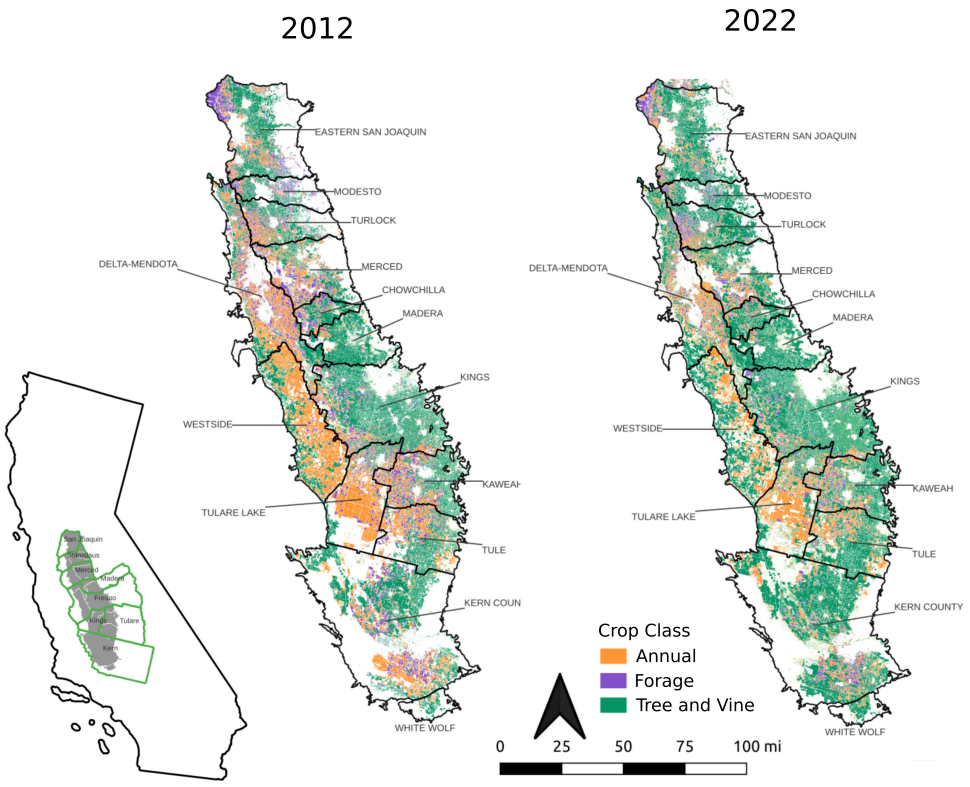

Figure 1.1: Land use in California's San Joaquin Valley in 2012 and 2022. Maps show the boundaries of the groundwater subbasins. Source: Chen et al. (2023)

In the past decade, the San Joaquin Valley has faced two prolonged drought periods: from 2012 to 2016 and from 2020 to 2022. These droughts have revealed the vulnerability of the region's food-water system, resulting in various consequences. These include significant economic costs to agriculture and related sectors (Medellin-Azuara et al., 2022; Medellín-Azuara et al., 2016), the emergence of dry domestic wells in disadvantaged communities (Méndez-Barrientos et al., 2022), and disparities in water curtailments leading to lower environmental flows (Stewart et al., 2020). Additionally, the distinctive climate of the region renders it highly susceptible to water shortages, which are expected to worsen due to climate change, including increased temperatures, heightened evapotranspiration rates, and diminished snowpack (Fernandez-Bou et al., 2021; Pathak et al., 2018).

Extensive deliberation has taken place regarding the implementation of demand and supply management strategies to achieve the sustainability objectives outlined by the state in the Sustainable Groundwater Management Act (SGMA). Demand-side management approaches include groundwater pumping restrictions and land fallowing (Escriva-Bou et al., 2023; Hanak et al., 2019); however, these policies entail significant economic costs. Additionally, numerous opportunities exist to develop adaptive policies that balance between sustainability goals and reduced economic impacts through coordinated water management between dry and wet years. State-level initiatives are also incorporating frameworks that incentivize strategic allocation of land and water resources to fulfill SGMA objectives while also addressing broader social and ecosystem benefits. Examples of such initiatives include cropland re-purposing (Fernandez-Bou et al., 2023) and groundwater recharge (Wendt et al., 2021). This dissertation offers a thorough and comprehensive analysis of these challenges and opportunities, providing an in-depth exploration of their complexities and potential implications.

1.3 Dissertation Overview

The general objective of this dissertation is to develop systemic understanding of San Joaquin Valley's food-water system using two modeling approaches, hydro-economic models and spatial statistical modeling, used to develop informed policy suggestions.

In Chapter 2, a global sensitivity analysis is conducted on a coupled hydro-economic model to identify vulnerabilities within the system that may significantly impact the effectiveness of groundwater management policies. This analysis characterizes the uncertainties inherent in the food-water system and examines the key influential factors that affect the performance of a potential groundwater pumping restriction.

In Chapter 3, the investigation into uncertainty is extended by integrating it into a simulation-optimization approach aimed at formulating adaptive and dynamic irrigation management policies. A bi-level optimization framework is developed, enabling the incorporation of feedback mechanisms between groundwater pumping and groundwater depth. Additionally, the framework uses Evolutionary Multi-Objective Direct Policy Search to effectively account for both economic objectives related to food production and sustainability objectives associated with groundwater man-

agement. Optimal policies are identified, and their performance is evaluated through robustness analysis. This chapter significantly contributes to enhancing our understanding of irrigation management strategies in the face of uncertainty, fostering the development of more adaptive groundwater management practices.

In Chapter 4 a statistical spatial analysis is performed to identify key factors in the food-water system that increase the risk of domestic wells to go dry during droughts. In this chapter multiple data sets are integrated such as reported dry wells, well completion records, groundwater levels, and land use information. Additionally, the used spatial model employs a Bayesian approach, to account for spatial autocorrelation among the observations. The model is able to predict the probability of domestic well failure within the Tule, Kaweah, Kings and Madera subbasins. Results provide valuable insights into the most significant factors within the system, which can guide the prioritization and development of effective groundwater management strategies.

Finally, in Chapter 5 insights and remarks on the research conducted in the main three chapters are included. The chapter also discusses the limitations and potential areas for further investigation, suggesting avenues for future exploration.

1.4 References

Banihabib, M. E., Mohammad Rezapour Tabari, M., & Mohammad Rezapour Tabari, M. (2019). Development of a Fuzzy Multi-Objective Heuristic Model for Optimum Water Allocation. *Water Resources Management*, *33*(11), 3673–3689. https://doi.org/10.1007/s11269-019-02323-7

Bierkens, M. F. P., & Wada, Y. (2019). Non-renewable groundwater use and groundwater depletion: A review. *Environmental Research Letters*, *14*(6), 063002. https://doi.org/10.1088/1748-9326/ab1a5f

Breyer, B., Zipper, S. C., & Qiu, J. (2018). Sociohydrological Impacts of Water Conservation Under Anthropogenic Drought in Austin, TX (USA). *Water Resources Research*, *54*(4), 3062–3080. https://doi.org/10.1002/2017WR021155

CDFA. (2022). *California agricultural statistics review 2021-2022* (tech. rep.). California Department of Food and Agriculture (CDFA). https://www.cdfa.ca.gov/Statistics/PDFs/2022_Ag_Stats_Review.pdf

Chen, B., Gramig, B., & Mieno, T. (2023). CropScapeR: Access Cropland Data Layer Data via the 'CropScape' Web Service. https://cran.r-project.org/web/packages/CropScapeR/index.html

Dalcin, A. P., Brêda, J. P. L. F., Marques, G. F., Tilmant, A., de Paiva, R. C. D., & Kubota, P. Y. (2023). The Role of Reservoir Reoperation to Mitigate Climate Change Impacts on Hydropower and Environmental Water Demands. *Journal of Water Resources Planning and Management*, *149*(4), 04023005. https://doi.org/10.1061/JWRMD5.WRENG-5810

Dalin, C., Wada, Y., Kastner, T., & Puma, M. J. (2017). Groundwater depletion embedded in international food trade. *Nature*, *543*(7647), 700–704. https://doi.org/10.1038/nature21403

de Graaf, I. E. M., van Beek, R. L. P. H., Gleeson, T., Moosdorf, N., Schmitz, O., Sutanudjaja, E. H., & Bierkens, M. F. P. (2017). A global-scale two-layer transient groundwater model: Development and application to groundwater depletion. *Advances in Water Resources*, *102*, 53–67. https://doi.org/10.1016/j.advwatres.2017.01.011

Deines, J. M., Kendall, A. D., Butler, J. J., & Hyndman, D. W. (2019). Quantifying irrigation adaptation strategies in response to stakeholder-driven groundwater management in the US High Plains Aquifer. *Environmental Research Letters*, *14*(4), 044014. https://doi.org/10.1088/1748-9326/aafe39

Deng, L., Guo, S., Yin, J., Zeng, Y., & Chen, K. (2022). Multi-objective optimization of water resources allocation in Han River basin (China) integrating efficiency, equity and sustainability. *Scientific Reports*, *12*(1), 798. https://doi.org/10.1038/s41598-021-04734-2

Di Baldassarre, G., Brandimarte, L., & Beven, K. (2016). The seventh facet of uncertainty: Wrong assumptions, unknowns and surprises in the dynamics of human–water systems. *Hydrological Sciences Journal*, *61*(9), 1748–1758. https://doi.org/10.1080/02626667.2015.1091460

Di Baldassarre, G., Sivapalan, M., Rusca, M., Cudennec, C., Garcia, M., Kreibich, H., Konar, M., Mondino, E., Mård, J., Pande, S., Sanderson, M. R., Tian, F., Viglione, A., Wei, J., Wei, Y., Yu, D. J., Srinivasan, V., & Blöschl, G. (2019). Sociohydrology: Scientific Challenges in

Addressing the Sustainable Development Goals. *Water Resources Research*, *55*(8), 6327–6355. https://doi.org/10.1029/2018WR023901

Elshall, A. S., Arik, A. D., El-Kadi, A. I., Pierce, S., Ye, M., Burnett, K. M., Wada, C. A., Bremer, L. L., & Chun, G. (2020). Groundwater sustainability: A review of the interactions between science and policy. *Environmental Research Letters*, *15*(9), 093004. https://doi.org/10.1088/1748-9326/ab8e8c

Escriva-Bou, A., Hanak, E., Cole, S., & Medellín-Azuara, J. (2023). *Policy Brief: The Future of Agriculture in the San Joaquin Valley* (tech. rep.). Public Policy Institute of California.

Famiglietti, J. S. (2014). The global groundwater crisis. *Nature Climate Change*, *4*(11), 945–948. https://doi.org/10.1038/nclimate2425

Fernandez-Bou, A. S., Ortiz-Partida, J. P., Pells, C., Classen-Rodriguez, L. M., Espinoza, V., Rodríguez-Flores, J. M., & Medellin-Azuara, J. (2021). *Regional Report for the San Joaquin Valley Region on Impacts of Climate Change* (California's Fourth Climate Assesment SUM-CCCA4-2021-003). California Natural Resources Agency. Sacramento. https://www.energy.ca.gov/sites/default/files/2022-01/CA4_CCA_SJ_Region_Eng_ada.pdf

Fernandez-Bou, A. S., Rodríguez-Flores, J. M., Guzman, A., Ortiz-Partida, J. P., Classen-Rodriguez, L. M., Sánchez-Pérez, P. A., Valero-Fandiño, J., Pells, C., Flores-Landeros, H., Sandoval-Solís, S., Characklis, G. W., Harmon, T. C., McCullough, M., & Medellín-Azuara, J. (2023). Water, environment, and socioeconomic justice in California: A multi-benefit cropland repurposing framework. *Science of The Total Environment*, *858*, 159963. https://doi.org/10.1016/j.scitotenv.2022.159963

Giuliani, M., Li, Y., Castelletti, A., & Gandolfi, C. (2016). A coupled human-natural systems analysis of irrigated agriculture under changing climate. *Water Resources Research*, *52*(9), 6928–6947. https://doi.org/10.1002/2016WR019363

Gupta, R. S., Hamilton, A. L., Reed, P. M., & Characklis, G. W. (2020). Can modern multi-objective evolutionary algorithms discover high-dimensional financial risk portfolio tradeoffs for snow-dominated water-energy systems? *Advances in Water Resources*, *145*, 103718. https://doi.org/10.1016/j.advwatres.2020.103718

Habibi Davijani, M., Banihabib, M. E., Nadjafzadeh Anvar, A., & Hashemi, S. R. (2016). Optimization model for the allocation of water resources based on the maximization of em-

ployment in the agriculture and industry sectors. *Journal of Hydrology*, *533*, 430–438. https://doi.org/10.1016/j.jhydrol.2015.12.025

Hanak, E., Escriva-Bou, A., Gray, B., Green, S., Harter, T., Jezdimirovic, J., Lund, J., Medellín-Azuara, J., Moyle, P., & Seavy, N. (2019). *Water and the Future of the San Joaquin Valley* (tech. rep.). https://doi.org/10.13140/RG.2.2.24360.83208

Harou, J. J., Pulido-Velazquez, M., Rosenberg, D. E., Medellín-Azuara, J., Lund, J. R., & Howitt, R. E. (2009). Hydro-economic models: Concepts, design, applications, and future prospects. *Journal of Hydrology*, *375*(3-4), 627–643. https://doi.org/10.1016/j.jhydrol.2009.06.037

Herman, J. D., Reed, P. M., Zeff, H. B., & Characklis, G. W. (2015). How Should Robustness Be Defined for Water Systems Planning under Change? *Journal of Water Resources Planning and Management*, *141*(10), 04015012. https://doi.org/10.1061/(ASCE)WR.1943-5452.0000509

Huggins, X., Gleeson, T., Kummu, M., Zipper, S. C., Wada, Y., Troy, T. J., & Famiglietti, J. S. (2022). Hotspots for social and ecological impacts from freshwater stress and storage loss. *Nature Communications*, *13*(1), 439. https://doi.org/10.1038/s41467-022-28029-w

Jasechko, S., & Perrone, D. (2020). California's Central Valley Groundwater Wells Run Dry During Recent Drought. *Earth's Future*, *8*(4). https://doi.org/10.1029/2019EF001339

Jasechko, S., & Perrone, D. (2021). Global groundwater wells at risk of running dry. *Science*, *372*(6540), 418–421. https://doi.org/10.1126/science.abc2755

Konar, M., Garcia, M., Sanderson, M. R., Yu, D. J., & Sivapalan, M. (2019). Expanding the Scope and Foundation of Sociohydrology as the Science of Coupled Human-Water Systems. *Water Resources Research*, *55*(2), 874–887. https://doi.org/10.1029/2018WR024088

Lall, U., Josset, L., & Russo, T. (2020). A Snapshot of the World's Groundwater Challenges. *Annual Review of Environment and Resources*, *45*(1), 171–194. https://doi.org/10.1146/annurev-environ-102017-025800

Leng, L., Jia, H., Chen, A. S., Zhu, D. Z., Xu, T., & Yu, S. (2021). Multi-objective optimization for green-grey infrastructures in response to external uncertainties. *Science of The Total Environment*, *775*, 145831. https://doi.org/10.1016/j.scitotenv.2021.145831

Levy, M. C., Lopes, A. V., Cohn, A., Larsen, L. G., & Thompson, S. E. (2018). Land Use Change Increases Streamflow Across the Arc of Deforestation in Brazil. *Geophysical Research Letters*, *45*(8), 3520–3530. https://doi.org/10.1002/2017GL076526

Levy, M. C., Neely, W. R., Borsa, A. A., & Burney, J. A. (2020). Fine-scale spatiotemporal variation in subsidence across California's San Joaquin Valley explained by groundwater demand. *Environmental Research Letters*, *15*(10), 104083. https://doi.org/10.1088/1748-9326/abb55c

Levy, Z. F., Jurgens, B. C., Burow, K. R., Voss, S. A., Faulkner, K. E., Arroyo-Lopez, J. A., & Fram, M. S. (2021). Critical Aquifer Overdraft Accelerates Degradation of Groundwater Quality in California's Central Valley During Drought. *Geophysical Research Letters*, *48*(17), e2021GL094398. https://doi.org/10.1029/2021GL094398

Liu, J., Dietz, T., Carpenter, S. R., Folke, C., Alberti, M., Redman, C. L., Schneider, S. H., Ostrom, E., Pell, A. N., Lubchenco, J., Taylor, W. W., Ouyang, Z., Deadman, P., Kratz, T., & Provencher, W. (2007). Coupled Human and Natural Systems. *AMBIO: A Journal of the Human Environment*, *36*(8), 639–649. https://doi.org/10.1579/0044-7447(2007)36[639:CHANS]2.0.CO;2

Liu, P.-W., Famiglietti, J. S., Purdy, A. J., Adams, K. H., McEvoy, A. L., Reager, J. T., Bindlish, R., Wiese, D. N., David, C. H., & Rodell, M. (2022). Groundwater depletion in California's Central Valley accelerates during megadrought. *Nature Communications*, *13*(1), 7825. https://doi.org/10.1038/s41467-022-35582-x

Lo Piano, S., Sheikholeslami, R., Puy, A., & Saltelli, A. (2022). Unpacking the modelling process via sensitivity auditing. *Futures*, *144*, 103041. https://doi.org/10.1016/j.futures.2022.103041

Lu, N., Liu, L., Yu, D., & Fu, B. (2021). Navigating trade-offs in the social-ecological systems. *Current Opinion in Environmental Sustainability*, *48*, 77–84. https://doi.org/10.1016/j.cosust.2020.10.014

Mall, N. K., & Herman, J. D. (2019). Water shortage risks from perennial crop expansion in California's Central Valley. *Environmental Research Letters*, *14*(10), 104014. https://doi.org/10.1088/1748-9326/ab4035

McPhail, C., Maier, H. R., Kwakkel, J. H., Giuliani, M., Castelletti, A., & Westra, S. (2018). Robustness Metrics: How Are They Calculated, When Should They Be Used and Why Do They Give Different Results? *Earth's Future*, *6*(2), 169–191. https://doi.org/10.1002/2017EF000649

Medellin-Azuara, J., Rodriguez-Flores, J. M., Cole, S., Escriva-Bou, A., Abatzoglou, J., Viers, J. H., & Santos, N. (2022). FIX ME!!!!On Assessing Drought Economic Impacts on Agriculture and Communities: Lessons Learned from California DroughtsFIX ME!!!! (Presenting Autor). https://scholar.google.com/citations?view_op=view_citation&hl=en&user=MJpJiPsAAAAJ&authuser=1&citation_for_view=MJpJiPsAAAAJ:ULOm3_A8WrAC

Medellín-Azuara, J., MacEwan, D., Howitt, R. E., & Sumner, D. A. (2016). *Economic Analysis of the 2016 California Drought on Agriculture* (tech. rep.). Center for Watershed Sciences. UC Davis, Davis, CA.

Mehrabi, A., Heidarpour, M., Safavi, H. R., & Rezaei, F. (2021). Assessment of the optimized scenarios for economic-environmental conjunctive water use utilizing gravitational search algorithm. *Agricultural Water Management*, *246*, 106688. https://doi.org/10.1016/j.agwat.2020.106688

Méndez-Barrientos, L. E., Fencl, A. L., Workman, C. L., & Shah, S. H. (2022). Race, citizenship, and belonging in the pursuit of water and climate justice in California. *Environment and Planning E: Nature and Space*, 25148486221133282. https://doi.org/10.1177/25148486221133282

Müller, M. F., & Levy, M. C. (2019). Complementary Vantage Points: Integrating Hydrology and Economics for Sociohydrologic Knowledge Generation. *Water Resources Research*, *55*(4), 2549–2571. https://doi.org/10.1029/2019WR024786

Null, S. E., Olivares, M. A., Cordera, F., & Lund, J. R. (2021). Pareto Optimality and Compromise for Environmental Water Management. *Water Resources Research*, *57*(10), e2020WR028296. https://doi.org/10.1029/2020WR028296

Nyahora, P. P., Babel, M. S., Ferras, D., & Emen, A. (2020). Multi-objective optimization for improving equity and reliability in intermittent water supply systems. *Water Supply*, *20*(5), 1592–1603. https://doi.org/10.2166/ws.2020.066

Ortiz Partida, J. P., Fernandez-Bou, A. S., Maskey, M., Rodriguez-Flores, J. M., Medellin-Azuara, J., Sandoval-Solis, S., Ermolieva, T., Wada, Y., & Kahil, T. (2023). Hydro-economic modeling of water resources management challenges: Current applications and future directions. *In-Preparation*.

Pathak, T., Maskey, M., Dahlberg, J., Kearns, F., Bali, K., & Zaccaria, D. (2018). Climate Change Trends and Impacts on California Agriculture: A Detailed Review. *Agronomy*, *8*(3), 25. https://doi.org/10.3390/agronomy8030025

Pérez-Blanco, C. D. (2022). Navigating Deep Uncertainty in Complex Human–Water Systems. In C. Kondrup, P. Mercogliano, F. Bosello, J. Mysiak, E. Scoccimarro, A. Rizzo, R. Ebrey, M. d. Ruiter, A. Jeuken, & P. Watkiss (Eds.), *Climate Adaptation Modelling* (pp. 169–178). Springer International Publishing. https://doi.org/10.1007/978-3-030-86211-4_20

Pérez-Blanco, C. D., González-López, H., & Hrast-Essenfelder, A. (2021). Beyond piecewise methods: Modular integrated hydroeconomic modeling to assess the impacts of adaptation policies in irrigated agriculture. *Environmental Modelling & Software*, *136*, 104943. https://doi.org/10.1016/j.envsoft.2020.104943

Polhill, J. G., Filatova, T., Schlüter, M., & Voinov, A. (2016). Modelling systemic change in coupled socio-environmental systems. *Environmental Modelling & Software*, *75*, 318–332. https://doi.org/10.1016/j.envsoft.2015.10.017

Qin, Y., Mueller, N. D., Siebert, S., Jackson, R. B., AghaKouchak, A., Zimmerman, J. B., Tong, D., Hong, C., & Davis, S. J. (2019). Flexibility and intensity of global water use. *Nature Sustainability*, *2*(6), 515–523. https://doi.org/10.1038/s41893-019-0294-2

Quinn, J. D., Reed, P. M., & Keller, K. (2017). Direct policy search for robust multi-objective management of deeply uncertain socio-ecological tipping points. *Environmental Modelling & Software*, *92*, 125–141. https://doi.org/10.1016/j.envsoft.2017.02.017

Reed, P. M., Hadka, D., Herman, J. D., Kasprzyk, J. R., & Kollat, J. B. (2013). Evolutionary multiobjective optimization in water resources: The past, present, and future. *Advances in Water Resources*, *51*, 438–456. https://doi.org/10.1016/j.advwatres.2012.01.005

Rong, Q., Cai, Y., Su, M., Yue, W., Yang, Z., & Dang, Z. (2019). A simulation-based bi-level multi-objective programming model for watershed water quality management under interval and

stochastic uncertainties. *Journal of Environmental Management*, *245*, 418–431. https://doi.org/10.1016/j.jenvman.2019.05.125

Scanlon, B. R., Rateb, A., Pool, D. R., Sanford, W., Save, H., Sun, A., Long, D., & Fuchs, B. (2021). Effects of climate and irrigation on GRACE-based estimates of water storage changes in major US aquifers. *Environmental Research Letters*, *16*(9), 094009. https://doi.org/10.1088/1748-9326/ac16ff

Schreckenberg, K., Mace, G. M., & Poudyal, M. (Eds.). (2018). *Ecosystem services and poverty alleviation: Trade-offs and governance*. Routledge, Taylor & Francis Group.

Stewart, I. T., Rogers, J., & Graham, A. (2020). Water security under severe drought and climate change: Disparate impacts of the recent severe drought on environmental flows and water supplies in Central California. *Journal of Hydrology X*, *7*, 100054. https://doi.org/10.1016/j.hydroa.2020.100054

Taylor, R. G., Scanlon, B., Döll, P., Rodell, M., van Beek, R., Wada, Y., Longuevergne, L., Leblanc, M., Famiglietti, J. S., Edmunds, M., Konikow, L., Green, T. R., Chen, J., Taniguchi, M., Bierkens, M. F. P., MacDonald, A., Fan, Y., Maxwell, R. M., Yechieli, Y., … Treidel, H. (2013). Ground water and climate change. *Nature Climate Change*, *3*(4), 322–329. https://doi.org/10.1038/nclimate1744

Torhan, S., Grady, C. A., Ajibade, I., Galappaththi, E. K., Hernandez, R. R., Musah-Surugu, J. I., Nunbogu, A. M., Segnon, A. C., Shang, Y., Ulibarri, N., Campbell, D., Joe, E. T., Penuelas, J., Sardans, J., Shah, M. a. R., & Team, t. G. A. M. (2022). Tradeoffs and Synergies Across Global Climate Change Adaptations in the Food-Energy-Water Nexus. *Earth's Future*, *10*(4), e2021EF002201. https://doi.org/10.1029/2021EF002201

Ward, F. A. (2021). Hydroeconomic Analysis to Guide Climate Adaptation Plans. *Frontiers in Water*, *3*. https://www.frontiersin.org/article/10.3389/frwa.2021.681475

Wendt, D. E., Loon, A. F. V., Scanlon, B. R., & Hannah, D. M. (2021). Managed aquifer recharge as a drought mitigation strategy in heavily-stressed aquifers. *Environmental Research Letters*, *16*(1), 014046. https://doi.org/10.1088/1748-9326/abcfe1

Worland, S. C., Steinschneider, S., & Hornberger, G. M. (2018). Drivers of Variability in Public-Supply Water Use Across the Contiguous United States. *Water Resources Research*, *54*(3), 1868–1889. https://doi.org/10.1002/2017WR021268

Wu, W., Zhou, Y., & Leonard, M. (2022). Evolutionary algorithm-based multiobjective reservoir operation policy optimisation under uncertainty. *Environmental Research Communications*, *4*(12), 121001. https://doi.org/10.1088/2515-7620/aca1fc

Wu, W.-Y., Lo, M.-H., Wada, Y., Famiglietti, J. S., Reager, J. T., Yeh, P. J.-F., Ducharne, A., & Yang, Z.-L. (2020). Divergent effects of climate change on future groundwater availability in key mid-latitude aquifers. *Nature Communications*, *11*(1), 3710. https://doi.org/10.1038/s41467-020-17581-y

Yuan, M., Chen, X., Liu, G., & Ren, H. (2022). Coordinated allocation of water resources and wastewater emission permits based on multi-objective optimization model: From the perspective of conflict between equity and economic benefits. *Journal of Cleaner Production*, *372*, 133733. https://doi.org/10.1016/j.jclepro.2022.133733

Yung, L., Louder, E., Gallagher, L. A., Jones, K., & Wyborn, C. (2019). How Methods for Navigating Uncertainty Connect Science and Policy at the Water-Energy-Food Nexus. *Frontiers in Environmental Science*, *7*. https://www.frontiersin.org/article/10.3389/fenvs.2019.00037

Chapter 2

Global Sensitivity Analysis of a Coupled Hydro-Economic Model and Groundwater Restriction Assessment

This chapter is published in the Water Resources Management journal:
Rodríguez-Flores, J. M., Valero Fandiño, J. A., Cole, S. A., Malek, K., Karimi, T., Zeff, H. B., Reed, P.M., Escriva-Bou, A., and Medellín-Azuara, J. (2022). Global Sensitivity Analysis of a Coupled Hydro-Economic Model and Groundwater Restriction Assessment. Water Resources Management, 36(15), 6115-6130. https://doi.org/10.1007/s11269-022-03344-5

2.1 Abstract

Assessing impacts on coupled food-water systems that may emerge from water policies, changes in economic drivers and crop productivity requires an understanding of dominant uncertainties. This paper assesses how a candidate groundwater pumping restriction and crop prices, crop yields, surface water price, electricity price, and parametric uncertainties shape economic and groundwater performance metrics from a coupled hydro-economic model (HEM) through a diagnostic global sensitivity analysis (GSA). The HEM used in this study integrates a groundwater

depth response, modeled by an Artificial Neural Network (ANN), into a calibrated Positive Mathematical Programming (PMP) agricultural production model. Results show that in addition to a groundwater pumping restriction, performance metrics are highly sensitive to prices and yields of perennial tree crops. These sensitivities become salient during dry years when there is a higher reliance on groundwater. Furthermore, results indicate that performing a GSA for two different water baseline conditions used to calibrate the production model, dry and wet, result in different sensitivity indices magnitudes and factor prioritization. Diagnostic GSA results are used to understand key factors that affect the performance of a groundwater pumping restriction policy. This research is applied to the Wheeler Ridge-Maricopa Water Storage District located in Kern County, California, region reliant on groundwater and vulnerable to surface water shortages.

2.2 Introduction

Worldwide groundwater demand for irrigation is increasing due to diminishing and variable surface water supplies that stress aquifer systems (Richey et al., 2015). For this reason it is important to assess how food production, aquifers and their feedback respond to water policies and economic and crop production changes. Models used to understand these relationships have intrinsic uncertainties in their input and calibration parameters. In order to develop better informed modeling support tools is important to assess how changes in the results are attributed to these uncertainties.

Modeling efforts have explored the dynamics and feedbacks of food-water systems using hydro-economic modeling approaches (Harou et al., 2009), factoring the particular characteristics of water and agricultural production systems. Various studies have used modular and response functions coupling taxonomies to represent the coevolution of agricultural production systems with surface water systems (Forni et al., 2016; Giuliani et al., 2016; Maneta et al., 2020) and groundwater systems (Afshar et al., 2020; Graveline, 2019; MacEwan et al., 2017), to assess impacts of exogenous changes and water policies.

As HEMs grow in their complexity, improved diagnostic tools to better map how inputs and calibration uncertainties shape the outputs become increasingly important. Sensitivity Analysis (SA) is a formalized methodology to study how the uncertainty in the output of a model is attributed

to uncertainties in the model inputs (Saltelli, 2002). Two general SA methods are used depending on the taxonomy of the model: local and global sensitivity analysis. Global sensitivity analysis is used for non-additive models where there are nonlinear interactions among inputs. The objective of this analysis is to quantify the variability of model outputs that result from direct and higher order effects (interactive effects) of uncertain inputs. Additionally, GSA considers the variation of all the uncertain inputs at the same time, whereas local SA is performed by varying one input at a time.

SA is widely employed in environmental and hydrologic modeling (Pianosi, 2016; Song et al., 2015), to explore inputs prioritization (Budamala and Baburao Mahindrakar, 2020; Hashemi and Mahjouri, 2022; Karimi et al., 2022), climate change uncertainties(Fayaz et al., 2020), and calibration performance (El Harraki et al., 2021). Despite the large use of HEMs in food-water systems, diagnostic sensitivity analysis is seldom performed and is often limited to exploring impacts on the outputs from a single input through scenario analysis without exploring all the uncertain space of inputs with some exceptions (D'Agostino et al., 2014; Ghadimi and Ketabchi, 2019; Singh, 2022). Furthermore, sensitivity analysis has also been applied to calibrated agricultural production models, where the diagnostic results were used to identify how changes in economic variables (Arribas et al., 2017; Shirzadi Laskookalayeh et al., 2022) and calibration parameters (Graveline and Merel, 2014) shape revenues and inputs allocation forecasts.

In this work, we contribute a coupled HEM and a GSA diagnostic framework for an improved understanding of the most consequential factors that shape the evolution of the food-water system in California's San Joaquin Valley (SJV), and provide insight for assessing a groundwater pumping restriction policy. The HEM used in this study uses a PMP model to emulate agricultural production, coupled with a groundwater response function (GRF), which was embedded in the PMP model through an ANN. Our diagnostic GSA explores uncertainties in economic, crop production, groundwater restriction and calibration factors. Additionally, we perform the diagnostic for two baseline conditions, to show how the selection of the baseline changes the results of the GSA and groundwater restriction impacts. This framework is applied for the Wheeler Ridge-Maricopa Water Storage District, a water district representative of the SJV.

This paper is organized as follows. In Section 2, we describe the study area and the agricultural and water characteristics of the water storage district. In Section 3, we lay out the

coupled hydro-economic modeling framework used in this paper, including a description of the calibration process and the GSA experiment. Results are summarized in Section 4, where we analyze the diagnostic insights from the GSA to clarify key factors shaping the performance metrics of the model. Finally, conclusions and areas for future research are described in Section 5.

2.3 Study area description

The Wheeler Ridge-Maricopa Water Storage District (Figure 2.1) is the third-largest district in crop acreage in Kern County, one of the most productive counties in the United States (USDA, 2019). Perennial crops are the commodities mainly produced in the district, including vines, subtropical fruit trees and nut trees. Perennials cropland has increased overtime as shown in Figure A2 of Appendix A. In the SJV, highly variable surface water supplies have significant impacts on aquifers as groundwater pumping for irrigation serves as an important backstop source of water during dry periods (Lund et al., 2018), affecting groundwater storage (Xiao et al., 2017; Yin et al., 2021) and groundwater depths (Vasco et al., 2019). With climate change, stress on groundwater is expected to exacerbate as changes in precipitation, temperature and snow-pack have impacts on surface water supply (Fernandez-Bou et al., 2021). Water stakeholders located on overdrafted groundwater basins are facing regulatory pressure to achieve groundwater sustainability following the objectives of the Sustainable Groundwater Management Act (SGMA) (DWR, 2021). Recent studies highlight the implementation of groundwater and land use controls on agriculture to achieve sustainability (Hanak et al., 2019), such as pumping restrictions (MacEwan et al., 2017; Miro and Famiglietti, 2019), pumping fees (Stone et al., 2022) and land fallowing (Bryant et al., 2020; Li et al., 2018; Van Schmidt et al., 2022). In this study, we assess a candidate groundwater pumping restriction while considering other uncertainties.

2.4 Methodological framework

The coupled HEM approach used in this paper integrates a groundwater depth response function, modeled using an ANN, in a calibrated agricultural production model. Both models were calibrated separately and coupled as explained in the following subsections.

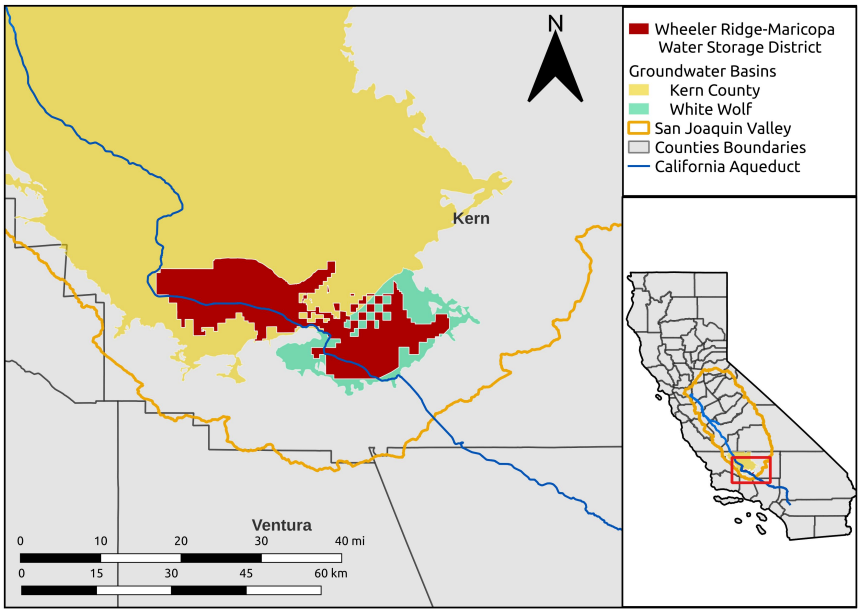

Figure 2.1: Wheeler Ridge-Maricopa Water Storage District located in the San Joaquin Valley, California. The district spans two groundwater basins: Kern County and White Wolf.

2.4.1 Agricultural production model

We modeled the agricultural production system following PMP (Howitt et al., 2012) using two baselines: the average of 2010-2012 (wet period) and the average of 2013-2015 (dry period). The average of these years was taken from observed data used in the calibration process. By using a time window average, we capture the average farmers behaviour during each water condition. The calibration process can be found in the Appendix A.

The calibrated model (Equations 2.1 to 2.6) maximizes the economic revenue at the water district level by optimizing the input allocation ($x_{i,j}$) of j={water, land, labor, other supplies} for production of crop i={almonds and pistachios, alfalfa, cotton, cucurbits, other deciduous, other truck, grain, other field, fresh tomatoes, processing tomatoes, onions and garlic, sugar beets, dry beans, pasture, subtropical, vine, potatoes, safflower, corn} and use of water (wat_w) by source w = {surface water, groundwater}. The second term in the objective function (Equation 2.1) is the crop specific exponential cost function, where the calibration parameters γ_i and δ_i are parameterized using dual values ($\bar{\lambda}_{land,i}$) obtained from solving the linear model in the Appendix A (Equations

A.1-A.4). δ_i equals $(\omega_{i,land} + \bar{\lambda}_{land,i})/(\gamma_i \exp(\gamma \bar{x}_{land,i}))$ where γ_i equals $1/\theta_i \bar{x}_i$, $\bar{x}_{land,i}$ is the baseline land use and θ_i is the own-price supply elasticity.

$$Max_{x_{i,j},wat_w} \prod = \sum_i (p_i yld_i y_i) - \sum_i (\delta_i \exp(\gamma_i x_{i,land})) - \sum_i \sum_{j \neq land,water} (\omega_{i,j} x_{i,j}) - \sum_w (\hat{\omega}_w wat_w) \tag{2.1}$$

Where p_i is the price by crop ($\$/ton$), and yld_i is the crop yield change coefficient. In the third term there is a linear cost of the use of inputs j, where $\omega_{i,j}$ is the marginal cost of each input per acre. Lastly $\widehat{\omega}_w$ is the cost per acre foot of water used from every source. The pumping cost ($\widehat{\omega}_{GW}$) is a function of depth and electricity price described in the Appendix A. y_i is the total production (tons) by crop given by a Constant Elasticity of Substitution (CES) production function with constant returns to scale (Debertin, 2012), defined as:

$$y_i = \tau_i [\sum_j \beta_{i,j} x_{i,j}^{\rho_i}]^{1/\rho_i} \tag{2.2}$$

Where τ_i is a scale parameter given by $\bar{y}_i \bar{x}_i / [\sum_j \beta_{i,j} x_{i,j}^{\rho_i}]^{1/\rho_i}$, where $\bar{y}_i$ is the baseline crop yield. The parameter $\beta_{i,j}$ represents the relative use of each input. The parameter ρ is equal to (σ-1)/σ where σ, elasticity of substitution, is 0.17 for all crops.

The optimization model has a set of resource constraints: land availability (Equation 2.3), surface water availability (Equation 2.5), and groundwater pumping restriction (Equation 2.6). Where b_{land} is the available land, b_{SW} is the available surface water and b_{GW} is the groundwater pumping capacity. GWR represents the groundwater pumping restriction policy.

$$\sum_i x_{i,land} \leq b_{land} \tag{2.3}$$

$$\sum_i x_{i,water} \leq \sum_w wat_w \tag{2.4}$$

$$wat_{SW} \leq b_{SW} \tag{2.5}$$

$$wat_{GW} \leq (1 - GWR)b_{GW} \tag{2.6}$$

2.4.2 Groundwater depth change response

In order to estimate the groundwater depth (GWD) change response from agricultural pumping, an ANN was calibrated. The groundwater depth change ($\Delta d_{g,t}$) at each year (t) of simulation is modeled at a water district level. The ANN was calibrated using data from twenty-four water districts within the Kern county region listed in Table A.1, and using a categorical variable to forecast district-specific changes (g). The ANN has nine input variables, one output variable, and two hidden layers, each with nine neurons, as shown in Figure 2.2. The variables used from the year of the simulation t and the previous year t-1 are: San Joaquin Valley Water Year Hydrologic Classification Index (WYI), total volume of surface water used for irrigation (VSW), total volume of groundwater used for irrigation at the end of the irrigation season (VGW), and volume of intentional groundwater recharge (VIR). Data sources for the calibration process are explained in Section 3.4. Details about the ANN calibration and validation results for Wheeler Ridge-Maricopa can be found in the Appendix A.

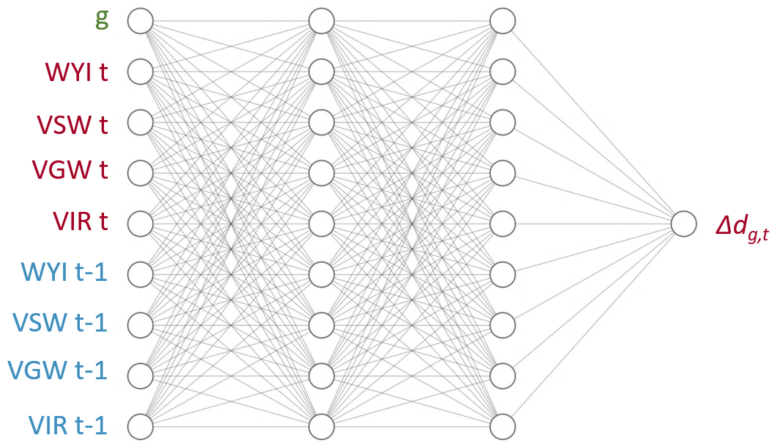

Figure 2.2: Artificial Neural Network (ANN) graphic representation which estimates the change in the average groundwater depth ($\Delta d_{g,t}$) by water district

2.4.3 Global sensitivity analysis

The economic production model and groundwater depth response neural network were calibrated and coupled in a single model in Python. The selected model input variables analyzed in the GSA are: crop prices, crop yield change coefficients, surface water price, price of electricity and crops own-price supply elasticities. Additionally, a potential groundwater restriction was included. Three outputs were analyzed in the diagnostic: groundwater depth change, total land use and total net revenue. Figure 2.3 shows the flow of inputs for the calibration of the model and simulation.

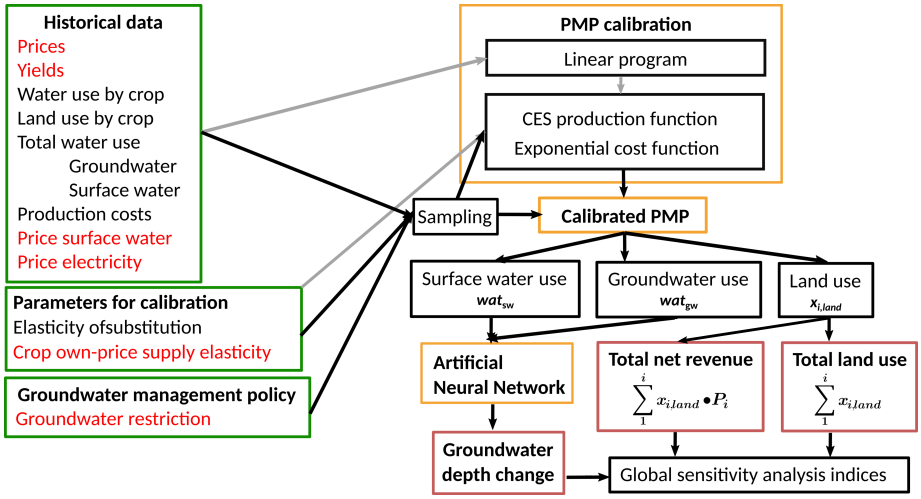

Figure 2.3: Global Sensitivity Analysis experiment. In red are the inputs selected for the GSA experiment from all the inputs used (green boxes). The gray arrows represent the flow of inputs for the calibration of the PMP model. The flow of inputs (in red) and outputs for the GSA experiment is depicted with black arrows. The yellow boxes represent the two models (PMP and ANN) and the red boxes represent the outputs of analysis. $P_i = \sum_{i,j}(p_i y_i - \omega_{i,j} x_{i,j}) x_{land,i}$

A variance-based GSA method, Sobol, was used for this study (Sobol, 2001). It uses the principle of variance decomposition to estimate the single interaction, higher order, and total effects of each input variable on the output. This method is computationally efficient, easy to interpret, and mathematically reliable.

Following Saltelli et al. (2010), the first order sensitivity index (S1) represents the contribution of a parameter X_i to the variance of the output Y given by Equation 2.7. $V(Y)$ is the

total variance of the output and $X_{\sim i}$ is a matrix of all parameters but X_i. The mean of Y is taken over all the possible values of $X_{\sim i}$ while keeping X_i constant. $S1_i$ is normalized so the first order indices have values between zero and $V(Y)$.

$$S1_i = \frac{V_{X_i}(E_{X_{\sim i}}(Y|X_i))}{V(Y)} \tag{2.7}$$

Using variance decomposition, Sobol indices capture interactions among parameters that are present due to nonlinearities in the model. The second order sensitivity (S2) is given by the joint effect of two parameters (X_i, X_j) on the variance of the output Y. This index is the result of the difference between the joint effect of the two parameters minus their first order effects as described by Equation 2.8.

$$S2_{ij} = V(E_{X_{\sim ij}}(Y|X_i, X_j)) - V(E_{X_{\sim i}}(Y|X_i)) - V(E_{X_{\sim j}}(Y|X_j)) \tag{2.8}$$

Finally the total order index (ST) for an input X_i is given by Equation 2.9. This represents the total effect of any input parameter X_i on the output Y, accounting for the first order effect and higher order effects. Where $V_{X_{\sim i}}(E_{X_i}(Y|X_{\sim i}))$ is the first order effect of $X_{\sim i}$.

$$ST_i = 1 - \frac{V_{X_{\sim i}}(E_{X_i}(Y|X_{\sim i}))}{V(Y)} \tag{2.9}$$

Since the distribution of the selected input variables is unknown we used the Saltelli sampling scheme (Saltelli, 2002), using minimum and maximum boundaries for each input (Table 2.1). For uncertainty on crop prices, we assume a relative price uncertainty of 20% and changes in yields of plus and minus 10% from the baseline as assessed by Medellín-Azuara et al. (2011) and Pathak et al. (2018). Crop prices show constant volatility as they are subject to global markets, while yield changes can be the result of farm-scale decisions (e.g. water stress, technology and fertilization) and climate factors. We used the baseline surface water price plus and minus 20% boundaries. For the price of electricity we used the minimum and maximum values reported in the analysis period. For own-price supply elasticities we used the minimum and maximum values found in the literature (Maneta et al., 2020; Russo et al., 2008; Volpe et al., 2010), or plus and minus 20% from the estimated values. Finally, we included a groundwater pumping restriction

policy, which can restrict up to 50% from the baseline groundwater pumped for each year. Values used for the GSA experiment are reported in Tables A.2-A.4 of the Appendix A.

Parameter	Name	Lower bound	Upper bound
p_i	Price by crop	80%	120%
yld_i	Yield change by crop	90%	110%
$\hat{\omega}_{SW}$	Price of surface water	80%	120%
$\omega_{electricity}$	Price of electricity	\$0.1/kWh	\$0.25/kWh
θ_i	Own price supply elasticity by crop	Lowest value in literature or 20% less than approximation	Highest value in literature or 20% more than approximation
GWR	Groundwater pumping restriction	0	50%

Table 2.1: Boundaries of input variables for Global Sensitivity Analysis Experiment

To perform this experiment we used the Python library SALib (Herman and Usher, 2017). The number of simulations to achieve significance and convergence on the sensitivity indices depend on the number of samples and number inputs (Saltelli et al., 2010). We performed simulations using 1,000 to 20,000 samples (n) for each input. The convergence of ST indices happened after n=2,000, however S1 indices converged after n=15,000. For the final simulations we chose n=20,000 samples for each input for a total of 2,080,000 state of the world simulations for the wet year conditions and 1,960,000 for the dry year conditions.

2.4.4 Data sources

Land use data is available from KCDAMS (2021). Crop water requirements were obtained from the California Department of Water Resources (DWR) (DWR, 2020a). Price and yield information was obtained at the county-level data for Kern (USDA, 2019). We assumed subsidies for crops that exhibit potentially negative marginal profitability under historical conditions. Costs of production were obtained from UC Davis Cost and Return Study estimates, using proxy crop costs per crop category (UC Davis, 2015). Agricultural surface water cost was estimated from rates published in the water district Agricultural Water Management Plans (DWR, 2020b). Surface water delivery, groundwater pumping and groundwater recharge amounts were obtained

from simulations of the California Food-Energy-Water Systems (CALFEWS) model(Zeff et al., 2021). Groundwater depths and pumping rates used for the ANN calibration were obtained from C2VSim-FG outputs (Brush and Dogrul, 2013) using the weighted-averaged groundwater depth to agricultural pumping. Water year classification was obtained from DWR (2020c). Additionally, the electricity costs, used in the pumping cost function, were obtained for agricultural customers reported by PG&E (2021).

2.5 Results and discussion

Results allow us to compare the sensitivity of groundwater depth change, total net revenue and total land use to input variable uncertainties. Figures 2.4 and 2.5 show the Sobol indices for wet year and dry year conditions, respectively. Second order indices are depicted by the ribbons of the chord-diagram. First order indices are the next outer circle, and total order indices are depicted in the outermost color circle. Variables related to the water supply (surface water price, price of electricity and groundwater restriction) are labeled as "water". Visualizations of the results were filtered to show the ten inputs with the highest ST for each output. The Python library used for the experiment, SALib, computes confidence intervals for the three indices, which satisfied a significance level of 0.05 for all the results. First order effects (S1) from Sobol were compared to Delta Moment-Independent Measure indices which can be found in the Appenix A (Tables A.5-A.10).

For wet year conditions (Figure 2.4), the results show that highest ranked input variables are the groundwater restriction and variables related to the most produced crops: vine, almonds and pistachios, other truck and subtropical. Allocation of land is highly sensitive to a restriction of groundwater pumping, which has a 68.3% ST. Additionally, the price of almonds and pistachios, price of other truck, and yield of cotton are among the most important inputs that affect land allocation based on their ST. Total net revenue is highly sensitive to price and yield of vine, the most produced crop in the district, and price of other truck crops.

For the wet year baseline 74% of irrigation was supplied from surface water, which price has a 13% ST to the groundwater depth change. Additionally, joint effects for GWD change are significant between price of almonds and pistachios with groundwater restriction (2.6% S2), which is also the largest joint effect of the study, and between the yield and price of almonds and

pistachios. Groundwater pumping restriction has the largest ST to GWD change of 73.08%.

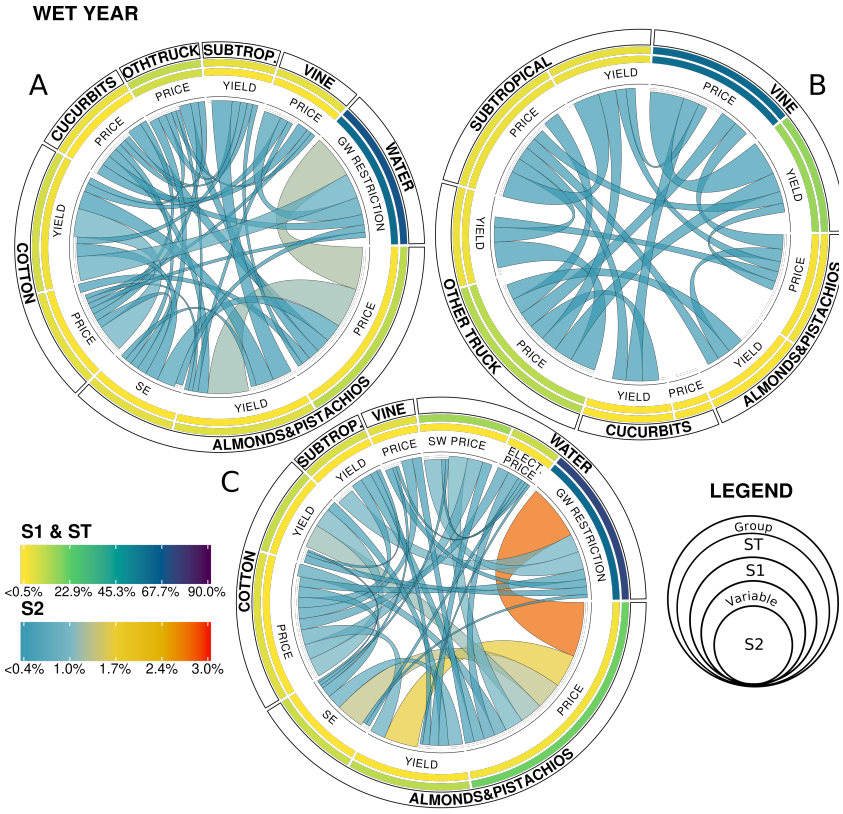

Figure 2.4: Results GSA for wet year conditions for Total Land Use (A), Total Net Revenue (B), and Groundwater Depth Change (C). SE=Supply Elasticity

As shown by the singular and joint effects, profitability changes due to crop price, yield and surface water price variation, have large impacts on land use and water use. This translates to changes in groundwater depth. The supply elasticity of almonds and pistachios used in the PMP calibration process has a total effect of 4% on total land use and 7.6% on groundwater depth change, showing the highest sensitivity indices from these calibration parameters in the analysis.

Results for the dry year are shown in Figure 2.5. Compared to the wet year, a lower number of inputs have large ST. Given a higher dependence on groundwater pumping (68.4% of the baseline water demand), crop production is less flexible and more sensitive to water shortages.

Expansion of perennial tree crops has been driven by increasing profits. However, these crops have a large water demand, 4 acre-feet per acre on average, making the food system vulnerable to water shortages. Groundwater restriction is the variable with the largest first order and total order effects on the total land allocation and groundwater depth change, with 90% ST.

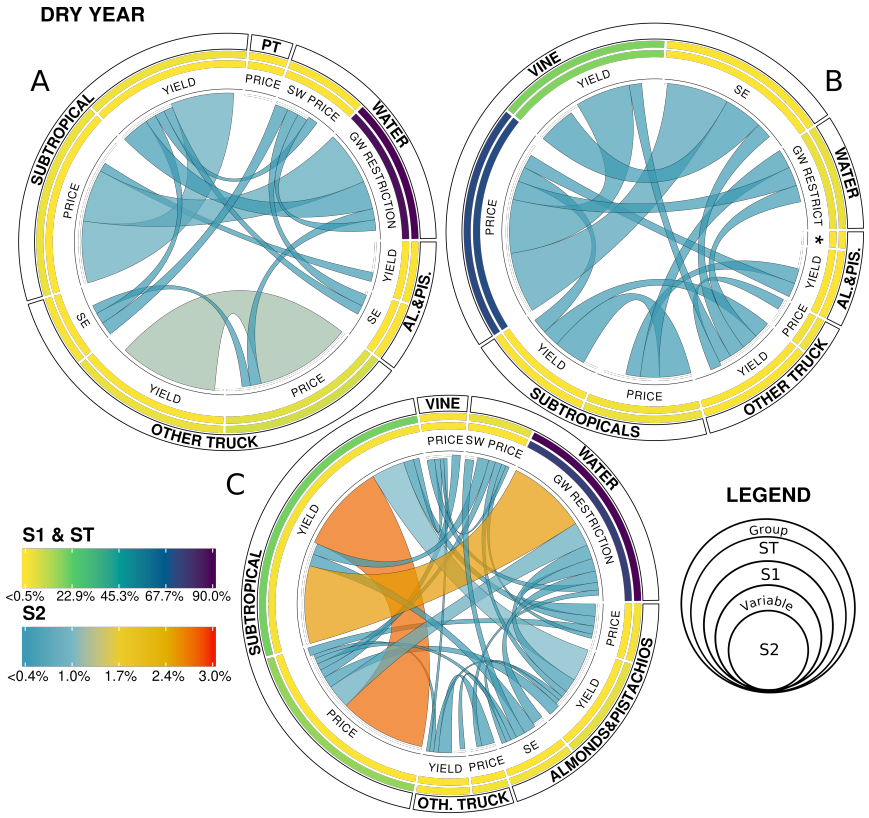

Figure 2.5: Results GSA for dry year conditions for Total Land Use (A), Total Net Revenue (B), and Groundwater Depth Change (C). *=Price, PT=Processing tomatoes, SE=Supply Elasticity, Al.&Pis.=Almonds and Pistachios

Total land use is sensitive to price of other truck crops with 7.0% ST. Total net revenue as in the wet year is highly sensitive to price and yield of vine. The groundwater depth changes is highly sensitive to yield and price of subtropical crops with ST of 20% and 15% respectively, which are highly contributed from the high joint effect between these two inputs (2.7% S2), and

the joint effect between subtropical crop yield and the groundwater restriction (2.5% S2).

By comparing wet and dry year conditions, we can observe that during a dry year S1 and ST effects of variables related to the most important crop groups are the most significant along with a groundwater restriction. This highlights the importance of groundwater, and that with a groundwater restriction the allocation of total land would likely be substantially reduced. S1 effects for the dry year are closer to representing the total variance of the outputs than in the wet year, meaning that direct effects are largely shaping the performance of the system. Additionally, during a wet year, multiple single and join effects are affecting the outputs of analysis, given the adaptation of farmers modeled by PMP in a year with more flexible water supply. In both years the price of electricity resulted in low indices, given the low electricity tariffs for agricultural users.

Other objectives beyond factor ranking can be achieved using the results of the diagnostic GSA. Factor fixing is a common practice that can reduce the uncertainty in the forecasts. Inputs with ST $\simeq 0$ can be fixed at any value in the space of the variation boundaries and will not affect the outputs. Since we are focusing on three outputs of the model and two base conditions, we have six total order indices for each input. Even though there are no inputs that satisfy this condition for all the outputs, some inputs show consistently low total order sensitivity, for example the supply elasticity of other deciduous and corn, yield of fresh tomatoes, and price of alfalfa and grain; suggesting that changes of these outputs would not have any significant effect to the outputs and can be fixed. In PMP modeling, crop own-price supply elasticities is one of the most uncertain inputs due to the limited information about them in the context of the SJV. Our analysis suggests that these parameters are candidates for factor fixing given their low ST.

Results from the diagnostic GSA can be used to explore the uncertainty space of the outputs, which can support stakeholders to identify areas of interest in the output space and trade-offs. Figure 2.6 shows the performance of the outputs at different percentage levels of groundwater pumping restrictions (color gradient). Trade-offs among outputs are depicted by the lines in the parallel-coordinate plot, each one represents the results from a state of the world simulated in the GSA experiment.

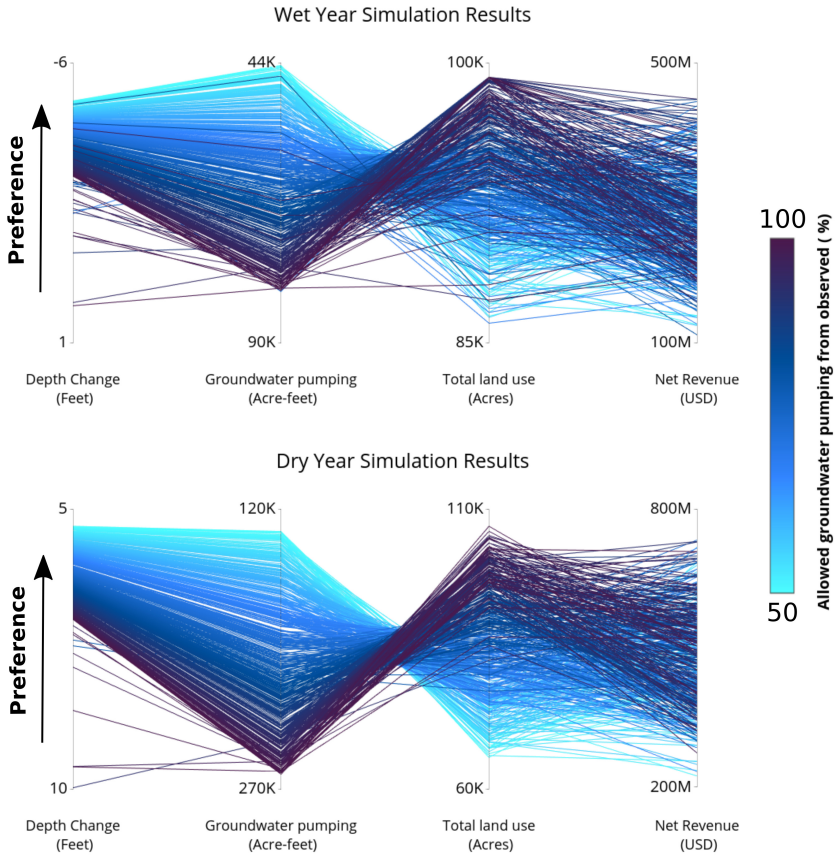

Figure 2.6: Random sample of five hundred scenarios for wet year and dry year from the diagnostic sensitivity analysis experiment

Our results show that the same level of pumping restriction can have different outcomes. For example, scenarios with a 50% pumping restriction in both water conditions can result in different levels of total land use and depth change. This is driven by the profitability of crops with high ST and high joint effects with the restriction policy, such as price and yield of almonds and pistachios, price and yield of subtropical crops and surface water price. The diagnostic GSA results show the dominant inputs and joint effects that explain the nuances in the trade-offs. Furthermore, the pumping restriction does not have a clear effect on the net revenue for which other inputs with higher ST have a greater impact. Stakeholders can use these results to identify specific scenarios

supported by the diagnostic GSA results and understand the drivers of particular results. Additionally, these results can inform policy makers about the expected magnitude of change in policy performance and the largest vulnerabilities in the system.

2.6 Conclusions

GSA diagnostic results inform how much each input and their joint effects impact three outputs of interest: total land use, total net revenue, and groundwater depth change. The diagnostic provides insight about dominant inputs (with high ST) or inputs (with ST $\simeq 0$) that can be fixed. The inclusion of a groundwater restriction policy allowed us to explore its impacts on the food-water system and how other dominant inputs can affect its performance. Even though the restriction parameter showed the largest sensitivity indices, other inputs also showed substantial total order effects. Changes in prices and yields of tree crops and vines can be considered vulnerabilities of the system and affect policy results and trade-offs among system performance metrics. Diagnostic results can be used to inform stakeholders about potential drivers of undesirable results, vulnerabilities and other elements to consider for the development of a robust policy. Future work will include other groundwater management policies such as a groundwater pumping fee and land restrictions.

Our findings show that significant differences in the diagnostic results emerge from two baseline water condition scenarios. We suggest that the use of the diagnostic framework shown in this study is applicable for any HEM. Furthermore, performing this diagnostic under different baselines is particularly important for studies of places with highly variable water supplies such as the San Joaquin Valley, and other places in Mediterranean, arid, and semi-arid climate regions.

2.7 Acknowledgements

This work was supported by the U.S. National Science Foundation (NSF) Innovations at the Nexus of Food, Energy and Water Systems (INFEWS) program (Award No. 1639268, Lead PI Characklis, University of North Carolina Chapel Hill). José M. Rodríguez-Flores was largely supported by a UC MEXUS-CONACYT Doctoral Fellowship. Cluster computing resources were

supplied using The Cube computer cluster at Cornell University Center for Advanced Computing.

2.8 References

Afshar, A., Tavakoli, M. A., & Khodagholi, A. (2020). Multi-Objective Hydro-Economic Modeling for Sustainable Groundwater Management. *Water Resources Management*, *34*(6), 1855–1869. https://doi.org/10.1007/s11269-020-02533-4

Arribas, I., Louhichi, K., Perni, Á., Vila, J., & Gómez-y-Paloma, S. (2017). Modelling Farmers' Behaviour Toward Risk in a Large Scale Positive Mathematical Programming (PMP) Model. In N. Tsounis & A. Vlachvei (Eds.), *Advances in Applied Economic Research* (pp. 625–643). Springer International Publishing. https://doi.org/10.1007/978-3-319-48454-9_42

Brush, C., & Dogrul, E. (2013). *User's Manual for the California Central Valley Groundwater-Surface Water Simulation Model (C2VSim), Version 3.02-CG.*

Bryant, B. P., Kelsey, T. R., Vogl, A. L., Wolny, S. A., MacEwan, D., Selmants, P. C., Biswas, T., & Butterfield, H. S. (2020). Shaping Land Use Change and Ecosystem Restoration in a Water-Stressed Agricultural Landscape to Achieve Multiple Benefits. *Frontiers in Sustainable Food Systems*, *4*. https://doi.org/10.3389/fsufs.2020.00138

Budamala, V., & Baburao Mahindrakar, A. (2020). Integration of Adaptive Emulators and Sensitivity Analysis for Enhancement of Complex Hydrological Models. *Environmental Processes*, *7*(4), 1235–1253. https://doi.org/10.1007/s40710-020-00468-x

D'Agostino, D. R., Scardigno, A., Lamaddalena, N., & El Chami, D. (2014). Sensitivity Analysis of Coupled Hydro-Economic Models: Quantifying Climate Change Uncertainty for Decision-Making. *Water Resources Management*, *28*(12), 4303–4318. https://doi.org/10.1007/s11269-014-0748-2

Debertin, D. L. (Ed.). (2012). *Agricultural Production Economics: The Art of Production Theory*. https://doi.org/10.22004/ag.econ.158320

DWR. (2020a). Agricultural Land & Water Use Estimates. http://water.ca.gov/Programs/Water-Use-And-Efficiency/Land-And-Water-Use/Agricultural-Land-And-Water-Use-Estimates

DWR. (2020b). Agricultural Land & Water Use Estimates. http://water.ca.gov/Programs/Water-Use-And-Efficiency/Land-And-Water-Use/Agricultural-Land-And-Water-Use-Estimates

DWR. (2020c). California Data Exchange Center (CDEC). https://cdec.water.ca.gov/reportapp/javareports?name=WSIHIST

DWR. (2021). Sustainable Groundwater Management Act (SGMA). https://water.ca.gov/Programs/Groundwater-Management/SGMA-Groundwater-Management

El Harraki, W., Ouazar, D., Bouziane, A., El Harraki, I., & Hasnaoui, D. (2021). Streamflow Prediction Upstream of a Dam Using SWAT and Assessment of the Impact of Land Use Spatial Resolution on Model Performance. *Environmental Processes*, *8*(3), 1165–1186. https://doi.org/10.1007/s40710-021-00532-0

Fayaz, N., Condon, L. E., & Chandler, D. G. (2020). Evaluating the Sensitivity of Projected Reservoir Reliability to the Choice of Climate Projection: A Case Study of Bull Run Watershed, Portland, Oregon. *Water Resources Management*, *34*(6), 1991–2009. https://doi.org/10.1007/s11269-020-02542-3

Fernandez-Bou, A. S., Ortiz-Partida, J. P., Pells, C., Classen-Rodriguez, L. M., Espinoza, V., Rodríguez-Flores, J. M., & Medellin-Azuara, J. (2021). *Regional Report for the San Joaquin Valley Region on Impacts of Climate Change* (California's Fourth Climate Assesment SUM-CCCA4-2021-003). California Natural Resources Agency. Sacramento. https://www.energy.ca.gov/sites/default/files/2022-01/CA4_CCA_SJ_Region_Eng_ada.pdf

Forni, L. G., Medellín-Azuara, J., Tansey, M., Young, C., Purkey, D., & Howitt, R. (2016). Integrating complex economic and hydrologic planning models: An application for drought under climate change analysis. *Water Resources and Economics*, *16*, 15–27. https://doi.org/10.1016/j.wre.2016.10.002

Ghadimi, S., & Ketabchi, H. (2019). Possibility of cooperative management in groundwater resources using an evolutionary hydro-economic simulation-optimization model. *Journal of Hydrology*, *578*, 124094. https://doi.org/10.1016/j.jhydrol.2019.124094

Giuliani, M., Li, Y., Castelletti, A., & Gandolfi, C. (2016). A coupled human-natural systems analysis of irrigated agriculture under changing climate. *Water Resources Research*, *52*(9), 6928–6947. https://doi.org/10.1002/2016WR019363

Graveline, N. (2019). Combining flexible regulatory and economic instruments for agriculture water demand control under climate change in Beauce. *Water Resources and Economics*, 100143. https://doi.org/10.1016/j.wre.2019.100143

Graveline, N., & Merel, P. (2014). Intensive and extensive margin adjustments to water scarcity in France's Cereal Belt. *European Review of Agricultural Economics*, *41*(5), 707–743. https://doi.org/10.1093/erae/jbt039

Hanak, E., Escriva-Bou, A., Gray, B., Green, S., Harter, T., Jezdimirovic, J., Lund, J., Medellín-Azuara, J., Moyle, P., & Seavy, N. (2019). *Water and the Future of the San Joaquin Valley* (tech. rep.). https://doi.org/10.13140/RG.2.2.24360.83208

Harou, J. J., Pulido-Velazquez, M., Rosenberg, D. E., Medellín-Azuara, J., Lund, J. R., & Howitt, R. E. (2009). Hydro-economic models: Concepts, design, applications, and future prospects. *Journal of Hydrology*, *375*(3-4), 627–643. https://doi.org/10.1016/j.jhydrol.2009.06.037

Hashemi, M., & Mahjouri, N. (2022). Global Sensitivity Analysis-based Design of Low Impact Development Practices for Urban Runoff Management Under Uncertainty. *Water Resources Management*. https://doi.org/10.1007/s11269-022-03140-1

Herman, J., & Usher, W. (2017). SALib: An open-source Python library for Sensitivity Analysis. *Journal of Open Source Software*, *2*(9), 97. https://doi.org/10.21105/joss.00097

Howitt, R. E., Medellín-Azuara, J., MacEwan, D., & Lund, J. R. (2012). Calibrating disaggregate economic models of agricultural production and water management. *Environmental Modelling & Software*, *38*, 244–258. https://doi.org/10.1016/j.envsoft.2012.06.013

Karimi, T., Reed, P., Malek, K., & Adam, J. (2022). Diagnostic Framework for Evaluating How Parametric Uncertainty Influences Agro-Hydrologic Model Projections of Crop Yields Under Climate Change. *Water Resources Research*, *58*(6), e2021WR031249. https://doi.org/10.1029/2021WR031249

KCDAMS. (2021). Kern County Department of Agriculture and Measurement Standards - Spatial Data. http://www.kernag.com/gis/gis-data.asp

Li, R., Ou, G., Pun, M., & Larson, L. (2018). Evaluation of Groundwater Resources in Response to Agricultural Management Scenarios in the Central Valley, California. *Journal of Water Resources Planning and Management*, *144*(12), 04018078. https://doi.org/10.1061/(ASCE)WR.1943-5452.0001014

Lund, J., Medellin-Azuara, J., Durand, J., & Stone, K. (2018). Lessons from California's 2012–2016 Drought. *Journal of Water Resources Planning and Management*, *144*(10), 04018067. https://doi.org/10.1061/(ASCE)WR.1943-5452.0000984

MacEwan, D., Cayar, M., Taghavi, A., Mitchell, D., Hatchett, S., & Howitt, R. (2017). Hydroeconomic modeling of sustainable groundwater management. *Water Resources Research*, *53*(3), 2384–2403. https://doi.org/10.1002/2016WR019639

Maneta, M., Cobourn, K., Kimball, J., He, M., Silverman, N., Chaffin, B., Ewing, S., Ji, X., & Maxwell, B. (2020). A satellite-driven hydro-economic model to support agricultural water resources management. *Environmental Modelling & Software*, *134*, 104836. https://doi.org/10.1016/j.envsoft.2020.104836

Medellín-Azuara, J., Howitt, R. E., MacEwan, D. J., & Lund, J. R. (2011). Economic impacts of climate-related changes to California agriculture. *Climatic Change*, *109*(S1), 387–405. https://doi.org/10.1007/s10584-011-0314-3

Miro, M. E., & Famiglietti, J. S. (2019). A framework for quantifying sustainable yield under California's Sustainable Groundwater Management Act (SGMA). *Sustainable Water Resources Management*, *5*(3), 1165–1177. https://doi.org/10.1007/s40899-018-0283-z

Pathak, T., Maskey, M., Dahlberg, J., Kearns, F., Bali, K., & Zaccaria, D. (2018). Climate Change Trends and Impacts on California Agriculture: A Detailed Review. *Agronomy*, *8*(3), 25. https://doi.org/10.3390/agronomy8030025

PG&E. (2021). Pacific Gas & Electric - Tariffs. https://www.pge.com/tariffs/rateinfo.shtml

Pianosi, F. (2016). Sensitivity analysis of environmental models: A systematic review with practical workflow. *Environmental Modelling*, 19.

Richey, A. S., Thomas, B. F., Lo, M.-H., Reager, J. T., Famiglietti, J. S., Voss, K., Swenson, S., & Rodell, M. (2015). Quantifying renewable groundwater stress with GRACE. *Water Resources Research*, *51*(7), 5217–5238. https://doi.org/10.1002/2015WR017349

Russo, C., Green, R., & Howitt, R. E. (2008). Estimation of Supply and Demand Elasticities of California Commodities. *SSRN Electronic Journal*. https://doi.org/10.2139/ssrn.1151936

Saltelli, A. (2002). Making best use of model evaluations to compute sensitivity indices. *Computer Physics Communications*, *145*(2), 280–297. https://doi.org/10.1016/S0010-4655(02)00280-1

Saltelli, A., Annoni, P., Azzini, I., Campolongo, F., Ratto, M., & Tarantola, S. (2010). Variance based sensitivity analysis of model output. Design and estimator for the total sensitivity

index. *Computer Physics Communications*, *181*(2), 259–270. https://doi.org/10.1016/j.cpc.2009.09.018

Shirzadi Laskookalayeh, S., Mardani Najafabadi, M., & Shahnazari, A. (2022). Investigating the effects of management of irrigation water distribution on farmers' gross profit under uncertainty: A new positive mathematical programming model. *Journal of Cleaner Production*, *351*, 131277. https://doi.org/10.1016/j.jclepro.2022.131277

Singh, A. (2022). Better Water and Land Allocation for Long-term Agricultural Sustainability. *Water Resources Management*. https://doi.org/10.1007/s11269-022-03208-y

Sobol, I. M. (2001). Global sensitivity indices for nonlinear mathematical models and their Monte Carlo estimates. *Mathematics and Computers in Simulation*, *55*(1), 271–280. https://doi.org/10.1016/S0378-4754(00)00270-6

Song, X., Zhang, J., Zhan, C., Xuan, Y., Ye, M., & Xu, C. (2015). Global sensitivity analysis in hydrological modeling: Review of concepts, methods, theoretical framework, and applications. *Journal of Hydrology*, *523*, 739–757. https://doi.org/10.1016/j.jhydrol.2015.02.013

Stone, K. M., Gailey, R. M., & Lund, J. R. (2022). Economic tradeoff between domestic well impact and reduced agricultural production with groundwater drought management: Tulare County, California (USA), case study. *Hydrogeology Journal*, *30*(1), 3–19. https://doi.org/10.1007/s10040-021-02409-w

UC Davis. (2015). Current Cost and Return Studies. https://coststudies.ucdavis.edu/en/current/

USDA. (2019). USDA - National Agricultural Statistics Service - California - County Ag Commissioners' Data Listing. https://www.nass.usda.gov/Statistics_by_State/California/Publications/AgComm/index.php

Van Schmidt, N. D., Wilson, T. S., & Langridge, R. (2022). Linkages between land-use change and groundwater management foster long-term resilience of water supply in California. *Journal of Hydrology: Regional Studies*, *40*, 101056. https://doi.org/10.1016/j.ejrh.2022.101056

Vasco, D. W., Farr, T. G., Jeanne, P., Doughty, C., & Nico, P. (2019). Satellite-based monitoring of groundwater depletion in California's Central Valley. *Scientific Reports*, *9*(1), 16053. https://doi.org/10.1038/s41598-019-52371-7

Volpe, R., Green, R., Heien, D., & Howitt, R. (2010). Estimating the Supply Elasticity of California Wine Grapes Using Regional Systems of Equations. *Journal of Wine Economics*, *5*(2), 219–235. https://doi.org/10.1017/S1931436100000924

Xiao, M., Koppa, A., Mekonnen, Z., Pagán, B. R., Zhan, S., Cao, Q., Aierken, A., Lee, H., & Lettenmaier, D. P. (2017). How much groundwater did California's Central Valley lose during the 2012–2016 drought? *Geophysical Research Letters*, *44*(10), 4872–4879. https://doi.org/10.1002/2017GL073333

Yin, J., Medellín-Azuara, J., Escriva-Bou, A., & Liu, Z. (2021). Bayesian machine learning ensemble approach to quantify model uncertainty in predicting groundwater storage change. *Science of The Total Environment*, *769*, 144715. https://doi.org/10.1016/j.scitotenv.2020.144715

Zeff, H. B., Hamilton, A. L., Malek, K., Herman, J. D., Cohen, J. S., Medellin-Azuara, J., Reed, P. M., & Characklis, G. W. (2021). California's food-energy-water system: An open source simulation model of adaptive surface and groundwater management in the Central Valley. *Environmental Modelling & Software*, *141*, 105052. https://doi.org/10.1016/j.envsoft.2021.105052

Chapter 3

Identifying robust adaptive irrigation operating policies to balance deeply uncertain economic food production and groundwater sustainability trade-offs

This chapter is currently in review in the Journal of Environmental Management: Rodríguez-Flores, J.M., Gupta, R.S., Zeff, H.B., Reed, P.M., Medellín-Azuara, J. (2023). Identifying robust adaptive irrigation operating policies to balance deeply uncertain economic food production and groundwater sustainability trade-offs.

3.1 Abstract

Increasing irrigation demand has heavily relied on groundwater use, especially in places with highly variable water supplies that are vulnerable to drought. Groundwater management in agriculture is becoming increasingly challenging given the growing effects from overdraft and groundwater depletion worldwide. However, multiple challenges emerge when seeking to develop sustainable groundwater management in irrigated systems, such as trade-offs between the eco-

nomic revenues from food production and groundwater resources, as well as the broad array of uncertainties in food-water systems. In this study we explore the applicability of Evolutionary Multi-Objective Direct Policy Search (EMODPS) to identify adaptive irrigation policies that water agencies and farmers can implement including operational decisions related to land use and groundwater use controls as well as groundwater pumping fees. The EMODPS framework yields state-aware, adaptive policies that respond dynamically as system state conditions change, for example with variable surface water (e.g., shifting management strategies across wet versus dry years). For this study, we focus on the Semitropic Water Storage district located in the San Joaquin Valley, California to provide broader insights relevant to ongoing efforts to improve groundwater sustainability in the state. Our findings demonstrate that adaptive irrigation policies can achieve sufficiently flexible groundwater management to acceptably balance revenue and sustainability goals across a wide range of uncertain future scenarios. Among the evaluated policy decisions, pumping restrictions and reductions in inflexible irrigation demands from tree crops are actions that can support dry-year pumping while maximizing groundwater storage recovery during wet years. Policies suggest that an adaptive pumping fee is the most flexible decision to control groundwater pumping and land use.

3.2 Introduction

As irrigation water demand increases due to increased crop acreage and droughts become more frequent, agricultural regions in the world are relying more on groundwater to make up for surface water losses. In Mediterranean climate regions, such as California, groundwater is the primary water source for buffering drought impacts on food production (Malmgren et al., 2022; Priyan, 2021). Aquifer systems' dynamics are sensitive to changes in temperature, precipitation, and surface water flows, that can be directly impacted by climate change (Cuthbert et al., 2019; W.-Y. Wu et al., 2020). However, one of the largest impacts from climate change are the resulting adaptation driven changes in land use and shifting water demands from human activities (R. G. Taylor et al., 2013). Globally, groundwater provides 43 percent of the total irrigation needs (Siebert et al., 2010), and its share is expected to increase as surface water scarcity increases (Bierkens and Wada, 2019). In California, the limits in coordinated and regulated groundwater management in

irrigation-based agriculture have led to decades of increasing stress and depletion of the state's aquifers (Vasco et al., 2019), affecting dependent ecosystems (Bierkens and Wada, 2019), limiting its access to shallow water-table reliant communities (Pauloo et al., 2020; Perrone and Jasechko, 2017), increasing land subsidence (Smith and Majumdar, 2020), reducing groundwater storage and storativity (Alam et al., 2021), and degradation of water quality (Levy et al., 2021).

The largest rate of groundwater depletion in California has been observed in the San Joaquin Valley (SJV) (Ojha et al., 2018). The SJV is the most important agricultural region in the United States by economic value (USDA, 2020), but also strongly susceptible to drought risk. Most of the region's snowpack and water supply comes from limited atmospheric-river driven events (Espinoza et al., 2018). Increasing temperatures and evapotranspiration linked to a warming climate are expected to further reduce snowpack runoff and surface water supply (Fernandez-Bou et al., 2021; Vahmani et al., 2022). Additionally, human factors such as increasing irrigation demand can exacerbate vulnerabilities to increasingly intense droughts (He et al., 2017). Over the past decade, the agricultural sector has been significantly impacted by multi-year droughts (Lund et al., 2018; Medellin-Azuara et al., 2022). Groundwater pumping is used as a buffer to reduce the negative impacts to agricultural production from surface water shortages, but increasing pumping and a lack of coordinated management have led to significant declines in groundwater levels and reductions in the regional aquifer's capacity to recover (Liu et al., 2022). Additionally, the SJV has seen a significant expansion of perennial tree crops, mainly almonds, which is the most important commodity by value in the region (USDA, 2020). Although highly profitable, the expansion of perennial tree crops represents a less flexible water demand and a higher financial risk to water shortages due to high establishment costs (Mall and Herman, 2019; Qin et al., 2019).

Given the consequences from overdraft in California, the 2014 Sustainable Groundwater Management Act (SGMA) (DWR, 2021b) was put in place to require critically over-drafted basins to achieve sustainability in terms of balancing their recharge and extraction by 2040. Groundwater Sustainability Agencies (GSAs) are locally formed agencies responsible for developing and enforcing policies to manage water conjunctively to address groundwater sustainability. The state defined guidelines in the Sustainable Management Criteria (DWR, 2017) that GSAs can use to develop management strategies to achieve sustainable goals, including sustainable groundwater levels. The sustainable criteria define a margin of operational flexibility where the groundwater

depth can go above the upper bound of the groundwater level range but not below the lower-bound depth where undesirable results (e.g., dry wells) may occur. Henceforth, the margin of operational flexibility will be referred to the groundwater level requirement as shown in Figure B1 in Appendix B. Within this framework, GSAs can develop flexible groundwater management strategies, allowing pumping during dry years and maximizing groundwater recovery during wet years. Overall, California's food production needs to adapt operational water and land allocation decisions and crop choice to achieve groundwater sustainability goals and be less vulnerable to surface water shortages.

Multiple challenges that are inherent to coupled food-water systems (Polhill et al., 2016) impact the development of groundwater management policies in the SJV. First, food-water systems are dynamic, where each component can evolve and lead to feed-backs (Filatova et al., 2016). Thus, management decisions need to adapt as the coupled system evolves. Second, water management policies may result in trade-offs between economic and sustainability objectives (McDermid et al., 2021; Null et al., 2021; Stone et al., 2022; Torhan et al., 2022). Lastly, there are intrinsic deep uncertainties (Stirling, 2010) that need to be considered to implement robust policies, including uncertain surface water supplies and crop prices. There is a growing base of literature focused on assessing management policies and mechanisms for groundwater sustainability in agriculture. Water and land use controls as well as economic instruments are the most common strategies that have been implemented. Examples of these mechanisms are groundwater pumping taxing and pricing (Madani and Dinar, 2013; Mulligan et al., 2014; Stone et al., 2022; S. Wang et al., 2023), pumping restrictions (Lan et al., 2021; MacEwan et al., 2017; Rodríguez-Flores et al., 2022; S. Wang et al., 2023; Young et al., 2021), pricing energy (Hrozencik et al., 2022), groundwater markets or water trading mechanisms (Khan and Brown, 2019; Kuwayama and Brozović, 2013; Safari et al., 2023), land fallowing (Van Schmidt et al., 2022) and land management (Bourque et al., 2019; Bryant et al., 2020; Li et al., 2018), implemented individually or utilized in conjunction (Graveline, 2020; Hrozencik et al., 2017). However, most of these studies do not capture the complexity of actually implementing these mechanisms in decision making. For example, they do not take into account intrinsic uncertainties such as annual variability in surface water supplies and the trade-offs between groundwater sustainability objectives and economic revenues.

Secondly, finding optimal groundwater management policies is a nontrivial task. Most

formulations that do so are characterized by non-linearity and non-convexity, and must consider a broad array of objectives that balance trade-offs across groundwater sustainability agencies and farmers (i.e., maximizing economic revenues and minimizing distance to groundwater). Heuristic methods such as multi-objective evolutionary algorithms (MOEAs) have been demonstrated in their ability to address these complexities and discover high quality approximations of optimal trade-offs among objectives that compose the Pareto-front (Reed et al., 2013). Thus, the resulting Pareto optimal approximate set of solutions are those where performance in any given objective cannot be achieved without degrading the performance in one or more of the remaining objectives (Coello et al., 2007). Even though heuristic optimization frameworks hold promise for aiding decision making in agriculture (Memmah et al., 2015), there are few applications addressing larger and more complex inter-connected food-water systems. Prior studies have focused on utilizing MOEAs in groundwater management controls (Afshar et al., 2020; Banihabib et al., 2019; Habibi Davijani et al., 2016; Hesamfar et al., 2023; Mehrabi et al., 2021; Salehi Shafa et al., 2023). This study expands the application of MOEAs to find coordinated optimal land and water use decisions to clarify groundwater sustainability and economic trade-offs in agriculture.

As reviewed by Thomann et al. (2020), there is a need for new groundwater management frameworks that are dynamic and adaptively responsive to observed system changes. In this study, we draw on Direct Policy Search (DPS) introduced by Rosenstein and Barto (2001) as a parameterization-simulation-optimization formulation where a control policy is parameterized using non-linear universal functions such as neural networks or radial basis functions. In DPS, the parameters of the control policy function are optimized rather than the decisions themselves using a simulation-optimization process to search for optimal operations for a system. The application of DPS to water systems was introduced by Koutsoyiannis and Economou (2003) in reservoir operations and subsequently extended to Evolutionary Multi-objective Direct Policy Search (EMODPS) formalized by Giuliani et al. (2014). As reviewed by Giuliani et al. (2021), the EMODPS framework has proven capable of discovering optimal dynamic adaptive control policies in a broad array of recent applications (Bertoni et al., 2021; Doering et al., 2021; Geressu et al., 2022; Gupta et al., 2020; Hamilton et al., 2022; Macian-Sorribes and Pulido-Velazquez, 2019; Veena et al., 2021; W. Wu et al., 2022). Additionally, EMODPS aids in the direct use of simulation models and overcoming the "curse of dimensionality" inherent to other control frameworks as Stochastic Dynamic

Programming that have been previously applied in agriculture (Giuliani et al., 2016; C. R. Taylor, 1993).

In this study, we formulate a 5-objective application of EMODPS where the resulting irrigation control policies utilize state information (e.g., surface water availability, groundwater depth and irrigation demand) to adaptively inform decisions related to pumping and land use controls as well as pricing pumping, for a given production year at the GSA level. The 5-objectives considered in this study include: maximize revenue from food production, minimize distance to groundwater (groundwater depth), maximize minimum economic revenue, minimize maximum groundwater depth change and maximize the number of years the groundwater level is at or below the groundwater level requirement. We further test the robustness of the resulting irrigation control policies (Groves et al., 2019; Kasprzyk et al., 2013; Lempert et al., 2013) by assessing how well they perform across a broader sampling of system conditions or states of the world (SOWs). Exploratory modeling-based evaluation of systems' robustness is being used across a broad array complex water management application contexts balancing human demands objectives, economic, sustainability and engineered performance (Bertoni et al., 2019; Graveline, 2020; Hadjimichael et al., 2020; Huskova, 2016; Miro et al., 2021; Moallemi et al., 2020; Quinn et al., 2018; Shuai et al., 2022; Trindade et al., 2019). Building off these examples, we identify robust irrigation control policies that consistently achieve performance goals for groundwater depth and economic revenues at the GSA level across a range of challenging SOWs.

A core technical contribution of this study is a novel application of a bi-level optimization framework where the hydro-economic model agricultural production model with a groundwater depth response function is nested within a broader MOEA-based search to find adaptive irrigation management policies that compose optimal groundwater sustainability and ecoomic revenue tradeoffs. This modeling framework is applied to the Semitropic Water Storage District (SWSD) GSA, which represents a broad set of groundwater sustainability agencies in the San Joaquin Valley. The objectives of this study are twofold. First, we use EMODPS to identify adaptive strategies that achieve groundwater sustainability and economic goals accounting for the characteristics of the food-water system. Second, we assess the robustness of the optimal policies within the context of the sustainable groundwater management criteria defined by the state of California.

3.3 Study area

The study area of this research is the SWSD, located in the SJV and the Kern County groundwater basin (Figure 3.1). The SWSD also operates its own Groundwater Sustainability Agency, which coordinates irrigation operations and water management strategies that can be implemented depending on the water budget of each year. Four possible management instruments are analyzed in this study: (1) a control on groundwater use, (2) a groundwater pumping fee that is implemented by the GSA, (3) total land use control, and (4) a perennial crops planting restriction. Other management strategies such as water market mechanisms and supply-side policies focused on augmenting groundwater storage, as managed aquifer recharge (Ulibarri et al., 2021), are out of the scope of this study. As has been seen in other regions of the SJV, there has been a significant expansion of almonds and other perennial crops in the SWSD over the past 10 years. Other important commodities in the district include vines, alfalfa, corn, cotton, and cucumbers shown in Appendix B Figure B2.

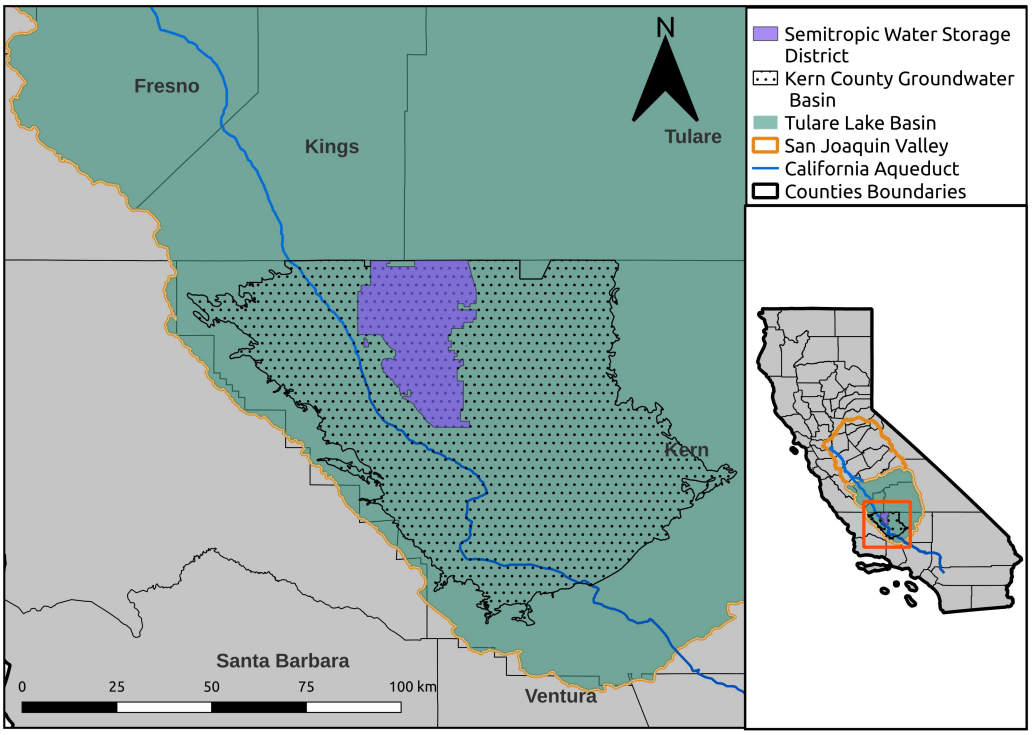

Figure 3.1: Semitropic Water Storage District study area located in the California's San Joaquin Valley.

3.3.1 Semitropic GSA Hydro-Economic model

In coupled food-water systems, Hydro-Economic Models have been used as decision support modeling tools to assess water policy and climate change adaptation decisions (Harou et al., 2009; Ward, 2021). HEMs are able to abstract stakeholders decisions (e.g., farmers) and hydrologic dynamics, as well as their feedback, by integrating economic models with hydrologic response functions (Harou et al., 2009). They have played an important role in supporting human and natural systems modeling studies focused on better understanding interdependent economic revenues and aquifer dynamics, as shown by MacEwan et al. (2017), Afshar et al. (2020), Graveline (2020) and Rodríguez-Flores et al. (2022). Additionally, HEMs have proven to be flexible in assisting assessments of the performance of water management policies under different climate scenarios across a range of space and time scales (Partida et al., 2023).

Economic model

The SWSD's food production system is modeled using a yearly net profit maximization at the irrigation district level. With this economic model, we can model land and water (surface and groundwater) allocation decisions for crop production. This model assumes that farmers make production decisions to maximize their net revenues by considering crop prices, surface water availability, price of surface water, price of electricity and water management policies. The mathematical model is based on Positive Mathematical Programming (PMP) formalized by Howitt (1995). PMP is a HEM method that uses observed agricultural production behavior to define a constrained non-linear optimization model, used to simulate water allocation for policy analysis assuming profit maximization (Graveline, 2020; Howitt et al., 2012; MacEwan et al., 2017; Rodríguez-Flores et al., 2019). In this study we implement a PMP calibration that uses a stochastic data assimilation method to calibrate the economic parameters described by Maneta and Howitt (2014) and Maneta et al. (2020). This calibration framework enables the update of the distribution of the calibration parameters every time data becomes available. More details on the calibration process are described in Appendix B.2.

For the calibration of the model, we use statistical data on prices, costs, water applied and yields for each crop category and water supply by source from 1998 to 2015. After the last year of historical observations was incorporated in the recursive data assimilation process, the final ensemble with 400 samples of the PMP calibration parameters $\theta_i = [\mu_i, \beta_{i,water}, \beta_{i,land}, \delta_i, \lambda_{i,land}, \lambda_{i,water}, \bar{\lambda}_{land}]$ are used in the economic model. Equations 3.1-3.7 define the PMP net profit maximization problem for food production within the SWSD that is nested in the MOEA for a Bi-level optimization problem (Section 3.4.2).

$$\underset{\substack{x_{i,land,t}\geq 0 \\ x_{i,water,t}\geq 0 \\ wat_{i,w,t}\geq 0}}{max} \sum_i \{p_{i,t}\mu_i(\beta_{i,land}x_{i,land,t}^{\rho_i} + \beta_{i,water}x_{i,water,t}^{\rho_i})^{\delta_i/\rho_i} - (\omega_{i,land} + \lambda_{i,land} + \bar{\lambda}_{land})x_{i,land,t} - (\omega_{SW,t} + \lambda_{i,water})wat_{i,SW,t} - (\omega_{GW,t} + \lambda_{i,water} + u_t^{GWF})wat_{i,GW,t}\} \tag{3.1}$$

subject to

$$\sum_{i} x_{i,land,t} \leq u_t^{TL} \tag{3.2}$$

$$\sum_{i \in PC} x_{i,land,t} \leq u_t^{PL} \tag{3.3}$$

$$\sum_{i \in PC} x_{i,land,t} \geq \sum_{i \in PC} x_{i,land,t-1} * 0.95 \tag{3.4}$$

$$x_{i,water,t} = wat_{i,SW,t} + wat_{i,GW_t} \tag{3.5}$$

$$\sum_{i} wat_{i,SW,t} \leq b_{SW,t} \tag{3.6}$$

$$\sum_{i} wat_{i,GW,t} \leq u_t^{GWP} \tag{3.7}$$

$$x_{i,water,t} \geq \bar{x}_{i,water} * 0.98 \tag{3.8}$$

Where Equation 3.1 represents the net revenue maximizing objective function, allocating $x_{land,i}$, total water $x_{water,i}$, surface water $wat_{SW,i}$ and groundwater $wat_{GW,i}$ to each crop i (Figure B2). $p_{i,t}$ is the price per ton of crop i. Crop production in the first term of Equation 3.1 is represented by a Constant Elasticity of Substitution (CES) production function (Debertin, 2012; Merel et al., 2010), with the two inputs, land and water. $\beta_{i,j=[land,water]}$ are the relative use of land and water. $\rho = (\sigma - 1)/\sigma$, where σ is the elasticity of substitution between inputs used to produce each crop. For this study we defined $\sigma = 0.17$ following Howitt et al. (2012). The scale parameter μ_i and δ_i are calibrated using the first order conditions of the first step of the PMP calibration process (Appendix B.2). The rest of the parameters used in the linear costs are the calibrated Lagrange multipliers $\lambda_{water}, \lambda_{land}$, associated to the observed water and land allocation per crop calibration constraints, respectively. Variable costs are linear and include cost of land ($\omega_{i,land}$) and the unit price of surface water ($\omega_{SW,t}$). In contrast the volumetric cost of groundwater pumping is given by $\omega_{GW,t}$, which is a function of price of electricity ($\omega_{E,t}$), the groundwater depth (GWD_t) and other parameters related to the characteristics of the wells (Appendix B.3). Additionally, a per cubic meter u_t^{GWF} pumping fee can be implemented on top of the pumping cost.

The PMP net revenue maximization problem is subject to land and water availability as well as the quantitative controls of groundwater and land use that are provided by the adaptive policies (Section 3.4). Equation 3.2 is a total land restriction where u_t^{TL} is the total land use

control that can be implemented in a year t. Equation 3.3 is an upper boundary perennial crops restriction u_t^{PL} that influences the expansion or reduction of land allocated to perennial crops, where $PC \in \{$Almonds and Pistachios, Subtropical, Other Deciduous and Vine$\}$. Maintaining the perennial crops removals to what has been observed historically, we add a perennial removal constraint (Equation 3.4) such that no more than 5 percent from the previous year perennial crops land can be allocated to other crops or taken out of production. Equation 3.5 is a mass balance restriction for each crop water use from both surface water and groundwater. Equation 3.6 is the surface water availability ($b_{SW,t}$) restriction. Equation 3.7 is the total groundwater pumping restriction where u_t^{GWP} is the maximum allowed groundwater pumping decision. u_t^{GWF}, u_t^{TL}, u_t^{PL}, u_t^{GWP} are the four management decision that this study assess formulated in the adaptive control policy (Section 3.4). Finally, we allow up to 2% deficit irrigation through Equation 3.8 which allows reductions in the applied water per unit of land ($\bar{x}_{i,water}$) with respect to baseline calibration conditions.

Groundwater Depth Response Function

The dynamics of groundwater in the San Joaquin Valley depend on many geological, hydrological, climate and human components. To represent the dynamics of groundwater depth level, we emulate the physical model Fine Grid California Central Valley Groundwater-Surface Water Simulation Model (C2VSIM-FG version 1.01) (DWR, 2021a) using a response function. C2VSIM-FG has a finite element grid of more than 35,000 elements for California's Central Valley California, and each element is able to link land surface, surface water and ground-water. The model detailed historical data (i.e., cropland use, crop water demand, surface water diversions, precipitation, soil moisture) to inform the simulations process. C2VSIM-FG simulates the period from 1973 to 2015 at a monthly time step. Water budgets are generated for each element in the grid including groundwater pumping and groundwater depth and can be post-processed to create water budgets for defined boundaries (group of elements). We use the water budget generated for the Semitropic Water Storage District's boundary as represented on the finite element grid.

From C2VSIM-FG outputs we used the weighted-average groundwater depth level to agricultural pumping. Since the economic model simulates farmers' decisions at a yearly time step, we use the groundwater depth change from the beginning of the water year (October) to the end of

the water year and irrigation season (September), and the total agricultural groundwater pumping in a water year to calibrate the response function. Figure B3 shows the simulated groundwater depth and agricultural pumping from C2VSIM-FG at the end of each water year from 1972-2016.

The groundwater depth change response function was calibrated using a Bayesian linear regression (Appendix B.4). The response function predicts the groundwater depth change each year as a function of total agricultural pumping. As shown by Equation 3.9, the ground water depth level at the beginning of the water year t (GWD_t) is calculated as the sum of the groundwater depth level at the beginning of the prior water year t-1 (GW_{t-1}) and the median of the predictive posterior distribution for groundwater depth change ($\overline{\Delta GWD}_{t-1}$) estimated at the end of the water year t-1. By embedding this function into the economic model defining the pumping cost as a function of the groundwater depth enables our ability to directly model the feed-back between food production and groundwater levels. In Appendix B.5 we show the capacity of the coupled hydro-economic model to replicate historical cropland, water allocation and groundwater depth dynamics.

$$GWD_t = GWD_{t-1} + \overline{\Delta GWD}_{t-1} \tag{3.9}$$

3.3.2 Stochastic time series

To run the model dynamically, we build Monte Carlo time series for economic and hydrologic conditions that are used to force the HEM. Each time series starts at $t_1 = 2016$. In our analysis, we included simulated surface water supplies to the irrigation district (Figure B12) from the California's Food-Energy-Water System simulation model (CALFEWS) (Zeff et al., 2021). These were simulated with down-scaled data from seven of the ten Global Circulation Models (GCMs) suggested by Pierce et al. (2018) (CCSM4, MIROC5, CanESM2, CNRM-CM5, GFDL-CM3, HadGEM2-CC and HadGEM2-ES), and using the Representative Concentration Pathway (RCP) 4.5 (moderate scenario) and 8.5 (high emissions scenario).

Additionally, we model uncertainties for the economic variables and calibration parameters of the economic model, summarized in Table 3.1. Crop prices $p_{i,t}$ were randomly sampled using the historical data from 1980 to 2020 (USDA, 2020) and the price of electricity ($\omega_{E,t}$) was sampled from the historical (2008-2021) reported by the Pacific Gas and Electricity Company (PG&E) for small and large agricultural users. The price of surface water ($\omega_{SW,t}$) is correlated to

the surface water deliveries depending on the water-year type(wet or dry) and randomly sampled from reported rates in the district using surface for different water supply conditions. All prices were adjusted for inflation using the consumer price index based on the year 2016. Finally a sample from the posterior distribution of the calibration parameters θ_i is sampled.

Table 3.1: Data Sources for Monte Carlo Time Series

Variable	Symbol	Units	Source
Crop prices	p_i	\$/ton	USDA (2020)
Price of electricity	$\omega_{E,t}$	$\$/Kwh$	PG&E (2021)
Price of surface water	$\omega_{SW,t}$	$\$/m^3$	SWSD reports
Surface water supply	$b_{SW,t}$	m^3	Zeff et al. (2021)
Calibration parameters	θ_i	-	PMP Calibration

3.4 Dynamic and Adaptive Decisions

Searching for adaptive groundwater management policies using DPS consists of finding parameters of the control policy function that yield the optimal control alternatives that compose the trade-offs between the groundwater sustainability and economic objectives. Different parametric functions can be used to model control policies, including linear, polynomial, neural networks, decision trees and radial basis functions (Giuliani et al., 2021; Giuliani et al., 2014). In this study, we used cubic radial basis functions (RBFs) to accommodate the complexity of the dynamic GSA level decisions that are coordinated and responsive to surface water supply conditions, crop-land decisions, and the groundwater depth observed at the beginning of a water year. The four decisions that comprise the control policy are: the groundwater pumping fee (GWF), total land restriction (TL), perennial cropland restriction (PL) and groundwater pumping restriction (GWP).

3.4.1 Direct Policy Search

Dynamic land and groundwater management decisions made at every yearly step t are represented by the vector u_t^D where $D \in \{GWP, TL, PL, GWF\}$ represent the four possible decisions. The control policy in Equation 10 equates to the outputs of a policy P^D, which is a mathematical function with two vector inputs: the structural parameters of the RBFs (ψ^D) and

system-state information vector ($I_{t'}$). The state information variables in $I_{t'}$ represent key components of the food-water system are observed in the current water year t or previous water year $t-1$.

$$u_t^D = P^D(I_{t'}|\psi^D) \tag{3.10}$$

In direct policy search, the use of RBFs has been shown to be an efficient way to represent complex sequential decisions. Recent applications include lake pollution control (Quinn et al., 2017), reservoir operations (Giuliani et al., 2021; Giuliani et al., 2014; Zatarain Salazar et al., 2017), sea-level rise protection (Garner and Keller, 2018), flood risk management (J. Wang and Johnson, 2023), and financial risk management in water-energy systems (Gupta et al., 2020; Hamilton et al., 2022). For this study, we define the control policy function P^D as a set of cubic radial basis functions given by Equation 3.11.

$$u_t^D = \phi^D \left(\sum_{m=1}^{M} w_m^D \sum_{j=1}^{J} \left| \frac{[I_{t'}]_j - c_{j,m}}{r_{j,m}} \right|^3 \right) \tag{3.11}$$

In Equation 11, ϕ^D is an outer function, w_m^D is the weight of M cubic radial basis functions. The weights can have values $0 \leq w_m \leq 1$ and are subject to $\sum_{m=1}^{M} m_m^D = 1$. The four decisions in the control policy share the same RBFs structure; hence the information vector $I_{t'}$ is shared for all decisions. Additionally, $c_{j,m} \in [-1, 1]$ and $r_{j,m} \in (0, 1]$ are the center and radius respectively shared by all the RBFs. $I_{t'}$ in Equation 3.12 is a vector with system state variables that inform the policies, where $\overline{GWD}_t$ is the normalized level to groundwater at the beginning of the year, $\overline{PCL}_{t-1}$ is the normalized area devoted for perennial crops production in the year $t-1$. $\bar{b}_{SW,t}$ is the normalized surface water available in year t. Normalization was performed using k^{GWD}, k^{TL}, k^{SW} to obtain $\overline{GWD}_t$, $\overline{PCL}_{t-1}$, $\bar{b}_{SW,t}$ respectively summarized in Table 3.2.

$$I_{t'} = [\overline{GWD}_t, \overline{PCL}_{t-1}, \bar{b}_{SW,t}] \tag{3.12}$$

Table 3.2: Normalization factors used in the control policy

Variable	Symbol	Units	Value
Normalization for cropland	k^{TL}	Kha	62
Normalization for groundwater pumping	k^{GW}	Mm^3	732
Normalization groundwater depth	k^{GWD}	m	198
Normalization for pumping fee	k^{GWF}	\$/m^3	0.5
Normalization surface water	k^{SW}	Mm^3	208

The function ϕ^D in Equation 3.11 can consist on two functions, a scaling function $\phi^{D,N}$ and constraint function $\phi^{D,C}$. z_t in Equation 3.13 is the argument to the ϕ^D, where $\phi^{D,N}$ is used to first constrain z_t values to lie between 0 and 1 and later scale them to the specific units of each irrigation management policy using the normalization factors in Table 3.2. $\phi^{D,C}$ is used to constrain the values of the candidate policy actions to be realistic considering other water balance and land constraints.

$$u_t^D = \phi^{D,C}(\phi^{D,N}(z_t)) \tag{3.13}$$

For the groundwater pumping restriction policy (u_t^{GWP}), Equation 3.14 scales the groundwater that farmers will have available to pump between zero and the pumping capacity of the district k^{GWP} (maximum observed pumping). Equation 3.15 constrains the groundwater pumping to be at least the difference between the water demand by perennial crops of the year $t-1$ and the surface water available in the year t.

$$z'_t = \phi^{GWP,N}(z_t) = k^{GWP} max(min(z_t, 1), 0) \tag{3.14}$$

$$u_t^{GWP} = \phi^{GWP,C}(z'_t) = max(z'_t, \sum_{i \in PCL} x_{i,water_{t\text{-}1}} - \ b_{SW,t}) \tag{3.15}$$

In Equation 3.16, where the scaling function ($\phi^{TL,N}$) results in the total land available that farmers can produce in the district for the year t and can have values between zero and the

total land in the district k^{TL} (maximum observed produced land). Additionally, Equation 3.17 constrains the total land decision to be at least the land used by perennial crops in the the year $t-1$.

$$z'_t = \phi^{TL,N}(z_t) = k^{TL} max(min(z_t, 1), 0) \tag{3.16}$$

$$u_t^{TL} = \phi^{TL,C}(z'_t) = max(z'_t, \sum_{i \in PC} x_{i,land_{t\text{-}1}}) \tag{3.17}$$

Equation 3.18 governs actions associated with perennial crops planting restriction (u_t^{PL}), where $\phi^{PL,N}$ results in the total land that can be allocated to perennial crops production with value between zero and the total land available in the district (k^{TL}). In Equation 3.19, $\phi^{PL,C}$ constrains the available land for perennial crops to be at least 95% of the previous year perennial crops land, and it limits the expansion of perennial crops to no more than 5% relative to the previous year $t-1$. These restrictions are applied to ensure that solutions of the perennial crop acreage control policy are realistic to what has been observed the region.

$$z'_t = \phi^{PL,N}(z_t) = k^{TL} max(min(z_t, 1), 0) \tag{3.18}$$

$$u_t^{PL} = \phi^{PL,C}(z'_t) = \begin{cases} \sum_{i \in PC} x_{i,land_{t\text{-}1}} * 1.05, & \text{if } \; z'_t > \sum_{i \in PC} x_{i,land_{t\text{-}1}} * 1.05 \\ \sum_{i \in PC} x_{i,land_{t\text{-}1}} * 0.95, & \text{elif } \; z'_t < \sum_{i \in PC} x_{i,land_{t\text{-}1}} * 0.95 \\ z'_t, & otherwise \end{cases} \tag{3.19}$$

Finally for the pumping fee control action (u_t^{GWF}), the function ϕ^{GWF} in Equation 3.20, scales the groundwater pumping fee that can have values between [0,k^{GWF}]. k^{GWF} is set to be $\$0.5/m^3$, hence the upper boundary of the pumping fee is 0.5 USD per cubic meter. This fee sums to the groundwater pumping cost in the objective function of the economic model (Equation 1).

$$u_t^{GWF} = \phi^{GWF,N}(z_t) = k^{GWF} max(min(z_t, 1), 0) \tag{3.20}$$

The dynamic control policy is represented by the set of Equations 3.11 to 3.20, where the vector of structural parameters $\psi = [w^D, c, r]$ of the RBFs is optimized. Since the information vector $I_{t'}$ of size J is shared across decisions in M number of RBF's the vectors of centers (c) and radii (r) are equal to $c = [c_{0,0}, ..., c_{J,M}]$ and $r = [r_{0,0}, ..., r_{J,M}]$.

3.4.2 Bi-level Optimization Problem

A core contribution of this study is the bi-level optimization framework illustrated in Figure 3.2. The Borg MOEA (Gupta et al., 2020; Hadka and Reed, 2013) is used to optimize the vector of structural parameters in the RBFs (Ψ). Each set of structural parameters define a control policy (Section 3.4) or set of annual groundwater management decisions (u^D) that are assessed using the HEM (Section 3.3.1) across N sampled Monte Carlo times series of T years (Section 3.3.2). Within its evaluations, the HEM then finds optimal land and water allocations for the first five years of each time series. At year t=5, the HEM initiates the implementation of the DPS-based management decisions and the evaluation of the overall evaluation of the performance objectives. This framework provides a multi-scale abstraction of dynamic and adaptive flexible groundwater management that has direct relevance to addressing the sustainability challenges discussed in Section 3.2. The bi-level optimization clarifies the performance trade-offs across the five objectives that represent the groundwater sustainability and economic goals of the GSA.

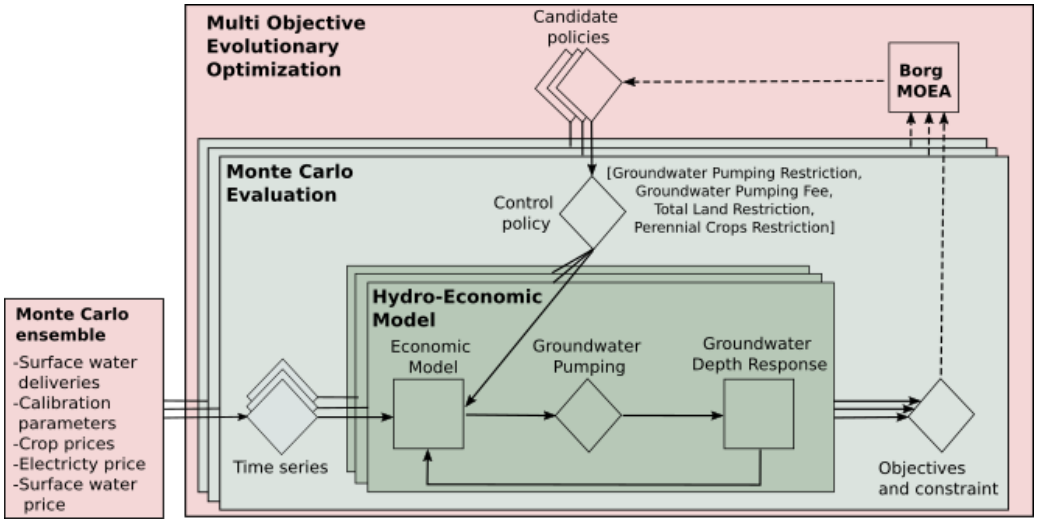

Figure 3.2: Bi-level optimization problem schematic adapted from Hamilton et al. (2022). Rectangles represent the modules that contain optimization and simulation models (squares) and inputs/outputs (diamonds). Dashed arrows depict the Borg MOEA feed-back process where the values of objectives and constraint are from performance metrics of HEM result of an implemented control policy.

The first level optimization focuses on the multi-objective evolutionary search to identify the trade-offs across the five performance objectives where the decision variables are the control policy parameters of the RBFs in the vector Ψ, used to parameterize the control policy.

$$\underset{\Psi}{argmin} = (-O_{avgrev}(\Psi), O_{avgdepth}(\Psi), -O_{worstrev}(\Psi), O_{worstdepth\Delta}(\Psi), -O_{depthrel}(\Psi)) \tag{3.21}$$

The first objective (O_{avgrev}) is to maximize the average total revenues from the average total net revenue of N ensemble realizations with T years. This objective represents the economic objective of farmers for revenue maximization. A lower boundary constraint for this objective is defined to achieve at least an average total revenue greater or equal than \$11 billion. This restriction constrains the algorithms from finding unrealistic policies far from farmers preferences.

$$O_{avgrev} = \frac{1}{N}\sum_{n=1}^{N}(\sum_{t=5}^{T}\pi_{n,t}) \tag{3.22}$$

$$O_{avgrev} \geq 11,000 \tag{3.23}$$

The second objective is the minimization of the average groundwater depth in meters below surface (m bls). The average groundwater depth is calculated over the years of management implementation (T-5) for each Monte Carlo realization, and then the average of these are taken over the N sampled Monte Carlo realizations.

$$O_{avgdepth} = \frac{1}{N}\sum_{n=1}^{N}(\frac{1}{T-5}\sum_{t=5}^{T}GWD_{n,t}) \tag{3.24}$$

The third objective is to maximize the 5th percentile of the minimum profits attained across the Monte Carlo samples. This metric represents a *max-min* objective formulation that is used to inform decision makers about the worst case 5th percentile of profits achieved in a given year. Even though there are economic factors included in the stochastic ensemble that can be drivers of low economic revenues, management decisions can be the main factors driving poor profits particularly during dry years, as shown by Rodríguez-Flores et al. (2022).

$$O_{worstrev} = Q5_N\left[\min_{t\in(5,...,T)}[\pi_{n,t}]\right] \tag{3.25}$$

The fourth objective is to minimize the 95th percentile of maximum groundwater depths change (m bls) attained across the Monte Carlo samples. This objective represents a *min-max* objective formulation focused on identifying the outcomes with significant increases in groundwater depth. The maximum groundwater depth level change is evaluated over each annual management implementation period and the Q95 operator takes the 95th percentile over all of the sampled Monte Carlo realizations.

$$O_{worstdepth\Delta} = Q95_N \left[\max_{t \in (5,\ldots,T)} [\overline{\Delta GWD}_t] \right] \tag{3.26}$$

As explained in Section 3.2, groundwater management allows groundwater depth to fluctuate in the marginal of operational flexibility. During dry years the groundwater depth can go above the groundwater level requirement but not beyond the minimum threshold with the expectation that in wet years it will recover. Thus, the fifth objective is to maximize the average fraction of years (reliability) that the groundwater depth is at the level requirement (GWD^{SGMA}) or below. For illustration purposes we used the 2015 groundwater level from C2VSim-FG as a measurable objective as it was the deepest year in the 2012-2016 drought Lund et al., 2018. Additionally, we included a constraint (Equation 3.28) that the reliability must be at least 20% (i.e., one of every five years).

$$O_{depthrel} = \frac{1}{N(T-5)} \sum_{n=1}^{N} (\sum_{t=5}^{T} \tau_{n,t}) \; where \; \tau_{n,t} = \begin{cases} 1, & GWD_{n,t} \leq GWD^{SGMA} \\ 0, & GWD_{n,t} > GWD^{SGMA} \end{cases} \tag{3.27}$$

$$O_{depthrel} \geq 0.2 \tag{3.28}$$

3.4.3 Robustness and Scenario Discovery Analysis

The bi-level multi-objective optimization problem presented in the prior section provides a direct means for understanding the management trade-offs for the SWSD GSA through analysis of a high quality approximations of the resulting Pareto front. Solutions in the Pareto front are each distinct control policies that prioritize a subset of objectives. Stakeholders can then choose acceptable policies based on their preferences. However, it is important that these policies can perform well in alternative SOWs beyond those used in the optimization that can change the decision makers' preferences from their initial expected trade-offs performance (Herman et al., 2015). Thus, we reevaluate these policies across a broader sampling of deep uncertainties (Section 3.3.2) to quantify their robustness. Different metrics can be used to measure the robustness of each control policy

which inherently represents a variety of farmers' and water managers' acceptability thresholds and their perception of risk (McPhail et al., 2018).

All of policies from the Pareto approximate set, are re-evaluated for deeply uncertain SOWs using N=1,000 sampled Monte Carlo realizations each covering T=30 years. Each sampled time series has a set of surface water supplies, crop prices, electricity price, surface water price and calibration parameters. For this study, we selected the domain criterion satisficing metric (Schneller and Sphicas, 1983) that quantifies the fraction of scenarios (rate of success) that achieve a minimum performance threshold, from a larger set of SOWs beyond those used in the EMODPS search. To illustrate this process, we defined an example of performance criteria and rates of success, shown in Table 3.3, all of which a control policy must achieve in N resolutions and 25 years of management implementation to be considered robust. These performance criteria include a minimum total revenue of $12,500 million (yearly expectation of 60% from the average yearly revenue between 2011 and 2015) and a groundwater depth requirement that the flexible management is expected to reach during wet years (depth observed in 2015). Additionally, a minimum perennial trees land in a year is defined to be at least 60% from the observed in 2015, as a metric of the reliability of keeping perennial trees at that minimum threshold. This framework to asses robustness is flexible and can support other definitions of robustness subject to stakeholders preferences.

Table 3.3: Performance Criteria for selection of robust policies

Criteria	Threshold	Units	Rate of Success
Minimum Total Revenue	> 12,500	M USD	$\geq$ 85%
Groundwater Depth Requirement	< 92	m bls	$\geq$ 20%
Minimum Perennial Trees Land	> 19,896	hectares	$\geq$ 85%

In order to identify the factors that cause solutions to fail to meet the robust performance criteria or poor performance, we use scenario discovery as is commonly employed in robust decision making frameworks (Kasprzyk et al., 2013; Lempert and Groves, 2010). For this study, we use the Patient Rule Induction Method (PRIM) (Friedman and Fisher, 1999; Kwakkel and Jaxa-Rozen, 2016), a statistical learning algorithm that provides factor mapping and visualization to identify uncertain input ranges that result in an outcome of particular interest (e.g., failing or succeeding in meeting the performance requirements). The PRIM algorithm classifies scenario boxes that capture values of key factors that cause a policy to succeed or fail in the meeting the performance requirements that define robustness (see Table 3.3), using the results from SOWs used in the robustness analysis. Using the exploratory modeling and analysis workbench (Kwakkel, 2017), we perform a feature scoring using the extra trees algorithm (Geurts et al., 2006) to identify what the most important uncertainties that drive candidate policies' vulnerabilities.

3.5 Computational Experiment

The search for optimal RBFs parameters in EMODPS is a non-convex problem (Giuliani et al., 2016) solved in this study using stochastic multi-objective evolutionary search. MOEAs are a popular tool for multi-objective optimization that iteratively improve a population of possible solutions until the population reaches a high quality representation of the Pareto front composed of the non-dominated solutions (Coello et al., 2007). For this study, we use the Borg MOEA (Hadka and Reed, 2013), a self-adaptive algorithm that employs probabilistic operators as ϵ-dominance, adaptive population sizing and time continuation through ϵ-progress. The Borg MOEA has been shown to have better time efficiency, scalability, and less sensitivity to its parameterizations in comparison to other MOEAs across a wide array of applications in the literature (Al-Jawad and Tanyimboh, 2017; Gupta et al., 2020; Reed et al., 2013; Seyedashraf et al., 2023; Zatarain Salazar et al., 2017).

Since the Borg MOEA is a stochastic algorithm, we estimate Pareto-front solutions using ten different random seeds (i.e., random initializations of the population) using the master-worker parallel configuration of Borg (Hadka and Reed, 2015). All the Borg MOEA parameters are set to the default values (Hadka and Reed, 2013) and ϵ-values (resolution) for each objective are summarized in Appendix B Table B3. The quality of the algorithm's runtime dynamics are evaluated through its hypervolume progress (Hadka and Reed, 2012) to prove that the search is reliable and effective given the number of function evaluations, shown in the Figure B13 of appendix B.

The economic model (Section 3.3.1) was formulated using the Python package Pyomo (Hart et al., 2011) and solved using the non-linear programming solver IPOPT (Wächter and Biegler, 2006). The decision variables in the economic model are the allocation of land and water (surface water and groundwater) to seventeen crop groups resulting in a total of 68 decision variables for each time step t. Additionally at each time step the groundwater depth change was estimated using the posterior predictive distribution of the parameters in the calibrated groundwater depth response function.

We performed the bi-level optimization process for an ensemble of N = 100 Monte Carlo realizations and T = 30 years for 50,000 candidate policy trials (function evaluations). One limitation of the bi-level optimization is the high computational demand that limited the number of sampled Monte Carlo realizations and function evaluations, however as shown the runtime analysis of hypervolume performance random seed consistently converge in approximately half of the 50,000 evaluations (Appendix B.7). A structure of M=4 RBFs (Equation 3.11) was selected given its good performance, resulting in 40 decision variables in the vector Ψ to be optimized with Borg MOEA. The selected Pareto-set with the best single seed approximation set was later validated by re-evaluating the solutions on a larger sampled set of independent Monte Carlo samples of size N = 1,000 to verify that reference set is stable. Results from the validation are shown in Figure B14 of the Appendix B. To inform the robustness analysis and scenario discovery we used a Monte Carlo ensemble of N = 1,000 expanding the assumed range of crop prices, surface water price and electricity price by %20 relative to the historical. All the computational experiments were performed using the MERCED cluster of the University of California Merced.

3.6 Results and Discussion

3.6.1 Policy Trade-offs and Dynamics

Figure 3.3 shows the selected Pareto-approximate set that spans different trade-offs among the five objectives in the problem. In the figure, the plotted location, size and color of each triangle represents the objective values associated with selected control policies (Ψ values). The size of the triangle depicts the 95th percentile of the maximum groundwater depth changes in a year, and the color gradient depicts the 5th percentile of the minimum revenue in a year. The star represents the hypothetical ideal solution that would allow for the smallest average groundwater depth while providing the highest possible revenue across the sustainable management implementation period. Characteristic behavior emerges particularly as average groundwater depth decreases, economic revenues (and minimum revenues) decrease as well. Average groundwater depth decreases also correspond to an increase in the reliability of meeting the groundwater level requirement. However, for some policies to attain one hundred percent reliability, they significantly limit groundwater pumping, including during dry years, which results in significantly lower total and minimum revenues. These solutions have strong reductions and limit flexibility in the management policies, potentially reducing the SWSD's preferences towards them. The maximum groundwater depth change (size of the triangles) attains values as those that have been observed in the historical record (Figure B3), highlighting the capacity of the policies to avoid larger depth changes even in drier future conditions. However, as expected the trade-offs illustrated in Figure 3.3 show that as the maximum depth changes reduce the Pareto-front shifts downwards due to lower average revenues.

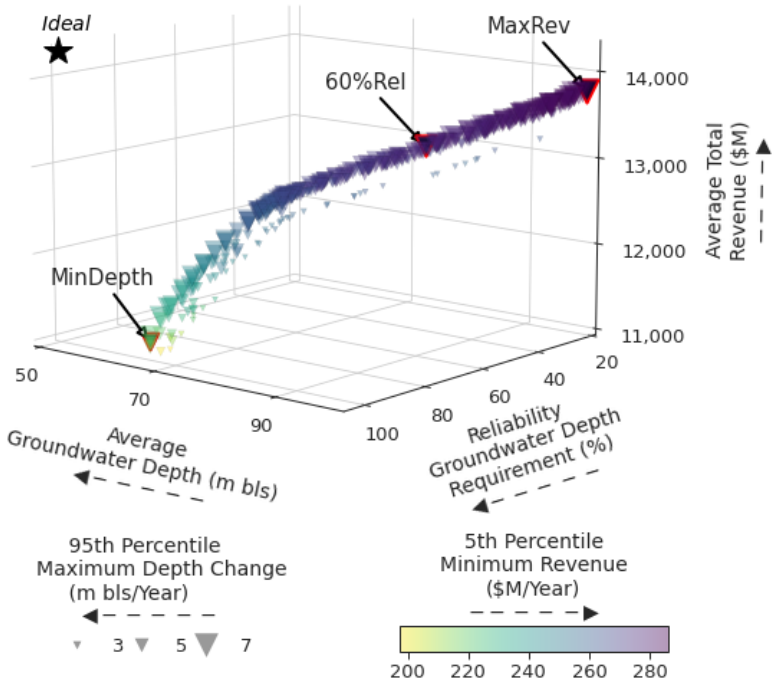

Figure 3.3: Pareto approximate set from the EMODPS experiment

To assess the adaptive capacity of the resulting policies to manage uncertain surface water supplies and economic conditions, we highlight three policies that capture a broad range of candidate preferences that stakeholders may hold when selecting a preferred solution from in the Pareto approximate shown in Figure 3.3. The policies selected for further analysis capture largest average total revenue (MaxRev), the lowest average groundwater depth (MinDepth), and a compromise with 60% average reliability of meeting the groundwater depth requirement (60%Rel). These solutions contain four different DPS-based irrigation management policies (Section 3.4) that would adapt under system state conditions. We asses their performance using the driest, wettest and largest standard deviation from the Monte Carlo sampled SOWs used in the evolutionary search (Section 3.3.2). We allow PMP to run without any DPS control policy for the first five years followed by a 25 years period of adaptive management based on simulating the DPS control policies implementation.

Figure 3.4 shows the temporal evolution of the dynamic management decisions and their

performance in the SWSD's food-water system using the SOW with the largest standard deviation on surface water deliveries (CANESM2 8.5). This surface water supply scenario captures interesting regional dynamics with interspersed dry and wet periods. In the initial 5 years before the management policies are implemented the perennial cropland expands with a reliance on groundwater pumping due to reduced surface water Figure 3.4 (a), and results in increasing the groundwater depth as shown in panel (g). Figure 3.4 panels (b)-(e) shows how the irrigation management decisions evolve, illustrating the dynamic and adaptive performance of the selected control policies. The total land planting restriction in Figure 3.4 (e), is the only decision that shows a non-implementation behavior for the selected policies, given that other decisions regulate land use via groundwater pumping panel (f) that result in a better performance of the system. In general, the 60%Rel and the MaxRev solutions show similar policy control behaviors, but with different magnitudes of restrictions and ground water pumping fee policies. Figure 3.4 panel (b) demonstrates that all three solutions implement groundwater restrictions during the initial stages of management. The solution with the lowest average groundwater depth (MinDepth) implements a continuous restriction that only relaxes during wet years. Policies show a declining land allocation to perennial crops from the initial area in Figure 3.4 panel (i). Given the flexibility that annual crops provide to the water budget, the three solutions decrease annual crops acreage at early stages of implementation with expansion during wet periods, shown in panel (j). These results confirm that sustainable groundwater management benefits from reducing the hard water demand imposed by perennial tree crops which has also been suggested in other studies (Mall and Herman, 2019; Qin et al., 2019) and an overall cropland reduction (Hanak et al., 2019).

During dry years, the control policies allow pumping to offset deficits in surface water, however none of the policies do not reach the region's suggested pumping capacity and limit pumping at a threshold (e.g., 460 Mm^3 for the MaxRev solution) as shown in Figure 3.4, which complies with the suggested safe yield by Miro and Famiglietti (2019) and MacEwan et al. (2017). Figure 3.4 panel (f) shows that reductions in planting perennial trees crops through the control policies use of perennials planting restriction. Control policies establish a pumping fee for the full implementation period, however use of a pumping fee peaks during wet years to limit the expansion of annual crops and maximize groundwater recovery. Implementing a pumping fee, illustrated in Figure 3.4 panel (c), can improve irrigation efficiency and control the expansion of cropland, particularly an-

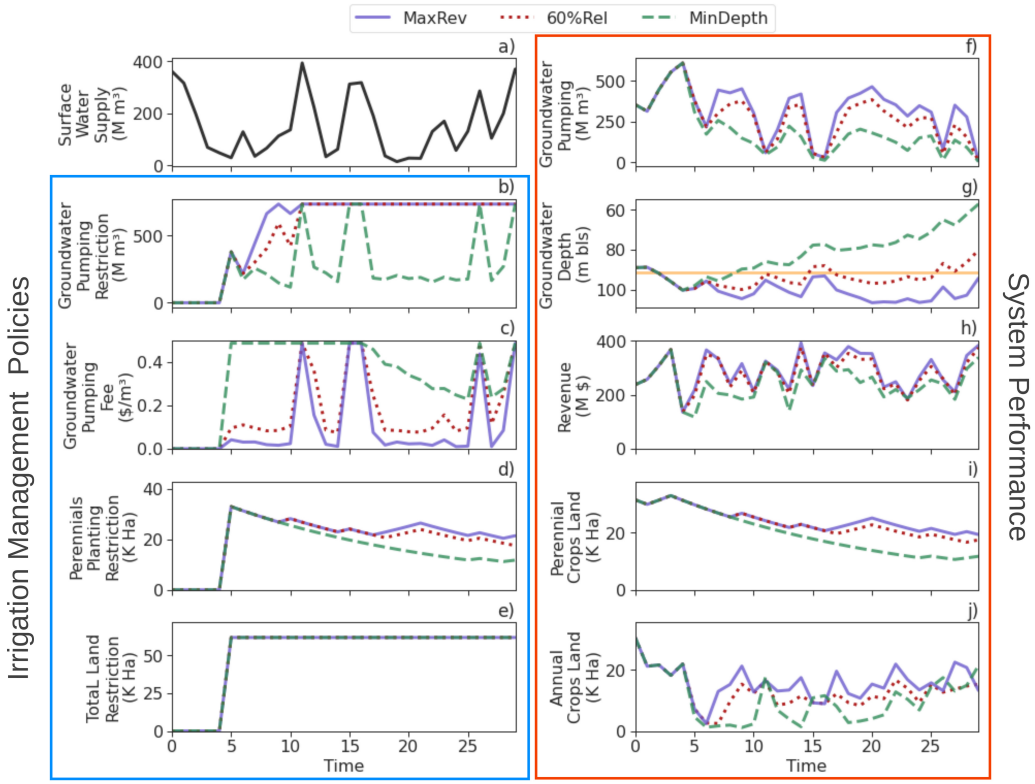

Figure 3.4: Performance of the dynamic and adaptive irrigation management policies and hydro-economic model performance over a 30 year realization period with 25 five years implementation of irrigation management decisions. Panel (a) shows the surface water deliveries. Panels (b)-(e) show the dynamic decisions in the control policy. Panels (f)-(j) show the performance of the food-water system. The orange line in Panel (g) depicts the groundwater depth requirement used in the experiment.

nual crops, during wet and dry years as suggested by Stone et al. (2022), Graveline (2020), and Khan and Brown (2019). The examined policy solutions suggest a pumping fee between $\$0.1/m^3$ and $\$0.2/m^3$ that increases up to $\$0.5/m^3$ during wet years to effectively encourage groundwater recovery.

Exploring the dynamic and adaptive behaviors of the three selected solutions along the Pareto approximate set distinguishes why they differ in their performance and provides insights into the drivers tacit to potential trade-offs of implementing the different management decisions. As shown in Figure 3.4 panel (g) implementing the MinDepth control policy results in a constant recovery of the groundwater depth, thus a larger groundwater depth requirement reliability. However, the MaxRev and %60Rel policies more actively exploit wet years and prescribe higher cropland than in the MinDepth solution. One key insight is that all of the control policies stopped the decline in groundwater depth observed in the historical record, allowing the groundwater depth to reach a maximum depth level where is feasible to recover and meet the groundwater depth requirement. Depending on the control policy, the largest groundwater depth and the number of years that achieve the measurable objective change. This suggests GSAs have the potential to achieve well designed flexible management strategies that maintain groundwater depths at levels where its capable post-drought recoveries. However, policies need to be flexible enough to allow groundwater depth to recover during wet years contrary to what has been observed during the past decades (Alam et al., 2021; Liu et al., 2022). Evolution of irrigation management policies and system performance in wet and dry conditions are shown in Figures C15-C16.

3.6.2 Robustness and Scenario Discovery Analysis

As explained in Section 3.4.3, solutions in the Pareto-approximate set (Figure 3.5) are re-evaluated in 1,000 alternative SOWs and their robustness is assessed using the three preference criteria and success requirements, summarized in Table 3.3. Filtering the initial full Pareto set for those solutions that comply with the three performance requirements yields twelve robust solutions illustrated in Figure 3.5. This family of solutions are clustered in the trade-offs space of the Pareto approximate set where reliability lies between 51% and 62%, average groundwater depth of 90 meters below surface, average total revenues between $13,291 and $13,382 million, and a minimum revenue per year between $272 and $279 thousand. These solutions achieve different levels of

maximum depth change, ranging from 4 to 6.5 m below surface.

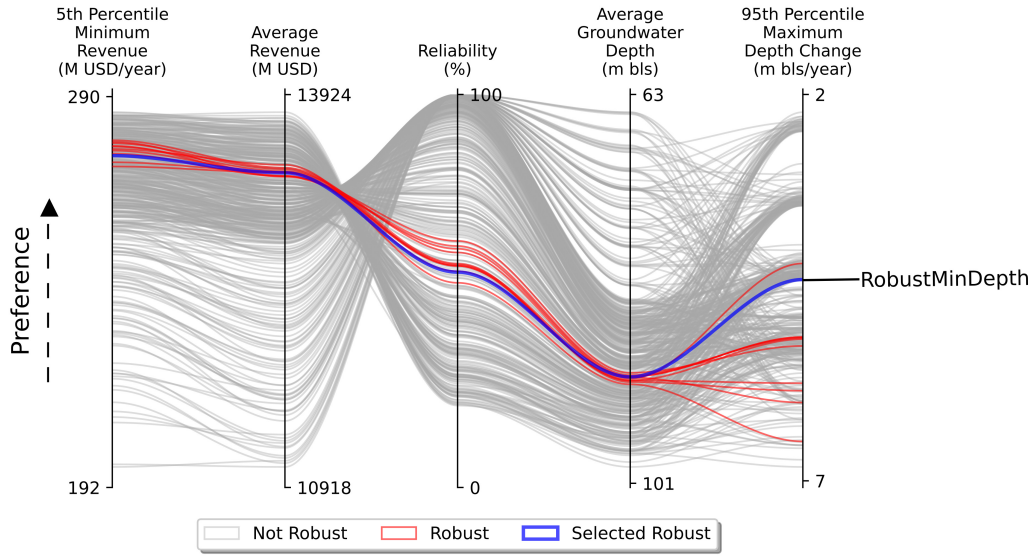

Figure 3.5: Highlighting policies from the Pareto approximate set shown Figure 3.3 that are classified as being robust policies (shown in red) as well as selected robust policy for further analysis (shown in blue). Policies in the Pareto approximate set that did not meet the satisfying criteria are shown in grey to provide the full trade-offs context.

For further analysis, we select the robust solution with lowest average minimum depth (RobustMinDepth) based on their re-evaluation across 1,000 alternative SOWs, depicted in blue in Figure 3.5. Consistent with the analysis in Section 3.6.1, the performance of the RobustMinDepth solution is assessed using the same random samples under dry, wet and largest standard deviation water supply scenarios. Figure 3.6 shows the performance of the RobustMinDepth solution under a scenario with the largest standard deviation on surface water deliveries (CANESM2 8.5). Compared to the policies analyzed in the previous section (Figure 3.4), RobustMinDepth performance is located between the performance of the MaxRev and 60%Rel solutions. RobustMinDepth allows higher revenues than the 60%Rel solution while meeting the groundwater depth requirement in all the water supply scenarios. In panel (g) from Figures 3.4 and 3.6 we can observe that compared to the MaxRev solution, RobustMinDepth does achieve the groundwater depth requirement in wet periods and achieves higher cropland compared to the 60%Rel solution . Additionally, RobustMin-

Depth solution achieves the groundwater level requirement in the driest scenario (shown in Figure B17) where the requirement is not achieved by MaxRevs in any implementation year. In the wet scenario (CNRM-CM5 8.5), shown in Figures B.18 in Appendix B, the RobustMinDepth solution achieves higher cropland of both annual and perennial crops than the 60%Rel solution (Figure B16).

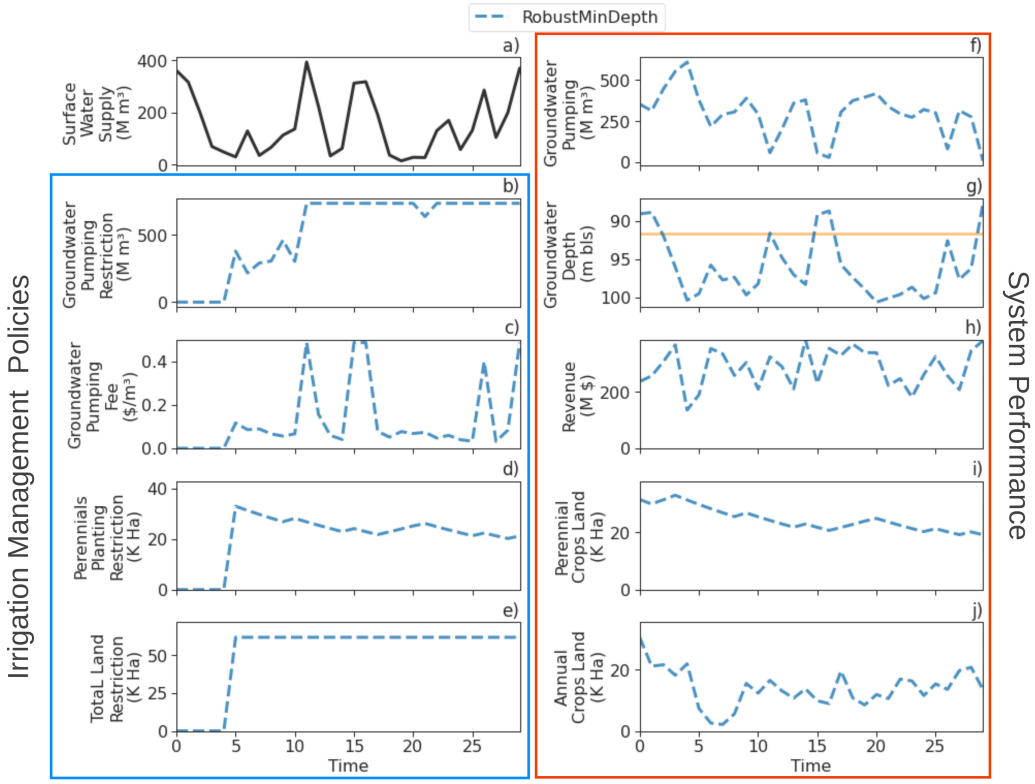

Figure 3.6: Performance of the selected dynamic and adaptive robust policies and hydro-economic model performance over a 30 year realization period with 25 five years implementation of irrigation management decisions. Panel (a) shows the surface water deliveries. Panels (b)-(e) show the dynamic decisions in the control policy. Panels (f)-(j) show the performance of the food-water system. The orange line in Panel (g) depicts the groundwater depth requirement used in the experiment.

Implementation of irrigation management policies between the selected robust solution

and those from the previous section shows similarities in the total land restriction (Figure 3.4 and 3.6 panel (e)), and decrease in perennial cropland (Figure 3.4 and 3.6 panel (d)). RobustMinDepth restricts perennial crops in the same magnitude as the MaxRev solution. The largest difference in the performance of irrigation management policies between the RobustMinDepth solution and the selected non robust polices is that RobustMinDepth implements a larger pumping restriction in early stages of implementation (Figure 3.6 panel (b)) than MaxRev and 60%Rel solutions (Figure 3.4 panel (b)). This results in lower annual cropland (Figure 3.4 and 3.6 panel (j)) and larger groundwater recovery (Figure 3.4 and 3.6 panel (g)) during the first years of implementation that later enables an increase in annual crops compared to the 60%Rel solution. This management of annual crops results in more optimal economic results. This policy also implements a groundwater pumping fee that controls pumping where the pumping fee is the same during wet periods as MaxRev but is higher in other years, shown in panel (c) of Figures 3.4 and 3.6. From the robust policy performance we can conclude that early recovery of groundwater levels can benefit the flexibility of future cropland allocation of annual crops and lower the reliability of higher pumping fee.

Beyond finding differences in the dynamic and adaptive behavior of different robust policies, another key question is what are the dominant drivers of their robustness as well as their ranges that lead to success or failure. In Figure 3.7, we further analyze what uncertainties dominantly control the ability of the RobustMinDepth solution to meet the three robustness performance requirements. The figure shows the combination of the three most important parameters, using the extra trees feature scoring (Figure B19 in Appendix B), that led the policy to succeed in meeting the performance criteria. Though perennials land is not an uncertain input but rather a PMP output (Section 3.3.2), this factor is included to provide insight on land management strategies that can be implemented in the SWSD and can lead to the failure of a policy. In Figure 3.7 each dot depicts the combination of two parameters sampled from 1,000 SOWs along with the output from PMP for average perennials land and the color of the dot represents if that SOW met (orange) or did not meet (green) the performance criteria listed in Table 3.3. The PRIM algorithm is able to identify the orthogonal parameter space where the policy meets the criteria depicted as a red square in the figure. Figure 3.7 demonstrates that low surface water deliveries leads to failure to meet the criteria, because peak water supply deliveries are needed to achieve groundwater depth recovery and

meet the groundwater depth level requirement. Average perennial land and price of almonds are important to meet the economic objectives of the SWSD. We can observe that the combination of low prices and low perennials land led to failure. Even though, the selected robust policy reduces perennials cropland, as show in Figure 3.6 panel (d), in the 1,000 sampled SOWs are scenarios where larger average perennials land cause the policy to not meet the criteria. In addition to the feature scoring for the robust performance criteria (Figure B19) we perform a second feature scoring for individual objectives, shown in Figure B20, where we identify the parameters that influence the most the capacity of the robust policy to achieve each objective. From these results we can conclude that perennial land and almond price are the parameters that influence total revenue objective the most and that the magnitude of wet years (75th Q of surface water deliveries) followed by the median surface water supplies and average perennial cropland are the parameters that have the largest impact on the average groundwater depth. The reliability objective is largely affected by median surface water supply and the magnitude of dry years (5th Q of surface water deliveries).

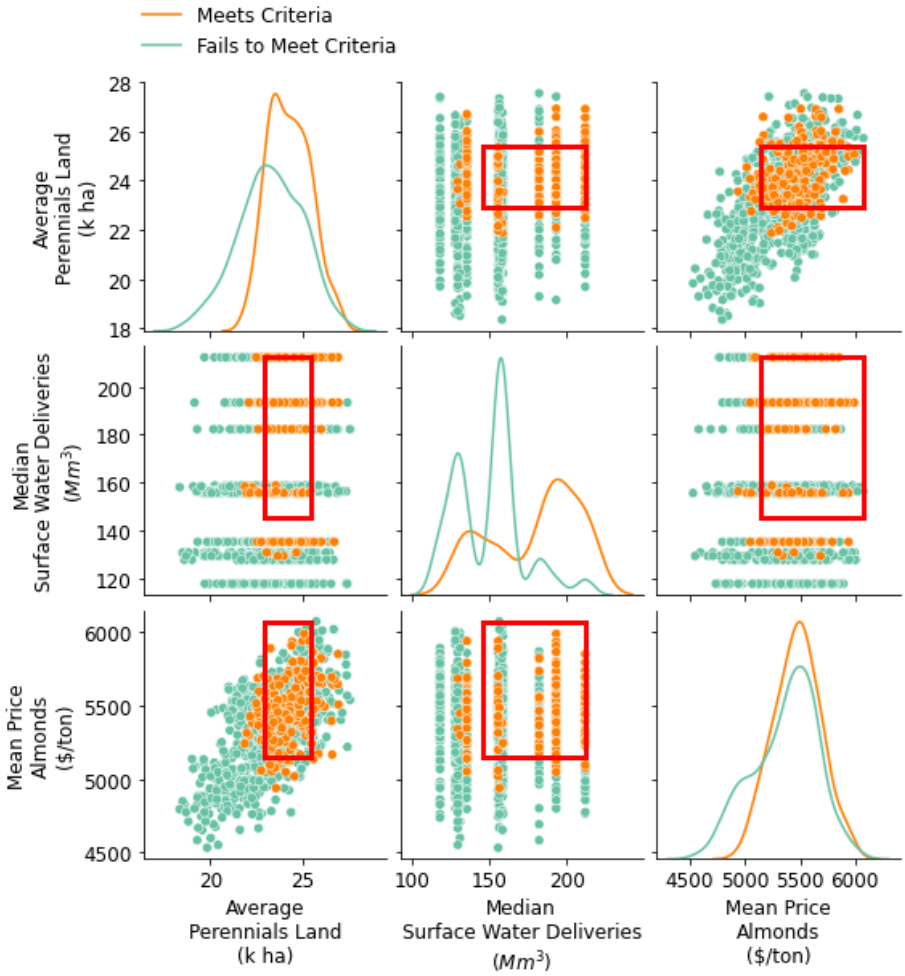

Figure 3.7: Combination of highest ranked parameters in the feature scoring that lead the RobustMinDepth solution to meet or fail the performance criteria (Table 3.3) using 1,000 alternative sampled SOWs. Each dot represents a different SOW. The diagonal plots show the marginal distribution of each parameter. In red is the PRIM box where the combination of parameters cause the policy to meet the robust performance criteria.

3.7 Discussion

This study contributes a novel assessment of the suitability of evolutionary multi-objective direct policy search to discover adaptive irrigation management strategies with a focus on meeting sustainable groundwater management. We assess the ability of EMODPS to help operationalize groundwater sustainable management that targets the yearly decisions of water managers and farmers within both sectors of the complex food-water system. Resulting policies were adaptive to changes in system conditions, showing flexibility between dry and wet years, that maximize total average revenue and lowest revenue in a year and minimize average groundwater depth and maximum groundwater depth in a year. This paper contributes to the body of literature that evaluates optimal land and water use controls and economic instruments (e.g., pumping fees) to achieve groundwater sustainability in agriculture.

This study was applied to the Semitropic Water Storage District GSA in Kern County, California, which represents a broad set of water agencies in overdrafted groundwater basins subject to groundwater sustainability legislation. Results from this study provide insight into the ongoing development and implementation of groundwater management policies which can be scaled up to other basins agencies in the state. Overall, we find that:

1. Reducing the proportion of perennial trees improves adaptation capacity by increasing water demand flexibility.

2. Annual crops can work as a buffer to support cropland increases during wet years and reductions during dry years.

3. In early groundwater management implementation, a groundwater restriction is needed to bring the groundwater depth to a level where GSAs can feasibly manage groundwater and reach the groundwater depth requirement.

4. A pumping fee policy shows promise in coordinating surface and groundwater use and incentivize sustainable pumping.

3.7.1 Limitations and Future Work

Climate change impacts in the region such as impacts on crop yields (Blanc et al., 2017) and increase on potential evapotranspiration (McEvoy et al., 2020; Vahmani et al., 2022) may occur but were not part of the present analysis. Additionally, surface water deliveries used in this study were obtained from the CALFEWS model (Zeff et al., 2021) which may have other intrinsic uncertainties not discussed in this study. Also, the groundwater depth response employed does not reflect the complexity of the aquifer dynamics, such as lateral flows from nearby basins, and surface-groundwater interactions beyond agricultural recharge among others. However, the groundwater response approach employed allows us to capture the general trend and response from groundwater pumping and recovery in the district. Crop prices used in the computational experiment were sampled from the historical record and may not reflect future conditions, which are difficult to forecast given their dependence on a highly dynamic globalized economy.

Future studies could consider increase groundwater via managed aquifer recharge (Alam et al., 2020) and potential participation in water markets (Arellano-Gonzalez et al., 2021; Hanak et al., 2019) that can potentially increase water availability and groundwater recovery. The results demonstrate that cropland reduction is a feasible strategy to achieve groundwater sustainability. However, developing cropland repurposing frameworks that can benefit groundwater sustainability, ecosystems and communities could have synergistic positive economic outcomes (Biggs et al., 2022; Espinoza et al., 2023; Fernandez-Bou et al., 2023). The multiple benefits from repurposing cropland could be included as additional objectives along with objectives that relate to benefits to the ecosystem and to communities. For example, maintaining the groundwater level at a level where domestic wells are protected or minimizing the number of domestic dry wells, which are shallower than agricultural wells and vulnerable to fail during droughts (Jasechko and Perrone, 2020). In addition a performance metric that captures the benefit of policies to protect groundwater reliant ecosystems. Future studies should consider expanding the study area to the San Joaquin Valley to demonstrate how multiple GSAs can develop conjunctive water use management strategies such as water markets. Finally, this study uses district-wide performance in its formulation; however nuances within the district due to the diversity of farm scale operations and commodities can exist. One of the key results is the implementation of a pumping fee, which should be

implemented considering the scale of farms as well as the commodity to achieve groundwater sustainability while achieving an equitable water access. This policy holds considerable potential to complement the highly subsidized energy rates for agriculture. While these rates have been beneficial to farmers, they inadvertently incentivize groundwater pumping. However, since energy rates vary throughout the day and season, the implementation of this policy should align with the same dynamic characteristics.

3.8 Acknowledgements

This work was supported by the California Department of Food and Agriculture grant agreement 21-0557-000-SO, by the Agriculture and Food Research Initiative Competitive Grant number 2021- 69012-35916 from the USDA National Institute of Food and Agriculture, and by the NSF INFEWS program grant number 1639268. José M. Rodríguez-Flores was partially supported by the UC Mexus-CONACYT scholarship. This research was conducted using MERCED cluster (NSF-MRI, #1429783) at the Cyberinfrastructure and Research Technologies (CIRT) from the University of California Merced. We acknowledge the support from students from the Water Systems Management Lab at UC Merced who supported data collection Spencer A. Cole, Elisa Gonzales and Kimberly Parra. VIC-CropSyst results used to estimate the crop yield elasticity to water were provided by Tina Karimi. Outputs from C2VSim-FG were provided by Jorge A. Valero Fandiño (UC Merced, Water Systems Management Lab). The views expressed in this work represent those of the authors and do not necessarily reflect the views or policies of the Semitropic WSD , the California Department of Water Resources or the California Department of Food and Agriculture.

Data Availability Statement

To access the Python code used for the computational experiment and visualization of the results readers can refer to the Github repository: https://github.com/josemrodriguezf/EMODPS_SGMA.

3.9 Bibliography

Afshar, A., Tavakoli, M. A., & Khodagholi, A. (2020). Multi-Objective Hydro-Economic Modeling for Sustainable Groundwater Management. *Water Resources Management*, *34*(6), 1855–1869. https://doi.org/10.1007/s11269-020-02533-4

Alam, S., Gebremichael, M., Ban, Z., Scanlon, B. R., Senay, G., & Lettenmaier, D. P. (2021). Post-Drought Groundwater Storage Recovery in California's Central Valley. *Water Resources Research*, *57*(10), e2021WR030352. https://doi.org/10.1029/2021WR030352

Alam, S., Gebremichael, M., Li, R., Dozier, J., & Lettenmaier, D. P. (2020). Can Managed Aquifer Recharge Mitigate the Groundwater Overdraft in California's Central Valley? *Water Resources Research*, *56*(8), e2020WR027244. https://doi.org/10.1029/2020WR027244

Al-Jawad, J. Y., & Tanyimboh, T. T. (2017). Reservoir operation using a robust evolutionary optimization algorithm. *Journal of Environmental Management*, *197*, 275–286. https://doi.org/10.1016/j.jenvman.2017.03.081

Arellano-Gonzalez, J., AghaKouchak, A., Levy, M. C., Qin, Y., Burney, J., Davis, S. J., & Moore, F. C. (2021). The adaptive benefits of agricultural water markets in California. *Environmental Research Letters*, *16*(4), 044036. https://doi.org/10.1088/1748-9326/abde5b

Banihabib, M. E., Mohammad Rezapour Tabari, M., & Mohammad Rezapour Tabari, M. (2019). Development of a Fuzzy Multi-Objective Heuristic Model for Optimum Water Allocation. *Water Resources Management*, *33*(11), 3673–3689. https://doi.org/10.1007/s11269-019-02323-7

Bertoni, F., Castelletti, A., Giuliani, M., & Reed, P. M. (2019). Discovering Dependencies, Trade-Offs, and Robustness in Joint Dam Design and Operation: An Ex-Post Assessment of the Kariba Dam. *Earth's Future*, *7*(12), 1367–1390. https://doi.org/10.1029/2019EF001235

Bertoni, F., Giuliani, M., Castelletti, A., & Reed, P. M. (2021). Designing With Information Feedbacks: Forecast Informed Reservoir Sizing and Operation. *Water Resources Research*, *57*(3), e2020WR028112. https://doi.org/10.1029/2020WR028112

Bierkens, M. F. P., & Wada, Y. (2019). Non-renewable groundwater use and groundwater depletion: A review. *Environmental Research Letters*, *14*(6), 063002. https://doi.org/10.1088/1748-9326/ab1a5f

Biggs, N. B., Shivaram, R., Lacarieri, E. A., Varkey, K., Hagan, D., Young, H., & Lambin, E. F. (2022). Landowner decisions regarding utility-scale solar energy on working lands: A qualitative case study in California. *Environmental Research Communications*, *4*(5), 055010. https://doi.org/10.1088/2515-7620/ac6fbf

Blanc, E., Caron, J., Fant, C., & Monier, E. (2017). Is current irrigation sustainable in the United States? An integrated assessment of climate change impact on water resources and irrigated crop yields. *Earth's Future*, *5*(8), 877–892. https://doi.org/10.1002/2016EF000473

Bourque, K., Schiller, A., Loyola Angosto, C., McPhail, L., Bagnasco, W., Ayres, A., & Larsen, A. (2019). Balancing agricultural production, groundwater management, and biodiversity goals: A multi-benefit optimization model of agriculture in Kern County, California. *Science of The Total Environment*, *670*, 865–875. https://doi.org/10.1016/j.scitotenv.2019.03.197

Bryant, B. P., Kelsey, T. R., Vogl, A. L., Wolny, S. A., MacEwan, D., Selmants, P. C., Biswas, T., & Butterfield, H. S. (2020). Shaping Land Use Change and Ecosystem Restoration in a Water-Stressed Agricultural Landscape to Achieve Multiple Benefits. *Frontiers in Sustainable Food Systems*, *4*. https://doi.org/10.3389/fsufs.2020.00138

Coello, C. C., Lamont, G. B., & Veldhuizen, D. A. v. (2007). *Evolutionary Algorithms for Solving Multi-Objective Problems* (2nd ed.). Springer US. https://doi.org/10.1007/978-0-387-36797-2

Cuthbert, M. O., Gleeson, T., Moosdorf, N., Befus, K. M., Schneider, A., Hartmann, J., & Lehner, B. (2019). Global patterns and dynamics of climate–groundwater interactions. *Nature Climate Change*, *9*(2), 137–141. https://doi.org/10.1038/s41558-018-0386-4

Debertin, D. L. (Ed.). (2012). *Agricultural Production Economics: The Art of Production Theory*. https://doi.org/10.22004/ag.econ.158320

Doering, K., Quinn, J., Reed, P. M., & Steinschneider, S. (2021). Diagnosing the time-varying value of forecasts in multiobjective reservoir control. *Journal of Water Resources Planning and Management*, *147*(7), 04021031.

DWR. (2017). *Sustainable Manage Criteria* (tech. rep.). California Department of Water Resources, Sustainable Groundwater Management Program. https://water.ca.gov/Programs/Groundwater-

Management / SGMA - Groundwater - Management / Best - Management - Practices - and - Guidance-Documents

DWR. (2021a). C2VSimFG Version 1.01. https://data.cnra.ca.gov/dataset/c2vsimfg-version-1-01

DWR. (2021b). Sustainable Groundwater Management Act (SGMA). https://water.ca.gov/Programs/Groundwater-Management/SGMA-Groundwater-Management

Espinoza, V., Bernacchi, L. A., Eriksson, M., Schiller, A., Hayden, A., & Viers, J. H. (2023). From fallow ground to common ground: Perspectives on future land uses in the San Joaquin valley under sustainable groundwater management. *Journal of Environmental Management*, *333*, 117226. https://doi.org/10.1016/j.jenvman.2023.117226

Espinoza, V., Waliser, D. E., Guan, B., Lavers, D. A., & Ralph, F. M. (2018). Global Analysis of Climate Change Projection Effects on Atmospheric Rivers. *Geophysical Research Letters*, *45*(9), 4299–4308. https://doi.org/10.1029/2017GL076968

Fernandez-Bou, A. S., Ortiz-Partida, J. P., Pells, C., Classen-Rodriguez, L. M., Espinoza, V., Rodríguez-Flores, J. M., & Medellin-Azuara, J. (2021). *Regional Report for the San Joaquin Valley Region on Impacts of Climate Change* (California's Fourth Climate Assesment SUM-CCCA4-2021-003). California Natural Resources Agency. Sacramento. https://www.energy.ca.gov/sites/default/files/2022-01/CA4_CCA_SJ_Region_Eng_ada.pdf

Fernandez-Bou, A. S., Rodríguez-Flores, J. M., Guzman, A., Ortiz-Partida, J. P., Classen-Rodriguez, L. M., Sánchez-Pérez, P. A., Valero-Fandiño, J., Pells, C., Flores-Landeros, H., Sandoval-Solís, S., Characklis, G. W., Harmon, T. C., McCullough, M., & Medellín-Azuara, J. (2023). Water, environment, and socioeconomic justice in California: A multi-benefit cropland repurposing framework. *Science of The Total Environment*, *858*, 159963. https://doi.org/10.1016/j.scitotenv.2022.159963

Filatova, T., Polhill, J. G., & van Ewijk, S. (2016). Regime shifts in coupled socio-environmental systems: Review of modelling challenges and approaches. *Environmental Modelling & Software*, *75*, 333–347. https://doi.org/10.1016/j.envsoft.2015.04.003

Friedman, J. H., & Fisher, N. I. (1999). Bump hunting in high-dimensional data. *Statistics and Computing*, *9*(2), 123–143. https://doi.org/10.1023/A:1008894516817

Garner, G. G., & Keller, K. (2018). Using direct policy search to identify robust strategies in adapting to uncertain sea-level rise and storm surge. *Environmental Modelling & Software*, *107*, 96–104. https://doi.org/10.1016/j.envsoft.2018.05.006

Geressu, R. T., Siderius, C., Rao Kolusu, S., Kashaigili, J., Todd, M. C., Conway, D., & Harou, J. J. (2022). Evaluating the sensitivity of robust water resource interventions to climate change scenarios. *Climate Risk Management*, *37*, 100442. https://doi.org/10.1016/j.crm.2022.100442

Geurts, P., Ernst, D., & Wehenkel, L. (2006). Extremely randomized trees. *Machine Learning*, *63*(1), 3–42. https://doi.org/10.1007/s10994-006-6226-1

Giuliani, M., Lamontagne, J. R., Reed, P. M., & Castelletti, A. (2021). A State-of-the-Art Review of Optimal Reservoir Control for Managing Conflicting Demands in a Changing World. *Water Resources Research*, *57*(12), e2021WR029927. https://doi.org/10.1029/2021WR029927

Giuliani, M., Castelletti, A., Pianosi, F., Mason, E., & Reed, P. M. (2016). Curses, Tradeoffs, and Scalable Management: Advancing Evolutionary Multiobjective Direct Policy Search to Improve Water Reservoir Operations. *Journal of Water Resources Planning and Management*, *142*(2), 04015050. https://doi.org/10.1061/(ASCE)WR.1943-5452.0000570

Giuliani, M., Mason, E., Castelletti, A., Pianosi, F., & Soncini-Sessa, R. (2014). Universal approximators for direct policy search in multi-purpose water reservoir management: A comparative analysis. *IFAC Proceedings Volumes*, *47*(3), 6234–6239. https://doi.org/10.3182/20140824-6-ZA-1003.01962

Graveline, N. (2020). Combining flexible regulatory and economic instruments for agriculture water demand control under climate change in Beauce. *Water Resources and Economics*, *29*. https://doi.org/10.1016/j.wre.2019.100143

Groves, D. G., Molina-Perez, E., Bloom, E., & Fischbach, J. R. (2019). Robust Decision Making (RDM): Application to Water Planning and Climate Policy. In V. A. W. J. Marchau, W. E. Walker, P. J. T. M. Bloemen, & S. W. Popper (Eds.), *Decision Making under Deep Uncertainty: From Theory to Practice* (pp. 135–163). Springer International Publishing. https://doi.org/10.1007/978-3-030-05252-2_7

Gupta, R. S., Hamilton, A. L., Reed, P. M., & Characklis, G. W. (2020). Can modern multi-objective evolutionary algorithms discover high-dimensional financial risk portfolio tradeoffs for snow-dominated water-energy systems? *Advances in Water Resources*, *145*, 103718. https://doi.org/10.1016/j.advwatres.2020.103718

Habibi Davijani, M., Banihabib, M. E., Nadjafzadeh Anvar, A., & Hashemi, S. R. (2016). Optimization model for the allocation of water resources based on the maximization of employment in the agriculture and industry sectors. *Journal of Hydrology*, *533*, 430–438. https://doi.org/10.1016/j.jhydrol.2015.12.025

Hadjimichael, A., Quinn, J., Wilson, E., Reed, P., Basdekas, L., Yates, D., & Garrison, M. (2020). Defining Robustness, Vulnerabilities, and Consequential Scenarios for Diverse Stakeholder Interests in Institutionally Complex River Basins. *Earth's Future*, *8*(7). https://doi.org/10.1029/2020EF001503

Hadka, D., & Reed, P. (2012). Diagnostic Assessment of Search Controls and Failure Modes in Many-Objective Evolutionary Optimization. *Evolutionary Computation*, *20*(3), 423–452. https://doi.org/10.1162/EVCO_a_00053

Hadka, D., & Reed, P. (2013). Borg: An Auto-Adaptive Many-Objective Evolutionary Computing Framework. *Evolutionary Computation*, *21*(2), 231–259. https://doi.org/10.1162/EVCO_a_00075

Hadka, D., & Reed, P. (2015). Large-scale parallelization of the Borg multiobjective evolutionary algorithm to enhance the management of complex environmental systems. *Environmental Modelling & Software*, *69*, 353–369. https://doi.org/10.1016/j.envsoft.2014.10.014

Hamilton, A. L., Characklis, G. W., & Reed, P. M. (2022). From Stream Flows to Cash Flows: Leveraging Evolutionary Multi-Objective Direct Policy Search to Manage Hydrologic Financial Risks. *Water Resources Research*, *58*(1). https://doi.org/10.1029/2021WR029747

Hanak, E., Escriva-Bou, A., Gray, B., Green, S., Harter, T., Jezdimirovic, J., Lund, J., Medellín-Azuara, J., Moyle, P., & Seavy, N. (2019). *Water and the Future of the San Joaquin Valley* (tech. rep.). https://doi.org/10.13140/RG.2.2.24360.83208

Harou, J. J., Pulido-Velazquez, M., Rosenberg, D. E., Medellín-Azuara, J., Lund, J. R., & Howitt, R. E. (2009). Hydro-economic models: Concepts, design, applications, and future prospects. *Journal of Hydrology*, *375*(3-4), 627–643. https://doi.org/10.1016/j.jhydrol.2009.06.037

Hart, W. E., Watson, J.-P., & Woodruff, D. L. (2011). Pyomo: Modeling and solving mathematical programs in Python. *Mathematical Programming Computation*, *3*(3), 219–260.

He, X., Wada, Y., Wanders, N., & Sheffield, J. (2017). Intensification of hydrological drought in California by human water management. *Geophysical Research Letters*, *44*(4), 1777–1785. https://doi.org/10.1002/2016GL071665

Herman, J. D., Reed, P. M., Zeff, H. B., & Characklis, G. W. (2015). How Should Robustness Be Defined for Water Systems Planning under Change? *Journal of Water Resources Planning and Management*, *141*(10), 04015012. https://doi.org/10.1061/(ASCE)WR.1943-5452.0000509

Hesamfar, F., Ketabchi, H., & Ebadi, T. (2023). Simulation-based multi-objective optimization framework for sustainable management of coastal aquifers in semi-arid regions. *Journal of Environmental Management*, *338*, 117785. https://doi.org/10.1016/j.jenvman.2023.117785

Howitt, R. E. (1995). A Calibration Method for Agricultural Economic Production Models. *Journal of Agricultural Economics*, *46*(2), 147–159. https://doi.org/10.1111/j.1477-9552.1995.tb00762.x

Howitt, R. E., Medellín-Azuara, J., MacEwan, D., & Lund, J. R. (2012). Calibrating disaggregate economic models of agricultural production and water management. *Environmental Modelling & Software*, *38*, 244–258. https://doi.org/10.1016/j.envsoft.2012.06.013

Hrozencik, R. A., Manning, D. T., Suter, J. F., Goemans, C., & Bailey, R. T. (2017). The Heterogeneous Impacts of Groundwater Management Policies in the Republican River Basin of Colorado. *Water Resources Research*, *53*(12), 10757–10778. https://doi.org/10.1002/2017WR020927

Hrozencik, R. A., Manning, D. T., Suter, J. F., & Goemans, C. (2022). Impacts of Block-Rate Energy Pricing on Groundwater Demand in Irrigated Agriculture. *American Journal of Agricultural Economics*, *104*(1), 404–427. https://doi.org/10.1111/ajae.12231

Huskova, I. (2016). Screening robust water infrastructure investments and their trade-offs under global change: A London example. *Global Environmental Change*, 12.

Jasechko, S., & Perrone, D. (2020). California's Central Valley Groundwater Wells Run Dry During Recent Drought. *Earth's Future*, *8*(4). https://doi.org/10.1029/2019EF001339

Kasprzyk, J. R., Nataraj, S., Reed, P. M., & Lempert, R. J. (2013). Many objective robust decision making for complex environmental systems undergoing change. *Environmental Modelling & Software*, *42*, 55–71. https://doi.org/10.1016/j.envsoft.2012.12.007

Khan, H. F., & Brown, C. M. (2019). Effect of Hydrogeologic and Climatic Variability on Performance of a Groundwater Market. *Water Resources Research*, *55*(5), 4304–4321. https://doi.org/10.1029/2018WR024180

Koutsoyiannis, D., & Economou, A. (2003). Evaluation of the parameterization-simulation-optimization approach for the control of reservoir systems. *Water Resources Research*, *39*(6). https://doi.org/10.1029/2003WR002148

Kuwayama, Y., & Brozović, N. (2013). The regulation of a spatially heterogeneous externality: Tradable groundwater permits to protect streams. *Journal of Environmental Economics and Management*, *66*(2), 364–382. https://doi.org/10.1016/j.jeem.2013.02.004

Kwakkel, J. H. (2017). The Exploratory Modeling Workbench: An open source toolkit for exploratory modeling, scenario discovery, and (multi-objective) robust decision making. *Environmental Modelling & Software*, *96*, 239–250. https://doi.org/10.1016/j.envsoft.2017.06.054

Kwakkel, J. H., & Jaxa-Rozen, M. (2016). Improving scenario discovery for handling heterogeneous uncertainties and multinomial classified outcomes. *Environmental Modelling & Software*, *79*, 311–321. https://doi.org/10.1016/j.envsoft.2015.11.020

Lan, L., Iftekhar, M. S., Fogarty, J., & Schilizzi, S. (2021). Performance of a uniform proportional "cut" to manage declining groundwater in Western Australia. *Journal of Hydrology*, *598*, 126421. https://doi.org/10.1016/j.jhydrol.2021.126421

Lempert, R. J., & Groves, D. G. (2010). Identifying and evaluating robust adaptive policy responses to climate change for water management agencies in the American west. *Technological Forecasting and Social Change*, *77*(6), 960–974. https://doi.org/10.1016/j.techfore.2010.04.007

Lempert, R. J., Popper, S. W., Groves, D. G., Kalra, N., Fischbach, J. R., Bankes, S. C., Bryant, B. P., Collins, M. T., Keller, K., Hackbarth, A., Dixon, L., LaTourrette, T., Reville, R. T., Hall, J. W., Mijere, C., & McInerney, D. J. (2013). *Making Good Decisions Without Predic-*

tions: Robust Decision Making for Planning Under Deep Uncertainty (tech. rep.). RAND Corporation. https://www.rand.org/pubs/research_briefs/RB9701.html

Levy, Z. F., Jurgens, B. C., Burow, K. R., Voss, S. A., Faulkner, K. E., Arroyo-Lopez, J. A., & Fram, M. S. (2021). Critical Aquifer Overdraft Accelerates Degradation of Groundwater Quality in California's Central Valley During Drought. *Geophysical Research Letters*, *48*(17), e2021GL094398. https://doi.org/10.1029/2021GL094398

Li, R., Ou, G., Pun, M., & Larson, L. (2018). Evaluation of Groundwater Resources in Response to Agricultural Management Scenarios in the Central Valley, California. *Journal of Water Resources Planning and Management*, *144*(12), 04018078. https://doi.org/10.1061/(ASCE)WR.1943-5452.0001014

Liu, P.-W., Famiglietti, J. S., Purdy, A. J., Adams, K. H., McEvoy, A. L., Reager, J. T., Bindlish, R., Wiese, D. N., David, C. H., & Rodell, M. (2022). Groundwater depletion in California's Central Valley accelerates during megadrought. *Nature Communications*, *13*(1), 7825. https://doi.org/10.1038/s41467-022-35582-x

Lund, J., Medellin-Azuara, J., Durand, J., & Stone, K. (2018). Lessons from California's 2012–2016 Drought. *Journal of Water Resources Planning and Management*, *144*(10), 04018067. https://doi.org/10.1061/(ASCE)WR.1943-5452.0000984

MacEwan, D., Cayar, M., Taghavi, A., Mitchell, D., Hatchett, S., & Howitt, R. (2017). Hydroeconomic modeling of sustainable groundwater management. *Water Resources Research*, *53*(3), 2384–2403. https://doi.org/10.1002/2016WR019639

Macian-Sorribes, H., & Pulido-Velazquez, M. (2019). Inferring efficient operating rules in multireservoir water resource systems: A review. *WIREs Water*, *7*(1), e1400. https://doi.org/10.1002/wat2.1400

Madani, K., & Dinar, A. (2013). Exogenous regulatory institutions for sustainable common pool resource management: Application to groundwater. *Water Resources and Economics*, *2-3*, 57–76. https://doi.org/10.1016/j.wre.2013.08.001

Mall, N. K., & Herman, J. D. (2019). Water shortage risks from perennial crop expansion in California's Central Valley. *Environmental Research Letters*, *14*(10), 104014. https://doi.org/10.1088/1748-9326/ab4035

Malmgren, K. A., C. Neves, M., Gurdak, J. J., Costa, L., & Monteiro, J. P. (2022). Groundwater response to climate variability in Mediterranean type climate zones with comparisons of California (USA) and Portugal. *Hydrogeology Journal*. https://doi.org/10.1007/s10040-022-02470-z

Maneta, M. P., & Howitt, R. (2014). Stochastic calibration and learning in nonstationary hydroeconomic models. *Water Resources Research*, *50*(5), 3976–3993. https://doi.org/10.1002/2013WR015196

Maneta, M., Cobourn, K., Kimball, J., He, M., Silverman, N., Chaffin, B., Ewing, S., Ji, X., & Maxwell, B. (2020). A satellite-driven hydro-economic model to support agricultural water resources management. *Environmental Modelling & Software*, *134*, 104836. https://doi.org/10.1016/j.envsoft.2020.104836

McDermid, S. S., Mahmood, R., Hayes, M. J., Bell, J. E., & Lieberman, Z. (2021). Minimizing trade-offs for sustainable irrigation. *Nature Geoscience*, *14*(10), 706–709. https://doi.org/10.1038/s41561-021-00830-0

McEvoy, D. J., Pierce, D. W., Kalansky, J. F., Cayan, D. R., & Abatzoglou, J. T. (2020). Projected Changes in Reference Evapotranspiration in California and Nevada: Implications for Drought and Wildland Fire Danger. *Earth's Future*, *8*(11), e2020EF001736. https://doi.org/10.1029/2020EF001736

McPhail, C., Maier, H. R., Kwakkel, J. H., Giuliani, M., Castelletti, A., & Westra, S. (2018). Robustness Metrics: How Are They Calculated, When Should They Be Used and Why Do They Give Different Results? *Earth's Future*, *6*(2), 169–191. https://doi.org/10.1002/2017EF000649

Medellin-Azuara, J., Escriva-Bou, A., Abatzoglou, J., Viers, J., Cole, S., Rodriguez-Flores, J., & Sumner, D. (2022). *Economic Impacts of the 2021 Drought on California Agriculture. Preliminary Report* (A report for the California Department of Food and Agriculture). University of California, Merced.

Mehrabi, A., Heidarpour, M., Safavi, H. R., & Rezaei, F. (2021). Assessment of the optimized scenarios for economic-environmental conjunctive water use utilizing gravitational search algorithm. *Agricultural Water Management*, *246*, 106688. https://doi.org/10.1016/j.agwat.2020.106688

Memmah, M.-M., Lescourret, F., Yao, X., & Lavigne, C. (2015). Metaheuristics for agricultural land use optimization. A review. *Agronomy for Sustainable Development*, *35*(3), 975–998. https://doi.org/10.1007/s13593-015-0303-4

Merel, P. R., Simon, L. K., & Yi, F. (2010). *A Fully Calibrated Generalized CES Programming Model of Agricultural Supply* (tech. rep. No. 60906). Agricultural and Applied Economics Association. https://ideas.repec.org/p/ags/aaea10/60906.html

Miro, M. E., & Famiglietti, J. S. (2019). A framework for quantifying sustainable yield under California's Sustainable Groundwater Management Act (SGMA). *Sustainable Water Resources Management*, *5*(3), 1165–1177. https://doi.org/10.1007/s40899-018-0283-z

Miro, M. E., Groves, D., Tincher, B., Syme, J., Tanverakul, S., & Catt, D. (2021). Adaptive water management in the face of uncertainty: Integrating machine learning, groundwater modeling and robust decision making. *Climate Risk Management*, *34*, 100383. https://doi.org/10.1016/j.crm.2021.100383

Moallemi, E. A., Kwakkel, J., de Haan, F. J., & Bryan, B. A. (2020). Exploratory modeling for analyzing coupled human-natural systems under uncertainty. *Global Environmental Change*, *65*, 102186. https://doi.org/10.1016/j.gloenvcha.2020.102186

Mulligan, K. B., Brown, C., Yang, Y.-C. E., & Ahlfeld, D. P. (2014). Assessing groundwater policy with coupled economic-groundwater hydrologic modeling. *Water Resources Research*, *50*(3), 2257–2275. https://doi.org/10.1002/2013WR013666

Null, S. E., Olivares, M. A., Cordera, F., & Lund, J. R. (2021). Pareto Optimality and Compromise for Environmental Water Management. *Water Resources Research*, *57*(10), e2020WR028296. https://doi.org/10.1029/2020WR028296

Ojha, C., Shirzaei, M., Werth, S., Argus, D. F., & Farr, T. G. (2018). Sustained Groundwater Loss in California's Central Valley Exacerbated by Intense Drought Periods. *Water Resources Research*, *54*(7), 4449–4460. https://doi.org/10.1029/2017WR022250

Partida, J. P. O., Fernandez-Bou, A. S., Maskey, M., Rodriguez-Flores, J. M., Medellin-Azuara, J., Sandoval-Solis, S., Ermolieva, T., Kanavas, Z., Sahu, R. K., Wada, Y., & Kahil, T. (2023). Hydro-economic modeling of water resources management challenges: Current applications and future directions. *Water Economics and Policy*. https://doi.org/10.1142/S2382624X23400039

Pauloo, R. A., Escriva-Bou, A., Dahlke, H., Fencl, A., Guillon, H., & Fogg, G. E. (2020). Domestic well vulnerability to drought duration and unsustainable groundwater management in California's Central Valley. *Environmental Research Letters*, *15*(4), 044010. https://doi.org/10.1088/1748-9326/ab6f10

Perrone, D., & Jasechko, S. (2017). Dry groundwater wells in the western United States. *Environmental Research Letters*, *12*(10), 104002. https://doi.org/10.1088/1748-9326/aa8ac0

PG&E. (2021). Pacific Gas & Electric - Tariffs. https://www.pge.com/tariffs/rateinfo.shtml

Pierce, W. D., Kalansky, F. J., & Cayan, R. D. (2018). *Climate, Drought, and Sea Level Rise Scenarios for California's Fourth Climate Change Assessment* (tech. rep. CNRA-CEC-2018-006). Scripps Institution of Oceanography. https://www.energy.ca.gov/sites/default/files/2019-11/Projections_CCCA4-CEC-2018-006_ADA.pdf

Polhill, J. G., Filatova, T., Schlüter, M., & Voinov, A. (2016). Modelling systemic change in coupled socio-environmental systems. *Environmental Modelling & Software*, *75*, 318–332. https://doi.org/10.1016/j.envsoft.2015.10.017

Priyan, K. (2021). Issues and Challenges of Groundwater and Surface Water Management in Semi-Arid Regions. In C. B. Pande & K. N. Moharir (Eds.), *Groundwater Resources Development and Planning in the Semi-Arid Region* (pp. 1–17). Springer International Publishing. https://doi.org/10.1007/978-3-030-68124-1_1

Qin, Y., Mueller, N. D., Siebert, S., Jackson, R. B., AghaKouchak, A., Zimmerman, J. B., Tong, D., Hong, C., & Davis, S. J. (2019). Flexibility and intensity of global water use. *Nature Sustainability*, *2*(6), 515–523. https://doi.org/10.1038/s41893-019-0294-2

Quinn, J. D., Reed, P. M., Giuliani, M., Castelletti, A., Oyler, J. W., & Nicholas, R. E. (2018). Exploring How Changing Monsoonal Dynamics and Human Pressures Challenge Multireservoir Management for Flood Protection, Hydropower Production, and Agricultural Water Supply. *Water Resources Research*, *54*(7), 4638–4662. https://doi.org/10.1029/2018WR022743

Quinn, J. D., Reed, P. M., & Keller, K. (2017). Direct policy search for robust multi-objective management of deeply uncertain socio-ecological tipping points. *Environmental Modelling & Software*, *92*, 125–141. https://doi.org/10.1016/j.envsoft.2017.02.017

Reed, P. M., Hadka, D., Herman, J. D., Kasprzyk, J. R., & Kollat, J. B. (2013). Evolutionary multiobjective optimization in water resources: The past, present, and future. *Advances in Water Resources*, *51*, 438–456. https://doi.org/10.1016/j.advwatres.2012.01.005

Rodríguez-Flores, J. M., Medellín-Azuara, J., Valdivia-Alcalá, R., Arana-Coronado, O. A., & García-Sánchez, R. C. (2019). Insights from a Calibrated Optimization Model for Irrigated Agriculture under Drought in an Irrigation District on the Central Mexican High Plains. *Water*, *11*(4), 858. https://doi.org/10.3390/w11040858

Rodríguez-Flores, J. M., Valero Fandiño, J. A., Cole, S. A., Malek, K., Karimi, T., Zeff, H. B., Reed, P. M., Escriva-Bou, A., & Medellín-Azuara, J. (2022). Global Sensitivity Analysis of a Coupled Hydro-Economic Model and Groundwater Restriction Assessment. *Water Resources Management*, *36*(15), 6115–6130. https://doi.org/10.1007/s11269-022-03344-5

Rosenstein, M. T., & Barto, A. G. (2001). Robot weightlifting by direct policy search. *International Joint Conference on Artificial Intelligence*, *17*, 839–846.

Safari, S., Sharghi, S., Kerachian, R., & Noory, H. (2023). A market-based mechanism for long-term groundwater management using remotely sensed data. *Journal of Environmental Management*, *332*, 117409. https://doi.org/10.1016/j.jenvman.2023.117409

Salehi Shafa, N., Babazadeh, H., Aghayari, F., & Saremi, A. (2023). Multi-objective planning for optimal exploitation of surface and groundwater resources through development of an optimized cropping pattern and artificial recharge system. *Ain Shams Engineering Journal*, *14*(2), 101847. https://doi.org/10.1016/j.asej.2022.101847

Schneller, G. O., & Sphicas, G. P. (1983). Decision making under uncertainty: Starr's Domain criterion. *Theory and Decision*, *15*(4), 321–336. https://doi.org/10.1007/BF00162111

Seyedashraf, O., Bottacin-Busolin, A., & Harou, J. J. (2023). Assisting decision-makers select multi-dimensionally efficient infrastructure designs – Application to urban drainage systems. *Journal of Environmental Management*, *336*, 117689. https://doi.org/10.1016/j.jenvman.2023.117689

Shuai, Y., He, X., & Yao, L. (2022). Robust optimization with equity and efficiency framework for basin-wide water resources planning. *Journal of Environmental Management*, *321*, 115834. https://doi.org/10.1016/j.jenvman.2022.115834

Siebert, S., Burke, J., Faures, J. M., Frenken, K., Hoogeveen, J., Döll, P., & Portmann, F. T. (2010). Groundwater use for irrigation – a global inventory. *Hydrology and Earth System Sciences*, *14*(10), 1863–1880. https://doi.org/10.5194/hess-14-1863-2010

Smith, R. G., & Majumdar, S. (2020). Groundwater Storage Loss Associated With Land Subsidence in Western United States Mapped Using Machine Learning. *Water Resources Research*, *56*(7), e2019WR026621. https://doi.org/10.1029/2019WR026621

Stirling, A. (2010). Keep it complex. *Nature*, *468*(7327), 1029–1031. https://doi.org/10.1038/4681029a

Stone, K. M., Gailey, R. M., & Lund, J. R. (2022). Economic tradeoff between domestic well impact and reduced agricultural production with groundwater drought management: Tulare County, California (USA), case study. *Hydrogeology Journal*, *30*(1), 3–19. https://doi.org/10.1007/s10040-021-02409-w

Taylor, C. R. (1993). Dynamic Programming and the Curses of Dimensionality. In *Applications of Dynamic Programming to Agricultural Decision Problems*. CRC Press.

Taylor, R. G., Scanlon, B., Döll, P., Rodell, M., van Beek, R., Wada, Y., Longuevergne, L., Leblanc, M., Famiglietti, J. S., Edmunds, M., Konikow, L., Green, T. R., Chen, J., Taniguchi, M., Bierkens, M. F. P., MacDonald, A., Fan, Y., Maxwell, R. M., Yechieli, Y., … Treidel, H. (2013). Ground water and climate change. *Nature Climate Change*, *3*(4), 322–329. https://doi.org/10.1038/nclimate1744

Thomann, J. A., Werner, A. D., Irvine, D. J., & Currell, M. J. (2020). Adaptive management in groundwater planning and development: A review of theory and applications. *Journal of Hydrology*, *586*, 124871. https://doi.org/10.1016/j.jhydrol.2020.124871

Torhan, S., Grady, C. A., Ajibade, I., Galappaththi, E. K., Hernandez, R. R., Musah-Surugu, J. I., Nunbogu, A. M., Segnon, A. C., Shang, Y., Ulibarri, N., Campbell, D., Joe, E. T., Penuelas, J., Sardans, J., Shah, M. a. R., & Team, t. G. A. M. (2022). Tradeoffs and Synergies Across Global Climate Change Adaptations in the Food-Energy-Water Nexus. *Earth's Future*, *10*(4), e2021EF002201. https://doi.org/10.1029/2021EF002201

Trindade, B. C., Reed, P. M., & Characklis, G. W. (2019). Deeply uncertain pathways: Integrated multi-city regional water supply infrastructure investment and portfolio management. *Advances in Water Resources*, *134*, 103442. https://doi.org/10.1016/j.advwatres.2019.103442

Ulibarri, N., Escobedo Garcia, N., Nelson, R. L., Cravens, A. E., & McCarty, R. J. (2021). Assessing the Feasibility of Managed Aquifer Recharge in California. *Water Resources Research*, *57*(3), e2020WR029292. https://doi.org/10.1029/2020WR029292

USDA. (2020). National Agricultural Statistics Service - California. https://www.nass.usda.gov/Statistics_by_State/California/index.php

Vahmani, P., Jones, A. D., & Li, D. (2022). Will Anthropogenic Warming Increase Evapotranspiration? Examining Irrigation Water Demand Implications of Climate Change in California. *Earth's Future*, *10*(1), e2021EF002221. https://doi.org/10.1029/2021EF002221

Van Schmidt, N. D., Wilson, T. S., & Langridge, R. (2022). Linkages between land-use change and groundwater management foster long-term resilience of water supply in California. *Journal of Hydrology: Regional Studies*, *40*, 101056. https://doi.org/10.1016/j.ejrh.2022.101056

Vasco, D. W., Farr, T. G., Jeanne, P., Doughty, C., & Nico, P. (2019). Satellite-based monitoring of groundwater depletion in California's Central Valley. *Scientific Reports*, *9*(1), 16053. https://doi.org/10.1038/s41598-019-52371-7

Veena, S., Singh, R., Gold, D., Reed, P., & Bhave, A. (2021). Improving Information-Based Coordinated Operations in Interbasin Water Transfer Megaprojects: Case Study in Southern India. *Journal of Water Resources Planning and Management*, *147*(11), 04021075. https://doi.org/10.1061/(ASCE)WR.1943-5452.0001456

Wächter, A., & Biegler, L. T. (2006). On the implementation of an interior-point filter line-search algorithm for large-scale nonlinear programming. *Mathematical Programming*, *106*(1), 25–57. https://doi.org/10.1007/s10107-004-0559-y

Wang, J., & Johnson, D. R. (2023). Incorporating learning into direct policy search for flood risk management. *Risk Analysis*. https://doi.org/10.1111/risa.14136

Wang, S., Tan, Q., Yang, P., Zhang, T., & Zhang, T. (2023). Development of an inexact simulation-evaluation model for the joint analysis of water pricing and groundwater allocation policies. *Journal of Environmental Management*, *329*, 116996. https://doi.org/10.1016/j.jenvman.2022.116996

Ward, F. A. (2021). Hydroeconomic Analysis to Guide Climate Adaptation Plans. *Frontiers in Water*, *3*. https://www.frontiersin.org/article/10.3389/frwa.2021.681475

Wu, W., Zhou, Y., & Leonard, M. (2022). Evolutionary algorithm-based multiobjective reservoir operation policy optimisation under uncertainty. *Environmental Research Communications*, *4*(12), 121001. https://doi.org/10.1088/2515-7620/aca1fc

Wu, W.-Y., Lo, M.-H., Wada, Y., Famiglietti, J. S., Reager, J. T., Yeh, P. J.-F., Ducharne, A., & Yang, Z.-L. (2020). Divergent effects of climate change on future groundwater availability in key mid-latitude aquifers. *Nature Communications*, *11*(1), 3710. https://doi.org/10.1038/s41467-020-17581-y

Young, R., Foster, T., Mieno, T., Valocchi, A., & Brozović, N. (2021). Hydrologic-Economic Trade-offs in Groundwater Allocation Policy Design. *Water Resources Research*, *57*(1), e2020WR027941. https://doi.org/10.1029/2020WR027941

Zatarain Salazar, J., Reed, P. M., Quinn, J. D., Giuliani, M., & Castelletti, A. (2017). Balancing exploration, uncertainty and computational demands in many objective reservoir optimization. *Advances in Water Resources*, *109*, 196–210. https://doi.org/10.1016/j.advwatres.2017.09.014

Zeff, H. B., Hamilton, A. L., Malek, K., Herman, J. D., Cohen, J. S., Medellin-Azuara, J., Reed, P. M., & Characklis, G. W. (2021). California's food-energy-water system: An open source simulation model of adaptive surface and groundwater management in the Central Valley. *Environmental Modelling & Software*, *141*, 105052. https://doi.org/10.1016/j.envsoft.2021.105052

Chapter 4

Drivers of domestic wells vulnerability during droughts in California's Central Valley

This chapter is currently in review in the Environmental Research Letters journal: Rodríguez-Flores, J.M., Fernandez-Bou, A.S., Ortiz-Partida, J.P. and Medellín-Azuara, J. Drivers of domestic wells vulnerability during droughts in California's Central Valley.

4.1 Abstract

Over the past decade, California has experienced two multiyear droughts, resulting in significant economic losses for the agricultural sector and limited water access for communities. Despite the recognition of water as a human right in the state, droughts consistently lead to the failure of thousands of domestic wells due to intensified groundwater pumping for irrigation purposes. In the Central Valley alone, groundwater sustains the livelihoods of thousands of individuals (and millions across the state) serving as the sole water source, rendering it vulnerable due to inadequate groundwater management. In this study, we present a spatial statistical model to identify critical localized factors within the food-water-human system that contribute to the vulnerability

of domestic wells during droughts. Our results indicate that the depth of domestic wells, density of domestic and agricultural wells, economic conditions, and the extent of perennial crops play significant roles in predicting well failures during droughts. We show the implications of addressing these factors within the context of ongoing groundwater sustainability initiatives, we propose strategies to safeguard the water source for thousands of individuals necessary to protect domestic wells.

4.2 Introduction

Groundwater in California is an important source of water for agriculture and human use. However, community water supply systems, small water supply systems, and households with private domestic wells are vulnerable to water shortages and water quality issues due to extended agricultural groundwater pumping (Levy et al., 2021; Pauloo et al., 2020; Smith et al., 2018). In the state, approximately 1.3 million people are served by domestic wells, mostly concentrated in the San Joaquin Valley with approximately 452,450 people (Pace et al., 2022). In 2012, California established a landmark law (Assembly Bill 685) recognizing the human right to water, ensuring that all individuals, including low-income and minority communities, are entitled to access clean, safe, and affordable water to drink, cook, and bathe. The recent occurrence of two consecutive drought periods (2012-2016 and 2020-2022) has exacerbated the depletion of groundwater levels, primarily due to intensified agricultural pumping practices, particularly in the San Joaquin Valley (Medellin-Azuara et al., 2022; Medellín-Azuara et al., 2016). As a consequence, thousands of domestic wells were reported dry, especially from rural disadvantaged communities, who have been severely impacted by unsustainable groundwater use (Feinstein et al., 2017; Klasic et al., 2022). Increasing risk to water shortages from groundwater sources for human consumption is not limited to California and the western United States (Perrone and Jasechko, 2017; Scanlon et al., 2021), similar challenges are observed in other semiarid regions worldwide, characterized by groundwater depletion (Bierkens and Wada, 2019; Gleeson et al., 2020; Huggins et al., 2022; Jasechko and Perrone, 2021; Mekonnen and Hoekstra, 2016) that have led to seek groundwater sustainability management (Elshall et al., 2020).

The vulnerability of California to drought stems from its Mediterranean climate, and high

dependence on snowpack and atmospheric rivers for water supply (Diffenbaugh et al., 2015; Gershunov et al., 2019; Payne et al., 2020), which results in multiyear drought periods and significant surface water shortages. The agricultural sector, which holds substantial economic importance in the region and is recognized as one of the most economically valuable in the United States (CDFA, 2022), heavily relies on groundwater extraction for irrigation purposes. During dry periods, there is a notable surge in the construction of agricultural wells and subsequent pumping (Jasechko and Perrone, 2020; Lund et al., 2018; Medellin-Azuara et al., 2022). This trend has triggered a range of adverse effects, including increased depth to groundwater (Liu et al., 2022; Vasco et al., 2022), reduced groundwater storage (Alam et al., 2021), land subsidence (Ojha et al., 2019) and deterioration of groundwater quality (Levy et al., 2021).

During the 2012 to 2016 drought, the California Department of Water Resources (DWR) established the Dry Well Reporting System (DWR, 2023a). Such platforms allows for voluntary reporting of domestic well failures and aims to provide water shortages mitigation assistance. Since its establishment in 2014 until the end of 2022, a total of 5,259 domestic wells have been reported as dry or failed in the state. The majority of these reported failures occurred during the past two drought periods, with 2,425 wells experiencing failure from 2014 to 2016 and 2,588 wells from 2020 to 2022. The greatest concentration of reported dry wells was observed in the Central Valley, where a total of 3,929 domestic wells were affected between 2014 and 2022. Significantly, the subbasins in the San Joaquin Valley (southern region of the Central Valley), namely Kaweah, Kings, Madera, and Tule, accounted for 2,878 of these reported dry wells (Figure 4.1). Given the substantial magnitude of domestic well failure and groundwater depletion (Figure C1), as well as the region's significant agricultural importance, these four subbasins serve as a representative case study area within the broader context of the Central Valley. Insights derived from studying this region can offer valuable perspectives for addressing domestic well vulnerability. Figure 1 (B) shows the number of agricultural and domestic wells by section of the Public Land Survey System (PLSS) and Figure 1 (C) the count by section of dry wells. We can see that the occurrence of domestic well failure happens mainly in high well density areas.

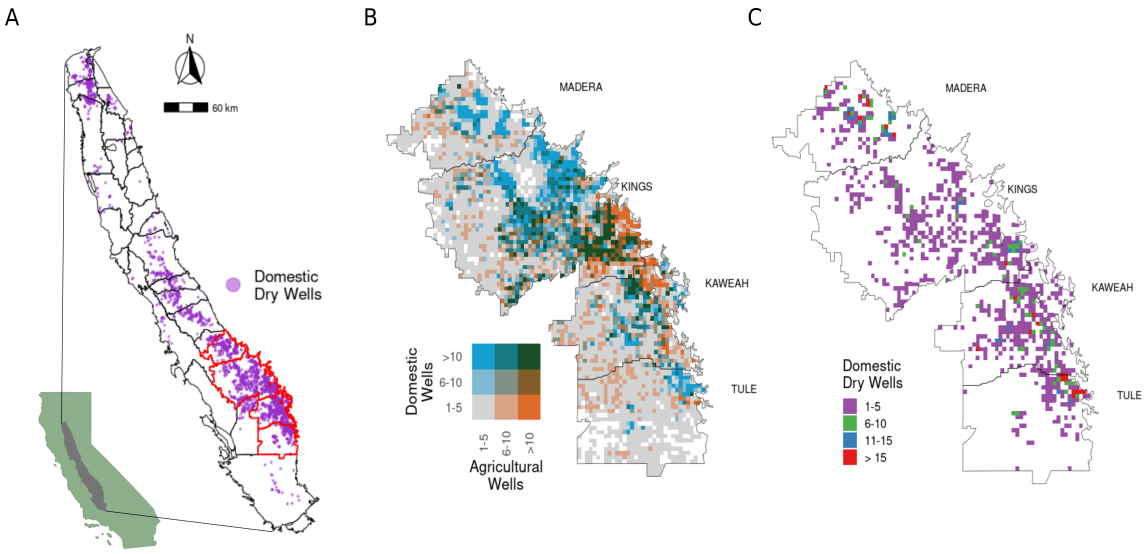

Figure 4.1: Figure A shows the location of reported domestic dry wells between 2014-2022 in the Central Valley California, highlighted in red color is the study area. Figure B shows the number of domestic and agricultural wells per section ($1mi^2$) of the build since 1970. Figure C shows the number of dry wells reported in the 2014-2022 period by PLSS section.

Since the California Sustainable Groundwater Management Act (SGMA) was signed in 2014, Groundwater Sustainability Agencies (GSAs) have been established to develop and implement Groundwater Sustainability Plans (GSPs). These plans aim to conceptualize water budgets, groundwater dynamics, and frame strategies for achieving sustainable groundwater management in each groundwater subbasin. However, since their submission in 2020 there have been inadequate representation of marginalized communities (Dobbin et al., 2023; Leach et al., 2021) and assessment of domestic well vulnerabilities within these plans. Thus, is crucial to gain a comprehensive understanding of the factors that contribute to domestic well failure, as this knowledge is vital for sustainable groundwater management and the protection of domestic wells. Notably, many of these factors can be addressed at the local level, particularly those related to agricultural practices and their associated impacts. For instance, agricultural wells, which are typically deeper and have higher yields than domestic wells (Perrone and Jasechko, 2019), contribute to localized drawdown and groundwater quality degradation (Gailey, 2023; Levy et al., 2021; Pauloo et al., 2020; Perrone

and Jasechko, 2017). Previous studies have focused on forecasting the occurrence of dry wells in the Tule subbasin (Gailey et al., 2019) and at a large scale in the Central Valley (Pauloo et al., 2020) or other basins in western USA (Perrone and Jasechko, 2017). These studies utilized interpolated groundwater levels and drilled depths of domestic wells to identify hotspots of dry wells or vulnerable wells in anticipation of future drought events. While these studies demonstrated high accuracy in predicting dry wells following groundwater declines, they did not comprehensively characterize key localized factors that contribute to the vulnerability of domestic wells.

In this study, we implement a spatial statistical model that utilizes publicly available spatial data sets, including reported dry wells, well completion records, groundwater levels and land use information. Our objective is to identify specific factors that contribute to the vulnerability of domestic wells during droughts. The used spatial model incorporates a Bayesian approach to account for spatial autocorrelation among observations. By employing this approach, we are able to predict the probability of failure of a domestic well within the four subbasins under investigation. Our model results provides valuable insights into the most significant factors within the food-water-human system which merit higher consideration for the development of effective groundwater management strategies.

4.3 Methods

4.3.1 Data and exploratory analysis

The spatial data set used in this study uses records on dry well reports, well completion reports, interpolated groundwater levels from monitoring wells, crop land use, surface water supply and poverty index. These data sets have different spatial resolutions and processing, explained in detail in the following sections. Each well in the data set is located in a section of 1 mi^2 (2.6 km^2) from the PLSS. When specific coordinates of the reported dry well or completed well are unknown the centroid of the section is registered as coordinates of the well by the DWR reporting system. For this reason, we used the PLSS section as reference location. We utilized two spatial resolutions to summarize the data sets for each well in the analysis (they are described in the following sections). First, the section where the well is located and adjacent sections referred as 9 mi^2 (23.3 km^2), depicted in yellow in Figure 4.2, and a second resolution using a 25 mi^2 polygon (64.7 km^2),

depicted in green in Figure 4.2, that includes second-level section neighbors.

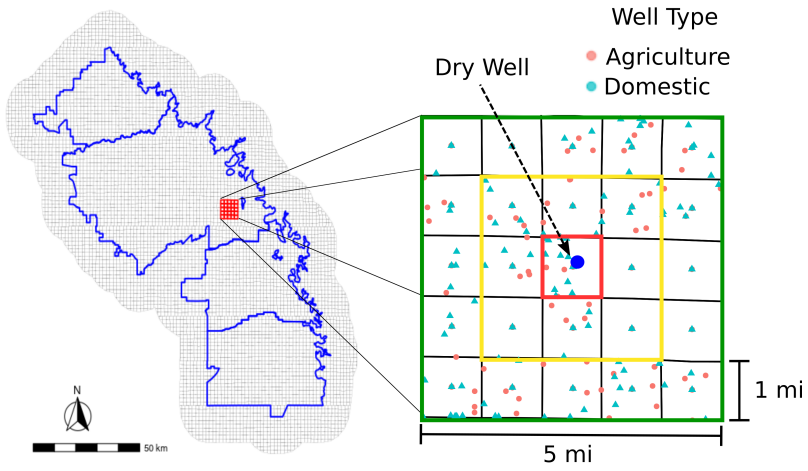

Figure 4.2: Example of dry well location, and surrounding agricultural and domestic wells. The section of the PLSS where a dry well is located is illustrated in red. The 9 mi^2 resolution is illustrated in yellow and the 25 mi^2 in green.

Dry wells and well completion reports

Domestic dry wells are voluntarily reported to the publicly available reporting system from DWR (2023a), which since 2014 collects domestic groundwater supply shortages. These reports are collected from individuals, local agencies, and organizations. Given the volunteer nature of the reports there are uncertainties on the location and well depths reported. Also, an potentially small omission bias from the non-reported dry wells is inherent to the data set and the analysis. However, is the only publicly available data set that collects systematically water shortages from domestic wells. To overcome some of the limitations of this data set, we used the upper boundary of the reported well depth if its a range and removed dry wells that did not report a well depth reported or is unclear. Figure 4.3 shows the count of reported dry wells in the study area before removing uncertain reports.

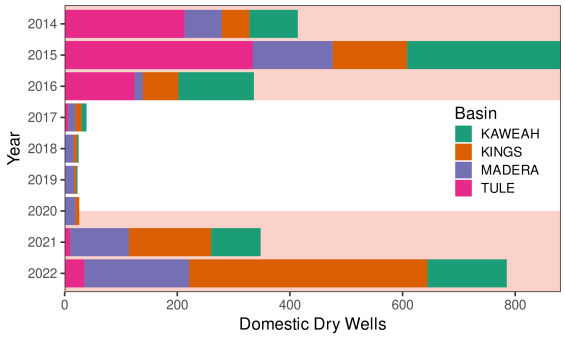

Figure 4.3: Number of dry wells in the four groundwater subbasins of the study area. The dry periods are highlighted in red.

Our data set contains selected dry wells and randomly sampled domestic wells from sections where no dry wells were reported in a way that we have a balance data set with equal number of dry and no dry wells by year and groundwater basin. We calculate the number of agricultural and domestic wells by section using the well completion reporting system from DWR (2023b). For each well and year of analysis we calculated number of wells at the two spatial resolutions (Figure 4.2). We assumed a lifespan of 30 years for domestic wells, as suggested by Pauloo et al. (2020) and Gailey et al. (2019), and 50 years for agricultural wells, from conversations with well drilling technicians. Given the geologic characteristics of California's Central Valley, wells can extract water from the unconfined, semiconfined, or confined aquifer. Given that most reported dry domestic wells (Figure C2) and domestic wells in the study area pump water from the unconfined to semiconfined aquifers, we selected agricultural wells and domestic wells that pump water from these two aquifers (Figures C3 and C4). For more details about this process refer to Appendix C. Additionally, we assumed that agricultural wells and domestic wells from the well completion reporting system may have been inactive by the year of analysis. To remove likely inactive agricultural and domestic wells we used interpolated groundwater levels for the unconfined and semiconfined aquifers (Section 4.3.1) and their location in relation to the top of the well screen, if reported. Otherwise, we used the well depth plus the median distance between the top and drilled depth (Table C1). The final number of estimated "active" wells was used to calculate wells density (number of wells divided by area for each well).

Groundwater Levels

Groundwater levels are reported in the DWR's periodic groundwater level measurements from monitoring wells. We followed the same classification process to the corresponding aquifer location and using only those from the unconfined to semi-confined aquifers. We validate our classification for the monitoring wells reported in the GSP's groundwater monitoring network of each GSA, available in the SGMA portal. Since we want to capture the conditions before each year's irrigation season, we used reported levels from January to April for each year between 2014 and 2022. Finally, we employed an ordinary kriging interpolation method following Pauloo et al. (2020), for the log-transformed ground- water levels, and the correction of Laurent (Laurent, 1963) to obtain unbiased groundwater level estimates. The spatial interpolation via kriging was performed using the gstat R package (Gräler et al., 2016). The final groundwater level raster was used in two ways, first to filter wells with top screens (or approximated top screen) shallower than the interpolated groundwater level, and second to calculate the ratio of the total drilled depth to the interpolated groundwater level for each well in the analysis, used as covariate in the statistical model.

Cropland

Cropland was obtained from the Cropland Data Layer (CDL), referred as CropScape, produced by USDA National Agricultural Statistics Service (NASS) (Boryan et al., 2011). We downloaded the spatial layers from 2014 to 2022 using the CropScapeR package for R (Chen et al., 2023). CropScape classifies each pixel, with 30 m resolution, into 134 different crops and other uses. We categorized crops into three categories: annual crops, perennial crops and forage crops. Table C2 in SM relates CDL crops to each category. Finally, using the cropland rasters (Figure C5) we calculated zonal statistics for each well, generated using the R package exactextractr (Baston, 2022).

Surface Water Supply

Surface water supplies in the San Joaquin Valley vary by water agency and irrigation district. Sources may contracts with state (Central Valley Project) or federal (State Water Project)

projects, water rights to divert water from rivers or streams, as well as transfers with other districts. Due to the lack of a spatial data set that relates each section of the PLSS to a surface water source, we used the historical allocations to each GSA. GSAs reported historical surface water allocation in their GSPs and in their yearly updates, both available in the SGMA portal.

Sociodemographic

We are interested to know if the socio-economic status affects the risk of domestic wells to cause residential water shortages. We hypothetize that lower income communities are often times isolated rural communities surrounded by agriculture, thus are likely more vulnerable to agricultural pumping. To characterize socioeconomic status, employed the poverty index from CalEnviroScreen 4.0 (OEHHA, 2021). This index represents the percent of population living below twice the federal poverty level at the census tract.

Exploratory data analysis

The curated data set contains 2,866 wells distributed in the four groundwater basins of the study area. The predictor variables or covariates of the model are summarized in Table 1, that also includes well depth and groundwater level used to calculate the ratio between well depth and groundwater level. These variables are selected to represent the localized characteristics of the system that can affect the domestic well vulnerability during dry years.

To identify relationships between covariates we estimated Pearson correlation coefficients, shown in Figure 4.4. The strongest positive correlation is between area of perennial crops and agricultural wells density. The largest negative correlations are between poverty and domestic wells density, surface water supply and poverty and rate of perennial crops and rate of annual crops. We measured the variance inflation factors (VIF) which resulted lower than 1.5 for all the variables indicating that there is no collinearity among them. Given that wells may be located in the same section or adjacent sections, spatial autocorrelation may exist between well failure conditions and covariates values. For this reason we tested for spatial autocorrelation using the Moran's I test, shown in Figure C6, where the test resulted in positive and significant spatial autocorrelation for all the variables up to 50 km between wells.

Variable	Description	Mean	Sd	Min	Max
r_area_perennial	Perennial crops proportion	0.34	0.13	0	0.9
r_area_annual	Annual crops proportion	0.19	0.11	0	0.66
r_area_forage	Forage crops proportion	0.071	0.053	0	0.38
r_well_depth_gw_level[1]	Ratio well depth to groundwater level	1.8	1.5	0.15	29
ag_wells_density	Density agricultural wells	0.0064	0.0052	0	0.028
dom_wells_density	Density domestic wells	0.014	0.018	0	0.12
Poverty	Poverty Index	45	18	3.8	85
Surface_Water[2]	Surface water supply (M m^3)	99	128	0	620
well_depth	Drilled well depth (m)	62.4	36.6	4.5	300
gw_level	Groundwater level Spring (m)	40.5	22.5	9.3	153

Table 4.1: Summary of the variables before standardization used in the statistical model for the $9mi^2$ resolution. Wells density and crop rate areas were calculated using $\approx$ 5,760 acres for each well's $9mi^2$ resolution polygon.[1] We used the groundwater level before the irrigation season [2]Surface water deliveries were used at the GSA scale, thus these values represent statistics across GSAs that can be inconsequential.

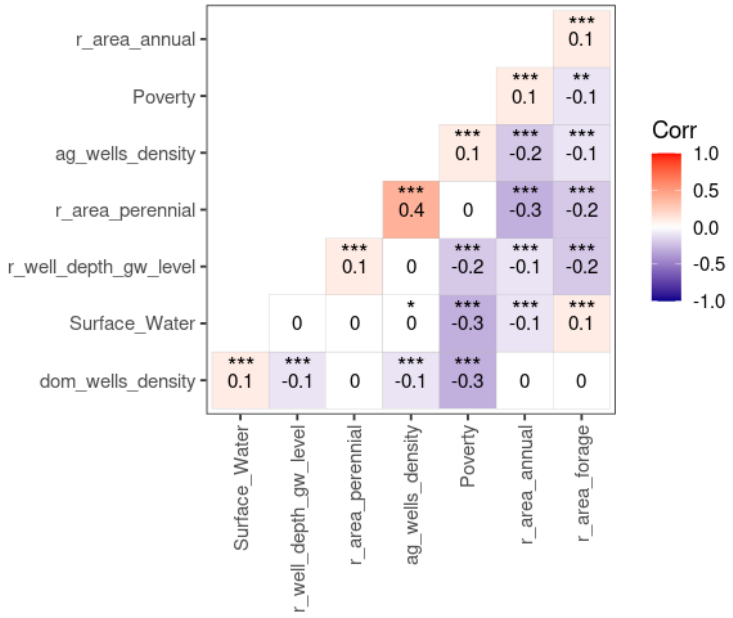

Figure 4.4: Pearson's correlation coefficients between covariates of the $9mi^2$ resolution data set. Asterisks represent the significance level of the coefficient, p < 0.05 (*), p < 0.01 (**) and p < 0.001 (***). Significance coefficients and figure were obtained using the ggcorrplot R package (Kassambara and Patil, 2022).

We fit linear models to identify the associations between domestic well failure and each covariate used in the spatial model (Section 4.3.2). Figure 4.5 shows results of the linear fits, where the orange line is the mean coefficient and in grey the 95% credible interval. Figure 4.5 (A) shows the ratio between well depth and groundwater level has the strongest negative association with well failure (Figure 5 (F)). We would expect a higher probability of domestic well failure in places with high domestic well density (Figure 5 (D)) and agricultural wells density (Figure 5 (E)). Cropland distribution (perennial, annual, and forage) shows similar positive association with domestic failure (Figure 5 (A) - (C)). Finally, in places with higher poverty index a higher probability of domestic well failure is expected. Since there is not data available on groundwater pumping at a fine resolution we asses if cropland ratio has an interaction effect with the agricultural wells density that can potentially affect domestic well failure, results are shown in (Figure C7). The exploration of these results provide insight on the individual effects of covariates to domestic failure before fitting the spatial model and that interaction effects between cropland rate and agricultural wells density should be included.

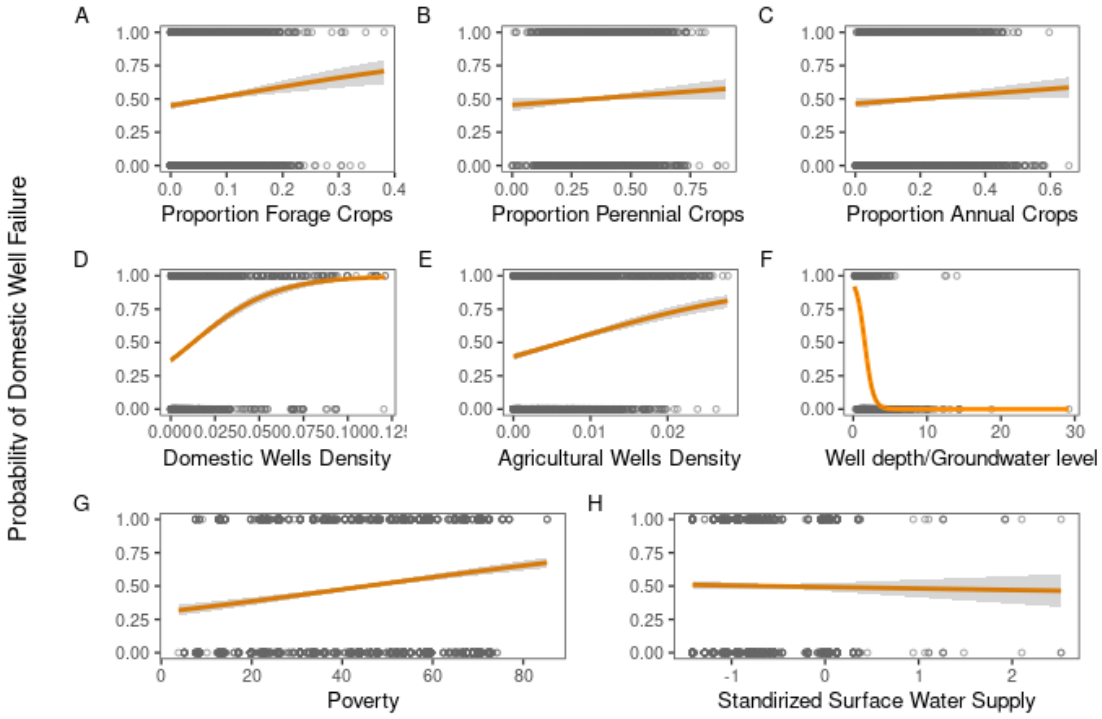

Figure 4.5: Results from performing linear fits for the covariates used in the study. The mean of the linear fit is depicted in orange and the estimated 95% credible interval. Dots represent observations of reported domestic well failure (1) or not (0). This analysis ignores spatial random effects and fits were generated using the model: $W_i \sim Bernoulli(p_i)$ where $logit(p_i) = \beta_j X_j$ and W_i = 1 if domestic well failure was reported and W_i = 0 if not.

4.3.2 Spatial model

We split the data into training and validation data sets, using block cross-validation, performed with the blockCV R package (Valavi et al., 2019). This splitting method is considered a robust approach for assessing predictive performance and error estimation of spatial models. We used 20% of the wells with equal number of positive or negative failure condition for validation. Additionally, variables were transformed using z-score standardization (mean of 0 and standard

deviation of 1) to interpret all the fixed-effect coefficients in the same scale. Surface water supply was standardized at the GSA scale to accurately capture the effect of deviations from the mean water supply.

The spatial model to predict the probability of domestic well failure was defined using the R-INLA package that relies on the Integrated Nested Laplace Approximation (INLA) for Bayesian inference (Blangiardo and Cameletti, 2015; Lindgren and Rue, 2015). R-INLA calculates a Gaussian Markov Random field to account for spatial autocorrelation via Stochastic Partial Differential Equation (SPDE) with a Matérn covariance function (Krainski et al., 2018). This method has proven to efficiently model spatially dependence of residuals and has been widely applied in socioenvironmental and environmental systems (Bosmans et al., 2022; Burchfield and Nelson, 2021; Expósito-Granados et al., 2019; Fichera et al., 2023; Gong et al., 2021; Jaffé et al., 2021; Ndolo et al., 2022; Nelson and Burchfield, 2017). The first step to approximate the SPDE is to create a mesh over the study region using a constrained refined Delaunay triangulation, where triangles define the basis of functions (Zuur et al., 2017). Multiple parameters are used to tune the triangulation, firstly we use the distances between wells (Figure C8) to define a distance of 16 km for the maximum edge length of the finer inner mesh and 80 km for the edge of triangles outside of it to avoid boundary effects. In addition, we define a cutoff value of 3 km (2 mi) that constrains assignment of wells with a distance of less than 3 km to single vertex, avoiding very small triangles. The final 537-vertices mesh is shown in Figure C9.

We predict domestic well failure (n=2,866 observations) using the model defined by Equation 1. Where W_i is the binary condition failure (W = 1) or no failure (W = 0) of a domestic well i. Equation 2 is the logit-link function for the Bernoulli probability function where p_i is the expected value of the probability of a well i to fail, α is the intercept, X_j is the j covariate of well i and β_j is the fixed effect coefficient. β_c are the interaction effects between crop categories (c={r_area_annual,r_area_perennial,r_area_forage}) and agricultural wells density. Additionally, we include a basin-level random intercept effects (iid) (β_g) to identify if well failure vulnerability changes across groundwater basins. S_i accounts for spatial random effects (SPDE). We use the R-INLA default uninformative priors.

$$W_i \sim Bernoulli(p_i) \tag{4.1}$$

$$logit(p_i) = \alpha + \sum_{j=1}^{9} \beta_j X_{j,i} + \sum_{c=1}^{3} \beta_c X_{c,i} X_{ag\_wells\_density,i} + \beta_g Basin_{g,i} + S_i \tag{4.2}$$

We run the model described by Equations 1 and 2 comparing different model configurations and two spatial resolutions ($9mi^2$ and $25mi^2$), defined in SM 6.1. Model configurations are defined to assess how information from different components of the human-food-water system affect the prediction of domestic well failure. We use different cross-validation and information criteria (Gelman et al., 2014) provided by R-INLA to compare ten model configurations (5 models and two spatial resolutions). These metrics include Deviance Information Criterion (DIC) (Spiegelhalter et al., 2002), Watanabe–Akaike information criterion (WAIC) (Watanabe, 2010), and Logarithmic Conditional Predictive Ordinate (LCPO) (Roos and Held, 2011). In addition, we calculate the Area Under the receiver operating characteristic Curve (AUC) (Fawcett, 2006) using the PresenceAbsence R package (Freeman, 2023). Lower DIC, WAIC and LCPO values suggest superior model performance and higher AUC suggest superior classification performance (true positive well failure and true negative well failure). Readers can refer to the following GitHub repository to access model script used for modeling, model diagnostics and visualization of results: https://github.com/josemrodriguezf/Domestic_Dry_Wells.

4.4 Results

Our model predicted well the probability of a well to go dry. The model described by Equations 1 and 2, using the 9 mi^2 resolution, resulted in the lowest DIC, WAIC, and LCPO, and highest AUC. The AUC is 0.88 for the fitting data set (Figure C10) and 0.92 for the validation data set (Figure C11), demonstrating good performance on domestic well failure prediction across space (Figure C12). The model shows no spatial autocorrelation of the residuals (Figure C13). Model results for all model configurations and spatial resolutions are shown in Table C3.

Figure 4.6(A) shows the mean and 95% credible intervals of the marginal posterior distribution of fixed effects and interaction effects. Figure 4.6(B) shows the posterior distribution for

groundwater subbasin specific random effects. Estimates are in the log-odds of a well to fail, and are also summarized in Tables C4 and C5. Each coefficient from covariates without interaction effects (sw, poverty, r_well_depth_gwlevel and dom_wells_density) are interpreted as the change in log-odds corresponding to a one standard deviation change in the covariate. The most important single effect predictor is the ratio between well depth and groundwater level that has a negative effect (-2.76 mean). In line with established expectations wells with deeper depths than the groundwater level are less probable to fail. However, other factors attribute to domestic well vulnerability as domestic wells density that has the largest positive coefficient (0.75 mean), followed by the poverty index (0.24 mean). Surface water deliveries distribution overlaps with zero, the rationale behind this value is that we focused on dry years to build the data set and there are no meaningful differences in surface water supplies across these drier years that can change the expectation of domestic well failure.

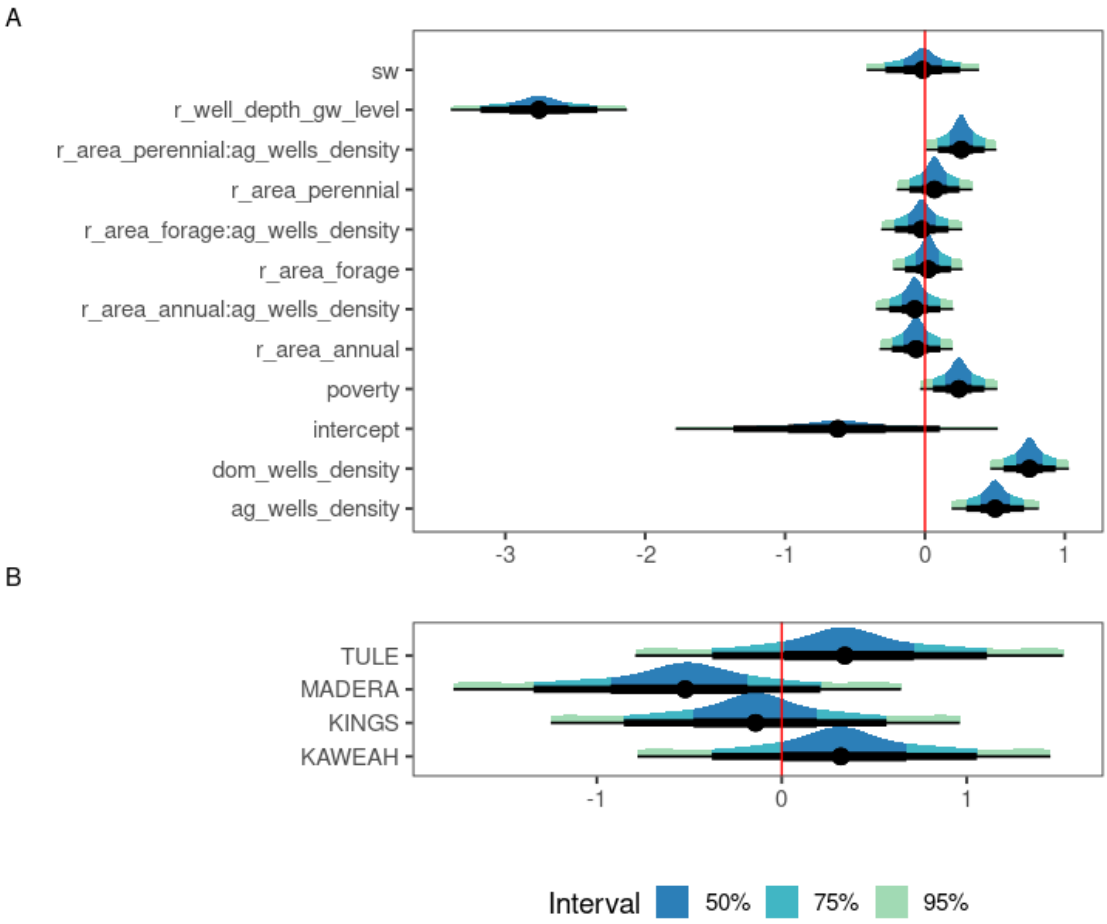

Figure 4.6: Posterior means and 95% credible intervals for fixed effects (A) and random effects by groundwater subbasin (B). Values are in log-odds scale. Surface water supply (sw), ratio between well depth and groundwater level (r_well_depth_gw_level), proportion perennial crops (r_area_perennial), proportion forage crops (r_area_forage), proportion annual crops (r_area_annual), poverty index (poverty), density agricultural wells (ag_wells_density) and domestic wells density (dom_wells_density).

In addition to the single fixed effects the model includes interaction effects between crop types and agricultural wells density. The most important interaction effect is the coefficient between perennial crops ratio and agricultural wells density. This coefficient represents the increase in

the agricultural wells density coefficient by an increase of perennial crops area by one standard deviation. Thus, an increase in perennial crops increases the effect that agricultural wells can have on domestic well failure. This coefficient can also be interpreted in the other direction, given an increase in agricultural wells density the expected impact of perennial crops to domestic well failure also increases. Although the coefficients for forage crops, annual crops and their interaction effects with agricultural wells density are not too far from zero, this does not imply that pumping to irrigate forage and annuals do not affect domestic wells, but rather these coefficients are less important predictors of domestic well failure considering all the other covariates in the model.

Finally, the model includes groundwater subbasin random effects which allow us to compare expected domestic well failure given the variability that exists across basins (e.g., geology, groundwater depletion, groundwater management, and land uses). Though the 75% credible intervals of these coefficients overlap with zero, we can observe that there is a higher expectation of domestic well failure in Tule and Kaweah subbasins than Madera and Kings subbasins. Finally, in Figure C14 we show the SPDE product of R-INLA.

4.5 Discussion

4.5.1 Domestic wells, agriculture and droughts

The results of our analysis suggest that domestic wells are most vulnerable when the distance between groundwater level and well depths are closer and is the most important factor that affects domestic well vulnerability (r_well_depth_gw_level variable). We examined the characteristics of wells drilled between 1970 and 2022 to better understand domestic wells vulnerability. Well drilling takes place more often during dry years, particularly during extended droughts (Figure C16). Kings subbasin shows the largest number of domestic and agricultural well construction with 60% of the wells in the study area (Figure C17). In the the four basins of analysis, agricultural wells have deeper depths than domestic wells (Figure C18). However, this difference changes across subbasins (Figure C19), the largest difference is found in the Tule subbasin where the mean agricultural well depth is 150 meters deeper than the mean domestic well depth, followed by Madera subbasin with a difference of 70 meters. In Kings and Kaweah subbasins this difference is around 30 meters. Shallower wells are more vulnerable than agricultural wells during droughts which is a common

characteristic of the Central Valley and other places in the western USA (Jasechko and Perrone, 2020; Pauloo et al., 2020; Perrone and Jasechko, 2019).

Domestic and agricultural pumping have a key role on localized groundwater dynamics. Even though there is lack of information about groundwater use or pumping rates data at the resolution of this study, results indicate that domestic wells located in areas with higher domestic wells density are more likely to go dry. Groundwater pumping causes a cone of depression with an ultimate drawdown of the water table (Bierkens and Wada, 2019; Condon and Maxwell, 2014). Agricultural wells are deeper (Figure C23) and have larger casing diameter (Figure C24) than domestic wells, resulting in larger drawdown than domestic wells. Additionally, higher wells density can potentially result in overlapping depression cones, leading to larger and deeper hot spots of groundwater drawdown. In the well completion reports, a drawdown is reported from the pumping test done after the well is completed, with median of 7.6 m and 4.6 m for agricultural and domestic wells respectively (Figure C25). During dry years, increased pumping leads to drawdown that can cause well failure before the groundwater table reaches a deeper level than the well perforation depth (Gailey et al., 2022). In addition, drawdown can create localized water quality degradation (Levy et al., 2021; Smith et al., 2018).

Results suggest that domestic wells in areas with higher rate of perennial crops are more vulnerable. The study area has shown an expansion of perennial crops, mainly nut trees such as almonds and pistachios. Though these crops are highly profitable they have higher evaporative demand (Hanak et al., 2019). Consequently, they require irrigation every year despite surface water shortages, relying on pumping. The increase of perennial crops and agricultural well drilling are correlated (Figure 3.4). This trend has been documented as one of the main drivers of continuous groundwater depletion, which also makes groundwater management more challenging and less flexible (Mall and Herman, 2019; Qin et al., 2019; Rodríguez-Flores et al., 2022).

4.5.2 Social impacts

Our results indicate that places with higher poverty index are more vulnerable to domestic well failure. As reviewed by Johnson and Belitz, 2015 and London et al., 2021, rural areas or outside of incorporated city boundaries are less likely to be served by municipal or other larger public water supply systems. Consequently, rural areas heavily depend on private domestic wells

for their water supply, which significantly increases their risks of water shortages and compromise their water quality (Aiken et al., 2023; Balazs and Ray, 2014; Hauptman et al., 2023; Horowitz et al., 2016; Pace et al., 2022; Tariqi and Naughton, 2021).

In the study area, there is a higher concentration of domestic wells in census tracts with a poverty index between 30 and 60. Areas with a poverty index between 0 and 30 have the second most number of domestic wells, followed by areas with high levels of poverty (between 60 and 90) (Figure C26). However, this trend changes for the reported dry wells. After areas with moderate poverty (30 to 60), high poverty areas reported the second most number of domestic dry wells (Figure C27). Well depths are similar for all areas despite of the poverty level (Figure C28), thus domestic well vulnerability of higher poverty areas arises from being more rural areas impacted by agriculture. These low-income communities are inhabited mostly by people of color (London et al., 2021; Méndez-Barrientos et al., 2022; Pace et al., 2022), who have limited infrastructure and are exposed to other environmental risks (Anderson et al., 2018; Fernandez-Bou, Ortiz-Partida, Dobbin, et al., 2021; Flores-Landeros et al., 2022). Though the poverty index is reported at the census tract level, which may misrepresent conditions of small rural communities designated to larger census tracts, the results are consistent with prior studies (Johnson and Belitz, 2015; Klasic et al., 2022; Perrone and Jasechko, 2017).

Numerous wells within the dry well reporting system reported solutions to address the water shortage. Common adaptations include lowering pumps and replacing dry wells with deeper wells (Gailey, 2023). However, drilling deeper wells entail higher upfront costs (Feinstein et al., 2017; Gailey et al., 2019; Perrone and Jasechko, 2019), larger operating cost (given the increased lift and energy use), and in some cases, deeper groundwater may contain elevated levels of salts or other contaminants making it unsuitable for domestic use (Kang and Jackson, 2016). For instance, the costs related to drilling domestic wells, typically fall within the range between $118 and $200 per meter (Gailey et al., 2022; SWRCB, 2022). This poses a burden for low-income communities to be self-sufficient considering that wells in the study area would need to be drilled deeper than 80 meters and in some places more than 100 meters. Thus, communities are compelled to depend on state's support like the "Small Community Drought Relief" that provides funds for household water storage tanks and hauled water, or depend on alternative resources such as tanker trucks and bottled water (London et al., 2021; Méndez-Barrientos et al., 2022).

Studies suggests that low-income or marginalized communities have been inadequately represented in the development of the groundwater sustainability plans (GSPs), leading to rather shortsighted planning strategies that overlook the water access and quality requirements of domestic well users in rural communities (Dobbin and Lubell, 2021; Dobbin et al., 2023; Leach et al., 2021; Perrone et al., 2023), despite being part of SGMA implementation objectives. For example, one of the metrics to guide sustainable groundwater planning is the establishment of a minimum threshold defined as "the quantitative value that represents the groundwater condition in each area that may cause an undesirable results (DWR, 2017). These thresholds are established in each GSP and in many cases prioritize agricultural wells depths to define this threshold, which as we discussed are deeper, leaving hundreds of domestic wells unprotected (Bostic, 2021; Perrone et al., 2023). Additionally, potential solutions are more likely to be successful if communities are engaged in the decision making process as suggested by Fernandez-Bou, Ortiz-Partida, Classen-Rodriguez, et al. (2021) and Espinoza, Bernacchi, et al. (2023). However, since GSPs were submitted in 2021 the state has reviewed them and required revision to address risk of domestic wells failure. At the time this study was being developed, six plans were rejected including the Kaweah and Tule subbasins where wells are more vulnerable, as indicated by the results.

4.5.3 Groundwater levels and domestic well failure trends

The reported depths of dry wells during the 2014 to 2016 period and the 2020 to 2022 period do not exhibit significant variations across the study area (Figure C30). However, there is a discernible shift in their spatial distribution. Although groundwater depletion and the occurrence of domestic dry wells are widespread phenomena that have been observed throughout the Central Valley (Jasechko and Perrone, 2020), we identify spatial nuances. The Tule subbasin saw the largest number of reported dry domestic wells during 2014-2016, followed by the Kaweah subbasin, whereas Kings and Madera subbasins reported the largest number of dry wells during between 2020 and 2022.

All groundwater subbasins have shown increasing groundwater levels (Figure C32), however to have a better understanding on particular conditions that led to well failure we further explore trends at the GSA level (Figure C33) that changed the spatial distribution of dry wells between the two droughts (Figure C34). The Eastern Tule GSA located in the Tule subbasin, exhibits one of

deepest water tables in the study area (Figure C35) and the highest count of reported dry wells, predominantly during the 2014-2016 period when most of the domestic wells in the subbasin failed. Despite groundwater recovery between the two drought periods, the 2020-2022 drought resulted in larger distance to groundwater (deeper than 100 m) leading to the failure of deeper domestic wells. GSAs in the Kings subbasin did not exhibit significant groundwater level increases prior to 2020 (Figure C36). However, during the 2020-2022 drought, substantial groundwater depletion that lead to shallow domestic wells failure. The County of Madera GSA in the Madera subbasin, has shown a constant rate increase in the water table since 2014 (Figure C37), that in 2020-2022 than in 2014-2016. Lastly the Kaweah subbasin shows the largest rate of groundwater depletion (Figure C38), after Tule subbasin, which increased the number of dry wells in 2020-2022 than in 2014-2016. Despite showing recovery of groundwater levels during the 2017-2019 wet years, groundwater levels reached deeper levels in the last drought (deeper than 50 m) leading to domestic well failure of shallow domestic wells of the area (median of 65 m).

In Figure C39, we show the drilled depths of domestic wells by GSA used to support this analysis and identify GSAs where domesic wells are more vulnerable given the trends on groundwater levels at the GSA level. In all GSAs, despite the recovery of groundwater depths during the wet years following the 2012-2016 drought and that surface water shortages during the 2020-2022 drought were not as profound and extended as during 2012-2016 (Figures C40 to C43), the lack of groundwater management, large pumping capacity and increased area of perennial crops led to increased groundwater levels and domestic well failure.

4.5.4 Implications for water and land management

Though the Sustainable Groundwater Management Act is in early implementation stages and the impacts of groundwater pumping during the last drought (2020-2022) showed again the lack of management. In the future strategies should be implemented by substantial pumping constraints (Escriva-Bou et al., 2020) and cropland retirement (Escriva-Bou et al., 2023), regardless of the upcoming dry periods in order to meet the 2040 sustainability goal. Based on our results groundwater management should address localized factors that are most influential in well failure risk. Which can be addressed by different land and water management actions, including strategic multibenefit cropland repurposing (Bourque et al., 2019; Bryant et al., 2020; Espinoza, Bernacchi,

et al., 2023; Fernandez-Bou et al., 2023). The objective of this approach is to retire cropland to reduce pumping (and water consumptive use), and allocate it to other less water intensive uses, while providing other benefits for communities and ecosystems. Another strategy is Managed Aquifer Recharge (MAR), designed to augment and restore groundwater by capturing and infiltrating excess surface water (Levintal et al., 2023; Marwaha et al., 2021; Ulibarri et al., 2021; Wendt et al., 2021). These projects can be strategically implemented nearby to communities to counterbalance localized groundwater drawdown.

Our findings indicate that the implementation of cropland repurposing, particularly of perennial crops, holds the potential to decrease the vulnerability of domestic wells. This finding aligns with the conclusions drawn by Fernandez-Bou et al. (2023), who studied the benefits of creating land use buffers around communities mostly by repurposing agricultural land. While the retirement of perennial crops from production may result in near term revenue losses for farming and reduced agricultural employment income for communities, previous research findings indicate that mitigation costs of dry wells might be higher with more drastic cost burdens for low-income communities (Bostic, 2021; Feinstein et al., 2017). Additionally, maintaining state programs to mitigate well failure, such as delivering water tanker trucks is economically costly and unsustainable (Feinstein et al., 2017; Méndez-Barrientos et al., 2022). For example the DWR's small community drought relief program had a budget of $190 million available in 2021, and $95 million to continue the program in 2022 in addition to $20 million allocated to the water storage tank and hauling program.

State initiatives have been created to facilitate cropland transition and alleviate its economic impacts. For example, the state's Department of Conservation created the Multibenefit Land Repurposing Program (MLRP), where the state has awarded multistake holder partnerships to fund planning and implementation of multibenefit cropland repurposing projects. Another example is the LandFlex program implemented by DWR in partnership with GSAs, that provides financial incentives to farmers that fallow land for each acre-foot (1,233 m^3) of water saved (up to $350/ acre-foot), as well as incentives for each permanently eliminated acre-foot of annual pumping ($1,000/ acre-foot) and incentives to perform climate resilient agricultural practices such as as removing permanent crops (up to $2,800/acre). Additionally, strategic cropland repurposing should consider the overall cost-effectiveness, which in some cases the expenses associated with retiring

cropland may outweigh the mitigation costs of domestic well failure. This highlights the importance of exploring alternative approaches, such as cost-sharing mechanisms (Stone et al., 2022) or financing options for the replacement of domestic wells.

Based on our findings, it is evident that a higher density of wells increases the vulnerability of domestic wells. GSAs should exercise control over the approval of new agricultural well drilling, taking into account the density of wells. Furthermore, comprehensive monitoring of pumping activities and groundwater levels should be conducted in regions characterized by a significant density of agricultural wells. The state passed a bill in 2022 (Assembly Bill 2201), which mandates that the approval of new agricultural well permits be subject to the oversight of GSAs. Notably, the potential impact of the new well's pumping on nearby domestic wells must be carefully considered before granting approval. Prior to the enactment of this bill, the approval process for agricultural wells solely rested with county authorities, often limited to paperwork requirements, without due consideration of the potential consequences associated with the long term water supply reliability of the authorized wells.

Lastly, consolidation of the water systems of unincorporated disadvantaged communities to nearby urban centralized water supply systems can guarantee water security. This has occurred with several communities already, such as East Portverville in the Tule subbasin where hundreds of houses experienced well failures between 2012 and 2016. While this solution may not be feasible for all the communities due to the large financial investment requirements (Klasic et al., 2022; Méndez-Barrientos et al., 2022) and wide separation to a public water supply system, environmental justice organizations are advocating in favor of it because of its multiple advantages. However, complexities associated with social dynamics post-consolidation need to be taken into account with community participation to have a successful implementation (Egge and Ajibade, 2023).

4.6 Limitations

Our study has limitations attributed to the characteristics of the utilized data sets, and we acknowledge the presence of inherent uncertainties. Many of these uncertainties pertain to publicly available data on groundwater levels, completed wells, and dry wells, which have been previously discussed (Jasechko et al., 2020; Pauloo et al., 2020; Gailey et al., 2019). We outline

the most significant limitations of the study. 1) DWR's voluntary reporting system of domestic well failures and well completion reports may underrepresent the total number of dry wells and number of wells that exists. The location of the wells is uncertain and often times the centroid of the nearest PLSS section is used. Additionally, the characteristics of the wells (e.g., well depth and screen location) may lack of accuracy. 2) There are temporal and spatial variations in the monitoring well data, which lead to inconsistencies in reporting groundwater levels. Since 2014 the number of monitoring wells has increased, however many of the monitoring wells do not report consistent measurements over the time of the study. 3) Given the inconsistencies in the monitoring wells data, the interpolated groundwater levels and wells classifications may have inaccuracies. 4) The land use information obtained from USDA's CropScape, relies on remote sensing which have classification errors (Espinoza, Booth, et al., 2023). However, in our study we are only interested in proportions for larger crop categories which reduces the uncertainty.

4.7 Conclusion

In this study, we conducted a comprehensive spatial analysis of domestic well failure in the Central Valley, California, focusing on the subbasins of Tule, Kaweah, Kings, and Madera. The region, known for its high levels of groundwater overdraft and susceptibility to droughts, has experienced a significant number of domestic well failures in recent years. We employ a reproducible modeling framework that integrates key components of the food-water-human system to understand domestic wells vulnerability. Notably, we identified the proximity between well depths and groundwater levels, the density of domestic and agricultural wells, and the extent of perennial crop areas as the most influential factors. These results highlight the importance of considering groundwater levels, well drilling, pumping and land management in sustainable groundwater management practices, particularly in areas where numerous individuals depend on unprotected self-supply groundwater sources. We discuss the implications of our findings within the context of current sustainable groundwater management implementation. We addressed some of the existing state-funded initiatives that can be employed, along with their limitations. Our study has broader applicability and can inform decision-making processes in other regions facing similar challenges in California, western USA or other semiarid areas where domestic wells are vulnerable to ground-

water depletion.

4.8 Limitations

Our study has several limitations that arise from the characteristics of the utilized data sets, and we acknowledge the presence of inherent uncertainties. Many of these uncertainties are related to publicly available data on groundwater levels, completed wells, and dry wells, which have been previously discussed Gailey et al., 2019; Jasechko and Perrone, 2020; Pauloo et al., 2020. We outline the most significant limitations of our study, which can be addressed in future research:

- The voluntary reporting system of domestic well failures and well completion reports by the DWR may lead to an underrepresentation of the total number of dry wells and the number of existing wells. Additionally, the uncertainty in the location of these wells often results in using the centroid of the nearest PLSS section, and the accuracy of well characteristics, such as well depth and screen location, may be lacking.

- The monitoring well data exhibit temporal and spatial variations, leading to inconsistencies in reporting groundwater levels. Although the number of monitoring wells has increased since 2014, many of them do not consistently provide measurements over the study period. Moreover, the spatial interpolation method using kyrgging may have limitations, necessitating exploration of other spatial interpolation techniques.

- The land-use information obtained from USDA's CropScape relies on remote sensing, which may introduce classification errors Espinoza, Booth, et al., 2023. However, our study focuses on proportions by large crop categories, which helps to reduce uncertainty.

- We used poverty as a socioeconomic index, but there are other important factors, such as race, that should be considered to better characterize communities and inform policy implementation to achieve environmental justice.

- The model was designed for dry periods, which may limit its ability to capture the effects of increased surface water supplies on domestic well vulnerability. Additionally, since the

model aggregates domestic wells and the majority of the domestic and reported dry wells are in more urbanized areas, isolated wells in rural areas may be misrepresented, reducing the reliability of the results for predicting domestic well failure.

4.9 Acknowledgements

This work was supported by the Agriculture and Food Research Initiative (competitive grant number 2021-69012-35916) from the USDA National Institute of Food and Agriculture and by the California Department of Food and Agriculture (grant agreement 21-0557-000-SO). José M. Rodríguez-Flores was partially supported by the UC Mexus-CONACYT scholarship. The views expressed in this work represent those of the authors and do not necessarily reflect the views of the funding agencies.

4.10 Bibliography

Aiken, M. L., Pace, C. E., Ramachandran, M., Schwabe, K. A., Ajami, H., Link, B. G., & Ying, S. C. (2023). Disparities in Drinking Water Manganese Concentrations in Domestic Wells and Community Water Systems in the Central Valley, CA, USA. *Environmental Science & Technology*. https://doi.org/10.1021/acs.est.2c08548

Alam, S., Gebremichael, M., Ban, Z., Scanlon, B. R., Senay, G., & Lettenmaier, D. P. (2021). Post-Drought Groundwater Storage Recovery in California's Central Valley. *Water Resources Research*, *57*(10), e2021WR030352. https://doi.org/10.1029/2021WR030352

Anderson, C. M., Kissel, K. A., Field, C. B., & Mach, K. J. (2018). Climate Change Mitigation, Air Pollution, and Environmental Justice in California. *Environmental Science & Technology*, *52*(18), 10829–10838. https://doi.org/10.1021/acs.est.8b00908

Balazs, C. L., & Ray, I. (2014). The Drinking Water Disparities Framework: On the Origins and Persistence of Inequities in Exposure. *American Journal of Public Health*, *104*(4), 603–611. https://doi.org/10.2105/AJPH.2013.301664

Baston, D. (2022). Exactextractr: Fast Extraction from Raster Datasets using Polygons. https://github.com/isciences/exactextractr

Bierkens, M. F. P., & Wada, Y. (2019). Non-renewable groundwater use and groundwater depletion: A review. *Environmental Research Letters*, *14*(6), 063002. https://doi.org/10.1088/1748-9326/ab1a5f

Blangiardo, M., & Cameletti, M. (2015). *Spatial and Spatio-temporal Bayesian Models with R - INLA*. John Wiley & Sons.

Boryan, C., Yang, Z., Mueller, R., & Craig, M. (2011). Monitoring US agriculture: The US Department of Agriculture, National Agricultural Statistics Service, Cropland Data Layer Program. *Geocarto International*, *26*(5), 341–358. https://doi.org/10.1080/10106049.2011.562309

Bosmans, J., Schipper, A., Mielke, K., Čengić, M., Gernaat, D., Vuuren, D. v., & Huijbregts, M. (2022). Determinants of the distribution of utility-scale photovoltaic power facilities across the globe. *Environmental Research Letters*, *17*(11), 114006. https://doi.org/10.1088/1748-9326/ac9851

Bostic, D. (2021). *At Risk: Public Supply Well Vulnerability Under California's Sustainable Groundwater Management Act* (tech. rep.). Pacific Institute.

Bourque, K., Schiller, A., Loyola Angosto, C., McPhail, L., Bagnasco, W., Ayres, A., & Larsen, A. (2019). Balancing agricultural production, groundwater management, and biodiversity goals: A multi-benefit optimization model of agriculture in Kern County, California. *Science of The Total Environment*, *670*, 865–875. https://doi.org/10.1016/j.scitotenv.2019.03.197

Bryant, B. P., Kelsey, T. R., Vogl, A. L., Wolny, S. A., MacEwan, D., Selmants, P. C., Biswas, T., & Butterfield, H. S. (2020). Shaping Land Use Change and Ecosystem Restoration in a Water-Stressed Agricultural Landscape to Achieve Multiple Benefits. *Frontiers in Sustainable Food Systems*, *4*. https://doi.org/10.3389/fsufs.2020.00138

Burchfield, E. K., & Nelson, K. S. (2021). Agricultural yield geographies in the United States. *Environmental Research Letters*, *16*(5), 054051. https://doi.org/10.1088/1748-9326/abe88d

CDFA. (2022). *California agricultural statistics review 2021-2022* (tech. rep.). California Department of Food and Agriculture (CDFA). https://www.cdfa.ca.gov/Statistics/PDFs/2022_Ag_Stats_Review.pdf

Chen, B., Gramig, B., & Mieno, T. (2023). CropScapeR: Access Cropland Data Layer Data via the 'CropScape' Web Service. https://cran.r-project.org/web/packages/CropScapeR/index.html

Condon, L. E., & Maxwell, R. M. (2014). Groundwater-fed irrigation impacts spatially distributed temporal scaling behavior of the natural system: A spatio-temporal framework for understanding water management impacts. *Environmental Research Letters*, *9*(3), 034009. https://doi.org/10.1088/1748-9326/9/3/034009

Diffenbaugh, N. S., Swain, D. L., & Touma, D. (2015). Anthropogenic warming has increased drought risk in California. *Proceedings of the National Academy of Sciences*, *112*(13), 3931–3936. https://doi.org/10.1073/pnas.1422385112

Dobbin, K. B., & Lubell, M. (2021). Collaborative Governance and Environmental Justice: Disadvantaged Community Representation in California Sustainable Groundwater Management. *Policy Studies Journal*, *49*(2), 562–590. https://doi.org/10.1111/psj.12375

Dobbin, K. B., Kuo, M., Lubell, M., Bostic, D., Mendoza, J., & Echeveste, E. (2023). Drivers of (in)equity in collaborative environmental governance. *Policy Studies Journal*, *51*(2), 375–395. https://doi.org/10.1111/psj.12483

DWR. (2017). *Sustainable Manage Criteria* (tech. rep.). California Department of Water Resources, Sustainable Groundwater Management Program. https://water.ca.gov/Programs/Groundwater-Management/SGMA-Groundwater-Management/Best-Management-Practices-and-Guidance-Documents

DWR. (2023a). Dry Well Reporting System Data. https://data.ca.gov/dataset/dry-well-reporting-system-data

DWR. (2023b). Well Completion Reports. https://data.ca.gov/dataset/well-completion-reports

Egge, M., & Ajibade, I. (2023). Water struggles and contested use: A capabilities assessment of household water security in marginalized communities. *Journal of Environmental Management*, *341*, 118047. https://doi.org/10.1016/j.jenvman.2023.118047

Elshall, A. S., Arik, A. D., El-Kadi, A. I., Pierce, S., Ye, M., Burnett, K. M., Wada, C. A., Bremer, L. L., & Chun, G. (2020). Groundwater sustainability: A review of the interactions between science and policy. *Environmental Research Letters*, *15*(9), 093004. https://doi.org/10.1088/1748-9326/ab8e8c

Escriva-Bou, A., Hui, R., Maples, S., Medellín-Azuara, J., Harter, T., & Lund, J. R. (2020). Planning for groundwater sustainability accounting for uncertainty and costs: An application to California's Central Valley. *Journal of Environmental Management*, *264*, 110426. https://doi.org/10.1016/j.jenvman.2020.110426

Escriva-Bou, A., Hanak, E., Cole, S., & Medellín-Azuara, J. (2023). *Policy Brief: The Future of Agriculture in the San Joaquin Valley* (tech. rep.). Public Policy Institute of California.

Espinoza, V., Bernacchi, L. A., Eriksson, M., Schiller, A., Hayden, A., & Viers, J. H. (2023). From fallow ground to common ground: Perspectives on future land uses in the San Joaquin valley under sustainable groundwater management. *Journal of Environmental Management*, *333*, 117226. https://doi.org/10.1016/j.jenvman.2023.117226

Espinoza, V., Booth, L. A., & Viers, J. H. (2023). Land Use Misclassification Results in Water Use, Economic Value, and GHG Emission Discrepancies in California's High-Intensity Agriculture Region. *Sustainability*, *15*(8), 6829. https://doi.org/10.3390/su15086829

Expósito-Granados, M., Castro, A. J., Lozano, J., Aznar-Sanchez, J. A., Carter, N. H., Requena-Mullor, J. M., Malo, A. F., Olszańska, A., Morales-Reyes, Z., Moleón, M., Sánchez-Zapata, J. A., Cortés-Avizanda, A., Fischer, J., & Martín-López, B. (2019). Human-carnivore relations: Conflicts, tolerance and coexistence in the American West. *Environmental Research Letters*, *14*(12), 123005. https://doi.org/10.1088/1748-9326/ab5485

Fawcett, T. (2006). An introduction to ROC analysis. *Pattern Recognition Letters*, *27*(8), 861–874. https://doi.org/10.1016/j.patrec.2005.10.010

Feinstein, L., Phurisamban, R., Ford, A., Tyler, C., & Crawford, A. (2017). *Drought and Equity in California* (tech. rep.). Pacific Institute.

Fernandez-Bou, A. S., Ortiz-Partida, J. P., Classen-Rodriguez, L. M., Pells, C., Dobbin, K. B., Espinoza, V., Rodríguez-Flores, J. M., Thao, C., Hammond Wagner, C. R., Fencl, A., Flores-Landeros, H., Maskey, M. L., Cole, S. A., Azamian, S., Gamiño, E., Guzman, A., Alvarado, A. G. F., Campos-Martínez, M. S., Weintraub, C., … Medellín-Azuara, J. (2021). 3 Challenges, 3 Errors, and 3 Solutions to Integrate Frontline Communities in Climate Change Policy and Research: Lessons From California. *Frontiers in Climate*, *3*. https://doi.org/10.3389/fclim.2021.717554

Fernandez-Bou, A. S., Ortiz-Partida, J. P., Dobbin, K. B., Flores-Landeros, H., Bernacchi, L. A., & Medellín-Azuara, J. (2021). Underrepresented, understudied, underserved: Gaps and opportunities for advancing justice in disadvantaged communities. *Environmental Science & Policy*, *122*, 92–100. https://doi.org/10.1016/j.envsci.2021.04.014

Fernandez-Bou, A. S., Rodríguez-Flores, J. M., Guzman, A., Ortiz-Partida, J. P., Classen-Rodriguez, L. M., Sánchez-Pérez, P. A., Valero-Fandiño, J., Pells, C., Flores-Landeros, H., Sandoval-Solís, S., Characklis, G. W., Harmon, T. C., McCullough, M., & Medellín-Azuara, J. (2023). Water, environment, and socioeconomic justice in California: A multi-benefit cropland repurposing framework. *Science of The Total Environment*, *858*, 159963. https://doi.org/10.1016/j.scitotenv.2022.159963

Fichera, A., King, R., Kath, J., Cobon, D., & Reardon-Smith, K. (2023). Spatial modelling of agro-ecologically significant grassland species using the INLA-SPDE approach. *Scientific Reports*, *13*(1), 4972. https://doi.org/10.1038/s41598-023-32077-7

Flores-Landeros, H., Pells, C., Campos-Martinez, M. S., Fernandez-Bou, A. S., Ortiz-Partida, J. P., & Medellín-Azuara, J. (2022). Community Perspectives and Environmental Justice in California's San Joaquin Valley. *Environmental Justice*, *15*(6), 337–345. https://doi.org/10.1089/env.2021.0005

Freeman, E. (2023). PresenceAbsence: Presence-Absence Model Evaluation. https://cran.r-project.org/web/packages/PresenceAbsence/index.html

Gailey, R. M. (2023). Factoring Impacts to Water Supply Well Operations into Groundwater Management Planning. *Groundwater*, *61*(1), 11–18. https://doi.org/10.1111/gwat.13280

Gailey, R. M., Lund, J. R., & Medellín-Azuara, J. (2019). Domestic well reliability: Evaluating supply interruptions from groundwater overdraft, estimating costs and managing economic externalities. *Hydrogeology Journal*, *27*(4), 1159–1182. https://doi.org/10.1007/s10040-019-01929-w

Gailey, R. M., Lund, J. R., & Philipp, J. R. (2022). Domestic-well failure mitigation and costs in groundwater management planning: Observations from recent groundwater sustainability plans in California, USA. *Hydrogeology Journal*. https://doi.org/10.1007/s10040-021-02431-y

Gelman, A., Hwang, J., & Vehtari, A. (2014). Understanding predictive information criteria for Bayesian models. *Statistics and Computing*, *24*(6), 997–1016. https://doi.org/10.1007/s11222-013-9416-2

Gershunov, A., Shulgina, T., Clemesha, R. E. S., Guirguis, K., Pierce, D. W., Dettinger, M. D., Lavers, D. A., Cayan, D. R., Polade, S. D., Kalansky, J., & Ralph, F. M. (2019). Precipitation regime change in Western North America: The role of Atmospheric Rivers. *Scientific Reports*, *9*(1), 9944. https://doi.org/10.1038/s41598-019-46169-w

Gleeson, T., Cuthbert, M., Ferguson, G., & Perrone, D. (2020). Global Groundwater Sustainability, Resources, and Systems in the Anthropocene.

Gong, W., Reich, B. J., & Chang, H. H. (2021). Multivariate spatial prediction of air pollutant concentrations with INLA. *Environmental Research Communications*, *3*(10), 101002. https://doi.org/10.1088/2515-7620/ac2f92

Gräler, B., Pebesma, E., & Heuvelink, G. (2016). Spatio-Temporal Interpolation using gstat. *The R Journal*, *8*(1), 204. https://doi.org/10.32614/RJ-2016-014

Hanak, E., Escriva-Bou, A., Gray, B., Green, S., Harter, T., Jezdimirovic, J., Lund, J., Medellín-Azuara, J., Moyle, P., & Seavy, N. (2019). *Water and the Future of the San Joaquin Valley* (tech. rep.). https://doi.org/10.13140/RG.2.2.24360.83208

Hauptman, B. H., Naughton, C. C., & Harmon, T. C. (2023). Using machine learning to predict 1,2,3-trichloropropane contamination from legacy non-point source pollution of groundwater in California's Central Valley. *Groundwater for Sustainable Development*, *22*, 100955. https://doi.org/10.1016/j.gsd.2023.100955

Horowitz, A. I., Moomaw, W. R., Liptzin, D., Gramig, B. M., Reeling, C., Meyer, J., & Hurley, K. (2016). A multiple metrics approach to prioritizing strategies for measuring and managing reactive nitrogen in the San Joaquin Valley of California. *Environmental Research Letters*, *11*(6), 064011. https://doi.org/10.1088/1748-9326/11/6/064011

Huggins, X., Gleeson, T., Kummu, M., Zipper, S. C., Wada, Y., Troy, T. J., & Famiglietti, J. S. (2022). Hotspots for social and ecological impacts from freshwater stress and storage loss. *Nature Communications*, *13*(1), 439. https://doi.org/10.1038/s41467-022-28029-w

Jaffé, R., Nunes, S., Santos, J. F. D., Gastauer, M., Giannini, T. C., Jr, W. N., Sales, M., Souza, C. M., Souza-Filho, P. W., & Fletcher, R. J. (2021). Forecasting deforestation in the Brazil-

ian Amazon to prioritize conservation efforts. *Environmental Research Letters*, *16*(8), 084034. https://doi.org/10.1088/1748-9326/ac146a

Jasechko, S., & Perrone, D. (2020). California's Central Valley Groundwater Wells Run Dry During Recent Drought. *Earth's Future*, *8*(4). https://doi.org/10.1029/2019EF001339

Jasechko, S., & Perrone, D. (2021). Global groundwater wells at risk of running dry. *Science*, *372*(6540), 418–421. https://doi.org/10.1126/science.abc2755

Johnson, T. D., & Belitz, K. (2015). Identifying the location and population served by domestic wells in California. *Journal of Hydrology: Regional Studies*, *3*, 31–86. https://doi.org/10.1016/j.ejrh.2014.09.002

Kang, M., & Jackson, R. B. (2016). Salinity of deep groundwater in California: Water quantity, quality, and protection. *Proceedings of the National Academy of Sciences*, *113*(28), 7768–7773. https://doi.org/10.1073/pnas.1600400113

Kassambara, A., & Patil, I. (2022). Ggcorrplot: Visualization of a Correlation Matrix using 'ggplot2'. https://cran.r-project.org/web/packages/ggcorrplot/index.html

Klasic, M., Fencl, A., Ekstrom, J. A., & Ford, A. (2022). Adapting to extreme events: Small drinking water system manager perspectives on the 2012–2016 California Drought. *Climatic Change*, *170*(3), 26. https://doi.org/10.1007/s10584-021-03305-8

Krainski, E. T., Gómez-Rubio, V., Bakka, H., Lenzi, A., Castro-Camilo, D., Simpson, D., Lindgren, F., & Rue, H. (2018). *Advanced Spatial Modeling with Stochastic Partial Differential Equations Using R and INLA*. CRC Press.

Laurent, A. G. (1963). The Lognormal Distribution and the Translation Method: Description and Estimation Problems. *Journal of the American Statistical Association*, *58*(301), 231–235. https://doi.org/10.1080/01621459.1963.10500844

Leach, W. D., An, B. Y., & Tang, S.-Y. (2021). Evaluating California's Sustainable Groundwater Management Act: The First Five Years of Governance and Planning. *JAWRA Journal of the American Water Resources Association*, *57*(6), 972–989. https://doi.org/10.1111/1752-1688.12967

Levintal, E., Kniffin, M. L., Ganot, Y., Marwaha, N., Murphy, N. P., & Dahlke, H. E. (2023). Agricultural managed aquifer recharge (Ag-MAR)—a method for sustainable groundwater

management: A review. *Critical Reviews in Environmental Science and Technology*, *53*(3), 291–314. https://doi.org/10.1080/10643389.2022.2050160

Levy, Z. F., Jurgens, B. C., Burow, K. R., Voss, S. A., Faulkner, K. E., Arroyo-Lopez, J. A., & Fram, M. S. (2021). Critical Aquifer Overdraft Accelerates Degradation of Groundwater Quality in California's Central Valley During Drought. *Geophysical Research Letters*, *48*(17), e2021GL094398. https://doi.org/10.1029/2021GL094398

Lindgren, F., & Rue, H. (2015). Bayesian Spatial Modelling with *R* - **INLA**. *Journal of Statistical Software*, *63*(19). https://doi.org/10.18637/jss.v063.i19

Liu, P.-W., Famiglietti, J. S., Purdy, A. J., Adams, K. H., McEvoy, A. L., Reager, J. T., Bindlish, R., Wiese, D. N., David, C. H., & Rodell, M. (2022). Groundwater depletion in California's Central Valley accelerates during megadrought. *Nature Communications*, *13*(1), 7825. https://doi.org/10.1038/s41467-022-35582-x

London, J. K., Fencl, A. L., Watterson, S., Choueiri, Y., Seaton, P., Jarin, J., Dawson, M., Aranda, A., King, A., Nguyen, P., Pannu, C., Firestone, L., & Bailey, C. (2021). Disadvantaged Unincorporated Communities and the Struggle for Water Justice in California. *14*(2).

Lund, J., Medellin-Azuara, J., Durand, J., & Stone, K. (2018). Lessons from California's 2012–2016 Drought. *Journal of Water Resources Planning and Management*, *144*(10), 04018067. https://doi.org/10.1061/(ASCE)WR.1943-5452.0000984

Mall, N. K., & Herman, J. D. (2019). Water shortage risks from perennial crop expansion in California's Central Valley. *Environmental Research Letters*, *14*(10), 104014. https://doi.org/10.1088/1748-9326/ab4035

Marwaha, N., Kourakos, G., Levintal, E., & Dahlke, H. E. (2021). Identifying Agricultural Managed Aquifer Recharge Locations to Benefit Drinking Water Supply in Rural Communities. *Water Resources Research*, *57*(3), e2020WR028811. https://doi.org/10.1029/2020WR028811

Medellin-Azuara, J., Escriva-Bou, A., Abatzoglou, J., Viers, J., Cole, S., Rodriguez-Flores, J., & Sumner, D. (2022). *Economic Impacts of the 2021 Drought on California Agriculture. Preliminary Report* (A report for the California Department of Food and Agriculture). University of California, Merced.

Medellín-Azuara, J., MacEwan, D., Howitt, R. E., & Sumner, D. A. (2016). *Economic Analysis of the 2016 California Drought on Agriculture* (tech. rep.). Center for Watershed Sciences. UC Davis, Davis, CA.

Mekonnen, M. M., & Hoekstra, A. Y. (2016). Four billion people facing severe water scarcity. *Science Advances*, *2*(2), e1500323. https://doi.org/10.1126/sciadv.1500323

Méndez-Barrientos, L. E., Fencl, A. L., Workman, C. L., & Shah, S. H. (2022). Race, citizenship, and belonging in the pursuit of water and climate justice in California. *Environment and Planning E: Nature and Space*, 25148486221133282. https://doi.org/10.1177/25148486221133282

Ndolo, V. A., Redding, D. W., Lekolool, I., Mwangangi, D. M., Odhiambo, D. O., Deka, M. A., Conlan, A. J. K., & Wood, J. L. N. (2022). Drivers and potential distribution of anthrax occurrence and incidence at national and sub-county levels across Kenya from 2006 to 2020 using INLA. *Scientific Reports*, *12*(1), 20083. https://doi.org/10.1038/s41598-022-24589-5

Nelson, K. S., & Burchfield, E. K. (2017). Effects of the Structure of Water Rights on Agricultural Production During Drought: A Spatiotemporal Analysis of California's Central Valley. *Water Resources Research*, *53*(10), 8293–8309. https://doi.org/10.1002/2017WR020666

OEHHA. (2021). CalEnviroScreen 4.0. https://oehha.ca.gov/calenviroscreen/report/calenviroscreen-40

Ojha, C., Werth, S., & Shirzaei, M. (2019). Groundwater Loss and Aquifer System Compaction in San Joaquin Valley During 2012–2015 Drought. *Journal of Geophysical Research: Solid Earth*, *124*(3), 3127–3143. https://doi.org/10.1029/2018JB016083

Pace, C., Balazs, C., Bangia, K., Depsky, N., Renteria, A., Morello-Frosch, R., & Cushing, L. J. (2022). Inequities in Drinking Water Quality Among Domestic Well Communities and Community Water Systems, California, 2011–2019. *American Journal of Public Health*, *112*(1), 88–97. https://doi.org/10.2105/AJPH.2021.306561

Pauloo, R. A., Escriva-Bou, A., Dahlke, H., Fencl, A., Guillon, H., & Fogg, G. E. (2020). Domestic well vulnerability to drought duration and unsustainable groundwater management in California's Central Valley. *Environmental Research Letters*, *15*(4), 044010. https://doi.org/10.1088/1748-9326/ab6f10

Payne, A. E., Demory, M.-E., Leung, L. R., Ramos, A. M., Shields, C. A., Rutz, J. J., Siler, N., Villarini, G., Hall, A., & Ralph, F. M. (2020). Responses and impacts of atmospheric rivers to climate change. *Nature Reviews Earth & Environment*, *1*(3), 143–157. https://doi.org/10.1038/s43017-020-0030-5

Perrone, D., & Jasechko, S. (2017). Dry groundwater wells in the western United States. *Environmental Research Letters*, *12*(10), 104002. https://doi.org/10.1088/1748-9326/aa8ac0

Perrone, D., & Jasechko, S. (2019). Deeper well drilling an unsustainable stopgap to groundwater depletion. *Nature Sustainability*, *2*(8), 773–782. https://doi.org/10.1038/s41893-019-0325-z

Perrone, D., Rohde, M. M., Hammond Wagner, C., Anderson, R., Arthur, S., Atume, N., Brown, M., Esaki-Kua, L., Gonzalez Fernandez, M., Garvey, K. A., Heidel, K., Jones, W. D., Khosrowshahi Asl, S., Munill, C., Nelson, R., Ortiz-Partida, J. P., & Remson, E. J. (2023). Stakeholder integration predicts better outcomes from groundwater sustainability policy. *Nature Communications*, *14*(1), 3793. https://doi.org/10.1038/s41467-023-39363-y

Qin, Y., Mueller, N. D., Siebert, S., Jackson, R. B., AghaKouchak, A., Zimmerman, J. B., Tong, D., Hong, C., & Davis, S. J. (2019). Flexibility and intensity of global water use. *Nature Sustainability*, *2*(6), 515–523. https://doi.org/10.1038/s41893-019-0294-2

Rodríguez-Flores, J. M., Valero Fandiño, J. A., Cole, S. A., Malek, K., Karimi, T., Zeff, H. B., Reed, P. M., Escriva-Bou, A., & Medellín-Azuara, J. (2022). Global Sensitivity Analysis of a Coupled Hydro-Economic Model and Groundwater Restriction Assessment. *Water Resources Management*, *36*(15), 6115–6130. https://doi.org/10.1007/s11269-022-03344-5

Roos, M., & Held, L. (2011). Sensitivity analysis in Bayesian generalized linear mixed models for binary data. *Bayesian Analysis*, *6*(2). https://doi.org/10.1214/11-BA609

Scanlon, B. R., Rateb, A., Pool, D. R., Sanford, W., Save, H., Sun, A., Long, D., & Fuchs, B. (2021). Effects of climate and irrigation on GRACE-based estimates of water storage changes in major US aquifers. *Environmental Research Letters*, *16*(9), 094009. https://doi.org/10.1088/1748-9326/ac16ff

Smith, R., Knight, R., & Fendorf, S. (2018). Overpumping leads to California groundwater arsenic threat. *Nature Communications*, *9*(1), 2089. https://doi.org/10.1038/s41467-018-04475-3

Spiegelhalter, D. J., Best, N. G., Carlin, B. P., & Van Der Linde, A. (2002). Bayesian Measures of Model Complexity and Fit. *Journal of the Royal Statistical Society Series B: Statistical Methodology*, *64*(4), 583–639. https://doi.org/10.1111/1467-9868.00353

Stone, K. M., Gailey, R. M., & Lund, J. R. (2022). Economic tradeoff between domestic well impact and reduced agricultural production with groundwater drought management: Tulare County, California (USA), case study. *Hydrogeology Journal*, *30*(1), 3–19. https://doi.org/10.1007/s10040-021-02409-w

SWRCB. (2022). *Supplemental Appendix E: Future socioeconomic indicator considerations for SSWSs and DWs* (tech. rep.). California State Water Resources Control Board.

Tariqi, A. Q., & Naughton, C. C. (2021). Water, Health, and Environmental Justice in California: Geospatial Analysis of Nitrate Contamination and Thyroid Cancer. *Environmental Engineering Science*, *38*(5), 377–388. https://doi.org/10.1089/ees.2020.0315

Ulibarri, N., Escobedo Garcia, N., Nelson, R. L., Cravens, A. E., & McCarty, R. J. (2021). Assessing the Feasibility of Managed Aquifer Recharge in California. *Water Resources Research*, *57*(3), e2020WR029292. https://doi.org/10.1029/2020WR029292

Valavi, R., Elith, J., Lahoz-Monfort, J. J., & Guillera-Arroita, G. (2019). blockCV: An r package for generating spatially or environmentally separated folds for k-fold cross-validation of species distribution models. *Methods in Ecology and Evolution*, *10*(2), 225–232. https://doi.org/10.1111/2041-210X.13107

Vasco, D. W., Kim, K. H., Farr, T. G., Reager, J. T., Bekaert, D., Sangha, S. S., Rutqvist, J., & Beaudoing, H. K. (2022). Using Sentinel-1 and GRACE satellite data to monitor the hydrological variations within the Tulare Basin, California. *Scientific Reports*, *12*(1), 3867. https://doi.org/10.1038/s41598-022-07650-1

Watanabe, S. (2010). Asymptotic Equivalence of Bayes Cross Validation and Widely Applicable Information Criterion in Singular Learning Theory. *Journal of Machine Learning Research*.

Wendt, D. E., Loon, A. F. V., Scanlon, B. R., & Hannah, D. M. (2021). Managed aquifer recharge as a drought mitigation strategy in heavily-stressed aquifers. *Environmental Research Letters*, *16*(1), 014046. https://doi.org/10.1088/1748-9326/abcfe1

Zuur, A. F., Ieno, E. N., & Saveliev, A. A. (2017). Spatial, temporal and spatial-temporal ecological data analysis with R-INLA. *Highland Statistics Ltd*, *1*.

Chapter 5

Conclusions

To develop an accurate analysis and informed policy suggestions of groundwater sustainability in the San Joaquin Valley, it is necessary to consider the characteristics of the coupled food-water system. This dissertation employed deductive and inductive approaches to explore the associations, feedbacks, adaptations, and trade-offs between agriculture and groundwater. In Chapters 2 and 3, we developed coupled hydro-economic models for two different regions, examining the feedback between agricultural groundwater pumping and changes in groundwater depth. Uncertainties related to water supplies, economic parameters, and calibration parameters were addressed within the modeling framework. In Chapter 2, we assessed the performance of the system under various scenarios to identify vulnerabilities and key factors that should be considered in implementing a potential groundwater pumping restriction. Global sensitivity analysis was used to identify factors that significantly influence the policy's performance and found that its is impacted mainly by surface water supply availability and perennial crop prices.

In Chapter 3, we proposed a modeling framework to search adaptive and dynamic irrigation management policies that can be adjusted annually based on conditions of the system such as surface water supply, groundwater levels, and the area of perennial crops. To achieve this, a novel bi-level optimization approach was implemented, additionally the Evolutionary Multi-Objective Direct Policy Search (EMODPS) framework was used to optimize candidate control policies. The system performance was explored under optimal policies and a robust policy considering potential

preferences. The results from the experiment were used to derive policy insights for achieving groundwater sustainability within the study area, with implications that extend to the entire San Joaquin Valley. In general these policies demonstrated the ability to adapt between dry and wet periods, balancing economic revenues and sustainable groundwater levels trade-offs.

Finally, Chapter 4 focused on identifying the primary factors contributing to domestic well vulnerability. Through spatial analysis, localized factors within the food-water-human system, that significantly impact groundwater dynamics and increase the risk of domestic well failures during droughts, were identified. The findings from this analysis provide insight into understanding the system during the two previous dry periods (2012-2016 and 2020-2022), characterized by a significant number of domestic well failures. These wells provide water to support marginalized communities, whose vulnerability to agricultural pumping externalities has been overlooked in the development of groundwater sustainability plans in the San Joaquin Valley. Localized factors shown in this Chapter should be considered for the protection of domestic wells, including well density, the extent of perennial crop cultivation, and well depths. In addition, the implications of these findings within the current policy context were discussed.

5.1 Main findings

The main findings of this dissertation are listed bellow, which unveil critical insights into the complex interplay between socioeconomic factors and groundwater sustainability.

- The utilization of coupled hydro-economic models demonstrated their potential in effectively capturing the feedback loop between agriculture and groundwater, enabling dynamic modeling of groundwater depth fluctuations and changes in pumping costs.
- The proposed hydro-economic modeling framework offers an efficient mean to address inherent uncertainties within the food-water system, facilitating policy search and assessment processes.
- The application of EMODPS showcased its efficacy in formulating adaptive and dynamic policies to ensure sustainable groundwater use, while balancing trade-offs between revenues and agricultural sustainability.

- Surface water availability and perennial crop prices were identified as the primary factors influencing the trade-offs between agricultural economic revenues and groundwater sustainability.

- To promote groundwater sustainability, policies need to exhibit adaptive behavior, accommodating wet and dry years by implementing measures such as pumping restrictions or fees to reduce overall pumping and maximize groundwater recovery during wet periods.

- Groundwater Sustainability Plans have established minimum thresholds considering factors as depths of agricultural wells. However, these threshold may fall short or be unrealistic as a feasible operational threshold considering the share of permanent crops and future water supplies.

- Reducing the extent of perennial cropland is essential to enhance the flexibility of groundwater sustainability agencies, enabling them to less costly curtail pumping during dry years while maintaining groundwater reserves at a sustainable yield. Additionally, the cultivation of some annual crops can serve as a flexible strategy to augment economic revenues during times of higher water availability and reduce water demand during droughts.

- During droughts, domestic wells are most vulnerable to fail when 1) their depths are close to the groundwater level, 2) are located in high domestic well density areas, and 3) could be affected by nearby agricultural wells' pumping.

- In order to protect domestic wells, policies should focus on managing land and pumping practices in their vicinity by mitigating the impact of agricultural pumping through land repurposing and groundwater pumping restrictions, that counteract drawdown resulting from increased pumping rates during dry periods.

- Localized strategic groundwater recharge and reduction of cropland area can reduce the susceptibility of domestic wells to failure, further emphasizing the need for comprehensive characterization of domestic wells depths and their vulnerabilities in groundwater sustainability planning. Additionally, local understanding of the crop production context (e.g., scale, commodity and ownership) is needed to develop the best cost-benefit strategies.

- To develop domestic well protection efforts that reduce disparities and ensure equitable assistance, it is essential to take into account socioeconomic factors, including race and income. By considering these factors, strategies can be more effective and inclusive strategies that address the specific needs and challenges faced by diverse communities, promoting environmental justice.

5.2 Future Work

This dissertation demonstrated novel modeling frameworks to study the coupled food-water system, which can be applied to other areas in California or places with groundwater depletion in the world. These used optimization frameworks showed advantages to model the feedback in the food-water system, such as easy application without relying on complex models to simulate groundwater depth - pumping dynamics. Additionally, was shown that characterizing the uncertainty in the system and policy planning can be done through Sensitivity Analysis and dynamic-adaptive formulations via EMODPS. Discovery of policies can be further extended with other strategies like groundwater management recharge and water markets, that can provide more flexibility in land and water management. In addition the multi-objective formulation could be extended to consider other objectives like ecosystem services or groundwater access to communities. Although the EMODPS framework demonstrated to be highly effective, its implementation requires substantial computational resources, such as cluster computing, which may not be readily available to many practitioners worldwide. Future work should explore how the strategies studied in this dissertation can be implemented, given the diversity of farms in the San Joaquin Valley, and while not negatively impacting small farmers, and benefiting other sectors such as domestic wells and ecosystems.

Further work should identify projects that can help building groundwater access resiliency for domestic wells. The findings presented in this dissertation underscore key factors that must be considered for effective domestic well protection. However, the successful implementation of land and water management strategies relies heavily on localized contexts (e.g., land ownership, water rights, and surface water contracts), necessitating further research to assess the feasibility of implementing proposed strategies. Additionally, exploring alternative strategies to balance overall

costs and benefits, while offsetting economic losses to agriculture need to be considered.

Appendix A

Supplementary Material for Chapter 2

A1 PMP calibration

The first step of the calibration process solves a linear optimization problem (equations A1 to A4), which maximizes a linear net profit objective function (equation A1) on land use for crop group i. Crop groups represent single crops or group of crops for which cost, prices and yield are selected based on a proxy crop within each group subindex, in our case the set i includes almonds and pistachios, alfalfa, cotton, cucurbits, other deciduous, other truck, grain, other field, fresh tomatoes, processing tomatoes, onions and garlic, sugar beets, dry beans, pasture, subtropical, vine, potatoes, safflower and corn. The PMP follows a two-step calibration process for which a constrained linear program is solved by restricting the model to the baseline (observed) land use in each time window, this is referred to as the calibration constraint set. A second set is conformed by the resources constraints, in these cases land and water. Lagrange multipliers obtained from the first optimization step on the calibration constraint set are used to parameterize an exponential cost function. A sub index to represent the two time windows was omitted since the mathematical representation is the same for both calibrations.

The linear optimization problem is formulated as:

$$Max_{x_{i,land}} \prod = \sum_{i} (p_i \cdot y_i - \sum_{j} \omega_{i,j} \cdot a_{i,j}) \cdot x_{i,land} \tag{A1}$$

Subject to:

$$\sum_i x_{i,land} \leq b_{land} \tag{A2}$$

$$\sum_i a_{i,water} \cdot x_{i,land} \leq b_{water} \tag{A3}$$

$$\sum_i x_{i,land} \leq \bar{x}_{i,land} + \epsilon \tag{A4}$$

Where p is the average price and y the average yield by crop group i. $\omega_{i,j}$ is the average cost by input j = water,land,labor,other supplies. For the case of $\omega_{i,water}$ we used a weighted price by volume since we are aggregating groundwater and surface water. Equations A2 and A3 represent the resources' constraints. The variables b_{land} and b_{water} represent the available land and water in the base case respectively, and $\alpha_{i,water}$ represents the use of water (acre-feet/acre) by crop group i. Lastly, equation S4 represents the calibration constraint, where $\bar{x}_{land,t}$ is the base historical land use. The linear program solves $x_{land,i}$ for and the Lagrange multipliers of the constraints λ_{land} and λ_{water} for the land and water availability constraints respectively, and $\bar{\lambda}_{land,i}$ for the crop specific calibration constraint (equation A4) which is used later in the calibration of the exponential cost function described below.

A2 Pumping cost

The unit (1 acre-foot) pumping cost of groundwater ($\widehat{\omega}_{GW}$) is given by the equation A5, where ω_{pump} is the capital cost of the well pump equals to $ 200,000, $A_{service}$ is the assumed pumping service area equals to 200 acres, $\widetilde{x}_{water}$ is the average irrigation demand per unit area equals to 4 acre-feet/acre, i is the discount rate equals to 0.05, n is the pump lifetime (20 years), ζ is the operation and maintenance costs for the pump equals to $\$0.082/(AFm)$,$\omega_{electricity}$ is the price of electricity ($/kWh) used in the sensitivity analysis, η_{pump} is the average pump efficiency equals to 0.7, h is the depth to groundwater in the water district (in feet), Q is the assumed pumping rate equals to 0.126 m^3/s, C is the Hazen-Williams coefficient equals to 120, and d is the pipe diameter

equals to 0.40 m. Pipe material is assumed to be cast-iron or steel (C = 120). The characteristic well is assumed to be a large production irrigation well (Q = 0.126 m^3/s, d = 0.4064 m).

$$\widehat{\omega}_{GW} = \left(\frac{\omega_{pump}}{A_{service}\widetilde{x}_{water}}\frac{i(1+i)^n}{(1+i)^n-1}\right) + \left(\zeta + \frac{3.354\omega_{electricity}}{\eta_{pump}}\right)\left(\frac{h}{3.28}\left(1+10.64\frac{hQ^{1.852}}{3.28C^{1.852}d^{4.8704}}\right)\right) \tag{A5}$$

A3 Water Districts Calibrated in the ANN

District Name
SEMITROPIC WSD
WEST KERN WD
WHEELER RIDGE-MARICOPA WSD
KERN DELTA WD
ARVIN-EDISON WSD
BELRIDGE WSD
LOST HILLS WD
NORTH KERN WSD
IMPROVEMENT DISTRICT NO. 4
SOUTHERN SAN JOAQUIN MUD
BERRENDA MESA WD
BUENA VISTA WSD
CAWELO WD
ROSEDALE-RIO BRAVO WSD
SHAFTER WASCO ID
HENRY MILLER WD
DELANO - EARLIMART ID
KERN - TULARE WATER DISTRICT
LOWER TULE RIVER ID
TULARE IRRIGATION DISTRICT
LINDMORE ID
SAUCELITO ID
PORTERVILE ID
LINDSAY-STRATHMORE ID
EXETER ID
TERRA BELLA ID

Table A1: List of irrigation and water districts used in the calibration of the Artificial Neural Network groundwater depth response.

A4 Performance ANN

Figure A1 shows the Wheeler Ridge-Maricopa's APD obtained from C2VSIM-FG and the regional ANN. The adjusted R-square for training and testing were 0.95 and 0.67, respectively,

whereas the Root Mean Square Error (RMSE) for training and testing were 4.73 and 8.18 ft, respectively. For the regional ANN, 80% of the records were randomly selected and used for its training and the 20% rest for its validation.

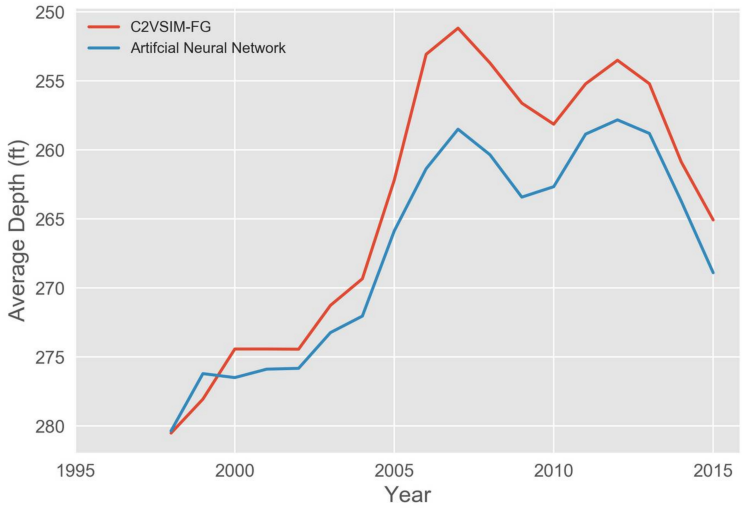

Figure A1: Average Potentiometric Depth for Wheeler Ridge-Maricopa first two layers from 1998 to 2015 comparing C2VSIM-FG output with the simulated ANN output

A5 Baseline Values

Name of input	Units	Base value	Name of input	Units	Base value
Price Vine	USD/Tonne	1746.48	Supply elasticity Vine	Unitless	0.13
Price Subtropical	USD/Tonne	687.21	Supply elasticity Subtropical	Unitless	0.13
Price Almonds and Pistachios	USD/Tonne	4022.1	Supply elasticity Almonds and Pistachios	Unitless	1
Price Other truck	USD/Tonne	659.14	Supply elasticity Other truck	Unitless	0.41
Price Cotton	USD/Tonne	5984.24	Supply elasticity Cotton	Unitless	0.68

Price Grain	USD/Tonne	586.83	Supply elasticity Grain	Unitless	0.74
Price Onions and Garlic	USD/Tonne	210.09	Supply elasticity Onions and Garlic	Unitless	0.41
Price Other Deciduous	USD/Tonne	2347.27	Supply elasticity Other Deciduous	Unitless	0.13
Price Potato	USD/Tonne	269.19	Supply elasticity Potato	Unitless	0.41
Price Processing Tomatoes	USD/Tonne	78.31	Supply elasticity Processing Tomatoes	Unitless	0.74
Price Cucurbits	USD/Tonne	295.12	Supply elasticity Cucurbits	Unitless	0.05
Price Alfalfa	USD/Tonne	254.32	Supply elasticity Alfalfa	Unitless	1.86
Price Fresh Tomatoes	USD/Tonne	640.76	Supply elasticity Safflower	Unitless	0.13
Price Safflower	USD/Tonne	1746.48	Supply elasticity Fresh Tomatoes	Unitless	1.06
Price Corn	USD/Tonne	60.77	Supply elasticity Corn	Unitless	0.74
Price Other Field	USD/Tonne	52.28	Supply elasticity Other Field	Unitless	1.3
Yield Vine	Tonne/acre	9.71	Price of surface water	USD/Tonne	112.2
Yield Subtropical	Tonne/acre	12.37	Price of electricity	USD/kWh	0.17
Yield Almonds and Pistachios	Tonne/acre	1.43			
Pice Other truck	Tonne/acre	16.88			
Yield Cotton	Tonne/acre	0.74			
Yield Grain	Tonne/acre	1.72			
Yield Onions and Garlic	Tonne/acre	19.02			
Yield Other Deciduous	Tonne/acre	2.49			

Yield Potato	Tonne/acre	22.08			
Yield Processing Tomatoes	Tonne/acre	50.23			
Yield Cucurbits	Tonne/acre	42.39			
Yield Alfalfa	Tonne/acre	8.18			
Yield Fresh Tomatoes	Tonne/acre	15.03			
Yield Corn	Tonne/acre	26.22			
Yield Other Field	Tonne/acre	21.26			
Yield Safflower	Tonne/acre	9.71			

Table A2: Base values used for the calibration of PMP and the ANN year 2011

Name of input	Units	Base value	Name of input	Units	Base value
Price Vine	USD/Tonne	2048	Supply elasticity Vine	Unitless	0.13
Price Subtropical	USD/Tonne	775.35	Supply elasticity Subtropical	Unitless	0.13
Price Almonds and Pistachios	USD/Tonne	7461.46	Supply elasticity Almonds and Pistachios	Unitless	1
Price Other truck	USD/Tonne	450	Supply elasticity Other truck	Unitless	0.41
Price Processing Tomatoes	USD/Tonne	79.96	Supply elasticity Processing Tomatoes	Unitless	0.74
Price Onions and Garlic	USD/Tonne	302.03	Supply elasticity Onions and Garlic	Unitless	0.41
Price Alfalfa	USD/Tonne	292.36	Supply elasticity Alfalfa	Unitless	1.86
Price Potato	USD/Tonne	221.45	Supply elasticity Potato	Unitless	0.41
Price Other Deciduous	USD/Tonne	1100	Supply elasticity Other Deciduous	Unitless	0.13

Price Cotton	USD/Tonne	6411.86	Supply elasticity Cotton	Unitless	0.68
Price Grain	USD/Tonne	454.15	Supply elasticity Grain	Unitless	0.74
Price Fresh Tomatoes	USD/Tonne	751.57	Supply elasticity Fresh Tomatoes	Unitless	1.06
Price Cucurbits	USD/Tonne	315.37	Supply elasticity Cucurbits	Unitless	0.05
Price Other Field	USD/Tonne	66.89	Supply elasticity Other Field	Unitless	1.3
Price Corn	USD/Tonne	57.11	Supply elasticity Corn	Unitless	0.74
Yield Vine	Tonne/acre	11.57	Price of surface water	USD/Tonne	153.25
Yield Subtropical	Tonne/acre	12.61	Price of electricity	USD/kWh	0.17
Yield Almonds and Pistachios	Tonne/acre	0.65			
Yield Other truck	Tonne/acre	19.56			
Yield Processing Tomatoes	Tonne/acre	45.72			
Yield Onions and Garlic	Tonne/acre	22.81			
Yield Alfalfa	Tonne/acre	7.16			
Yield Potato	Tonne/acre	27.74			
Yield Other Deciduous	Tonne/acre	7.51			
Yield Cotton	Tonne/acre	0.81			
Yield Grain	Tonne/acre	2.34			
Yield Fresh Tomatoes	Tonne/acre	15.92			
Yield Cucurbits	Tonne/acre	39.18			

Yield Other Field	Tonne/acre	17.1			
Yield Corn	Tonne/acre	28.38			

Table A3: Base values used for the calibration of PMP and the ANN year 2015

A6 Boundaries for Supply elasticites

Crop Group	Lower Bound	Upper bound
Alfalfa	0.44	1.86
Almonds and Pistachios	0.2	1
Corn	0.1	0.74
Cotton	0.55	0.68
Cucurbits	0.05	0.08
Fresh Tomatoes	0.27	1.06
Grain	0.35	0.74
Onions and Garlic	0.2	0.6
Other deciduous	0.02	0.13
Other truck	0.2	0.6
Potatoes	0.2	0.6
Processing Tomatoes	0.4	0.74
Safflower	0.2	0.6
Subtropicals	0.026	0.156
Vine	0.003	0.37
Other Field	0.35	1.3

Table A4: Supply elasticities boundaries

A7 Base line data

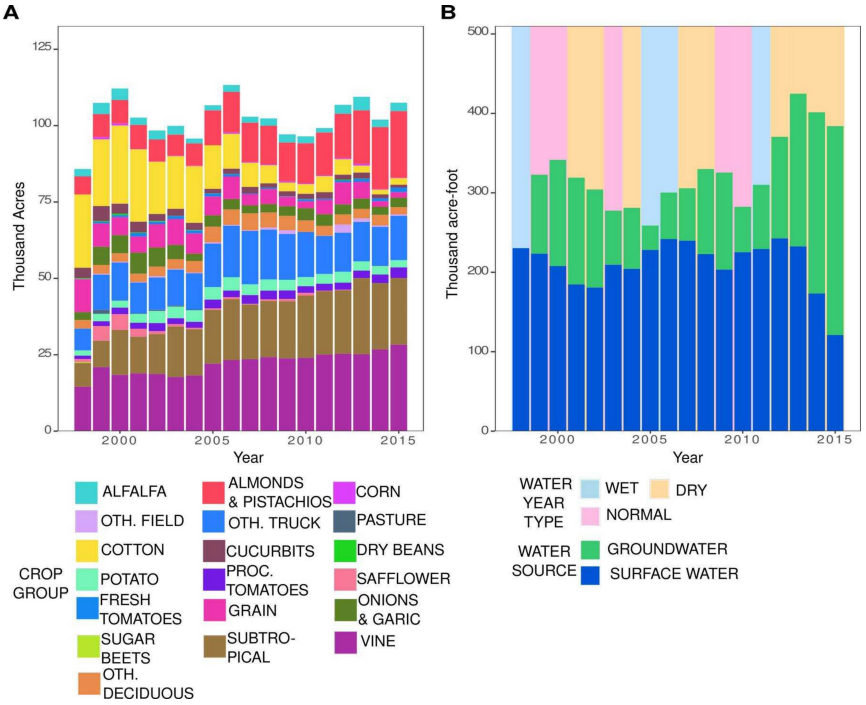

Figure A2: Historical cropland use (KCDAMS) and water use Zeff et al., 2021 for Wheeler Ridge-Maricopa, from 1998 to 2015.

The historical water use shows an increasing demand for water, of which the proportion supplied from groundwater pumping has increased in the last years. During dry periods, groundwater offsets the lack of surface water to meet the demand, as observed in the 2012-2015 drought. On the other hand, the land devoted to perennial crops such as vine, subtropical and almonds and pistachios has increased in the last years. This land configuration has several implications on the adaptation of farmers to water and economic shocks, since these crops have high establishment costs, any shock to the production system represents a risk to the investment and capability to irrigate tree crops. Transitions to perennial crops represent a "hardening" of water demand as they cannot be readily deficit irrigated or fallowed without long-term consequences. Other representative crops for the years of analysis include other truck crops, processing tomatoes and onions and garlic.

For this study, we focus on two baselines under different water supply conditions. The year 2011 was chosen to represent a wet year conditions and 2015 a dry year. For the wet year, the surface water

73.9% of irrigation demand, while for the critical dry year, surface water supplied 31.5%. The total land use was 99,200 acres and 107,500 acres during the year 2011 and 2015, respectively. The approximate total net revenue for these years, calculated as price times yield minus water costs, land cost and cost of labor and other supplies given the historical cropland use was 248 million USD in 2011 and 459 million USD in 2015. The large difference of total net revenue between the two years is result of a higher price of almonds in 2015. The use of two calibrations with extreme types of water year gives us the ability to compare how the sensitivities of the system vary in different water conditions and inform the best strategies to improve the forecast and quality of the coupled model.

A8 Comparison Sensitivity Indices

The next tables show the first order Delta Moment-Independent and Sobol Indices and significance levels for the three output metrics and two water conditions. Notice that there are negative values in Sobol indixes these are direct outputs form SALib when an index already converged to zero this might get negative values, hence these can be considered zero.

Input Variable	**Delta**		**Sobol**	
	S1	S1_conf	S1	S1_conf
Alfalfa Price	0.0007	0.0001	0.0004	0.0017
Almonds and Pistachios Price	0.0189	0.0005	0.0207	0.0130
Corn Price	0.0005	0.0001	0.0002	0.0007
Cotton Price	0.0025	0.0001	-0.0008	0.0045
Cucurbits Price	0.0028	0.0002	-0.0012	0.0019
Fresh Tomatoes Price	0.0005	0.0001	0.0004	0.0006
Grain Price	0.0003	0.0001	0.0006	0.0010
Onions and Garlic Price	0.0005	0.0001	0.0000	0.0011
Other Deciduous Price	0.0005	0.0001	0.0003	0.0008
Other Truck Price	0.0014	0.0001	0.0005	0.0020
Potatoes Price	0.0006	0.0001	-0.0005	0.0007
Processing Tomatoes Price	0.0007	0.0001	0.0000	0.0011
Safflower Price	0.0006	0.0001	0.0003	0.0006
Subtropical Price	0.0016	0.0001	0.0021	0.0031
Vine Price	0.0027	0.0001	0.0029	0.0044

Other Field Price	0.0002	0.0000	0.0002	0.0005
Alfalfa Yield	0.0011	0.0001	0.0008	0.0016
Almonds and Pistachios Yield	0.0062	0.0002	0.0071	0.0073
Corn Yield	0.0005	0.0001	0.0002	0.0007
Cotton Yield	0.0080	0.0003	0.0071	0.0063
Cucurbits Yield	0.0013	0.0001	0.0002	0.0016
Fresh Tomatoes Yield	0.0003	0.0001	-0.0001	0.0006
Grain Yield	0.0006	0.0001	-0.0002	0.0009
Onions and Garlic Yield	0.0010	0.0001	0.0006	0.0018
Other Deciduous Yield	0.0003	0.0001	0.0004	0.0010
Other Truck Yield	0.0004	0.0001	0.0004	0.0013
Potatoes Yield	0.0004	0.0001	0.0001	0.0008
Processing Tomatoes Yield	0.0003	0.0001	0.0000	0.0008
Safflower Yield	0.0004	0.0001	0.0001	0.0005
Subtropical Yield	0.0038	0.0002	0.0038	0.0044
Vine Yield	0.0009	0.0001	0.0011	0.0023
Other Field Yield	0.0006	0.0001	0.0000	0.0005
Surface Water Price	0.0075	0.0002	0.0043	0.0083
Supply Elasticity Alfalfa	0.0003	0.0001	0.0000	0.0009
Supply Elasticity Almonds and Pistachios	0.0041	0.0002	0.0036	0.0064
Supply Elasticity Corn	0.0003	0.0001	0.0003	0.0007
Supply Elasticity Cotton	0.0003	0.0001	-0.0002	0.0007
Supply Elasticity Cucurbits	0.0003	0.0001	0.0003	0.0007
Supply Elasticity Fresh Tomatoes	0.0004	0.0001	-0.0003	0.0006
Supply Elasticity Grain	0.0004	0.0001	0.0000	0.0006
Supply Elasticity Onions and Garlic	0.0004	0.0001	-0.0002	0.0009
Supply Elasticity Other Deciduous	0.0017	0.0002	-0.0001	0.0006
Supply Elasticity Other Truck	0.0003	0.0001	-0.0003	0.0008
Supply Elasticity Potatoes	0.0011	0.0001	0.0003	0.0008
Supply Elasticity Processing Tomatoes	0.0005	0.0001	-0.0001	0.0008
Supply Elasticity Safflower	0.0005	0.0001	0.0001	0.0007
Supply Elasticity Subtropical	0.0007	0.0001	0.0008	0.0020

Supply Elasticity Vine	0.0017	0.0001	0.0014	0.0025
Supply Elasticity Other Field	0.0006	0.0001	-0.0005	0.0005
Groundwater Restriction	0.6019	0.0019	0.6138	0.0252
Electricity Price	0.0023	0.0002	0.0017	0.0044

Table A5: First Order Delta Moment-Independent and Sobol Indices for Ground Water Depth Change-Wet Year

Input Variable	Delta		Sobol	
	S1	S1_conf	S1	S1_conf
Groundwater Restriction	0.5952	0.0013	0.6010	0.0139
Electricity Price	0.0012	0.0001	0.0012	0.0022
Surface Water Price	0.0002	0.0000	-0.0019	0.0027
Alfalfa Price	0.0004	0.0001	-0.0026	0.0019
Almonds and Pistachios Price	0.0146	0.0004	0.0133	0.0069
Corn Price	0.0005	0.0001	-0.0008	0.0021
Cotton Price	0.0082	0.0003	0.0094	0.0043
Cucurbits Price	0.0037	0.0002	0.0025	0.0041
Fresh Tomatoes Price	0.0006	0.0001	0.0009	0.0020
Grain Price	0.0083	0.0002	0.0103	0.0027
Onions and Garlic Price	0.0019	0.0001	0.0011	0.0021
Other Deciduous Price	0.0003	0.0001	0.0008	0.0018
Other Field Price	0.0003	0.0001	-0.0007	0.0019
Other Truck Price	0.0730	0.0006	0.0724	0.0068
Potatoes Price	0.0027	0.0001	0.0006	0.0021
Processing Tomatoes Price	0.0047	0.0002	0.0025	0.0029
Safflower Price	0.0004	0.0001	-0.0004	0.0018
Subtropical Price	0.0009	0.0001	0.0001	0.0032
Vine Price	0.0076	0.0002	0.0066	0.0041
Supply Elasticity Alfalfa	0.0002	0.0000	-0.0015	0.0021
Supply Elasticity Almonds and Pistachios	0.0030	0.0002	0.0060	0.0039
Supply Elasticity Corn	0.0003	0.0001	-0.0001	0.0021

Supply Elasticity Cotton	0.0003	0.0001	0.0018	0.0021
Supply Elasticity Cucurbits	0.0002	0.0000	-0.0021	0.0018
Supply Elasticity Fresh Tomatoes	0.0003	0.0001	-0.0010	0.0020
Supply Elasticity Grain	0.0010	0.0001	0.0009	0.0019
Supply Elasticity Onions and Garlic	0.0011	0.0001	0.0001	0.0022
Supply Elasticity Other Deciduous	0.0015	0.0001	0.0000	0.0019
Supply Elasticity Other Field	0.0005	0.0001	-0.0014	0.0023
Supply Elasticity Other Truck	0.0009	0.0001	-0.0008	0.0027
Supply Elasticity Potatoes	0.0009	0.0001	0.0011	0.0024
Supply Elasticity Processing Tomatoes	0.0004	0.0001	-0.0004	0.0022
Supply Elasticity Safflower	0.0005	0.0001	-0.0007	0.0018
Supply Elasticity Subtropical	0.0008	0.0001	-0.0006	0.0028
Supply Elasticity Vine	0.0025	0.0002	0.0034	0.0036
Alfalfa Yield	0.0007	0.0001	-0.0009	0.0017
Almonds and Pistachios Yield	0.0036	0.0002	0.0073	0.0046
Corn Yield	0.0005	0.0001	-0.0004	0.0018
Cotton Yield	0.0242	0.0004	0.0257	0.0050
Cucurbits Yield	0.0009	0.0001	0.0029	0.0040
Fresh Tomatoes Yield	0.0003	0.0001	-0.0013	0.0023
Grain Yield	0.0080	0.0002	0.0072	0.0028
Onions and Garlic Yield	0.0054	0.0002	0.0046	0.0026
Other Deciduous Yield	0.0003	0.0001	0.0012	0.0021
Other Field Yield	0.0003	0.0000	0.0000	0.0019
Other Truck Yield	0.0173	0.0003	0.0173	0.0035
Potatoes Yield	0.0008	0.0001	0.0015	0.0024
Processing Tomatoes Yield	0.0014	0.0001	0.0000	0.0021
Safflower Yield	0.0002	0.0001	0.0001	0.0016
Subtropical Yield	0.0057	0.0002	0.0063	0.0038
Vine Yield	0.0022	0.0001	0.0023	0.0021

Table A6: First Order Delta Moment-Independent and Sobol Indices for Total Land Use -Wet Year

Input Variable	Delta		Sobol	
	S1	S1_conf	S1	S1_conf
Groundwater Restriction	0.0034	0.0002	0.0031	0.0014
Electricity Price	0.0004	0.0001	-0.0002	0.0010
Surface Water Price	0.0013	0.0001	0.0007	0.0013
Alfalfa Price	0.0001	0.0000	0.0000	0.0008
Almonds and Pistachios Price	0.0169	0.0004	0.0157	0.0026
Corn Price	0.0002	0.0001	-0.0005	0.0008
Cotton Price	0.0006	0.0001	-0.0004	0.0009
Cucurbits Price	0.0037	0.0002	0.0032	0.0018
Fresh Tomatoes Price	0.0001	0.0000	-0.0007	0.0010
Grain Price	0.0001	0.0000	-0.0003	0.0007
Onions and Garlic Price	0.0003	0.0001	-0.0002	0.0007
Other Deciduous Price	0.0005	0.0001	0.0000	0.0009
Other Deciduous Price	0.0002	0.0000	-0.0009	0.0008
Other Truck Price	0.1061	0.0008	0.1055	0.0065
Potatoes Price	0.0017	0.0001	0.0008	0.0014
Processing Tomatoes Price	0.0004	0.0001	-0.0012	0.0009
Safflower Price	0.0001	0.0000	-0.0008	0.0007
Subtropical Price	0.0306	0.0005	0.0312	0.0039
Vine Price	0.5970	0.0007	0.5962	0.0149
Other Field Price	0.0003	0.0001	-0.0006	0.0010
Other Field Price	0.0003	0.0001	-0.0005	0.0010
Other Field Price	0.0002	0.0001	-0.0003	0.0009
Other Field Price	0.0002	0.0001	0.0000	0.0008
Other Field Price	0.0003	0.0001	-0.0004	0.0008
Other Field Price	0.0003	0.0001	0.0000	0.0010
Other Field Price	0.0005	0.0001	-0.0007	0.0008
Other Field Price	0.0005	0.0001	-0.0001	0.0008
Other Field Price	0.0002	0.0001	0.0001	0.0008
Other Field Price	0.0001	0.0000	-0.0010	0.0008
Other Field Price	0.0016	0.0001	-0.0003	0.0011

Other Field Price	0.0003	0.0001	-0.0012	0.0009
Other Field Price	0.0001	0.0000	-0.0003	0.0010
Other Field Price	0.0001	0.0000	-0.0007	0.0007
Other Field Price	0.0002	0.0000	-0.0012	0.0009
Other Field Price	0.0002	0.0001	-0.0013	0.0011
Alfalfa Yield	0.0001	0.0000	-0.0006	0.0009
Almonds and Pistachios Yield	0.0045	0.0002	0.0043	0.0017
Corn Yield	0.0001	0.0000	-0.0007	0.0009
Cotton Yield	0.0004	0.0001	-0.0003	0.0009
Cucurbits Yield	0.0011	0.0001	0.0013	0.0018
Fresh Tomatoes Yield	0.0001	0.0000	-0.0005	0.0009
Grain Yield	0.0004	0.0002	-0.0010	0.0011
Onions and Garlic Yield	0.0003	0.0001	-0.0003	0.0007
Other Deciduous Yield	0.0012	0.0001	-0.0008	0.0011
Other Deciduous Yield	0.0001	0.0000	-0.0007	0.0009
Other Truck Yield	0.0266	0.0004	0.0262	0.0037
Potatoes Yield	0.0004	0.0001	-0.0008	0.0011
Processing Tomatoes Yield	0.0002	0.0000	-0.0006	0.0010
Safflower Yield	0.0001	0.0000	-0.0009	0.0010
Subtropical Yield	0.0320	0.0005	0.0313	0.0043
Vine Yield	0.1503	0.0009	0.1485	0.0072

Table A7: First Order Delta Moment-Independent and Sobol Indices for Total Net Revenue-Wet Year

Input Variable	Delta		Sobol	
	S1	S1_conf	S1	S1_conf
Grain Price	0.0001	0.0003	0.0001	0.0004
Alfalfa Price	-0.0007	0.0008	-0.0008	0.0009
Almonds and Pistachios Price	-0.0010	0.0023	-0.0008	0.0028
Corn Price	-0.0001	0.0002	-0.0001	0.0003
Cotton Price	-0.0004	0.0007	-0.0004	0.0009

Cucurbits Price	-0.0002	0.0005	-0.0004	0.0008
Fresh Tomatoes Price	-0.0001	0.0006	-0.0002	0.0011
Onions and Garlic Price	-0.0007	0.0006	-0.0010	0.0009
Other Deciduous Price	-0.0001	0.0006	-0.0002	0.0008
Other Deciduous Price	0.0000	0.0000	0.0000	0.0000
Other Truck Price	-0.0005	0.0021	0.0004	0.0035
Potatoes Price	-0.0004	0.0006	-0.0006	0.0009
Processing Tomatoes Price	-0.0004	0.0007	-0.0004	0.0009
Subtropical Price	0.0039	0.0074	0.0042	0.0082
Vine Price	-0.0001	0.0018	-0.0001	0.0018
Grain Yield	-0.0001	0.0005	-0.0002	0.0007
Alfalfa Yield	-0.0003	0.0014	-0.0004	0.0014
Almonds and Pistachios Yield	0.0005	0.0038	0.0008	0.0037
Corn Yield	0.0000	0.0002	-0.0001	0.0003
Cotton Yield	-0.0008	0.0010	-0.0010	0.0012
Cucurbits Yield	-0.0004	0.0005	-0.0006	0.0007
Fresh Tomatoes Yield	0.0001	0.0003	0.0002	0.0005
Onions and Garlic Yield	-0.0003	0.0003	-0.0005	0.0005
Other Deciduous Yield	0.0000	0.0001	0.0001	0.0003
Other Deciduous Yield	0.0002	0.0003	0.0004	0.0005
Other Truck Yield	0.0000	0.0011	0.0002	0.0027
Potatoes Yield	0.0001	0.0003	0.0002	0.0005
Processing Tomatoes Yield	-0.0001	0.0004	-0.0001	0.0006
Subtropical Yield	0.0148	0.0106	0.0148	0.0110
Vine Yield	-0.0001	0.0011	-0.0003	0.0012
Price Surface Water	0.0003	0.0037	0.0006	0.0038
Other Field Price	-0.0001	0.0001	-0.0002	0.0002
Other Field Price	-0.0004	0.0006	-0.0002	0.0009
Other Field Price	-0.0016	0.0023	-0.0019	0.0022
Other Field Price	-0.0001	0.0001	-0.0002	0.0002
Other Field Price	-0.0001	0.0001	-0.0002	0.0003
Other Field Price	-0.0003	0.0005	-0.0005	0.0007

Other Field Price	0.0000	0.0002	-0.0002	0.0008
Other Field Price	-0.0002	0.0002	-0.0003	0.0003
Other Field Price	-0.0002	0.0005	-0.0004	0.0007
Other Field Price	-0.0001	0.0003	-0.0002	0.0005
Other Field Price	-0.0002	0.0007	-0.0005	0.0008
Other Field Price	-0.0001	0.0002	-0.0001	0.0003
Other Field Price	0.0000	0.0003	0.0001	0.0005
Other Field Price	0.0003	0.0018	0.0003	0.0017
Other Field Price	0.0003	0.0008	0.0001	0.0011
Groundwater Restriction	0.7527	0.0239	0.7377	0.0230
Price Electricity	0.0000	0.0002	0.0000	0.0003

Table A8: First Order Delta Moment-Independent and Sobol Indices for Total Net Revenue-Wet Year

Input Variable	Delta		Sobol	
	S1	S1_conf	S1	S1_conf
Grain Price	0.0001	0.0004	0.0001	0.0000
Alfalfa Price	0.0003	0.0005	0.0002	0.0001
Almonds and Pistachios Price	0.0018	0.0011	0.0012	0.0001
Corn Price	0.0002	0.0004	0.0001	0.0000
Cotton Price	0.0001	0.0008	0.0004	0.0001
Cucurbits Price	0.0005	0.0006	0.0003	0.0001
Fresh Tomatoes Price	0.0007	0.0008	0.0008	0.0001
Onions and Garlic Price	0.0006	0.0005	0.0005	0.0001
Other Deciduous Price	0.0004	0.0005	0.0003	0.0000
Other Deciduous Price	0.0000	0.0000	0.0012	0.0002
Other Truck Price	0.0476	0.0052	0.0471	0.0006
Potatoes Price	0.0005	0.0005	0.0003	0.0001
Processing Tomatoes Price	0.0017	0.0011	0.0021	0.0001
Subtropical Price	0.0013	0.0036	0.0010	0.0001
Vine Price	0.0000	0.0007	0.0005	0.0001

Grain Yield	0.0004	0.0004	0.0002	0.0000
Alfalfa Yield	0.0005	0.0008	0.0001	0.0000
Almonds and Pistachios Yield	0.0022	0.0016	0.0022	0.0001
Corn Yield	0.0002	0.0003	0.0015	0.0001
Cotton Yield	0.0006	0.0006	0.0002	0.0000
Cucurbits Yield	0.0004	0.0005	0.0001	0.0000
Fresh Tomatoes Yield	0.0001	0.0003	0.0001	0.0001
Onions and Garlic Yield	0.0004	0.0006	0.0003	0.0001
Other Deciduous Yield	-0.0004	0.0007	0.0007	0.0001
Other Deciduous Yield	-0.0003	0.0005	0.0002	0.0001
Other Truck Yield	0.0091	0.0029	0.0095	0.0003
Potatoes Yield	-0.0002	0.0008	0.0002	0.0000
Processing Tomatoes Yield	0.0008	0.0008	0.0014	0.0001
Subtropical Yield	0.0031	0.0028	0.0016	0.0001
Vine Yield	0.0002	0.0007	0.0001	0.0000
Price Surface Water	0.0020	0.0019	0.0003	0.0001
Other Field Price	0.0001	0.0004	0.0002	0.0001
Other Field Price	-0.0002	0.0004	0.0001	0.0000
Other Field Price	0.0004	0.0012	0.0001	0.0000
Other Field Price	0.0002	0.0002	0.0001	0.0000
Other Field Price	0.0003	0.0005	0.0003	0.0000
Other Field Price	0.0005	0.0006	0.0006	0.0001
Other Field Price	-0.0002	0.0005	0.0003	0.0001
Other Field Price	0.0003	0.0003	0.0001	0.0000
Other Field Price	0.0006	0.0005	0.0005	0.0001
Other Field Price	0.0004	0.0004	0.0002	0.0001
Other Field Price	0.0088	0.0020	0.0076	0.0002
Other Field Price	-0.0001	0.0004	0.0001	0.0000
Other Field Price	-0.0001	0.0005	0.0001	0.0000
Other Field Price	0.0003	0.0009	0.0001	0.0000
Other Field Price	0.0006	0.0011	0.0002	0.0000
Groundwater Restriction	0.8685	0.0139	0.8690	0.0007

Price Electricity	0.0000	0.0004	0.0001	0.0000

Table A9: First Order Delta Moment-Independent and Sobol Indices for Total Land Use-Dry Year

Input Variable	Delta		Sobol	
	S1	S1_conf	S1	S1_conf
Groundwater Restriction	0.0316	0.0005	0.0315	0.0038
Price Electricity	0.0011	0.0001	0.0010	0.0006
Price Surface Water	0.0003	0.0001	0.0003	0.0007
Alfalfa Price	0.0001	0.0001	-0.0001	0.0002
Almonds and Pistachios Price	0.0019	0.0001	0.0024	0.0011
Corn Price	0.0002	0.0001	0.0000	0.0001
Cotton Price	0.0001	0.0000	-0.0001	0.0002
Cucurbits Price	0.0003	0.0001	0.0001	0.0003
Fresh Tomatoes Price	0.0008	0.0001	0.0007	0.0006
Grain Price	0.0012	0.0001	0.0000	0.0001
Onions and Garlic Price	0.0019	0.0002	0.0010	0.0006
Other Deciduous Price	0.0013	0.0001	0.0003	0.0004
Other Deciduous Price	0.0001	0.0000	0.0000	0.0000
Other Truck Price	0.0184	0.0004	0.0182	0.0030
Potatoes Price	0.0004	0.0001	0.0005	0.0004
Processing Tomatoes Price	0.0001	0.0000	0.0000	0.0003
Subtropical Price	0.0237	0.0004	0.0234	0.0032
Vine Price	0.7077	0.0006	0.7077	0.0142
Other Field Price	0.0002	0.0000	0.0000	0.0001
Other Field Price	0.0001	0.0000	0.0001	0.0004
Other Field Price	0.0035	0.0002	0.0001	0.0001
Other Field Price	0.0004	0.0001	0.0000	0.0000
Other Field Price	0.0002	0.0001	-0.0001	0.0002
Other Field Price	0.0001	0.0000	0.0000	0.0002
Other Field Price	0.0002	0.0000	0.0000	0.0002
Other Field Price	0.0004	0.0001	0.0000	0.0001

Other Field Price	0.0001	0.0000	0.0001	0.0001
Other Field Price	0.0001	0.0000	-0.0001	0.0001
Other Field Price	0.0009	0.0001	0.0007	0.0005
Other Field Price	0.0016	0.0001	0.0000	0.0001
Other Field Price	0.0002	0.0001	0.0000	0.0001
Other Field Price	0.0001	0.0000	0.0002	0.0003
Other Field Price	0.0007	0.0001	0.0006	0.0015
Alfalfa Yield	0.0001	0.0000	0.0000	0.0002
Almonds and Pistachios Yield	0.0032	0.0002	0.0033	0.0014
Corn Yield	0.0002	0.0000	0.0000	0.0001
Cotton Yield	0.0001	0.0000	0.0000	0.0001
Cucurbits Yield	0.0002	0.0001	0.0001	0.0001
Fresh Tomatoes Yield	0.0003	0.0001	0.0003	0.0004
Grain Yield	0.0001	0.0000	0.0000	0.0001
Onions and Garlic Yield	0.0003	0.0000	0.0001	0.0003
Other Deciduous Yield	0.0003	0.0001	0.0000	0.0004
Other Deciduous Yield	0.0002	0.0001	0.0000	0.0001
Other Truck Yield	0.0047	0.0002	0.0051	0.0017
Potatoes Yield	0.0002	0.0000	0.0000	0.0004
Processing Tomatoes Yield	0.0001	0.0000	0.0000	0.0002
Subtropical Yield	0.0061	0.0002	0.0060	0.0020
Vine Yield	0.1783	0.0009	0.1786	0.0080

Table A10: First Order Delta Moment-Independent and Sobol Indices for Total Net Revenue-Dry Year

A9 Bibliography

Zeff, H. B., Hamilton, A. L., Malek, K., Herman, J. D., Cohen, J. S., Medellin-Azuara, J., Reed, P. M., & Characklis, G. W. (2021). California's food-energy-water system: An open source simulation model of adaptive surface and groundwater management in the Central Valley.

Environmental Modelling & Software, *141*, 105052. https://doi.org/10.1016/j.envsoft.2021.105052

Appendix B

Supplementary Material for Chapter 3

B1 Flexible Sustainable Groundwater Management

The Sustainable Management Criteria (DWR, 2017) defines:

- Sustainable groundwater management as *"the management and use of groundwater in a manner that can be maintained during the planning and implementation horizon without causing undesirable results."*
- Measurable objectives is *"the specific, quantifiable goals for the maintenance or improvement of groundwater conditions that have been included in an adopted Plan."*
- The minimum threshold is *"the quantitative value that represents the groundwater condition in each representative monitoring well site that when exceeded, may cause an undesirable result."*

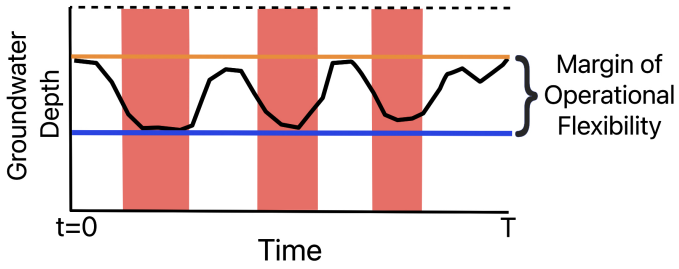

Figure B1: Conceptual behavior of groundwater depth under sustainable management. Dashed line represents the reference ground surface level, orange line depicts the upper bound of groundwater depth level and blue line represents the lower-bound depth. Red rectangles depict dry periods when groundwater depth increases.

B2 Economic Model Calibration

We used a Positive Mathematic Programing (PMP) (Howitt, 1995) calibration that employs a stochastic data assimilation process to calibrate the economic model (Maneta et al., 2020). With this calibration we address two objectives: avoid the assumption that farmers will behave as a particular year or average of years but rather capturing the mid-term farmers behavior using all the data available from 1999 to 2015, and second, we account for the uncertainty in the calibration parameters inherited from uncertain inputs used in the calibration. This stochastic framework enables us to update the distribution of parameters as new observations become available. We adapted the Python code used by Maneta et al. (2020) that performs a Monte Carlo recursive Bayesian estimator based on the ensemble Kalman Filter (enKF) (Evensen, 1994). The enKF uses uses the calibration conditions to recursively update the distribution of the parameters using historical data on crop production, land use, water use, own-price supply elasticities, crop yield response to water (elasticity) and production costs. The optimality conditions to perform the stochastic assimilation follow the PMP calibration described by Mérel et al. (2011) which uses using a generalized Constant Elasticity of Substitution (CES) production function as a concave production function, and the calibration of the Lagrange multipliers used in the linear costs of land and water explained by Garnache, Mérel, et al. (2017).

The goal of the calibration stage is to replicate observed inputs allocation to crops and yield. Following the necessary and sufficient optimality conditions or Karush-Kuhn-Tucker conditions of the maximization problem (Equations B1) that are solved so the model calibration parameters can reproduce the observed allocation of inputs land and water per crop ($\tilde{x}_{i,land}, \tilde{x}_{i,water}$).

$$\max_{\substack{x_{i,land}\geq 0 \\ x_{i,water}\geq 0}} \sum_i \{p_i \mu_i (\beta_{i,land} x_{i,land}^{\rho_i} + \beta_{i,water} x_{i,water}^{\rho_i})^{\delta_i/\rho_i} - (\omega_{i,land}) x_{i,land} - (\omega_{i,water}) x_{i,water}\}$$

subject to:

$$\sum_i x_{i,land} \leq b_{land}[\bar{\lambda}_{land}] \tag{B1}$$

$$x_{i,land} = \tilde{x}_{i,land}[\lambda_{i,land}]$$

$$x_{i,water} = \tilde{x}_{i,water}[\lambda_{i,water}]$$

Where $\mu_i, \beta_{i,water}, \beta_{i,land}, \delta_i, \rho_i$ are the calibration parameters used the CES production function (Mérel et al., 2011) and $\lambda_{i,land}, \lambda_{i,water}, \bar{\lambda}_{land}$ the Lagrange multipliers for the total land and crop-specific use of inputs restrictions. The crop-specific input use restriction guarantees that the solution will reproduce the observed input use. p_i is the crop price per crop and $\omega_{i,land}$ and $\omega_{i,water}$ represent the average land and water costs. For the case of water such cost is weighted by the proportion of surface and groundwater baseline use. Even though the economic model described in Section 2.1.1 solves for two sources of water (groundwater and surface water), the calibration was performed aggregating both sources of water. Calibration parameters and crop specific Lagrange multipliers are obtained for the crop groups $i \in$ {Alfalfa, Almonds and Pistachios, Corn, Cotton, Cucurbits, Dry Beans, Fresh Tomatoes, Grain, Onions and Gralic, Other Deciduous, Other Field, Other Truck, Pasture, Processing Tomatoes, Safflower, Subtropical and Vine} shown in Figure B1.

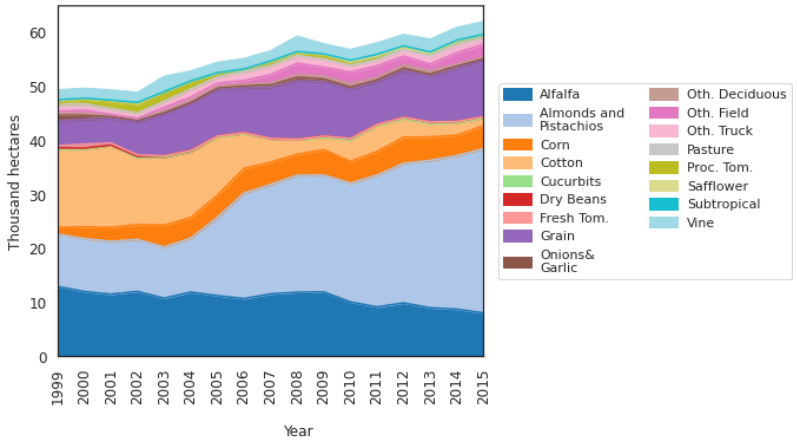

Figure B2: Historical cropland of Semitropic WSD

The PMP maximization problem defined by the set of Equations B1 can be formulated following its first order optimality conditions and arranged as a set of nonlinear equations as proposed by Garnache, Mérel, et al. (2017). Where on the left-hand side of Equations B2 are the observed quantities and on the right-hand side are the model functions that include the parameters that we are estimating.

$$
\begin{aligned}
&-p_i\tilde{y}_i\tilde{y}_{i,water} = (\omega_{i,land} + \lambda_{i,land} + \bar{\lambda}_{land})\tilde{x}_{i,land} - p_i\tilde{y}_i\delta_i \\
&p_i\tilde{y}_i\tilde{y}_{i,water} = (\omega_{i,water} + \lambda_{i,water})\tilde{x}_{i,water} \\
&\tilde{\eta}_i = \frac{\delta_i}{1-\delta}\left\{1 - \frac{\frac{b_i}{\delta_i(1-\delta_i)}}{\sum_i[\frac{b_i}{\delta_i(1-\delta_i)} + \frac{\sigma_i b_i \tilde{y}_{i,water}}{\delta_i(\delta_i - \tilde{y}_{i,water})}]}\right\}, b_i = \frac{(\tilde{x}_{i,land})^2}{p_i\tilde{y}_i} \\
&\tilde{y}_{i,water} = \delta_i\left(\frac{\beta_{i,water}(\tilde{x}_{i,land})^{\rho_i}}{\beta_{land,i}(\tilde{x}_{i,land})^{\rho_i} + \beta_{i,water}(\tilde{x}_{i,water})^{\rho_i}}\right) \\
&\tilde{y}_i = \mu_i(\beta_{i,land}x_{i,land}^{\rho_i} + \beta_{i,water}x_{i,water}^{\rho_i})^{\delta_i/\rho_i} \\
&\sum_i\{(2\tilde{x}_{i,land}p_i\tilde{y}_i\tilde{y}_{i,water}) = \sum_i -2(\omega_{i,land} + \lambda_{land})(\tilde{x}_{i,land})^2 + 2\tilde{x}_{i,land}p_i\tilde{y}_i\delta_i\} \\
&1 = \beta_{i,water} + \beta_{i,land}
\end{aligned}
\tag{B2}
$$

Where $\tilde{x}_{i,land}$, $\tilde{x}_{i,water}$, $\tilde{y}_i$ are the observed land use, water use and yield for each crop respectively, $\tilde{y}_{i,water}$ is the crop specific water yield elasticity and $\tilde{\eta}_i$ is the exogenous own price crop supply elasticity. $\rho_i = (\sigma_i - 1)/\sigma_i$ where σ represents the elasticity of substitution between land and water, which was fixed to $\sigma = 0.17$ as shown to be a good approximation (Howitt et al., 2012). Equations B2 are embeded in a stochastic assimilation process to calibrate recursively the calibration parameters, in the vector $\theta_i = [\mu_i, \beta_{i,water}, \beta_{i,land}, \delta_i, \lambda_{i,land}, \lambda_{i,water}, \bar{\lambda}_{land}]$, following the stochastic data assimilation framework described by Maneta et al. (2020).

Data used in the calibration are from various sources, spatial scales, and specific crops or groups of crops. This lack of specific spatial and crop type resolution creates uncertainty in the estimators. Data sources include crop grouping categories defined by the Department of Water Resources (DWR) that reports water applied to each group by county and year, different individual crops are included in each group for which we selected a price and yield from USDA (2020). Agricultural production costs were obtained from UC Davis Cost and Return Studies (UC Davis, 2015) using average costs from crops within each group. Historical annual land use was obtained from the Kern County Spatial Data (KCDAMS, 2020). Own-price crop supply elasticity were obtained from (Rodríguez-Flores et al., 2022). Finally, the yield elasticity to water was calculated following the process in Appendix B.2.1. All data sources are summarized in Table B1.

Observation	Symbol	Units	Source
Crop prices	p_i	\$/ton	USDA (2020)
Price of electricity	$\omega_{E,t}$	$\$/Kwh$	PG&E (2021)
Price of surface water	$\omega_{SW,t}$	$\$/m^3$	Irrigation districts reports
Surface water supply	$b_{SW,t}$	m^3	Zeff et al. (2021)
Land cost	$\omega_{i,land}$	$\$/ha$	UC Davis (2015)
Pumping cost	$\omega_{GW,t}$	$\$/m^3$	Pumping cost function (Section A.2)
Crop yield	y_i	ton/ha	USDA (2020)
Crop yield-water elasticity	$\tilde{y}_{i,water}$	-	SM 2.1
Crop supply elasticity	$\tilde{\eta}_i$	-	Rodríguez-Flores et al. (2022)
Applied water	$\tilde{x}_{i,water}$	m^3/ha	DWR (2020a)
Land use	$\tilde{x}_{i,land}$	ha	KCDAMS, 2020[1]

Table B1: Data sources for Economic model calibration

Following the data-assimilation process we first set the ensemble size with 400 samples using the first year of observations (1999). We began by stabilizing the model parameters to start with correct values spinning up the data assimilation process using observations from 1999 until the ensemble stabilized. We found that the parameters stabilized with 40 repetitions of the spin up process, after which we use observations from 2000 to 2015 to sequentially perform the data assimilation process. We tune manually the parameters used in the Kalman filter, variance smoothing parameter and background parameter ensemble variance, until we find the best results. With the final calibration, we found that the model closely reproduces the historical allocation of land and water to all the crops but for the Cotton category which has been observed a decline in acreage over the observed years. However, the calibration closely resembles the last years of historical data which show a clear positive trend in perennial tree crops.

B2.1 Yield Elasticity to Water Use

Crop yield elasticity to water ($\tilde{y}_{i,water}$) represents the response of yield to changes in water applied, as percent change in yield to a percent change in applied water. To estimate this parameter we used two approaches, first for crops Alfalfa, Corn, Almonds (in Almonds and Pistachios category), and Wheat (in Grain category) we used the VIC-CropSyst model (Malek et al., 2017) calibrated for a spatial grid in the study area and using different irrigation systems. Crop yield responses were estimated by reducing applied water (deficit irrigation), responses from VIC-CropSyst (V-CS) were later used to estimate the crop yield water elasticity ($\tilde{y}_{i,water}$) using following a sigmoidal yield response function (Equation B3) described by Mérel et al. (2014). We fitted the sigmoidal response function using a nonlinear regression solving for

$\alpha_{i,1}, \alpha_{i,2}, \alpha_{i,3}$. With the estimates from solving this regression the crop-specific yield response to water changes was later calculated using Equation B4. using the reference water applied ($\tilde{x}_{i,water}$) and reference yield ($\tilde{y}_i$) used in the PMP calibration (average of the historical).

$$\hat{y}_{i,V-CS} = \frac{\alpha_{i,1}}{1 + exp\left(-\frac{\hat{x}_{i,water,V-CS} - \alpha_{i,2}}{\alpha_{i,3}}\right)} \tag{B3}$$

$$\tilde{y}_{i,water} = \frac{\tilde{x}_{i,water} exp\left(-\frac{\tilde{x}_{i,water} - \bar{\alpha}_{i,2}}{\bar{\alpha}_{i,3}}\right) \hat{y}_i}{\bar{\alpha}_{i,1}\bar{\alpha}_{i,3}} \tag{B4}$$

For the rest of the crops we used the applied water by crop category from DWR (2020a) and yield from the most representative crop within each group using the land reported by USDA (2020), both reported at a county level and using the data from 1998 to 2015. We estimated the elasticity through least squares (Equation B5) as the slope between the natural logarithm of production and the natural logarithm of water used. We compared our results with other published values for crops in California, specially for San Joaquin Valley (Garnache, Mérel, et al., 2017; Mérel et al., 2014).

$$ln(\tilde{y}_{i,t}) = \tilde{y}_{i,water} ln(\tilde{x}_{i,water,t}) \tag{B5}$$

B3 Groundwater Pumping Cost

The unitary ($\$1/m^3$) pumping cost ω_{GW} is given by the Equation B3, where $\omega_{pump} = \$200,000$ is the capital cost of the well, $A_{service} = 80$ ha is the assumed pumping service area, $\widetilde{x}_{water} = 4,933 m^3/ha$ is the assumed average irrigation demand per unit area, $i = 0.05$ is the discount rate, $n = 20$ is the pump years lifetime, $\zeta = \$6.6 \times 10^{-5}/m^3 m$ is the variable operation and maintenance costs for the pump, $\omega_{E,t}\$/kWh$ is the price of electricity, $\eta_{pump} = 0.7$ is the average pump efficiency, GWD_t is the potentiometric depth (meters) of the irrigation district in the year t, Q is the assumed pumping rate $0.1261 m^3/s$, C is the Hazen-Williams coefficient, pipe is assumed to be cast-iron or steel for which C = 0.12680, and $d = 0.4m$ is the pipe diameter.

$$\omega_{GW,t} = \left(\frac{\omega_{pump}}{A_{service}\widetilde{x}_{water}} \frac{i(1+i)^n}{(1+i)^n - 1}\right) + \left(\zeta + \frac{\omega_{E,t}}{\eta_{pump}}\right)\left(GWD_t + 10.67 \frac{GWD_t Q^{1.852}}{C^{1.852} d^{4.8704}}\right) \tag{B6}$$

B4 Calibration Groundwater Depth Response Function

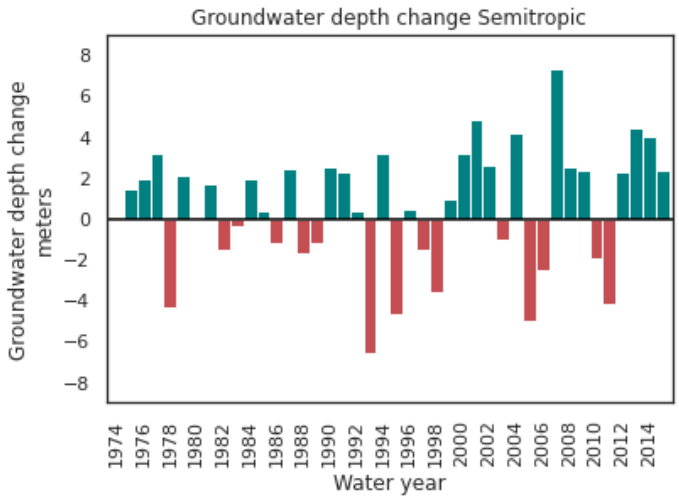

Figure B3: Changes on distance to groundwater depth from C2VSIM-FG

We used Bayesian linear regression to simulate the groundwater depth response to agricultural pumping. We used C2VSIM-FG (DWR, 2021) simulation outputs from 1973 to 2015, from which we used the Groundwater Pumping at the beginning and end of each water year t (GWP_t) to predict the groundwater depth change at the end of the irrigation season in a year (ΔGWD) as a function of the total agricultural pumping in year t GWP_t and t-1 GWP_{t-1}. Additionally, we include Water year Type of year t (WY_t) and Water Year type of year t-1 (WY_{t-1}) as index variables. The water year type categories are: Wet, Normal and Dry. Normal category includes above and bellow normal categories and Dry water year includes Critical and Dry types, all of them are defined by the Water Year Hydrologic Classification Indices of the California Department of Water Resources (DWR, 2020b). As shown by (MacEwan et al., 2017), using the water type variable we can capture information related to hydro-logical processes that shift how agricultural pumping affect groundwater depth levels.

Using groundwater pumping of the year t and $t-1$ and water year type (Wet, Normal and Dry) of the year t and $t-1$ as index variables we fitted different Bayesian linear modes. Pooled model (or fixed-effects) assigns same model parameters (intercept and slopes) across water year types. Un-pooled model assigns different parameters to each water year type as if water-year type is independent and have different intercepts and slopes. Finally, the Hierarchical model (or random-effects or multi-level) assigns different parameters to each water-year type varying intercepts or slopes (or both) across water-year type categories,

this models enables the statistical model to learn how the agricultural pumping affects the groundwater depth change in each water year type while learning this effect from all the water wear types at the same time.

Groundwater pumping (GWP_t, GWP_{t-1}) and change of depth to groundwater (ΔGWD_t) were normalized using the z-score normalization. Bayesian modeling uses a maximum entropy distribution to define the likelihood of the output, for this study we use Student's-t distribution to model the groundwater depth change probability distribution. The characteristics of the Student's t distribution makes it a more robust distribution to include extreme values and that can improve the MCMC sampling process. Additionally we need to define priors of the parameters (or unobserved variables). For this study we defined Gaussian priors for the intercept and slopes in all the model variations. As we expect that the relationship between groundwater depth change and change being positive for which case we centered the Gaussian distribution on the positive side for GWP_t and a less informative distribution centered in 0 for GWP_{t-1}. Additionally an exponential distribution for the standard deviation priors and Gamma distribution for the degrees of freedom of the Student-t's distribution prior.

- P1: Pooled, $\mu_t = \alpha + \beta_1 GWP_t$
- P2: Pooled with lag on pumping, $\mu_t = \alpha + \beta_1 GWP_t + \beta_2 GWP_{t-1}$
- U1: Unpooled, $\mu_t = \alpha_{WY_t} + \beta_{1,WY_t} GWP_t$
- U2: Unpooled with lag on pumping, $\mu_t = \alpha_{WY_t} + \beta_{1,WY_t} GWP_t + \beta_{2,WY_t} GWP_t$
- U3: Unpooled with lag on pumping and slope, $\mu_t = \alpha_{WY_t} + \gamma_{WY_{t-1}} + \beta_{1,WY_t} GWP_t + \beta_{2,WY_t} GWP_t$
- H1: Hirerarchical with varying intercept, $\mu_t = \alpha_{WY_t} + \beta_1 GWP_t$
- H2: Hirerarchical with varying intercept and varying slope, $\mu_t = \alpha_{WY_t} + \beta_{1,WY_t} GWP_t$
- H3: Hirerarchical with varying slopes, $\mu_t = \alpha_t + \beta_{1,WY_t} GWP_t + \beta_{2,WY_t} GWP_t$
- H4: Hirerarchical with varying intercept and slopes, $\mu_t = \alpha_{WY_t} + \beta_{1,WY_t} GWP_t + \beta_{2,WY_t} GWP_t$
- H5: Hirerarchical with varying intercepts and slopes, $\mu_t = \alpha_{WY_t} + \gamma_{WY_{t-1}} + \beta_{1,WY_t} GWP_t + \beta_{2,WY_t} GWP_t$

Models were fit using a Markov Chain Monte Carlo (MCMC) sampling method using the probabilistic programming Python package PyMC (Salvatier et al., 2016). Model selection was done using the Leave-one-out Cross-validation (LOO-CV) as estimate of the out-of-sample predictive fit (Vehtari et al., 2017), selecting the model with the highest log-scale LOO-CV or with he best out-of-sample prediction (Figure B3). The LOO-CV validation results are summarized in the Figure B8. Where the best model is the hirerarchical model with varying intercepts (H5), however the model with unpooled effects in intercepts and pumping (U3) was selected since is a simpler model and has a LOO close to H5. Hence, obtaining similar predictive power for a more computational efficient model.

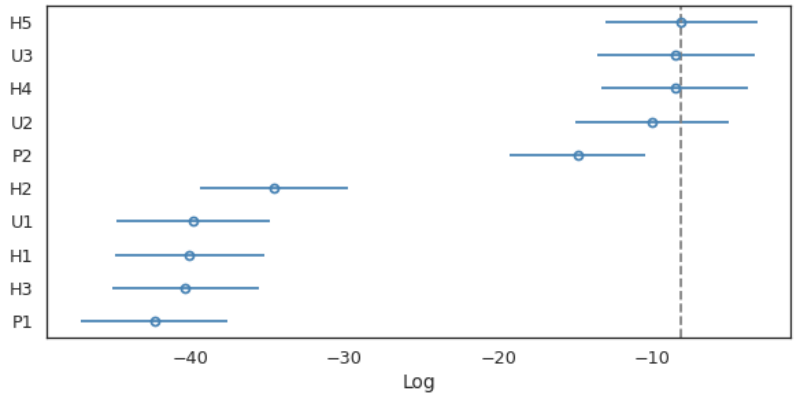

Figure B4: Leave-one-out cross-validation results

The selected model is an unpooled model with priors defined in Equations B1. Table B1 shows the results from the model U3 summarizing the distribution of the posterior distribution of the parameters. In Figure B1 we show that calibrated response function can predict correctly the groundwater depth change with an $r^2 = 0.90 (r^2 std = 0.007)$.

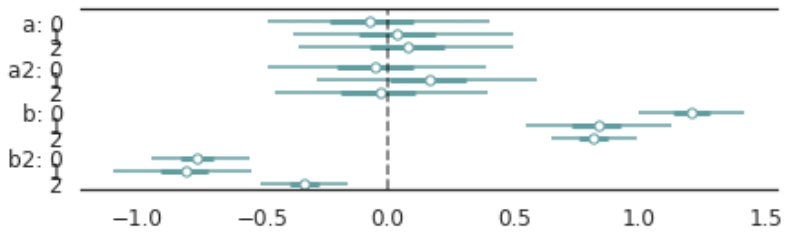

Figure B5: Posterior Distributions of the parameters, where 0 is Wet Year, 1 is Normal Year and 2 is Dry Year

Table B2: Marginal posterior distributions of the parameters of Groundwater Depth Response

Parameter	Mean	Sd	HDI 2.5%	HDI 97.5%
$\alpha_{1[Wet_t]}$	-0.063	0.232	-0.478	0.405
$\alpha_{1[Normal_t]}$	0.041	0.223	-0.379	0.501
$\alpha_{1[Dry_t]}$	0.079	0.217	-0.356	0.494
$\gamma_{1[Wet_t]}$	-0.057	0.224	-0.481	0.393
$\gamma_{1[Normal_t]}$	0.159	0.225	-0.285	0.588
$\gamma_{1[Dry_t]}$	-0.041	0.217	-0.453	0.400
$\beta_{1[Wet_{t\text{-}1}]}$	1.207	0.107	0.995	1.419
$\beta_{1[Normal_{t\text{-}1}]}$	0.829	0.148	0.550	1.126
$\beta_{1[Dry_{t\text{-}1}]}$	0.817	0.088	0.649	0.991
$\beta_{2[Wet_{t\text{-}1}]}$	-0.757	0.100	-0.940	-0.551
$\beta_{2[Normal_{t\text{-}1}]}$	-0.807	0.141	-1.094	-0.543
$\beta_{2[Dry_{t\text{-}1}]}$	-0.336	0.088	- 0.507	-0.159
σ	0.235	0.037	0.169	0.310
ν	20.470	12.859	2.469	45.244

$$
\begin{aligned}
\Delta GWD_t &\sim \textit{Student-t}(\mu_t, \sigma, \nu) \\
\mu_t &= \alpha_{WY_t} + \gamma_{WY_{t-1}} + \beta_{1WY_t} GWP_t + \beta_{2WYR_{t-1}} GWP_{t-1} \\
\alpha_j &= Normal(0, 0.5) \\
\gamma_j &= Normal(0, 0.5) \\
\beta_{1j} &= Normal(0.5, 0.5) \quad for j = \{Wet, Normal, Dry\} \\
\beta_{2j} &= Normal(0, 0.5) \\
\sigma &= Exponential(1) \\
\nu &= Gamma(2, 0.1)
\end{aligned}
\tag{B7}
$$

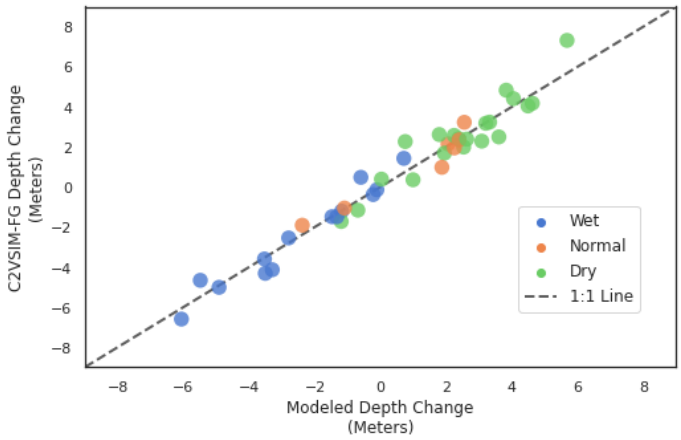

Figure B6: Results groundwater depth response function and C2VSIM-FG (DWR, 2021). Dots represent the median of each posterior predictive distribution of groundwater depth change, colors represent the water-year type in year t.

B5 Calibrated Hydro-Economic Model Performance

The following figures show the performance from running dynamically the coupled hydro-economic model with the last set of calibration parameters obtained from the data assimilation process (with 400 samples) over historical water available conditions. The model was let free to optimize dynamically land and water allocation decisions to assess its capacity to replicate observed conditions.

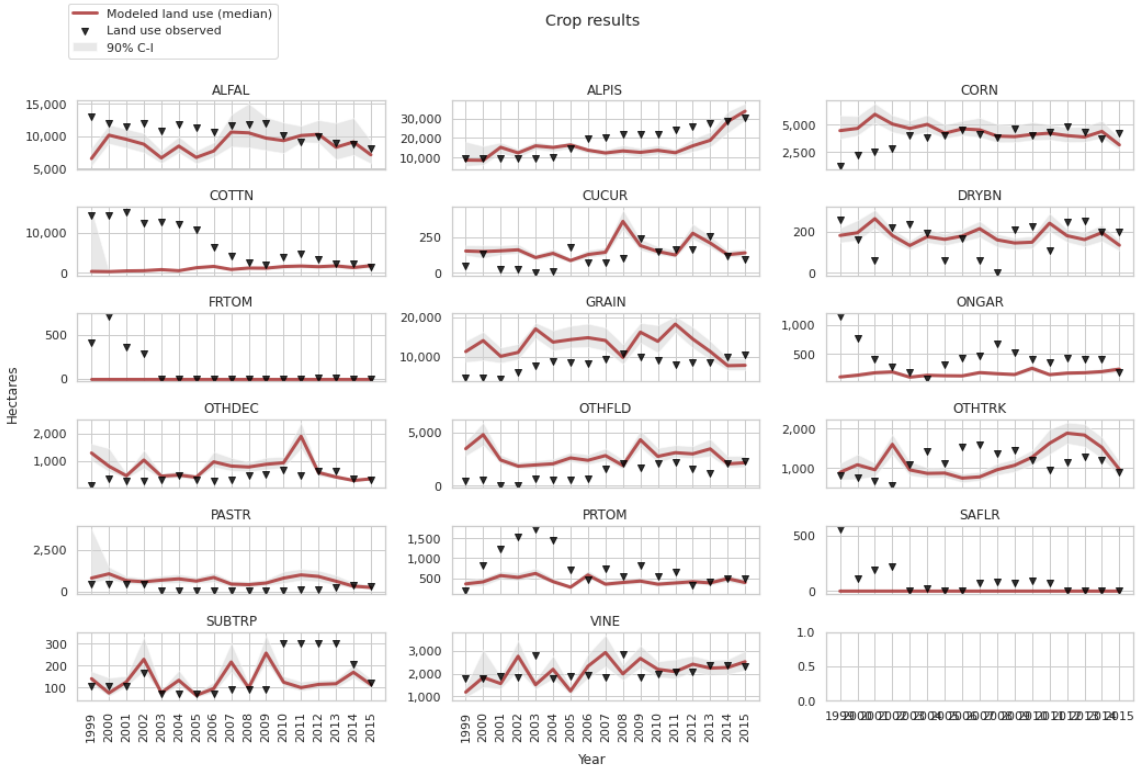

Figure B7: Land allocation from Hydro-economic model and observed

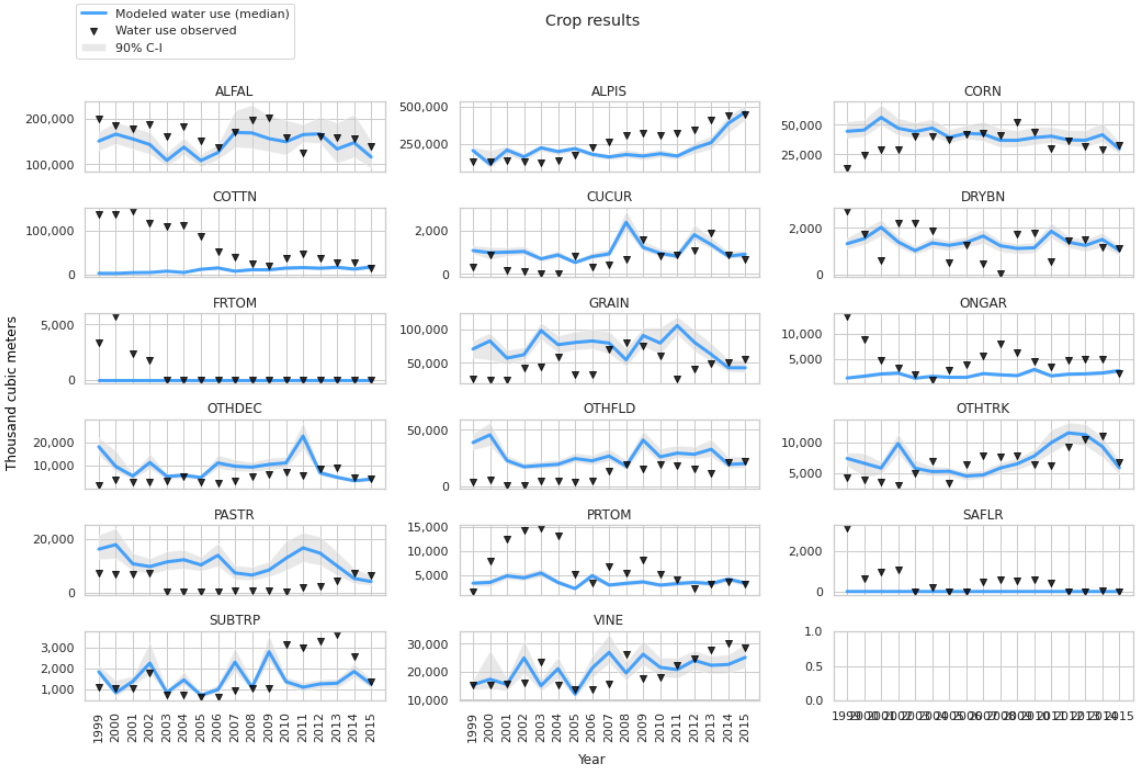

Figure B8: Water allocation from Hydro-economic model and observed

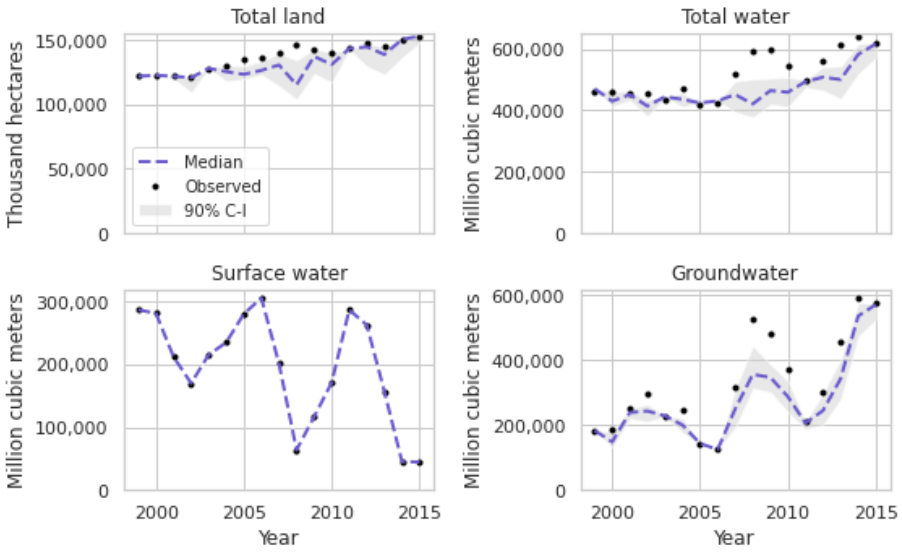

Figure B9: Total water allocation by source from Hydro-economic model and observed

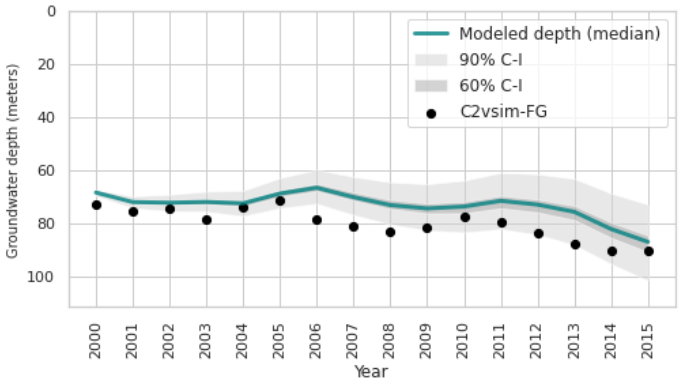

Figure B10: Simulated groundwater depth from running coupled hydro-economic model dynamically and observed groundwater depth from DWR (2021)

Table B3: Epsilon values used for the Borg MOEA

Objective	Epsilon
Maximize Average Total Revenues (O1)	30
Minimize Average Groundwater Depth (O2)	1.8
Maximize 5th Percentile Revenue in a year (O3)	1
Minimize 95th Groundwater Depth Change in a year (O4)	0.9
Reliability (O5)	0.01

B6 Surface Water Deliveries used in Computational Experiment

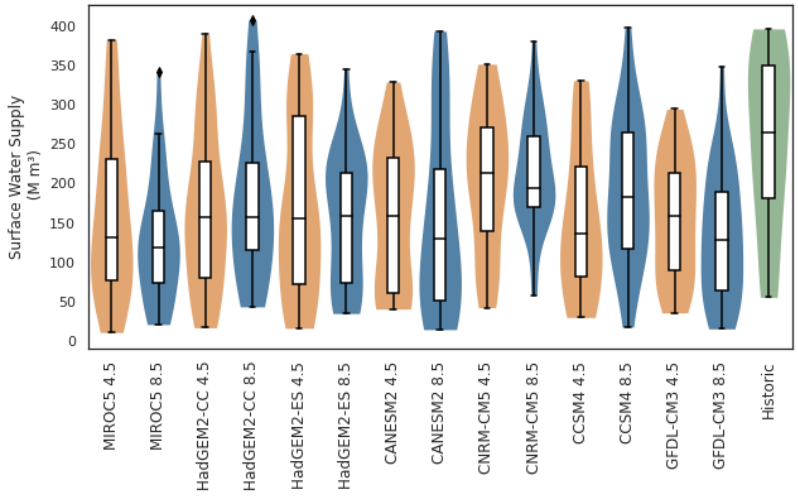

Figure B11: Distribution of historical (1999-2015) and surface water deliveries from CALFEWS (2016-2045) used in this study

B7 Borg Epsilon values and Hypervolume from Random Seeds

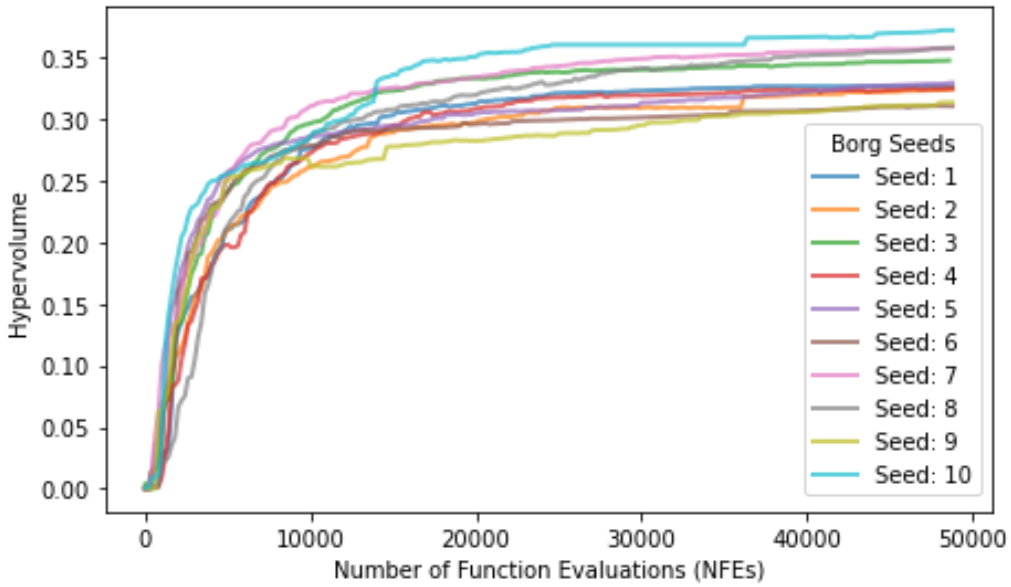

Figure B12: Hypervolume from 10 random seeds used in Borg MOEA

B8 Pareto-approximate set validation

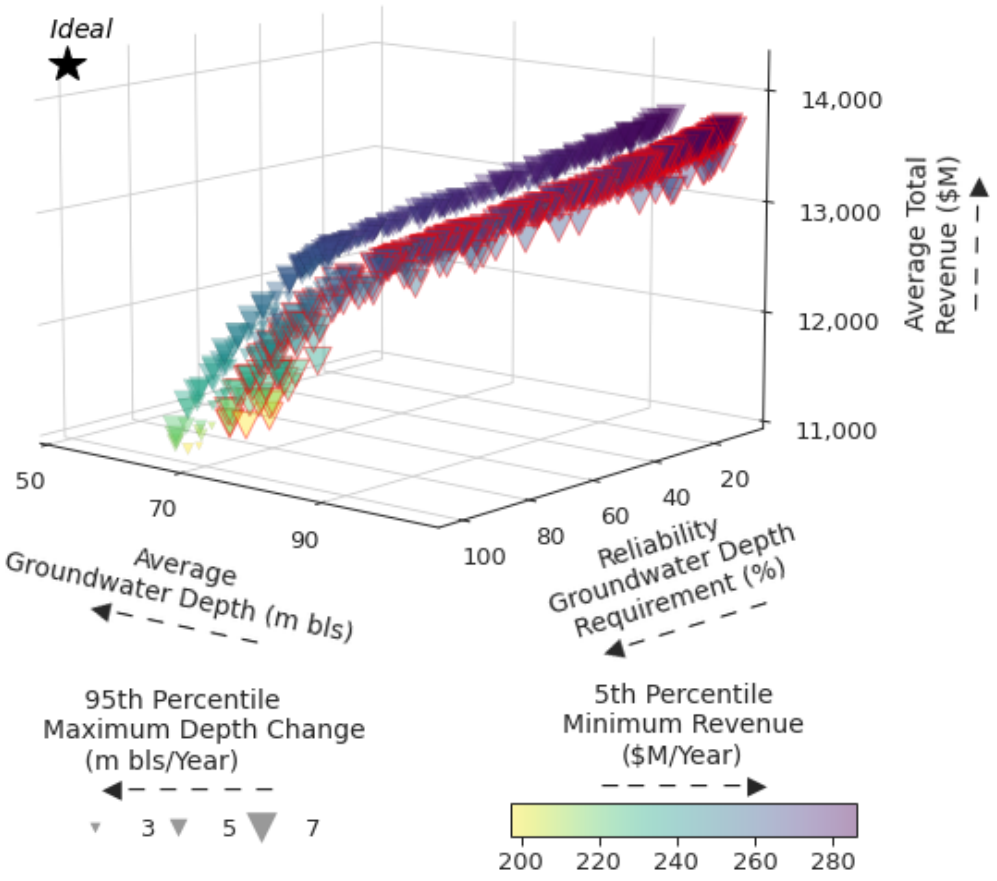

Figure B13: Reference pareto set was re-evaluated using a larger independent set of 1,000 sets of sampled SOWs. Triangles with red edge represent the re-evaluated set and triangles without edge the original optimized solution.

B9 Performance selected Policies

The following figures show the performance of the selected solutions in Section 3.5.

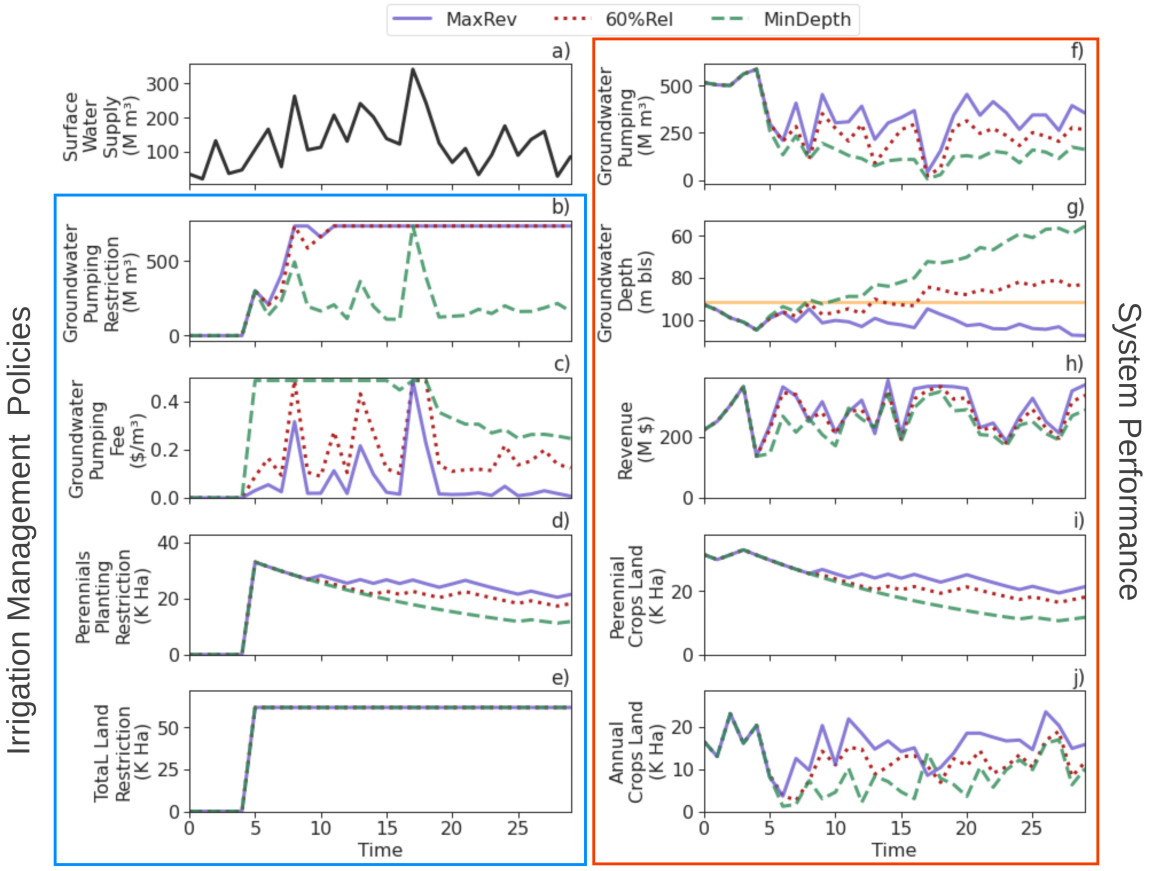

Figure B14: Performance selected policies, shown in Figure 3.5, under driest average surface water deliveries (MIROC 8.5). Panel (a) shows the surface water deliveries. Panels (b) - (e) show the dynamic decisions in the control policy. Panels (f)-(j) show the performance of the food-water system. The orange line in Sub-figure (g) depicts the measurable objective used in the experiment

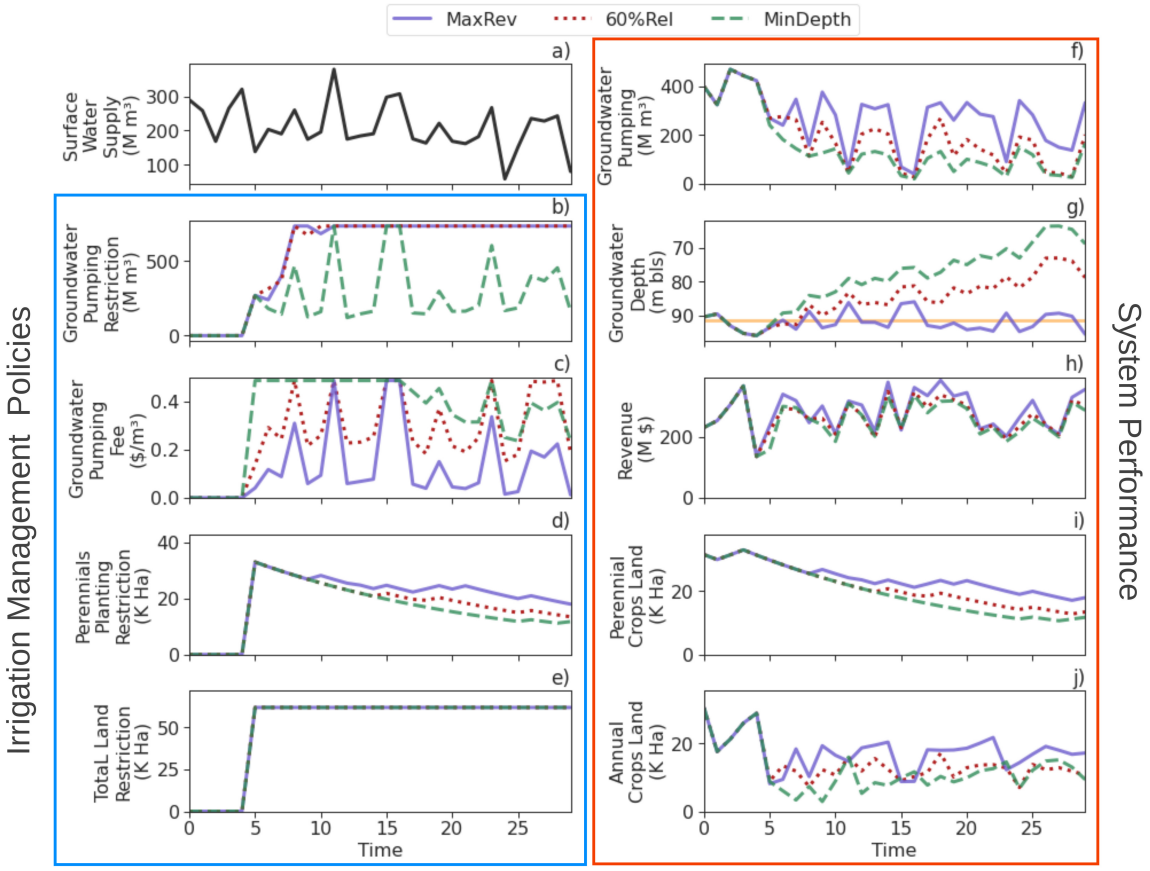

Figure B15: Performance selected policies, shown in Figure 3.5, under largest (wet) average surface water deliveries (CNRM-CM5 8.5). Panel (a) shows the surface water deliveries. Panels (b) - (e) show the dynamic decisions in the control policy. Panels (f)-(j) show the performance of the food-water system. The orange line in Sub-figure (g) depicts the measurable objective used in the experiment

B10 Performance selected Robust Policies

The following figures show the performance of the selected robust solutions in Section 5.1

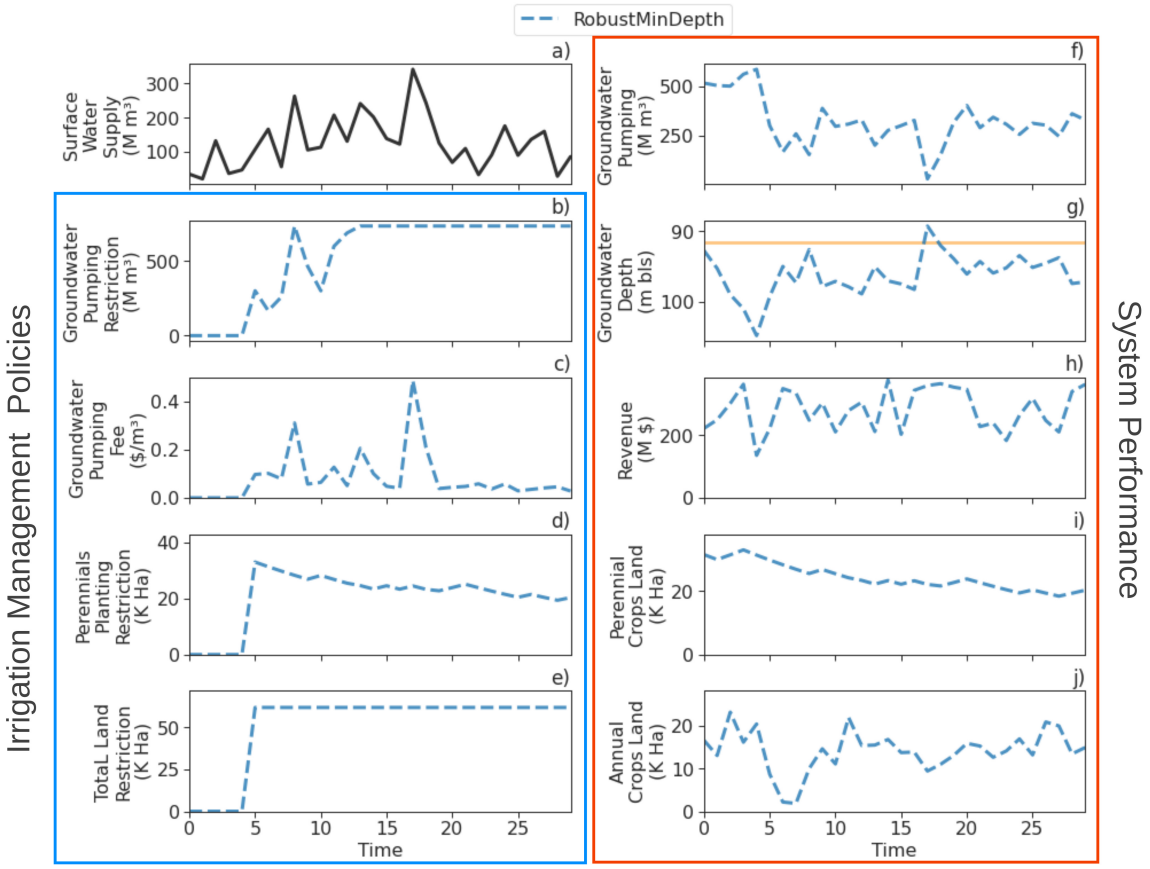

Figure B16: Performance Robust Policy under driest average surface water deliveries (MIROC 8.5). Panel (a) shows the surface water deliveries. Panels (b) - (e) show the dynamic decisions in the control policy. Panels (f)-(j) show the performance of the food-water system. The orange line in Sub-figure (g) depicts the measurable objective used in the experiment

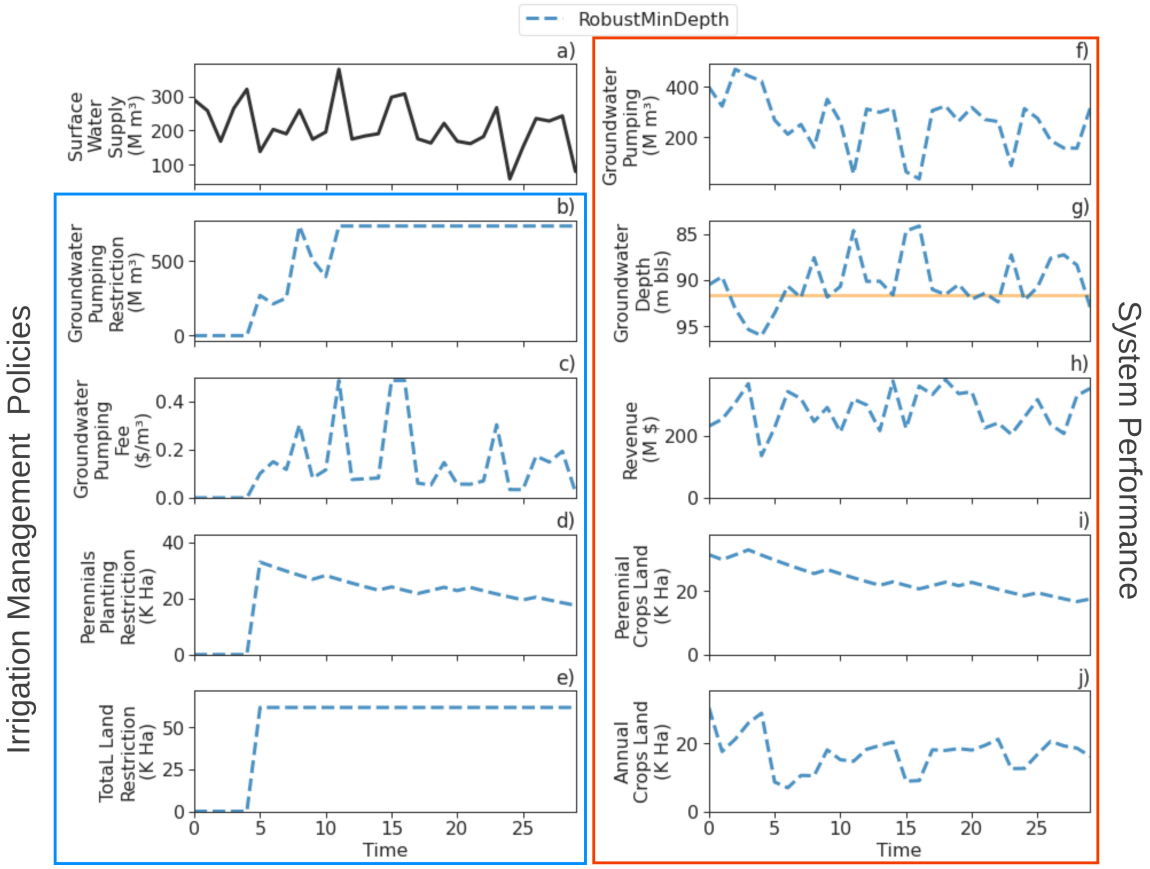

Figure B17: Performance Robust Policy under largest (wet) average surface water deliveries (CNRM-CM5 8.5). Panel (a) shows the surface water deliveries. Panels (b) - (e) show the dynamic decisions in the control policy. Panels (f)-(j) show the performance of the food-water system. The orange line in Sub-figure (g) depicts the measurable objective used in the experiment

B11 Feature Scoring

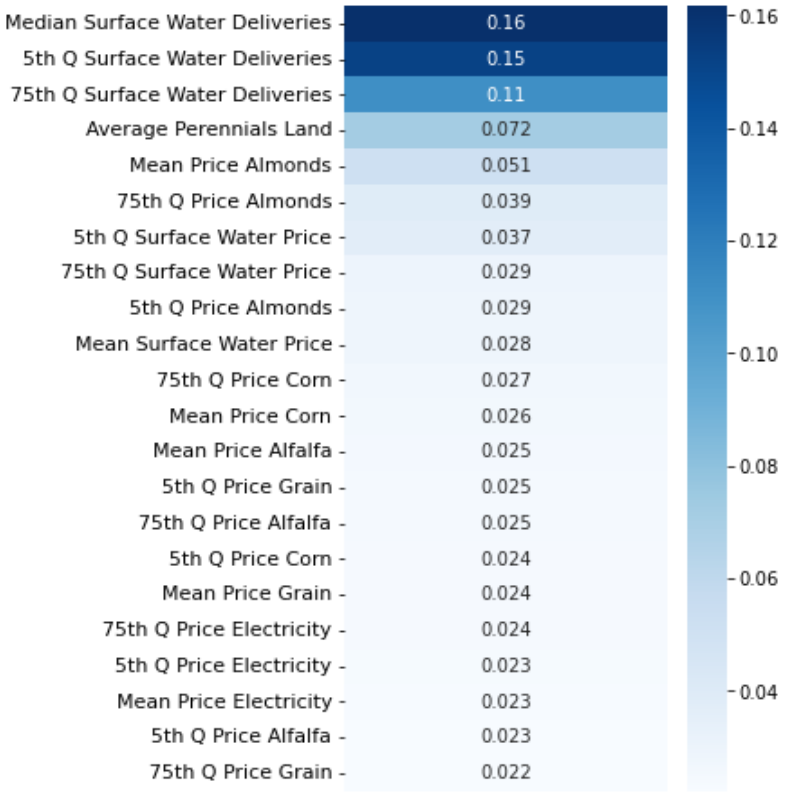

Figure B18: Feature Scoring for the RobustMinDepth solution

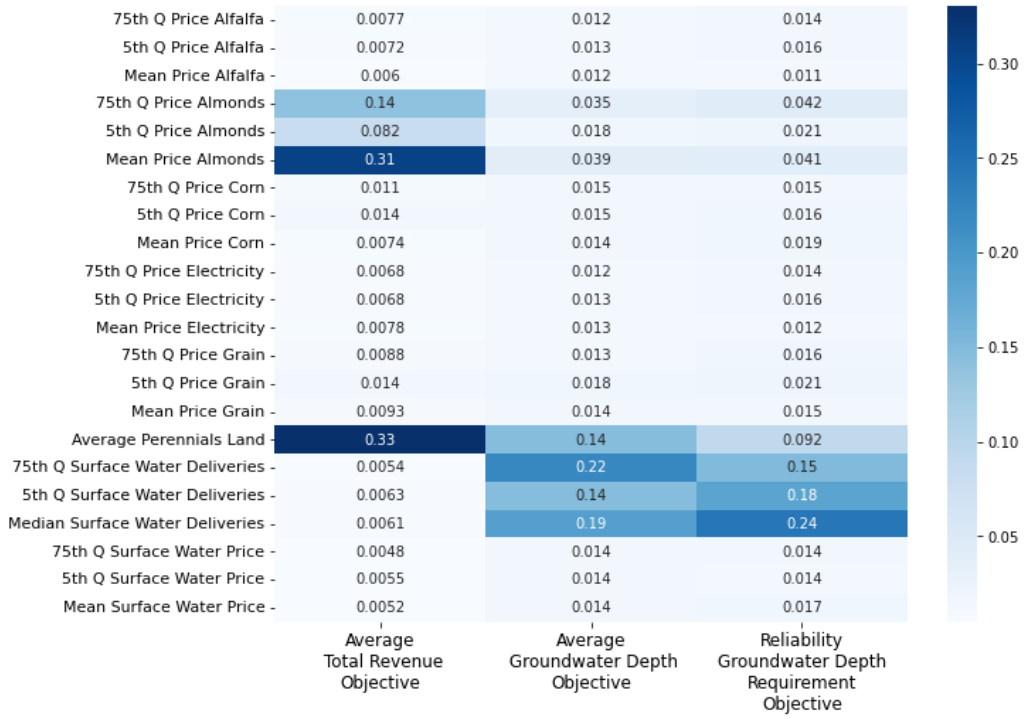

Figure B19: Feature Scoring for the RobustMinDepth solution for each objective

Bibliography

DWR. (2017). *Sustainable Manage Criteria* (tech. rep.). California Department of Water Resources, Sustainable Groundwater Management Program. https://water.ca.gov/Programs/Groundwater-Management/SGMA-Groundwater-Management/Best-Management-Practices-and-Guidance-Documents

DWR. (2020a). Agricultural Land & Water Use Estimates. http://water.ca.gov/Programs/Water-Use-And-Efficiency/Land-And-Water-Use/Agricultural-Land-And-Water-Use-Estimates

DWR. (2020b). California Data Exchange Center (CDEC). https://cdec.water.ca.gov/reportapp/javareports?name=WSIHIST

DWR. (2021). C2VSimFG Version 1.01. https://data.cnra.ca.gov/dataset/c2vsimfg-version-1-01

Evensen, G. (1994). Sequential data assimilation with a nonlinear quasi-geostrophic model using Monte Carlo methods to forecast error statistics. *Journal of Geophysical Research: Oceans*, *99*(C5), 10143–10162. https://doi.org/10.1029/94JC00572

Garnache, C., Mérel, P., Howitt, R., & Lee, J. (2017). Calibration of shadow values in constrained optimisation models of agricultural supply. *European Review of Agricultural Economics*, *44*(3), 363–397. https://doi.org/10.1093/erae/jbx005

Garnache, C., Mérel, P. R., Lee, J., & Six, J. (2017). The social costs of second-best policies: Evidence from agricultural GHG mitigation. *Journal of Environmental Economics and Management*, *82*, 39–73. https://doi.org/10.1016/j.jeem.2016.10.004

Howitt, R. E. (1995). A Calibration Method for Agricultural Economic Production Models. *Journal of Agricultural Economics*, *46*(2), 147–159. https://doi.org/10.1111/j.1477-9552.1995.tb00762.x

Howitt, R. E., Medellín-Azuara, J., MacEwan, D., & Lund, J. R. (2012). Calibrating disaggregate economic models of agricultural production and water management. *Environmental Modelling & Software*, *38*, 244–258. https://doi.org/10.1016/j.envsoft.2012.06.013

KCDAMS. (2020). Kern County Spatial Data. http://www.kernag.com/gis/gis-data.asp

MacEwan, D., Cayar, M., Taghavi, A., Mitchell, D., Hatchett, S., & Howitt, R. (2017). Hydroeconomic modeling of sustainable groundwater management. *Water Resources Research*, *53*(3), 2384–2403. https://doi.org/10.1002/2016WR019639

Malek, K., Stöckle, C., Chinnayakanahalli, K., Nelson, R., Liu, M., Rajagopalan, K., Barik, M., & Adam, J. C. (2017). VIC–CropSyst-v2: A regional-scale modeling platform to simulate the nexus of climate, hydrology, cropping systems, and human decisions. *Geoscientific Model Development*, *10*(8), 3059–3084. https://doi.org/10.5194/gmd-10-3059-2017

Maneta, M., Cobourn, K., Kimball, J., He, M., Silverman, N., Chaffin, B., Ewing, S., Ji, X., & Maxwell, B. (2020). A satellite-driven hydro-economic model to support agricultural water resources management. *Environmental Modelling & Software*, *134*, 104836. https://doi.org/10.1016/j.envsoft.2020.104836

Mérel, P., Simon, L. K., & Yi, F. (2011). A Fully Calibrated Generalized Constant-Elasticity-of-Substitution Programming Model of Agricultural Supply. *American Journal of Agricultural Economics*, *93*(4), 936–948. https://doi.org/10.1093/ajae/aar029

Mérel, P., Yi, F., Lee, J., & Six, J. (2014). A Regional Bio-economic Model of Nitrogen Use in Cropping. *American Journal of Agricultural Economics*, *96*(1), 67–91. https://doi.org/10.1093/ajae/aat053

PG&E. (2021). Pacific Gas & Electric - Tariffs. https://www.pge.com/tariffs/rateinfo.shtml

Rodríguez-Flores, J. M., Valero Fandiño, J. A., Cole, S. A., Malek, K., Karimi, T., Zeff, H. B., Reed, P. M., Escriva-Bou, A., & Medellín-Azuara, J. (2022). Global Sensitivity Analysis of a Coupled Hydro-Economic Model and Groundwater Restriction Assessment. *Water Resources Management*, *36*(15), 6115–6130. https://doi.org/10.1007/s11269-022-03344-5

Salvatier, J., Wiecki, T., & Fonnesbeck, C. (2016). Probabilistic programming in Python using PyMC3. *PeerJ Comput. Sci.* https://doi.org/10.7717/PEERJ-CS.55

UC Davis. (2015). Current Cost and Return Studies. https://coststudies.ucdavis.edu/en/current/

USDA. (2020). National Agricultural Statistics Service - California. https://www.nass.usda.gov/Statistics_by_State/California/index.php

Vehtari, A., Gelman, A., & Gabry, J. (2017). Practical Bayesian model evaluation using leave-one-out cross-validation and WAIC. *Statistics and Computing*, *27*(5), 1413–1432. https://doi.org/10.1007/s11222-016-9696-4

Zeff, H. B., Hamilton, A. L., Malek, K., Herman, J. D., Cohen, J. S., Medellin-Azuara, J., Reed, P. M., & Characklis, G. W. (2021). California's food-energy-water system: An open source simulation model of adaptive surface and groundwater management in the Central Valley. *Environmental Modelling & Software*, *141*, 105052. https://doi.org/10.1016/j.envsoft.2021.105052

Appendix C

Supplementary Material for Chapter 4

C1 Groundwater Depletion Study Area

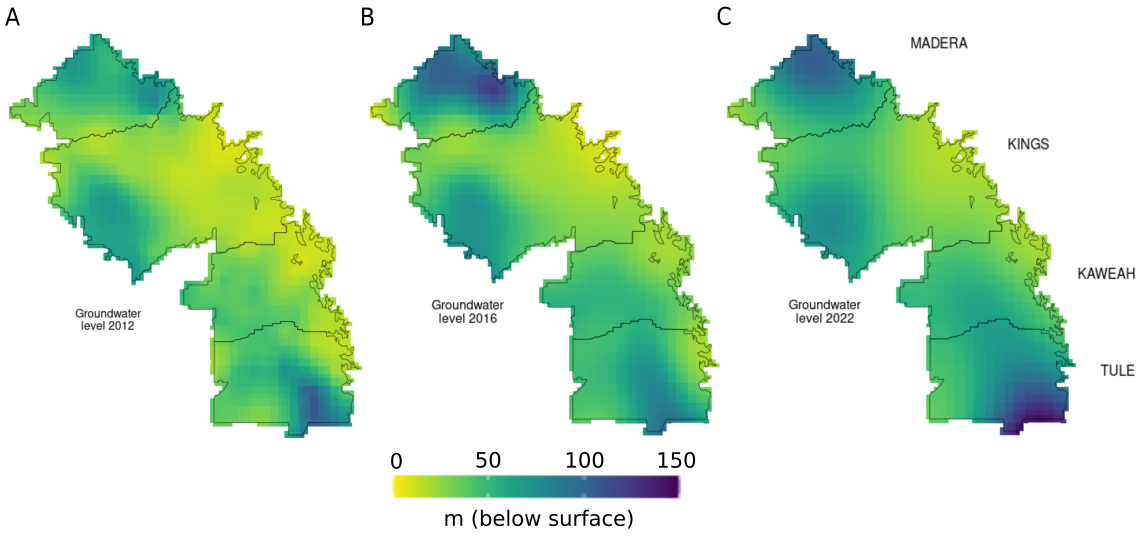

Figure C1: Groundwater Depth for 2012, 2016 and 2022 in the study area in meters bellow ground surface

C2 Wells data cleaning and aquifer location

Well completion reports collect data on characteristics of the total drilled depth (well depth) and location of top and bottom of the screen (water intake). However, not all the wells report depths, and screen location. In the study area 87% of the wells in the well completion reports have well depth and 60% bottom and top of the screen. Additionally out of 2,751 monitoring wells that have reported a measurement groundwater levels in the study area (and buffer) between 2014 and 2022, 61% have well depth and 54% have bottom of the screen. Finally, 49% of the dry wells in the study area did not report well depth or is uncertain. We used a buffer around the study area of 10 miles (17 km) to consider wells from the well completion report in sections that are in neighbor sections to the ones in the study area as shown in Figure 4.2 of the main text.

To approximate from what aquifer each well is pumping or measuring levels (for monitoring wells) from, we used the stratigraphy of the C2VSim-FG (DWR, 2021) that has the thickens of the Corcoran clay (Aquitard) and the confined and unconfined depths across the Central Valley for each vertix in a finite element spatial grid. We first assign to each well the closest node or vertix of the finite element grid from C2VSim-FG. In order to assign an aquifer to each well from well completion, dry well reports and monitoring wells we used two approaches. First, if the well has a reported bottom of the screen (the one closest to the ground surface screen if multiple), and this is shallower than the unconfined aquifer depth plus aquitard we assigned the well to the unconfined aquifer. If the bottom of the screen is deeper than the unconfined aquifer depth plus aquitard and shallower than the depth of unconfined aquifer depth plus aquitard plus confined aquifer depth we assigned it to the confined aquifer. C2Vsim-FG also has a deep layer aquifer, referred as Deep Aquifer in Figures C3 and C4 where little pumping occurs. For wells that do not have a reported bottom of the well screen we used the same process using the well depth as reference minus the median distance between well depth and bottom of the screen by type of well and basin (Table C1). For monitoring wells we used the well depth minus the median distance between well depth and bottom of the screen of both domestic wells and agricultural wells.

A second step in the process of cleaning the wells data, was to filter for each year those wells that have been built to that point in time but were likely inactive due to groundwater table being deeper than the water intake of the well (well is dry). For this process we used the well depth minus the median distance between well depth and bottom of the screen (Table C1), as a conservative estimate. Since we used interpolated groundwater levels, there might be uncertainties with these approximations, thus we assumed that only wells whose bottom of the screens are shallower (from ground surface) than the groundwater level may be inactive. However, when groundwater levels are bellow the top of the screen, wells may start failing.

Well Type	Subbasin	Well Variable	mean	median
agriculture	KAWEAH	Bottom Screen Location	103.4	85.3
domestic	KAWEAH	Bottom Screen Location	64.6	59.1
agriculture	KINGS	Bottom Screen Location	84.9	75.9
domestic	KINGS	Bottom Screen Location	56.9	48.8
agriculture	MADERA	Bottom Screen Location	155.3	150.9
domestic	MADERA	Bottom Screen Location	92.3	84.7
agriculture	TULE	Bottom Screen Location	212.3	184.4
domestic	TULE	Bottom Screen Location	70.9	56.4
agriculture	KAWEAH	Distance Bottom Screen to Well Depth	17.1	6.4
domestic	KAWEAH	Distance Bottom Screen to Well Depth	9.9	5.8
agriculture	KINGS	Distance Bottom Screen to Well Depth	12.2	6.1
domestic	KINGS	Distance Bottom Screen to Well Depth	8.6	3.0
agriculture	MADERA	Distance Bottom Screen to Well Depth	18.4	6.1
domestic	MADERA	Distance Bottom Screen to Well Depth	12.2	6.1
agriculture	TULE	Distance Bottom Screen to Well Depth	25.5	6.1
domestic	TULE	Distance Bottom Screen to Well Depth	10.7	4.6
agriculture	KAWEAH	Screen Interval (Bottom – Top)	44.9	30.5
domestic	KAWEAH	Screen Interval (Bottom – Top)	25.3	18.3
agriculture	KINGS	Screen Interval (Bottom – Top)	39.8	34.7
domestic	KINGS	Screen Interval (Bottom – Top)	18.0	12.2
agriculture	MADERA	Screen Interval (Bottom – Top)	56.1	46.3
domestic	MADERA	Screen Interval (Bottom – Top)	19.7	12.2
agriculture	TULE	Screen Interval (Bottom – Top)	82.4	64.0
domestic	TULE	Screen Interval (Bottom – Top)	23.3	18.0
agriculture	KAWEAH	Top Screen Location	58.5	54.9
domestic	KAWEAH	Top Screen Location	39.3	35.4
agriculture	KINGS	Top Screen Location	45.1	39.6
domestic	KINGS	Top Screen Location	38.9	35.1
agriculture	MADERA	Top Screen Location	99.3	85.3
domestic	MADERA	Top Screen Location	72.6	70.1
agriculture	TULE	Top Screen Location	129.9	112.8
domestic	TULE	Top Screen Location	47.6	39.6
agriculture	KAWEAH	Well Depth	120.5	103.6
domestic	KAWEAH	Well Depth	74.5	67.1
agriculture	KINGS	Well Depth	97.1	89.9
domestic	KINGS	Well Depth	65.5	56.4
agriculture	MADERA	Well Depth	173.8	162.5
domestic	MADERA	Well Depth	104.5	94.8
agriculture	TULE	Well Depth	237.7	219.5
domestic	TULE	Well Depth	81.6	68.6

Table C1: Summary statistics for wells in Well Completion Reports

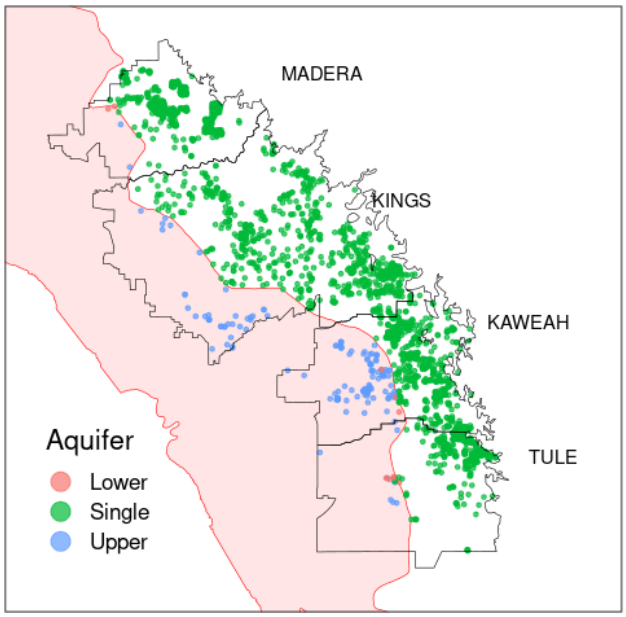

Figure C2: Aquifer location of dry wells (reported between 2014 and 2022). The Corcoran clay is depicted in red.

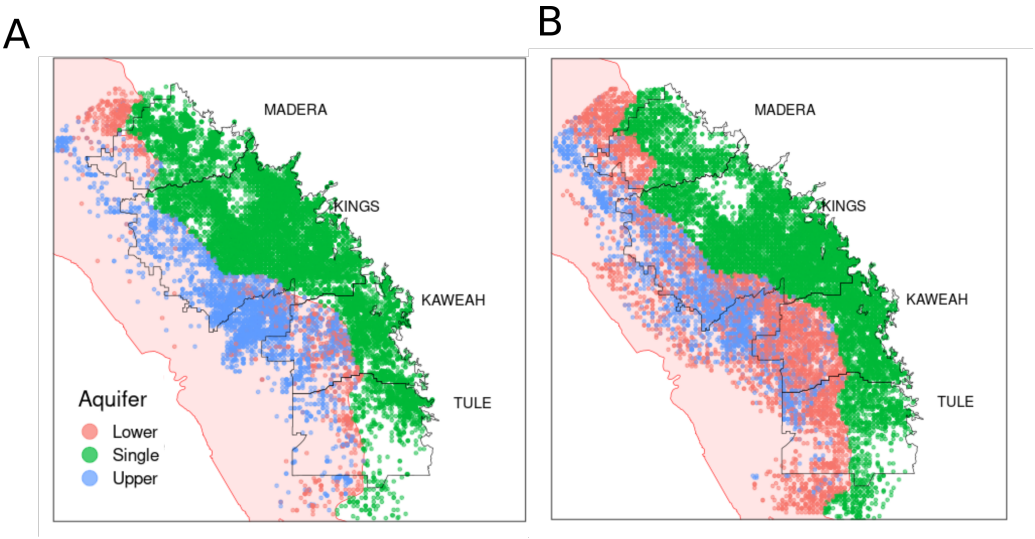

Figure C3: Aquifer location of domestic (A) and agricultural (B) wells, reported between 1970 and 2022. The Corcoran clay is depicted in red.

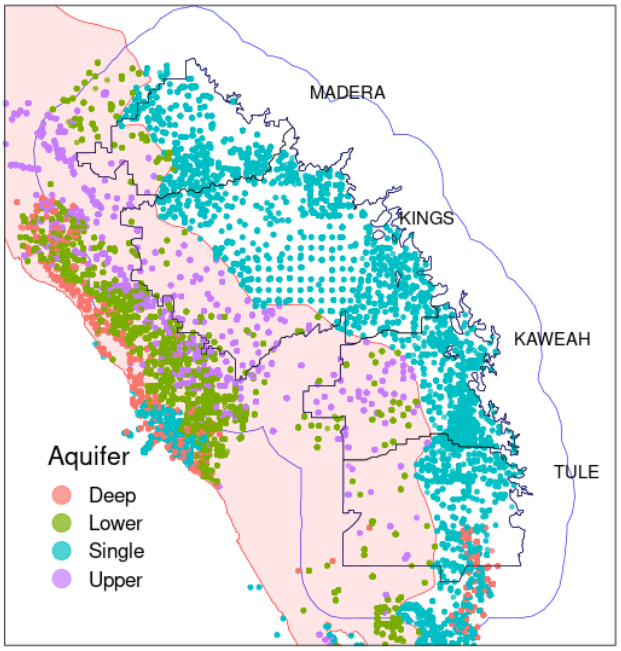

Figure C4: Aquifer location of selected monitoring wells. We used a buffer around the study area of 10 miles (depicted in blue) for selected monitoring wells from the single and upper aquifers to perform the spatial interpolation. The Corcoran clay is depicted in red.

C3 CDL Cropland

CDL_code	Crop	Crop_group	Class
1	Corn	Corn	Forage
2	Cotton	Cotton	Annual
3	Rice	Rice	Annual
4	Sorghum	Field and Grain	Annual
5	Soybeans	Field and Grain	Annual
6	Sunflower	Field and Grain	Annual
10	Peanuts	Truck	Annual
11	Tobacco	Field and Grain	Annual
12	Sweet Corn	Corn	Annual
13	Pop or Orn Corn	Corn	Annual
14	Mint	Truck	Annual
21	Barley	Field and Grain	Annual
22	Durum Wheat	Field and Grain	Annual
23	Spring Wheat	Field and Grain	Annual
24	Winter Wheat	Field and Grain	Annual
25	Other Small Grains	Field and Grain	Annual
26	Dbl Crop WinWht/Soybeans	Field and Grain	Annual
27	Rye	Field and Grain	Annual
28	Oats	Field and Grain	Annual
29	Millet	Field and Grain	Annual
30	Speltz	Field and Grain	Annual
31	Canola	Field and Grain	Annual
32	Flaxseed	Field and Grain	Annual
33	Safflower	Field and Grain	Annual
34	Brassica napus	Field and Grain	Annual
35	Mustard	Field and Grain	Annual
36	Alfalfa	Alfalfa	Forage
37	Other Hay/Non Alfalfa	Field and Grain	Forage
38	Camelina	Field and Grain	Annual

39	Buckwheat	Field and Grain	Annual
41	Sugarbeets	Field and Grain	Annual
42	Dry Beans	Beans Dry	Annual
43	Potatoes	Potatoes	Annual
44	Other Crops	Truck	Annual
45	Sugarcane	Field and Grain	Annual
46	Sweet Potatoes	Potatoes	Annual
47	Misc Vegs Fruits	Truck	Annual
48	Watermelons	Cucurbits	Annual
49	Onions	Onions and Garlic	Annual
50	Cucumbers	Cucurbits	Annual
51	Chick Peas	Truck	Annual
52	Lentils	Truck	Annual
53	Peas	Truck	Annual
54	Tomatoes	Tomatoes	Annual
55	Caneberries	Berries	Annual
56	Hops	Truck	Annual
57	Herbs	Truck	Annual
58	Clover/Wildflowers	Pasture	Non Ag
59	Sod/Grass Seed	Pasture	Annual
60	Switchgrass	Non Ag	Non Ag
61	Fallow/Idle Cropland	Fallow	Fallow
62	Pasture/Grass	Pasture	Non Ag
63	Forest	Non Ag	Non Ag
64	Shrubland	Non Ag	Non Ag
65	Barren	Non Ag	Non Ag
66	Cherries	Orchard	Orchard
67	Peaches	Orchard	Orchard
68	Apples	Orchard	Orchard
69	Grapes	Vine	Orchard
70	Christmas Trees	Non Ag	Non Ag
71	Other Tree Crops	Orchard	Orchard

72	Citrus	Orchard	Orchard
74	Peas	Orchard	Orchard
75	Almonds	Almonds	Orchard
76	Walnuts	Orchard	Orchard
77	Pears	Orchard	Orchard
82	Developed	Urban	Developed
83	Water	Non Ag	Non Ag
87	Wetlands	Non Ag	Non Ag
88	Nonag/Undefined	Non Ag	Non Ag
92	Aquaculture	Non Ag	Non Ag
111	Open Water	Non Ag	Non Ag
112	Perennial Ice/Snow	Non Ag	Non Ag
121	Developed/Open Space	Urban	Developed
122	Developed/Low Intensity	Urban	Developed
123	Developed/Med Intensity	Urban	Developed
124	Developed/High Intensity	Urban	Developed
131	Barren	Non Ag	Non Ag
141	Deciduous Forest	Non Ag	Non Ag
142	Evergreen Forest	Non Ag	Non Ag
143	Mixed Forest	Non Ag	Non Ag
152	Shrubland	Non Ag	Non Ag
176	Grassland/Pasture	Pasture	Non Ag
190	Woody Wetlands	Non Ag	Non Ag
195	Herbaceous Wetlands	Non Ag	Non Ag
204	Pistachios	Pistachios	Orchard
205	Triticale	Field and Grain	Annual
206	Carrots	Truck	Annual
207	Asparagus	Truck	Annual
208	Garlic	Onions and Garlic	Annual
209	Cantaloupes	Cucurbits	Annual
210	Prunes	Orchard	Orchard
211	Olives	Orchard	Orchard

212	Oranges	Orchard	Orchard
213	Honeydew Melons	Cucurbits	Annual
214	Broccoli	Truck	Annual
215	Avocados	Orchard	Orchard
216	Peppers	Truck	Annual
217	Pomegranates	Orchard	Orchard
218	Nectarines	Orchard	Orchard
219	Greens	Lettuce	Annual
220	Plums	Orchard	Orchard
221	Strawberries	Berries	Orchard
222	Squash	Cucurbits	Annual
223	Apricots	Orchard	Orchard
224	Vetch	Field and Grain	Annual
225	Dbl Crop WinWht/Corn	Field and Grain	Annual
226	Dbl Crop Oats/Corn	Field and Grain	Annual
227	Lettuce	Lettuce	Annual
228	Dbl Crop Triticale/Corn	Field and Grain	Annual
229	Pumpkins	Cucurbits	Annual
230	Dbl Crop Lettuce/Durum Wht	Lettuce	Annual
231	Dbl Crop Lettuce/Cantaloupe	Lettuce	Annual
232	Dbl Crop Lettuce/Cotton	Lettuce	Annual
233	Dbl Crop Lettuce/Barley	Lettuce	Annual
234	Dbl Crop Durum Wht/Sorghum	Field and Grain	Annual
235	Dbl Crop Barley/Sorghum	Field and Grain	Annual
236	Dbl Crop WinWht/Sorghum	Field and Grain	Annual
237	Dbl Crop Barley/Corn	Field and Grain	Annual
238	Dbl Crop WinWht/Cotton	Field and Grain	Annual
239	Dbl Crop Soybeans/Cotton	Field and Grain	Annual
240	Dbl Crop Soybeans/Oats	Field and Grain	Annual
241	Dbl Crop Corn/Soybeans	Field and Grain	Annual
242	Blueberries	Berries	Orchard
243	Cabbage	Lettuce	Annual

244	Cauliflower	Truck	Annual
245	Celery	Truck	Annual
246	Radishes	Truck	Annual
247	Turnips	Field and Grain	Annual
248	Eggplants	Truck	Annual
249	Gourds	Cucurbits	Annual
250	Cranberries	Berries	Orchard
254	Dbl Crop Barley/Soybeans	Field and Grain	Annual

Table C2: Relation of CDL codes and crop categories

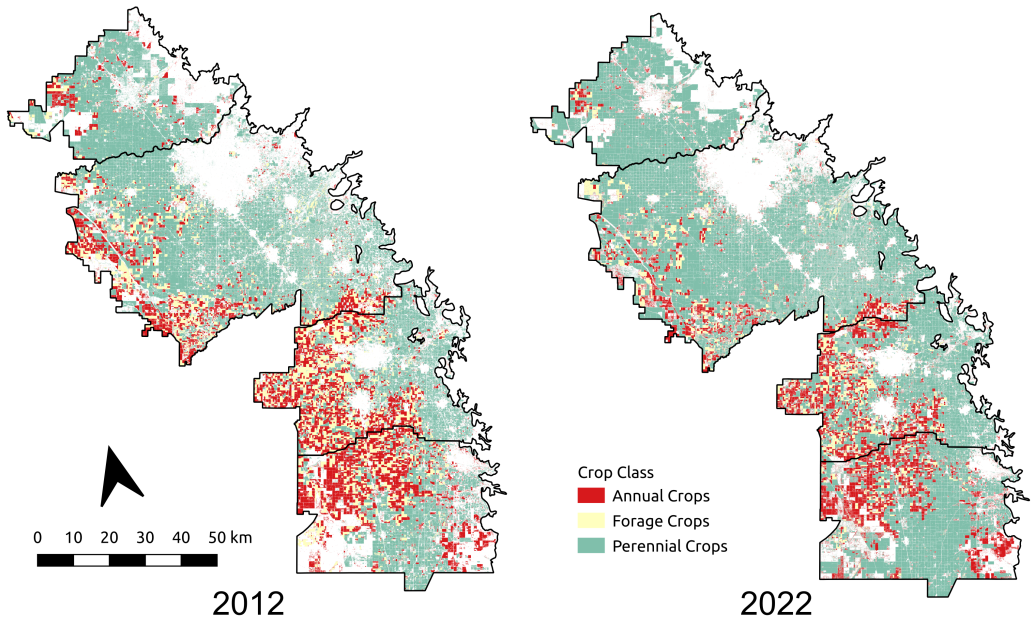

Figure C5: Land use of 2012 and 2022 showing an increase of perennial crops in the time period. Data source: USDA CropScape (Chen et al., 2023)

C4 Spatial autocorrelaion

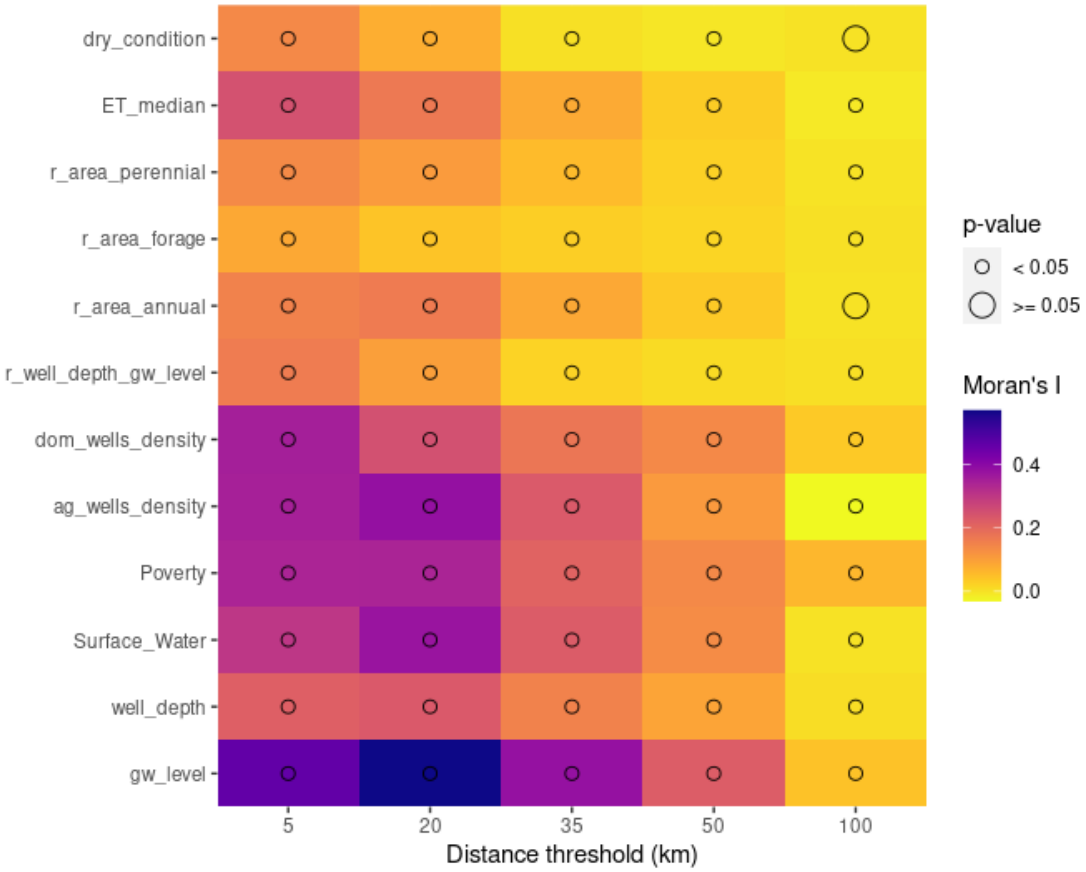

Figure C6: Moran's I test to test for spatial auto-correlation for the variables used as covariates in the model.

C5 Interaction effects

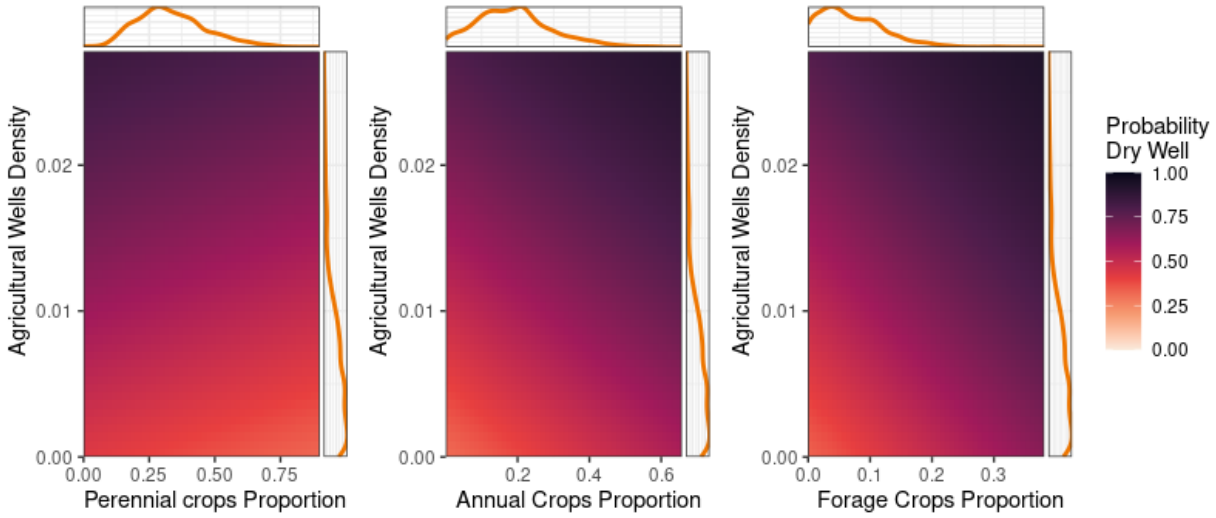

Figure C7: Results from performing linear fits of covariates used in the study. The mean of the linear fit is depicted in orange and the estimated 95% credible interval. Dots represent observations of reported domestic well failure (1) or not (0). This analysis ignores spatial random effects and fits were generated using the model: $W_i \sim Bernoulli(p_i)$ where $logit(p_i) = \sum_j^2 \beta_j X_j$ and W_i = 1 if domestic well failure was reported and W_i = 0 if not.

C6 Spatial model configurations and results

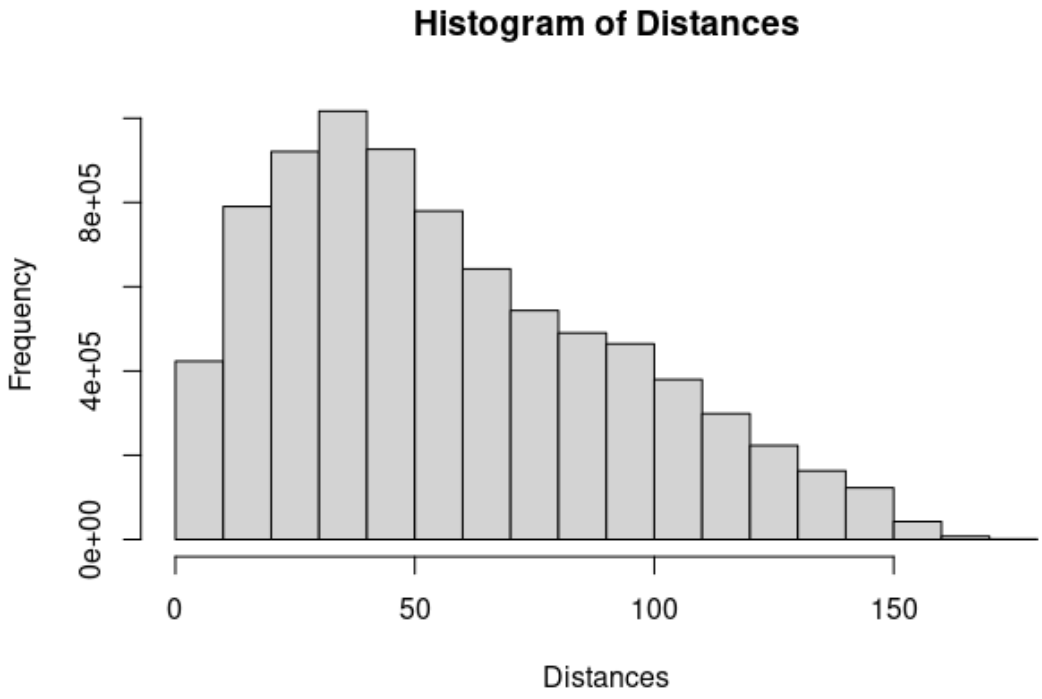

Figure C8: Histogram of distances between wells selected for the study.

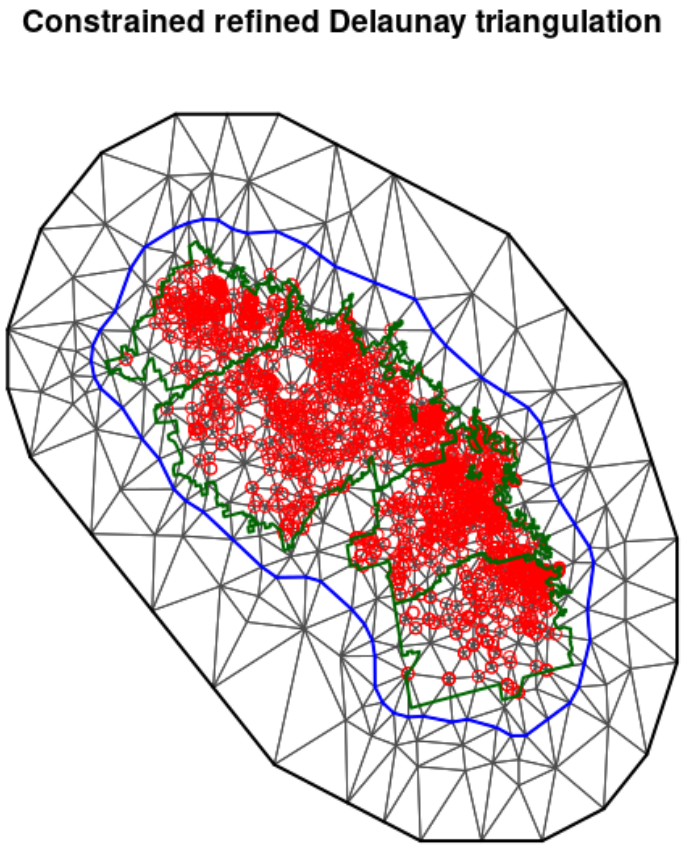

Figure C9: Constraint Delaunay triangulation. In green is depicted the groundwater basins of the study area. Reported dry wells are depicted in red. We constraint the boundary between smaller and larger triangles (in blue).

C6.1 Model Configurations

$$W_i = intercept + S_i + r\_area\_perennial + r\_area\_annual + r\_area\_forage \quad \text{(C1)}$$

$$W_i = intercept + S_i + sw + ag\_wells\_density + dom\_wells\_density \quad \text{(C2)}$$

$$W_i = intercept + S_i + r\_area\_perennial + r\_area\_annual + r\_area\_forage + r\_well\_depth\_gw\_level + sw + dom\_wells\_density + ag\_wells\_density \quad \text{(C3)}$$

$$W_i = intercept + S_i + r\_area\_perennial + r\_area\_annual + r\_area\_forage + r\_well\_depth\_gw\_level + sw + dom\_wells\_density + ag\_wells\_density + \beta_g Basin_g + ag\_wells\_density : r\_area\_perennial + ag\_wells\_density : r\_area\_annual + ag\_wells\_density : r\_area\_forage \quad \text{(C4)}$$

$$W_i = intercept + S_i + r\_area\_perennial + r\_area\_annual + r\_area\_forage + r\_well\_depth\_gw\_level + sw + dom\_wells\_density + ag\_wells\_density + \beta_g Basin_g + ag\_wells\_density : r\_area\_perennial + ag\_wells\_density : r\_area\_annual + ag\_wells\_density : r\_area\_forage + poverty \quad \text{(C5)}$$

data scale	model	AUC	AUC.SD	DIC	WAIC	LCPO
$9mi^2$	C1	0.55	0.01	2933.33	2933.41	1466.70
$9mi^2$	C2	0.87	0.01	2135.28	2140.60	1070.30
$9mi^2$	C3	0.87	0.01	2132.56	2137.64	1068.82
$9mi^2$	C4	0.89	0.01	2043.24	2048.84	1024.42
$9mi^2$	C5	0.89	0.01	2034.63	2040.26	1020.13
$25mi^2$	C1	0.56	0.01	2923.56	2923.60	1461.80
$25mi^2$	C2	0.86	0.01	2196.44	2201.23	1100.62
$25mi^2$	C3	0.86	0.01	2193.17	2197.77	1098.88
$25mi^2$	C4	0.88	0.01	2122.62	2127.71	1063.86
$25mi^2$	C5	0.88	0.01	2115.32	2120.54	1060.27

Table C3: Results by model and data resolution

C6.2 Results selected model

	mean	sd	0.025quant	0.5quant	0.975quant	mode	kld
intercept	-0.63	0.24	-1.12	-0.62	-0.15	-0.61	0.00
r_area_perennial	0.07	0.07	-0.07	0.07	0.20	0.07	0.00
r_area_annual	-0.06	0.07	-0.19	-0.06	0.07	-0.06	0.00
r_area_forage	0.02	0.06	-0.10	0.02	0.14	0.02	0.00
r_well_depth_gw_level	-2.76	0.16	-3.07	-2.76	-2.45	-2.76	0.00
sw	-0.01	0.10	-0.21	-0.01	0.18	-0.01	0.00
dom_wells_density	0.75	0.07	0.61	0.75	0.89	0.75	0.00
ag_wells_density	0.50	0.08	0.35	0.50	0.66	0.50	0.00
poverty	0.24	0.07	0.11	0.24	0.38	0.24	0.00
r_area_perennial:ag_wells_density	0.26	0.06	0.13	0.26	0.38	0.26	0.00
r_area_annual:ag_wells_density	-0.07	0.07	-0.21	-0.07	0.06	-0.07	0.00
r_area_forage:ag_wells_density	-0.02	0.07	-0.17	-0.02	0.12	-0.02	0.00

Table C4: Fixed-effect results

Groundwater Subbasin	mean	sd	0.025quant	0.5quant	0.975quant	mode	kld
Madera	-0.53	0.26	-1.10	-0.52	-0.08	-0.48	0.00
Kings	-0.14	0.23	-0.61	-0.14	0.32	-0.14	0.00
Kaweah	0.33	0.23	-0.12	0.32	0.82	0.30	0.00
Tule	0.35	0.24	-0.10	0.34	0.87	0.31	0.00

Table C5: Random-effect results

C7 Additional figures selected model performance

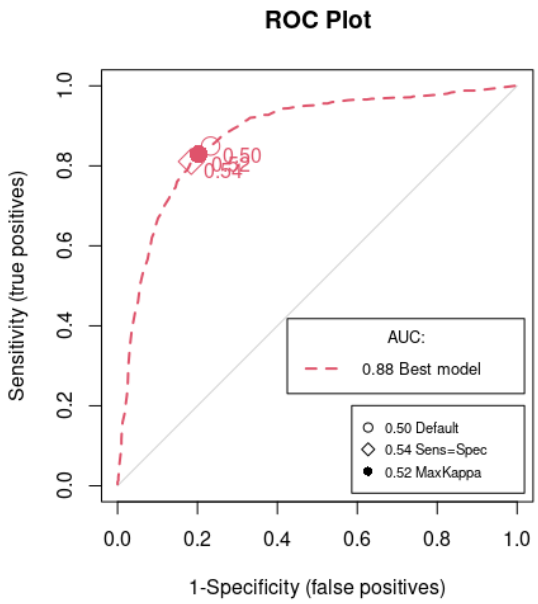

Figure C10: ROC curve for the model S5 wih $9mi^2$ ($23.3km^2$) data resolution, using training data set. 1 is a perfect classifier.

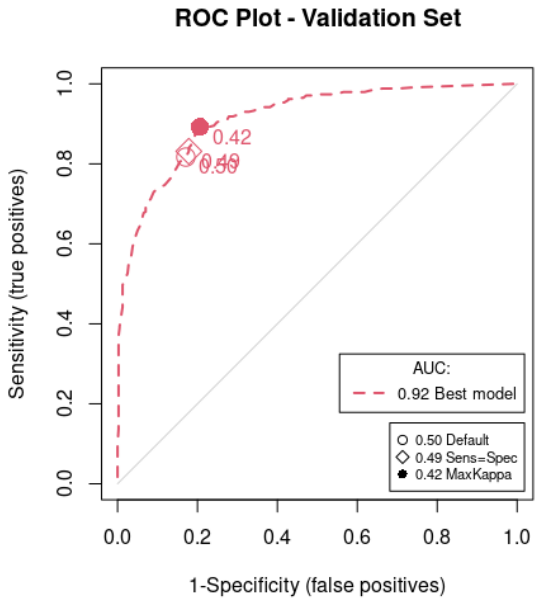

Figure C11: ROC curve for the model S5 wih $9mi^2$ ($23.3km^2$) data resolution, using validation data set. 1 is a perfect classifier.

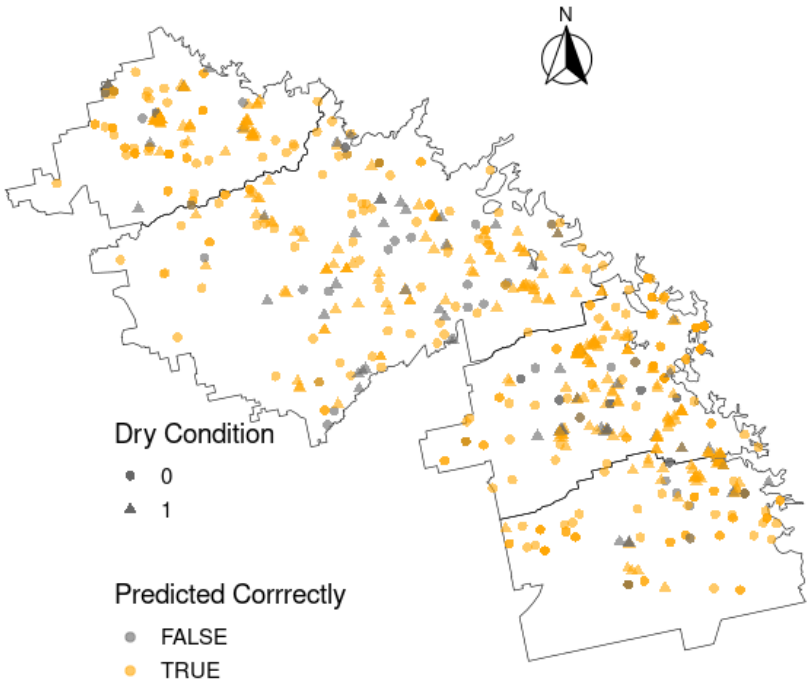

Figure C12: Validation of domestic well failure prediction

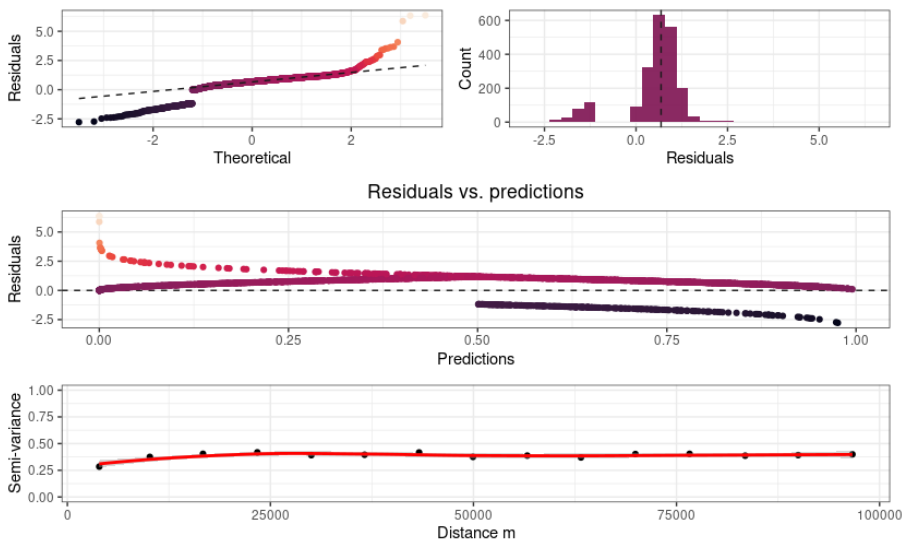

Figure C13: Residuals of the selected model S5 wih $9mi^2$ ($23.3km^2$) data resolution

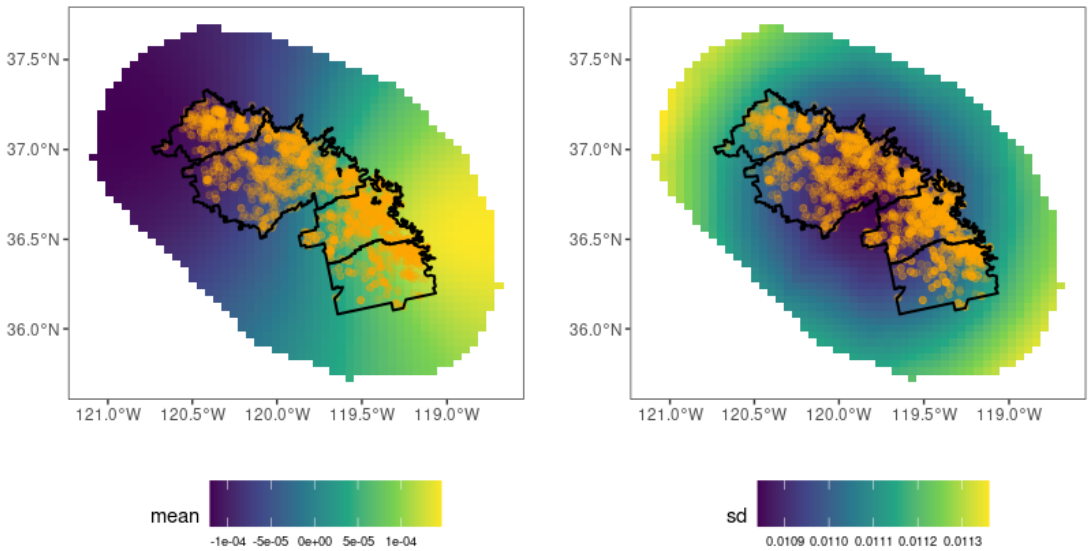

Figure C14: Stochastic Partial Differential Equations (SPDE) result from R-INLA

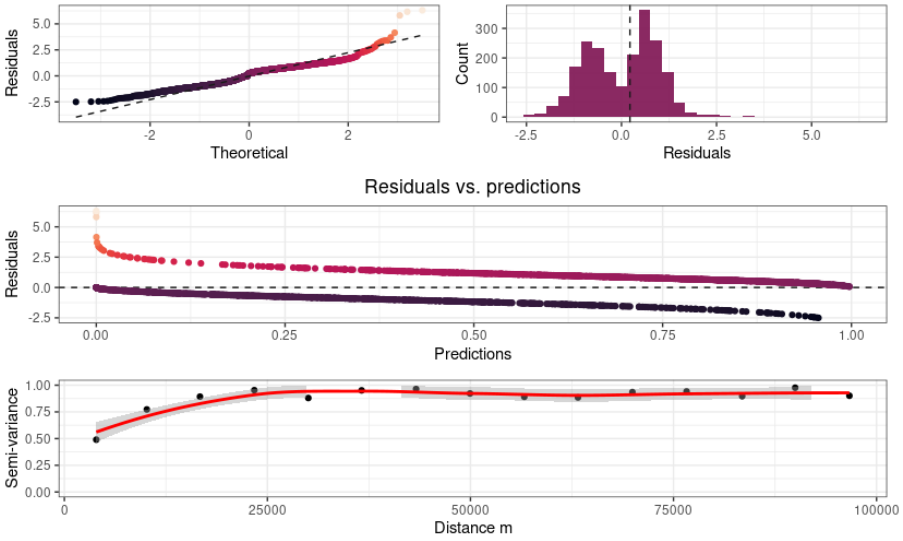

Figure C15: Residuals of selected model without the spatial random effects

C8 Well Completion Reports Analysis

C8.1 Supporting figures

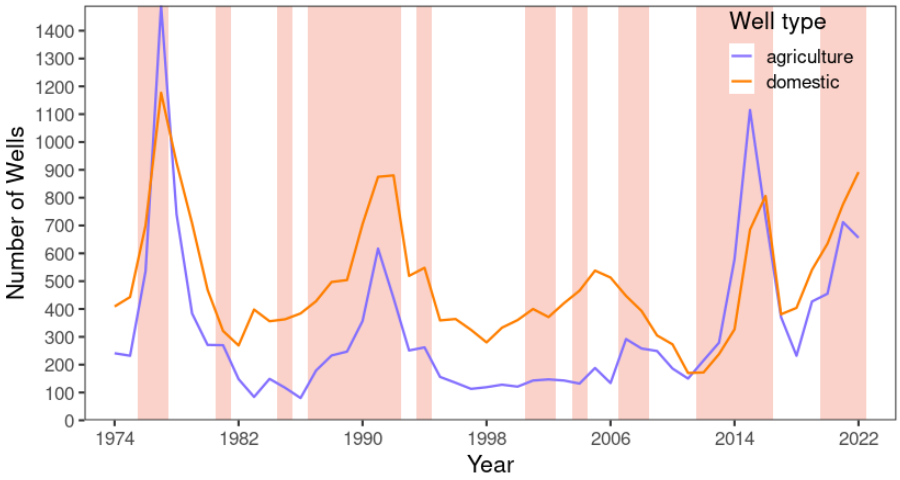

Figure C16: Evolution of well drilling for agricultural and domestic wells in the study area.In red we highlight dry periods based on the San Joaquin River Index (dry).

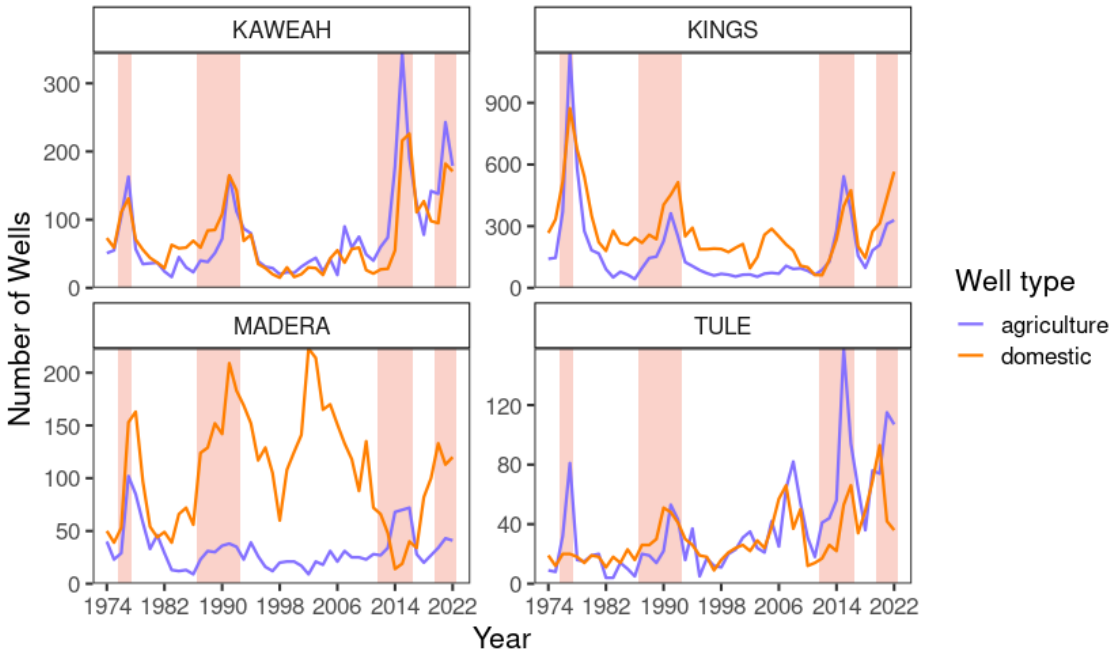

Figure C17: Evolution of well drilling for agricultural and domestic wells by groundwater subbasin in the study area. In red we highlight dry periods based on the San Joaquin River Index (critical dry).

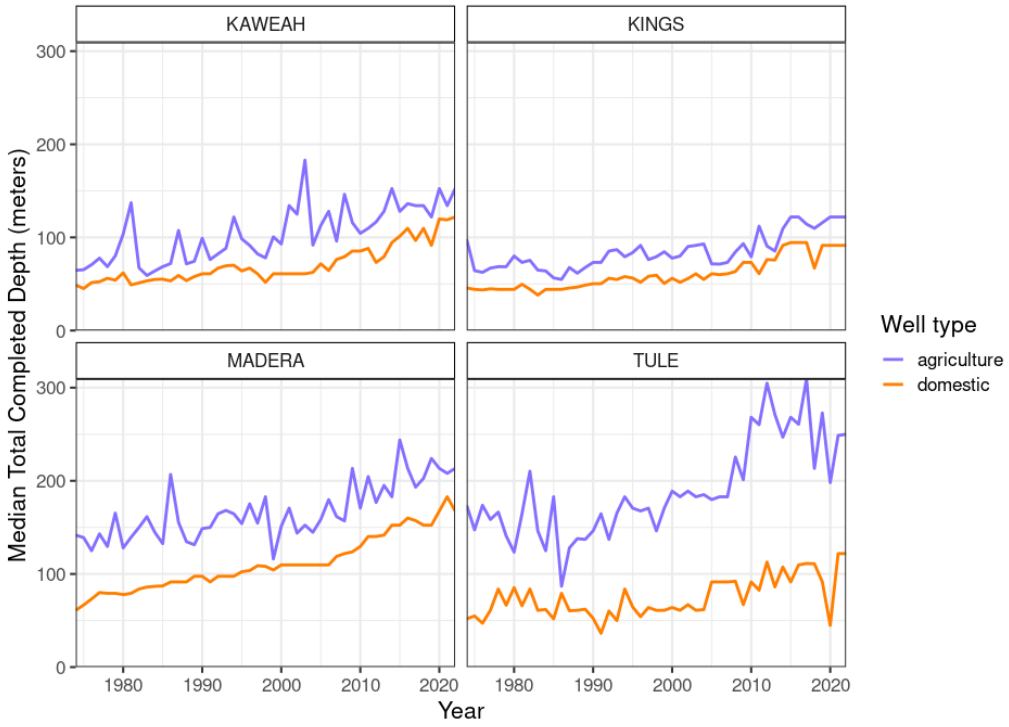

Figure C18: Median of completed drilled depths from the ground surface for agricultural and domestic wells in the study area form 1970 to 2022.In red we highlight critical dry periods based on the San Joaquin River Index (dry and critical dry).

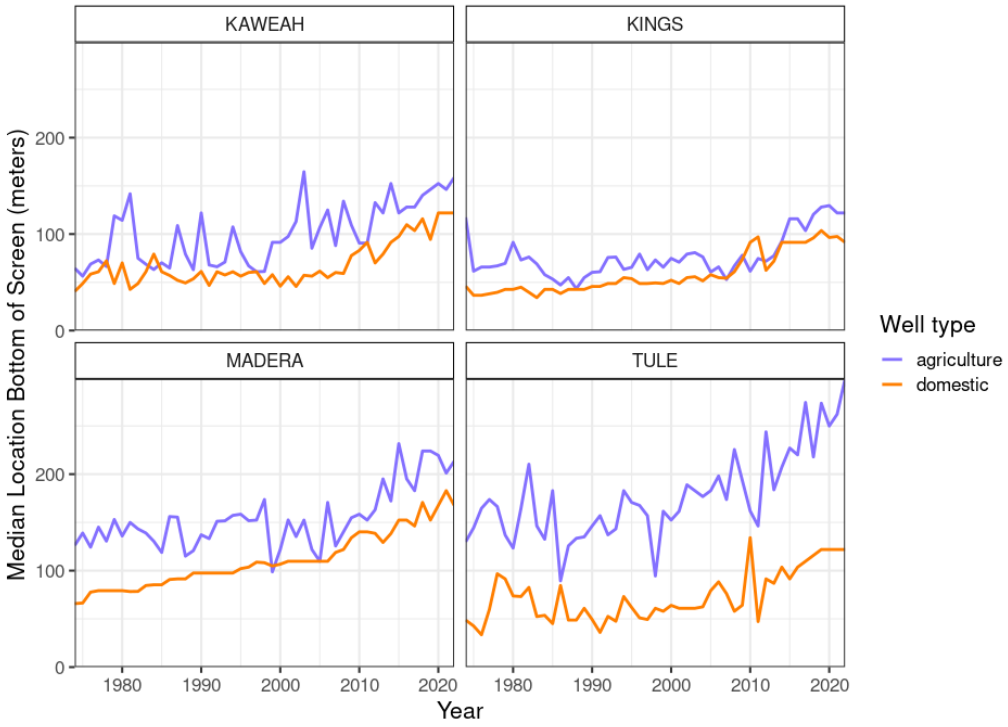

Figure C19: Median of distance to bottom of screen location from ground surface level for agricultural and domestic wells in the study area form 1970 to 2022.

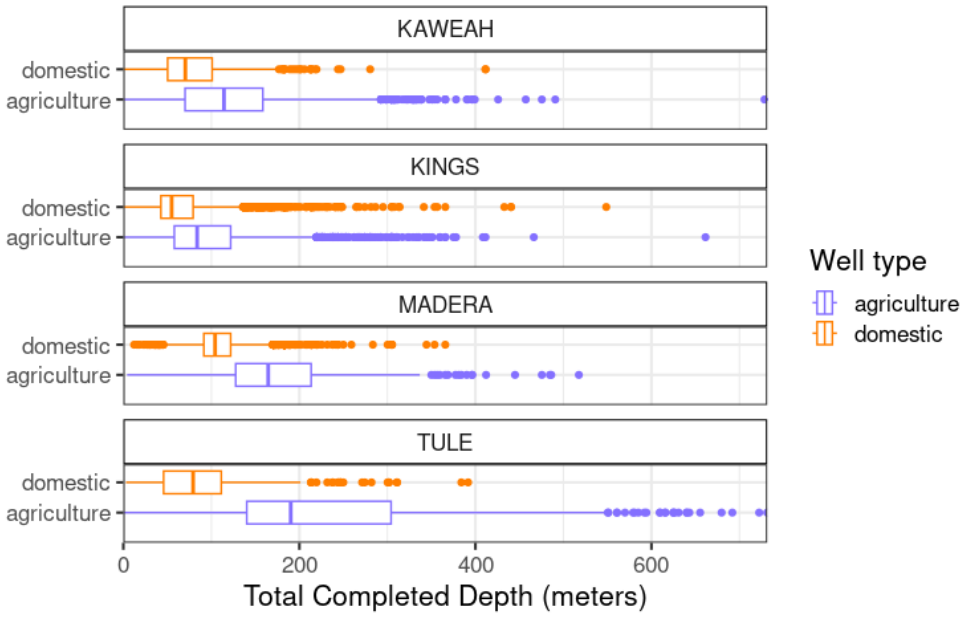

Figure C20: Distribution of well depths of domestic and agricultural wells by subbasin.

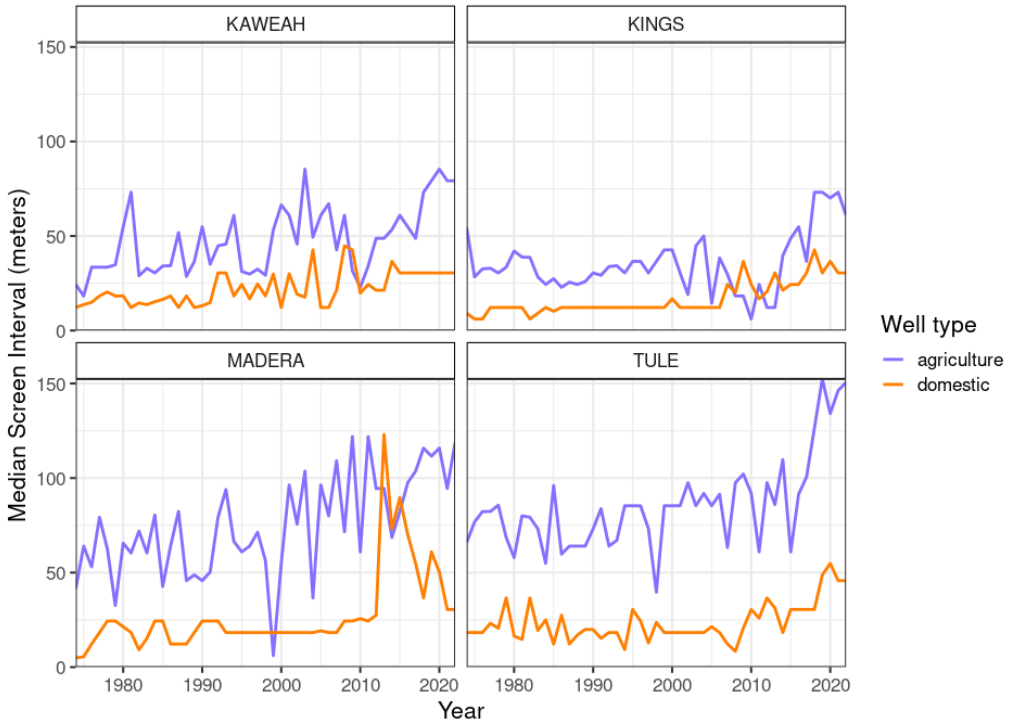

Figure C21: Median of screen interval distance (bottom screen - top screen) for agricultural and domestic wells in the study area form 1970 to 2022.

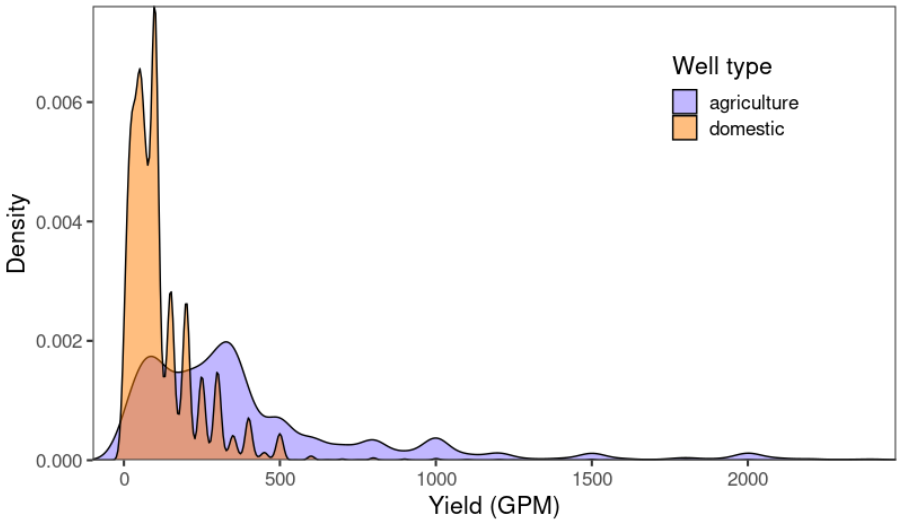

Figure C22: Density of well yield for agricultural and domestic wells. This is reported from the pumping test performed after the well is completed.

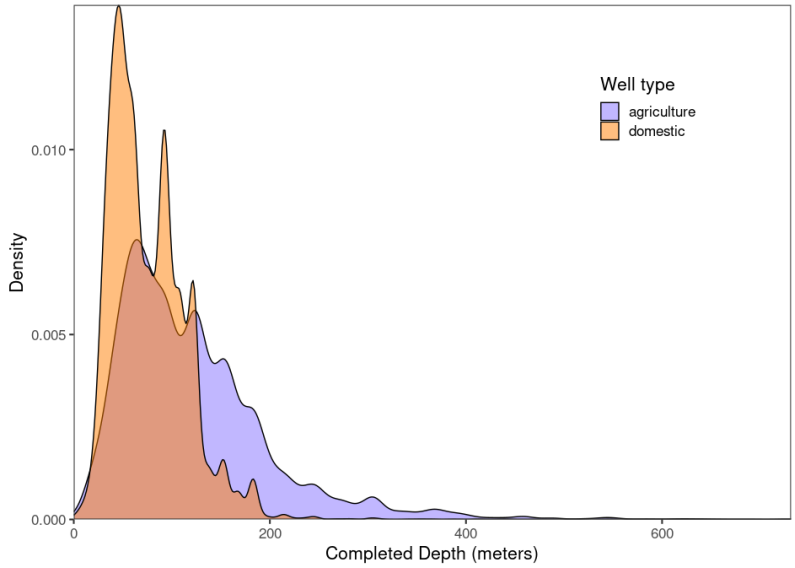

Figure C23: Density of well depth for agricultural and domestic wells.

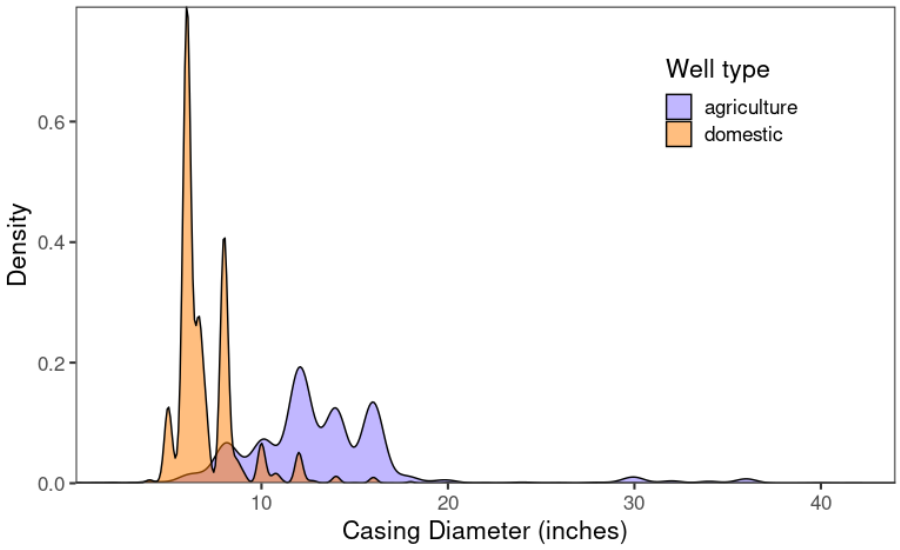

Figure C24: Density of well casing diameter for agricultural and domestic wells.

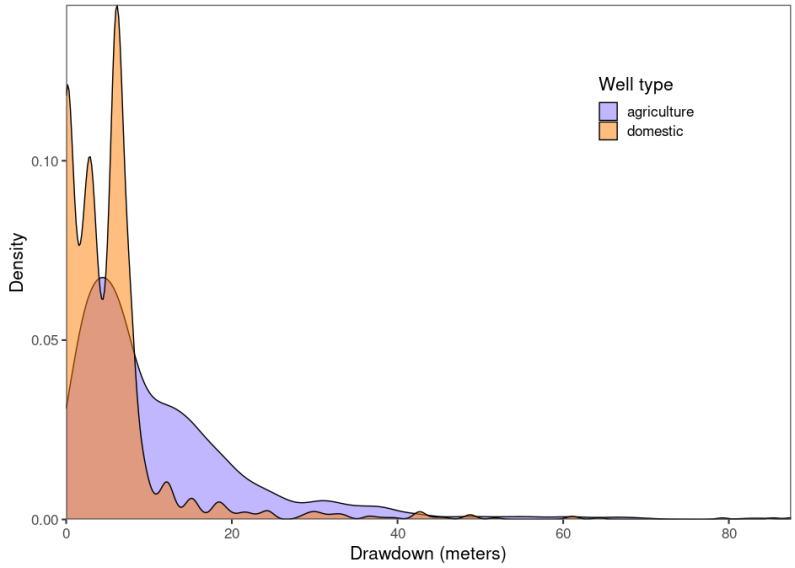

Figure C25: Density of well drawdown for agricultural and domestic wells. This is reported from the pumping test performed after the well is completed.

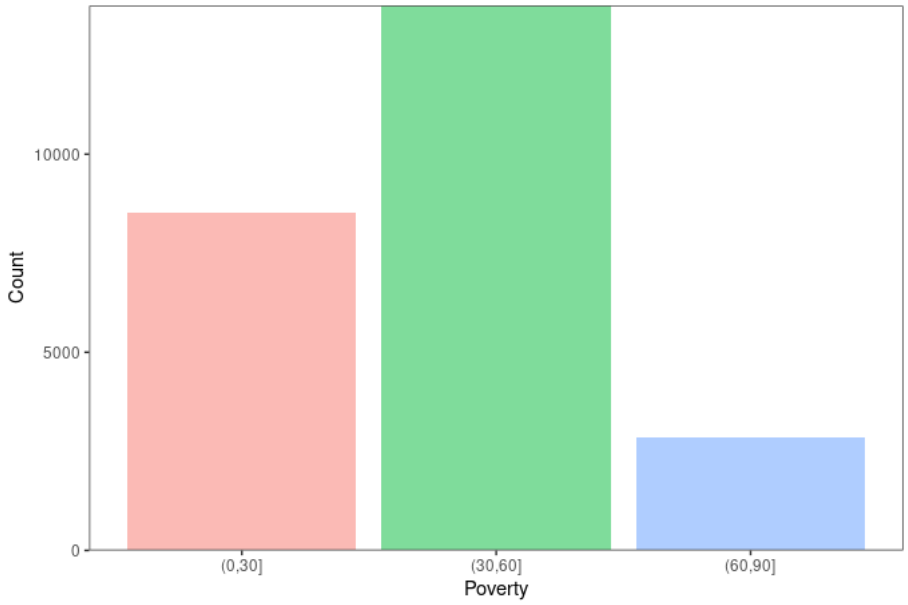

Figure C26: Number of domestic wells (1970-2022) by poverty index category

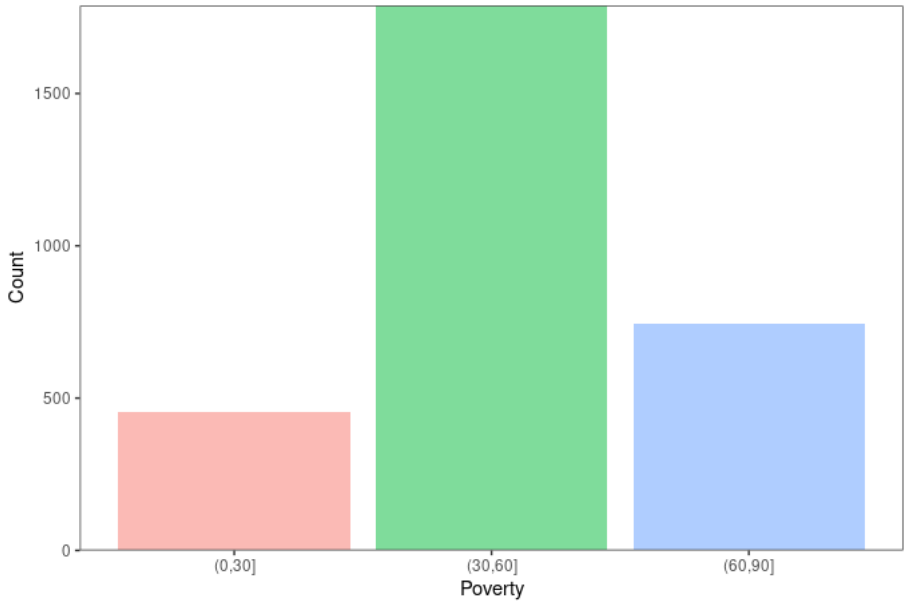

Figure C27: Number of reported dry wells (2014-2022) by poverty index category

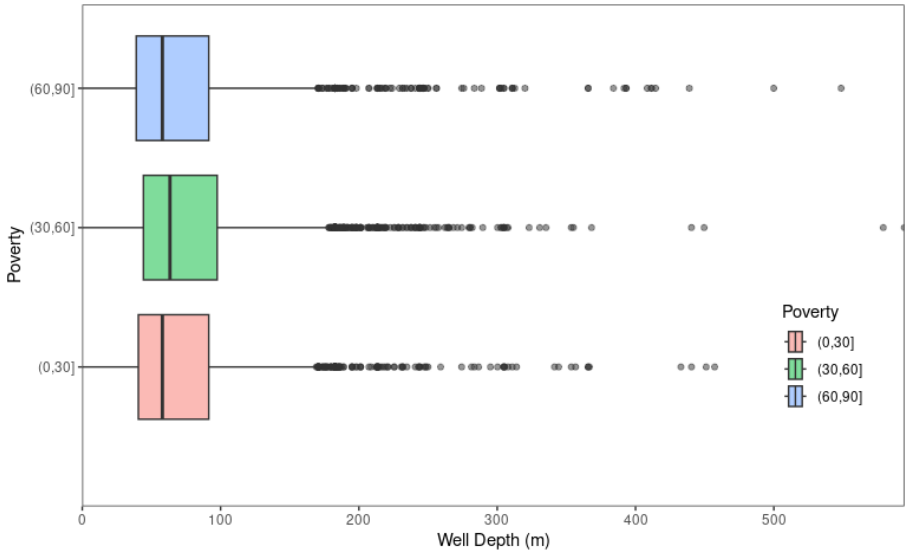

Figure C28: Domestic well depths by poverty index category

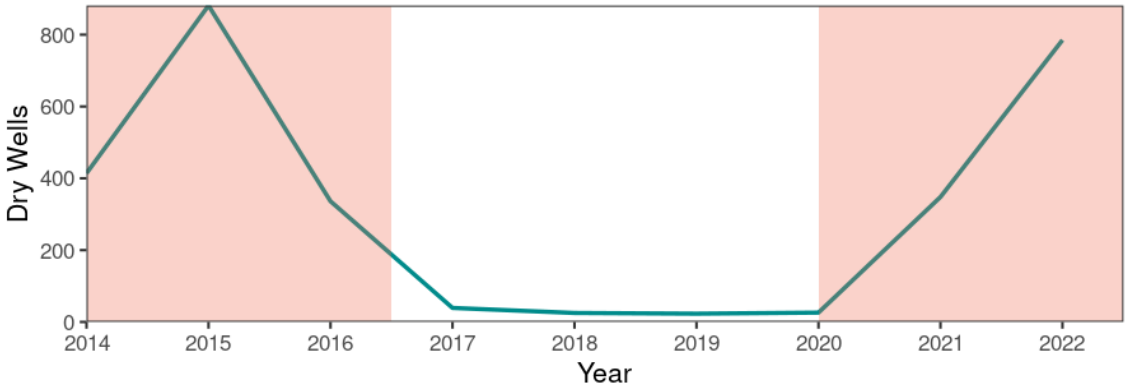

Figure C29: Total dry wells in the study area from 2014 to 2022

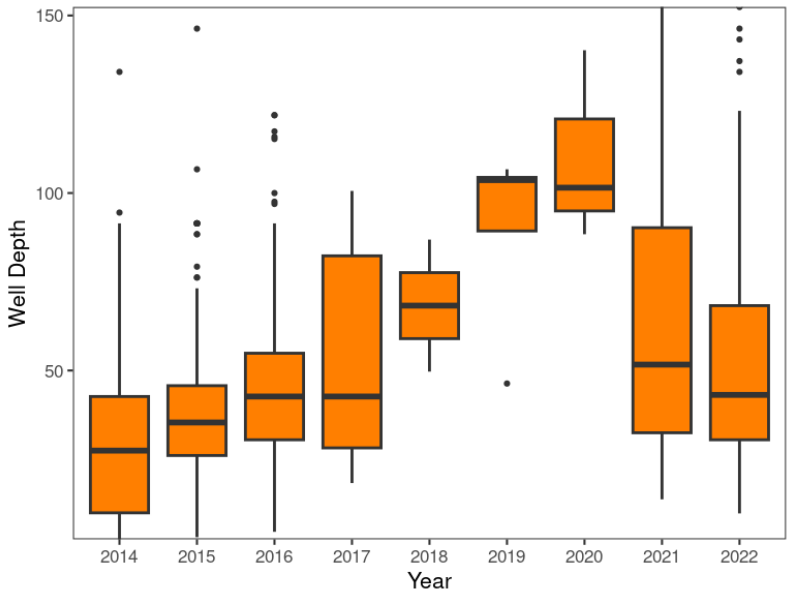

Figure C30: Well depths of reported domestic dry wells in the study area

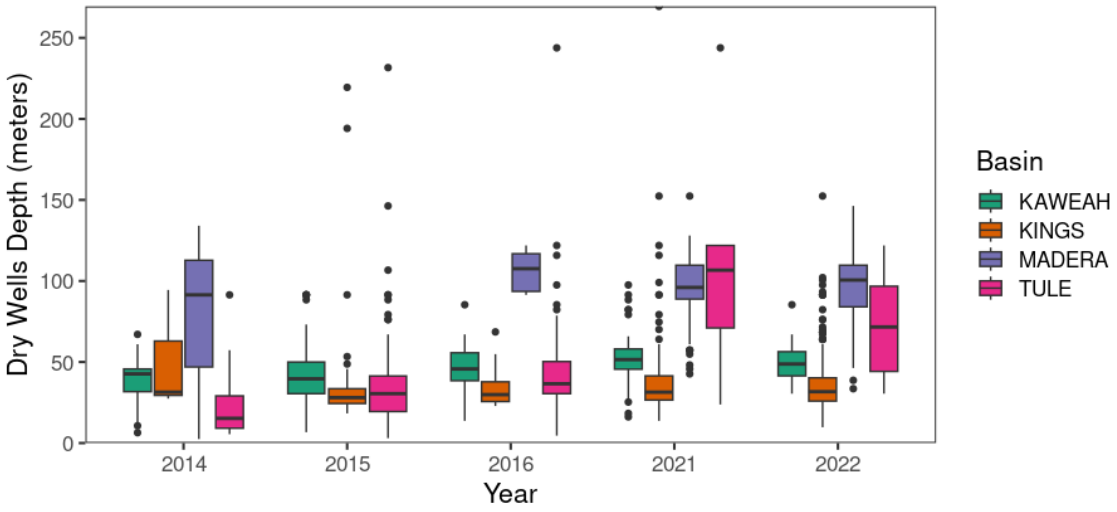

Figure C31: Well depths of reported dry wells in the study area by groundwater subbasin

C9 GSA scale Figures

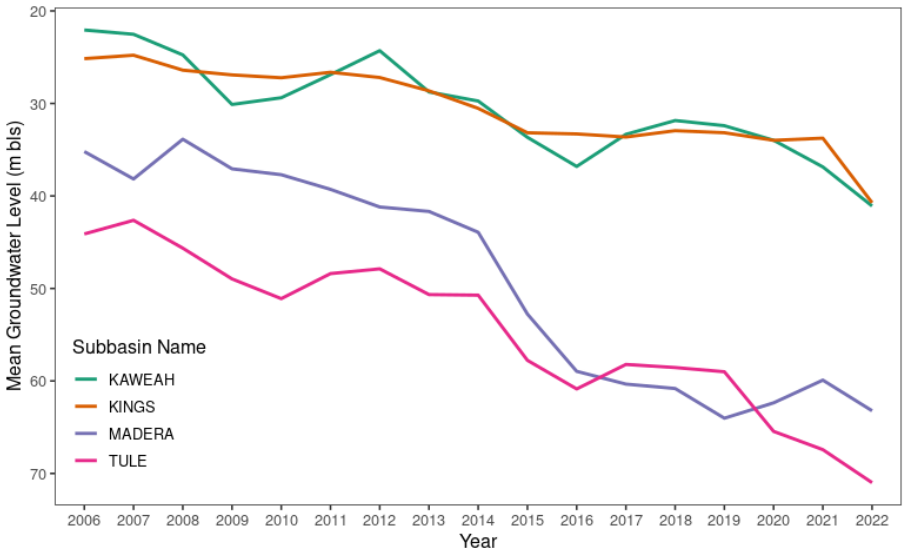

Figure C32: Mean groundwater depth (in meters bellow surface) by groundwater subbasin from 2005 to 2022

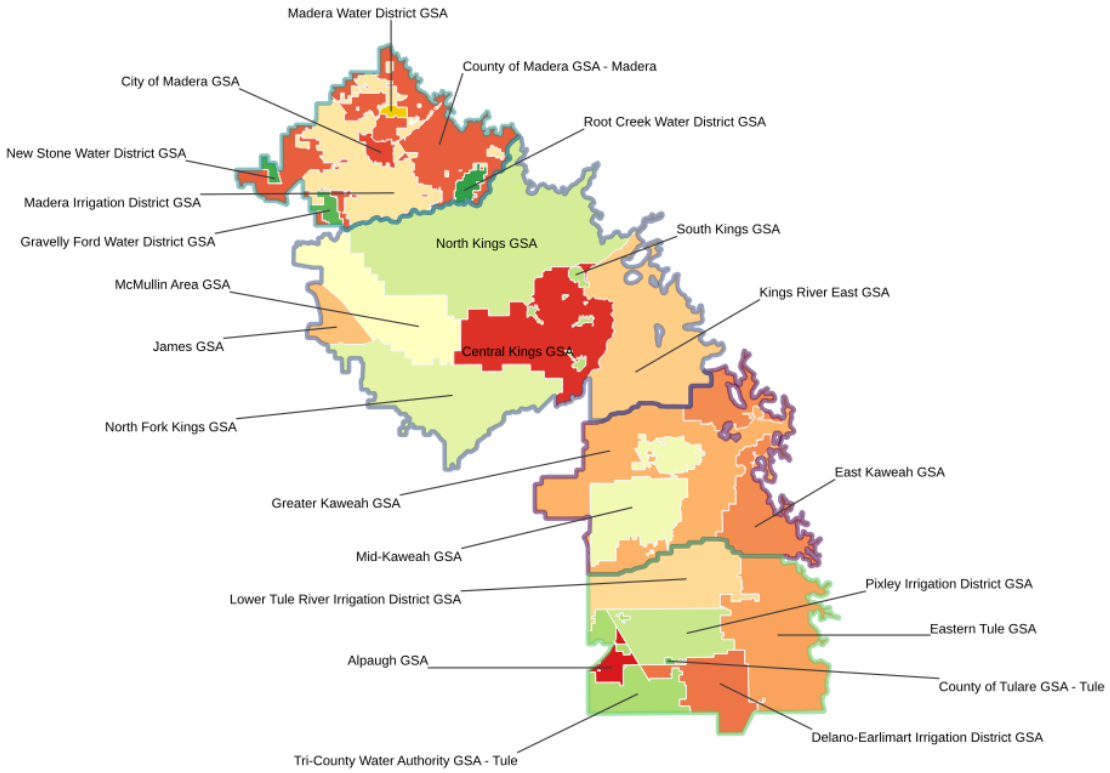

Figure C33: GSAs in the four subbasins of the study area

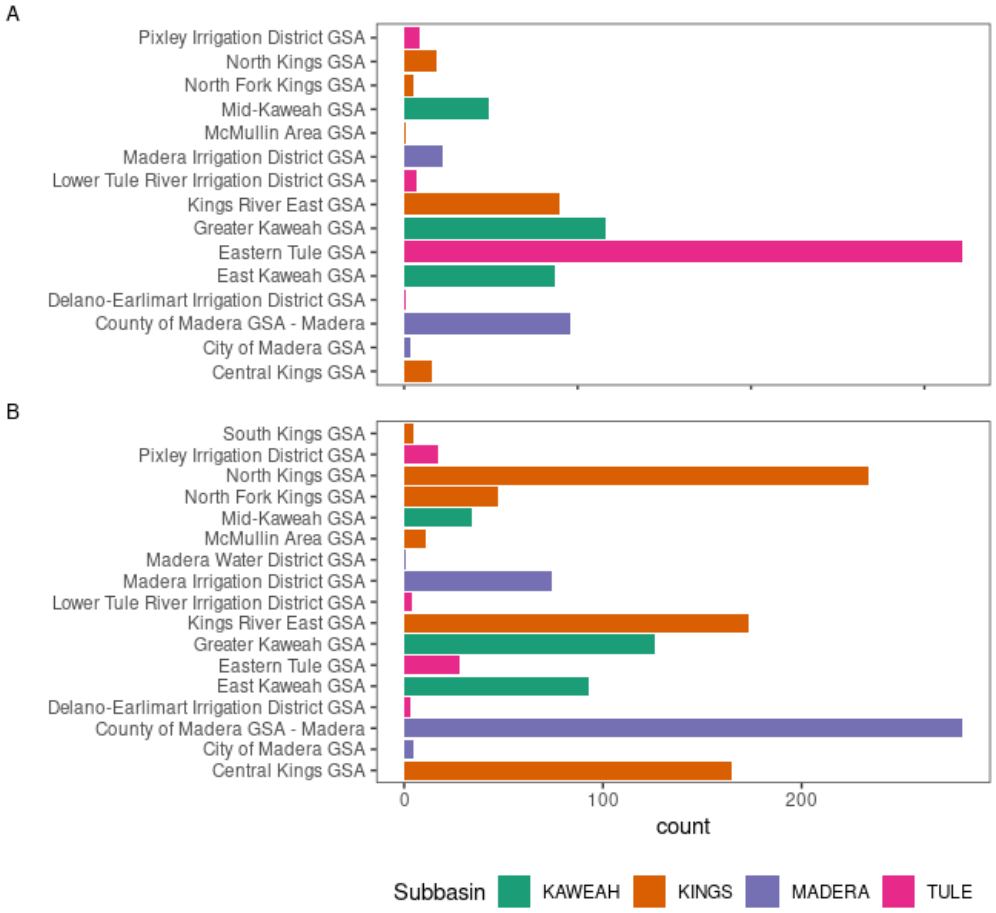

Figure C34: Number of reported dry wells by GSA from 2014-2016 (A) and 2020-2022 (B)

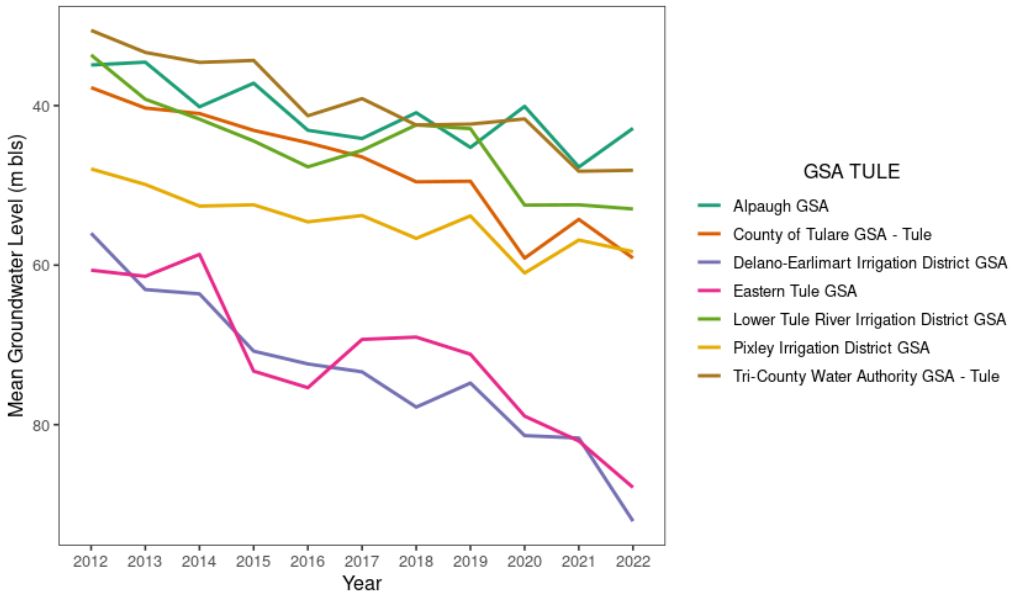

Figure C35: Mean groundwater depth (in meters bellow surface) by GSA in Tule subbasin from 2012 to 2022

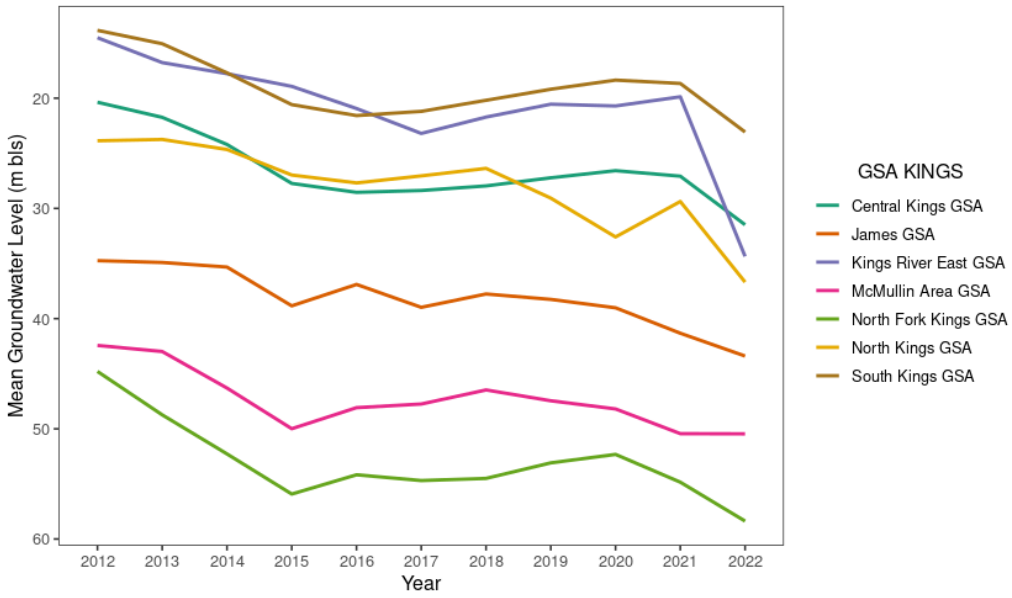

Figure C36: Mean groundwater depth (in meters bellow surface) by GSA in Kings subbasin from 2012 to 2022

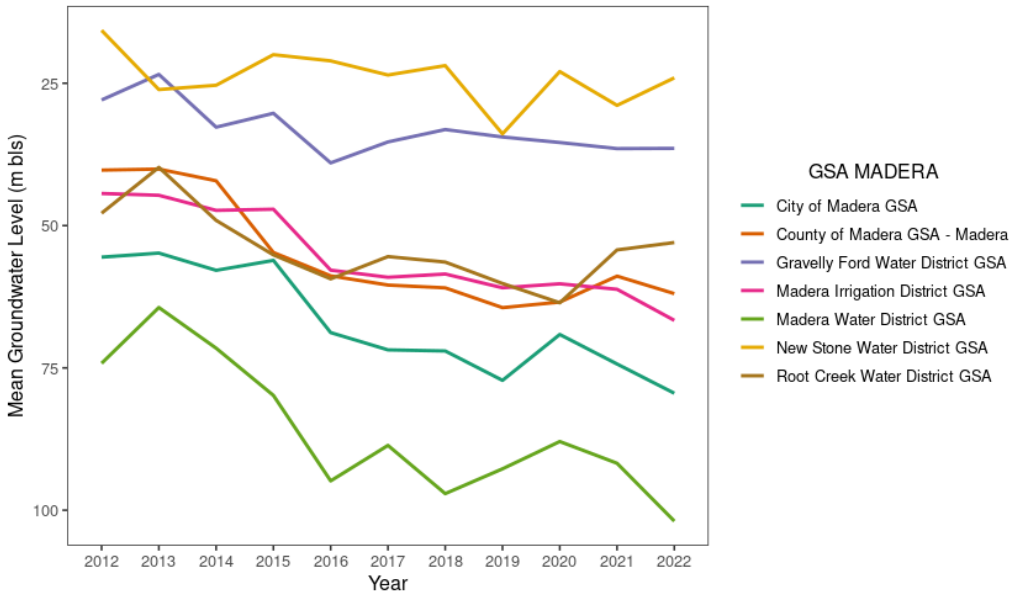

Figure C37: Mean groundwater depth (in meters bellow surface) by GSA in Madera subbasin from 2012 to 2022

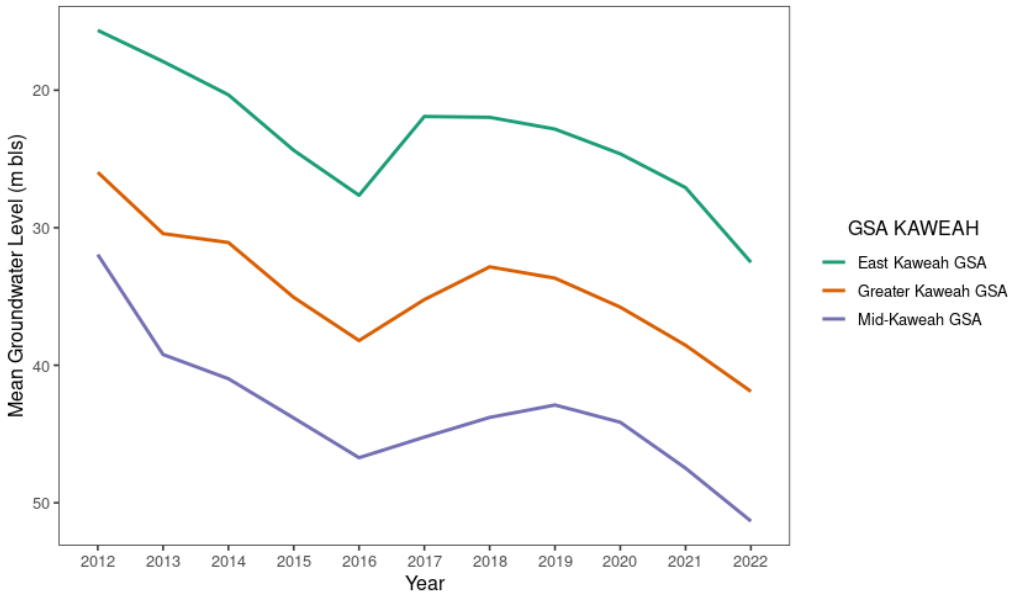

Figure C38: Mean groundwater depth (in meters bellow surface) by GSA in Kaweah subbasin from 2012 to 2022

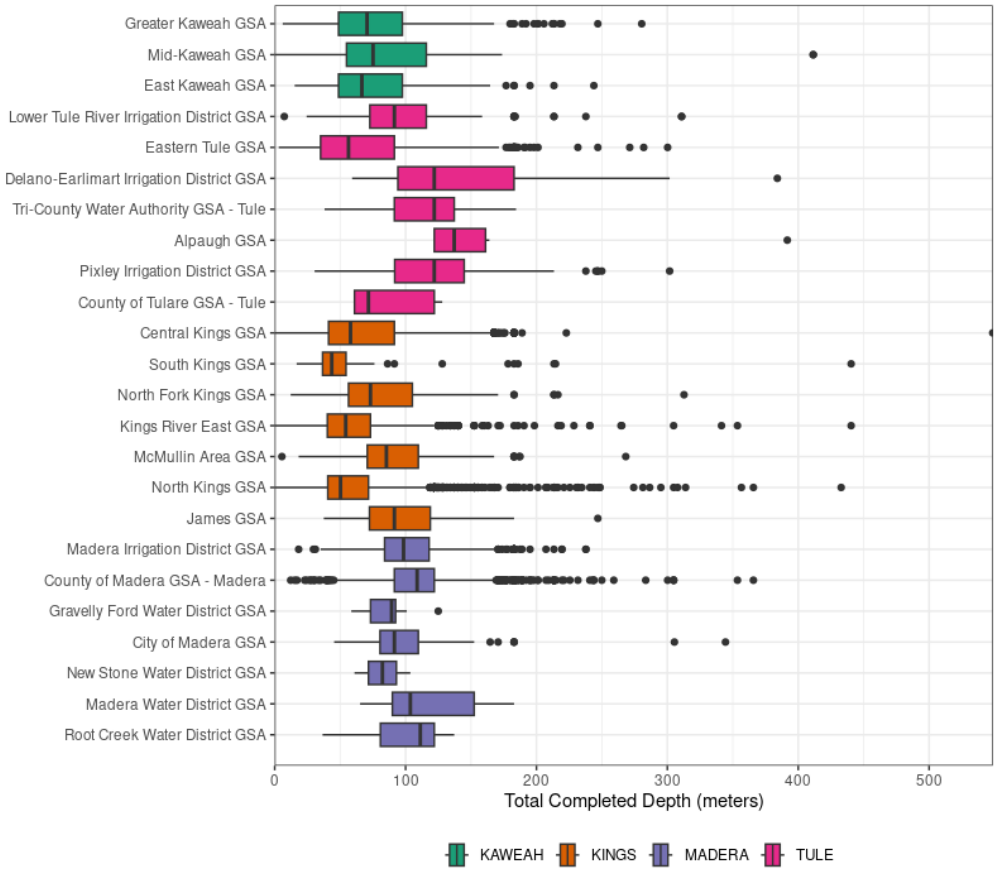

Figure C39: Drilled well depths (in meters bellow surface) by GSA

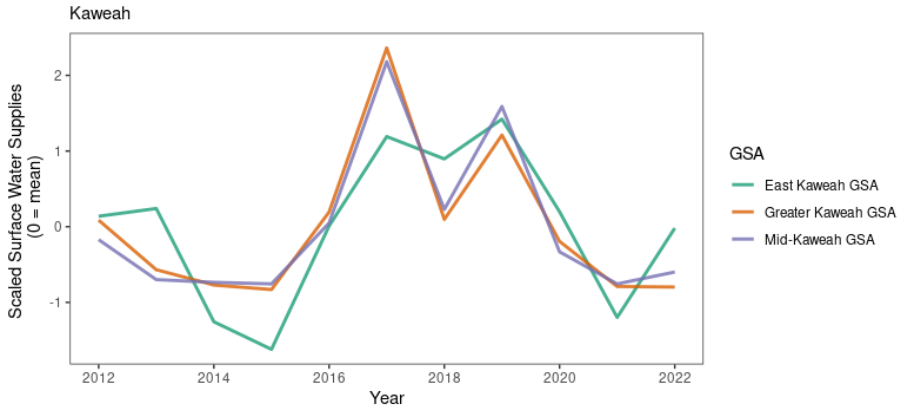

Figure C40: Mean centered surface water deliveries by GSA in Kaweah subbasin from 2012 to 2022

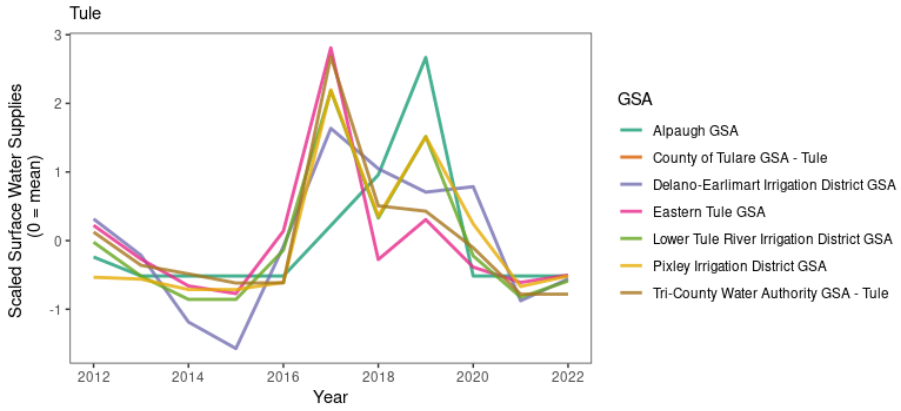

Figure C41: Mean centered surface water deliveries by GSA in Tule subbasin from 2012 to 2022

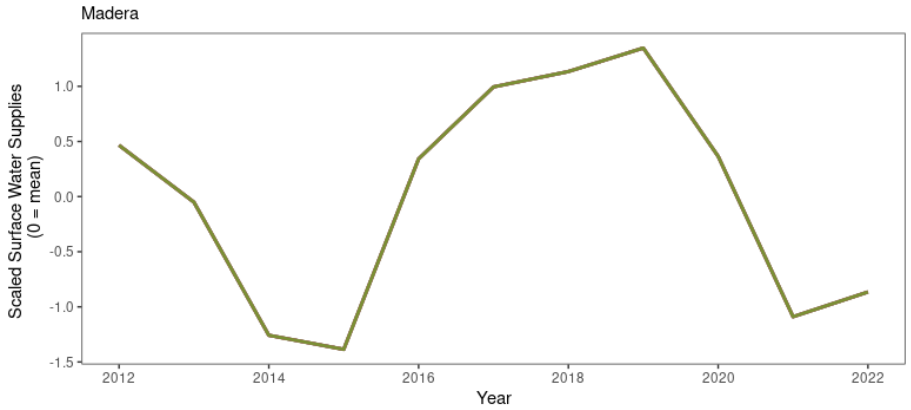

Figure C42: Mean centered surface water deliveries in Madera subbasin from 2012 to 2022

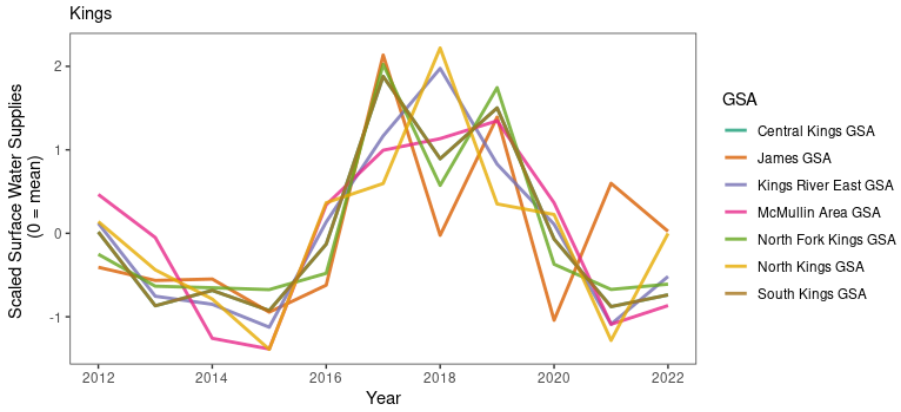

Figure C43: Mean centered surface water deliveries by GSA in Tule subbasin from 2012 to 2022

Bibliography

Chen, B., Gramig, B., & Mieno, T. (2023). CropScapeR: Access Cropland Data Layer Data via the 'CropScape' Web Service. https://cran.r-project.org/web/packages/CropScapeR/index.html

DWR. (2021). C2VSimFG Version 1.01. https://data.cnra.ca.gov/dataset/c2vsimfg-version-1-01